

THE JENNER INSTITUTE
DEVELOPING INNOVATIVE VACCINES



UNIVERSITY OF OXFORD

Identification and Selection of Novel Mycobacterial Antigens using Immunopeptidomics and Immunoinformatics for the Development of Subunit Vaccines Against Tuberculosis

Salem Salman Almujri
Linacre College
Jenner institute
University of Oxford

Thesis submitted for the degree of Doctor of Philosophy in Clinical Medicine

Michaelmas 2022

Supervisors:
Prof. Helen McShane
Dr. Nicola Ternette
Dr. Paulo Bettencourt
Dr. Iman Satti

ABSTRACT

In response to the urgent need for an effective vaccine against tuberculosis (TB), mass spectrometry-based immunopeptidomics was employed to identify novel mycobacterial antigens. Human macrophages (differentiated THP-1 cells) were utilised as an *in-vitro* model of TB, in which mycobacterial peptides presented on major histocompatibility complex (MHC) molecules were identified. As a result, 64 and 81 mycobacterial proteins derived from the Bacille Calmette-Guérin (BCG) vaccine and *Mycobacterium tuberculosis* (MTB) were discovered, respectively. The identified proteins were prioritised based on their T-cell epitope repertoire through the use of immunoinformatics tools *in silico*, resulting in a list of potential candidate antigens. This approach efficiently facilitated the identification and prioritisation of novel mycobacterial antigens, in which T-cell responses and the diversity of human leukocyte antigen (HLA) alleles were considered. The top candidate antigens (hisD, metE and mmpL12) were selected for screening in mice through the application of mycobacterial growth inhibitory assays (MGIAs) to evaluate their protective properties. MGIA was used as an *ex-vivo* surrogate assay for an *in-vivo* MTB challenge experiment. The mouse groups that were vaccinated with metE (either in the form of plasmid DNA or as a protein with adjuvant) conferred protection compared with unvaccinated mice. The metE-DNA vaccine induced polyfunctional CD4+ T cells expressing interferon-gamma (IFNγ), tumour necrosis factor-alpha (TNFα), and interleukin-2 (IL-2), whereas the metE-AddaS03 vaccine elicited a range of CD4+ T cells that expressed TNFα, IL-2, IL-4, and IL-17. Both the metE-DNA and metE-AddaS03 vaccines significantly induced the production of immunoglobulin G (IgG) antibodies compared with the naïve group;

when the vaccines were compared, the antibody concentration that was induced by the metE-AddaS03 vaccine was 16-fold higher than that induced by the metE-DNA vaccine. The findings of this work show that the metE protein is a novel protective candidate that merits further development for inclusion in a subunit vaccine against TB.

Interestingly, IFNγ was found to enhance the expression and the total number of identified peptides that were associated with HLA-DR significantly compared with HLA-DQ and HLA-DP. The effects of mycobacterial infection and IFNγ treatment on the surface expression of HLA-DR alleles (HLA-DRB1*0101, -DRB1*1501 and -DRB5*0101) expressed by THP-1 cells were investigated quantitatively. Mass spectrometry-based quantitative proteomics was used to analyse the expression levels of HLA-DR proteins obtained from the same samples used for immunopeptidomics. Without IFNγ treatment, DRB1*0101 was dominantly expressed compared with DRB1*1501 and DRB5*0101. In contrast, when the sample was treated with IFNγ, DRB1*1501 was up-regulated more than DRB1*0101. Compared with uninfected samples, the levels of HLA-DRA1 and -DRB1*0101 showed a decreasing trend upon infection, whereas levels of DRB1*1501 and DRB5*0101 increased or remained unchanged. When the mycobacterial peptides were predicted according to their binding affinity, 55% of peptides were assigned as ligands for DRB1*0101, compared with about 24.3% and 20.7% assigned as ligands for DRB1*1501 and DRB5*0101, respectively. To expand this further to the whole sequence, 76% of the tested antigens (47 antigens) were predicted to contain more peptides for DRB1*0101 than for DRB1*1501. The data collected in this work suggest that mycobacteria may evade T-cell recognition as they target HLA-DR alleles that are more likely to present their antigens (i.e. they inhibit the HLA-DRB1*0101 allele and avoid being presented by the DRB1*1501 allele).

TABLE OF CONTENTS

Abstract I

Table of Contents III

List of Tables VII

List of Figures VIII

List of Abbreviations X

Acknowledgements XII

Chapter 1 1

1.1 Background 2

1.2 Immunopathogenesis of TB 3

1.3 Natural immunity to TB 3

1.3.1 Innate immunity 3

1.3.2 Adaptive immunity 10

1.3.3 Granuloma 15

1.4 Vaccines for TB 16

1.5 Novel antigen discovery 21

1.6 MHC structure and function 27

1.7 Animal models 29

1.8 Mycobacterial growth inhibition assays (MGIAs) 30

1.9 Thesis aims 33

Chapter 2 34

2.1 Reagents and solutions 35

2.2 Cell culture and *in-vitro* infection 37

2.2.1 THP-1 cells 37

2.2.2 BCG and MTB culture and freezing 38

2.2.3 Infection of THP-1 cells with MTB for immunopeptidomics 39

2.2.4 Removal of MTB from the lysate 39

2.2.5 Flow cytometry 40

2.2.6 Quantification of mycobacteria 40

2.3 MS-based immunopeptidomics and proteomics 41

2.3.1 IP of peptide-MHC complex 41

2.3.2 Purification of HLA peptides 42

2.3.3 MS and data analysis 42

2.3.4 Data analysis for immunopeptidomics 43

2.3.5 MHC protein digestion and peptide purification 44

2.3.6 Data analysis for quantitative proteomics 44

2.4 *In silico* analysis and computational tools 45

2.4.1 T-cell MHC-II prediction 45

2.4.2 Non-homologous protein identification 46

2.4.3 Peptide yield after trypsin digestion 46

2.5 Plasmid amplification and purification 47

2.5.1 Escherichia coli transformation 47

2.5.2 Plasmid purification 48

2.6 Confirmation of inserts and expression 49

2.6.1 Agarose gel electrophoresis 49

2.6.2 Western blotting 50

2.6.3 Flow cytometry 52

2.7 Animal experiments 53

2.7.1 CB6F1 Mice 53

2.7.2 Immunisation 54

2.7.3 MGIA 54

2.7.4 Enzyme-linked immunosorbent assay (ELISA) 55

2.7.5 Enzyme-linked immunospot (ELISpot) 56

2.7.6 Intracellular cytokine staining 57

2.8 Statistical analyses 60

Chapter 3 61

3.1 Introduction 62

3.2 Aims of the work described in this chapter 64

3.3 Results 66

3.3.1 Profiling identified MHC peptides 66

3.3.2 Prediction of binding motifs 68

3.3.3 Optimisation of MTB macrophage-infected model 71
3.3.4 Profiling identified MHC peptides upon MTB-infected macrophages 75
3.3.5 Selection and prioritisation of candidate antigens 78
3.4 Discussion 84
3.5 Conclusion and future work 91
Chapter 4 92
4.1 Introduction 93
4.2 Aims of the work described in this chapter 95
4.3 Results 96
4.3.1 HLA expression upon IFNγ treatment 96
4.3.2 Identification of unique peptides that represent HLA-DR chains 97
4.3.3 Quantification of α or β chains of HLA-DR alleles by use of MS 100
4.3.4 Comparisons of each HLA-DR chain across experimental conditions 101
4.3.5 Analysis of human immunopeptidome (BCG experiments) 102
4.3.6 Quantification of HLA proteins and analysis of human immunopeptidome (MTB experiments) 104
4.3.7 Prediction of binding affinity through the use of whole antigen sequences 106
4.3.8 Effect of small molecules on HLA expression 107
4.3.9 Effect of Tubastatin A on HLA expression 109
4.4 Discussion 111
4.5 Conclusions 117
4.6 Ongoing and Future work 119
Chapter 5 120
5.1 Introduction 121
5.2 Aims of the work described in this chapter 123
5.3 Results 124
5.3.1 Construction of candidate antigens as DNA vaccines 124
5.3.2 Confirmation of correctly sized inserts and plasmid expressions *in vitro* 125
5.3.3 Antigen Evaluation using MGIA 126
5.3.4 Vaccination with metE inhibited mycobacterial growth 129
5.3.5 Exploring antigen secretion 130
5.3.6 Vaccination with metE conferred protection 132

5.3.7 Assessment of T cell responses induced by metE vaccinations 134
5.3.8 Assessment of antibody responses induced by metE vaccinations 139
5.4 Discussion 143
5.5 Research limitations 151
5.6 Conclusions 151
5.7 Ongoing and future work 152
Chapter 6 153
6.1 Summary of main findings of work described in Chapter 3 154
6.1.1 Future work 155
6.2 Summary of main findings of work described in Chapter 4 155
6.2.1 Ongoing work 158
6.2.2 Future work 159
6.3 Summary of main findings of work described in Chapter 5 160
6.3.1 Ongoing work 161
6.3.2 Future work 161
Chapter 7 163
7.1 Identified BCG peptides 164
7.2 Identified MTB peptides 167
7.3 Prioritisation of identified antigens 170
7.3.1 Characterisation of identified peptides 170
7.3.2 Prediction of HLA-DR peptides 176
7.3.3 Prediction of HLA-DP and HLA-DQ peptides 178
7.3.4 Prediction of H2 peptides 180
7.3.5 Prediction of HLA-I peptides 182
References 184

LIST OF TABLES

Table 1.1 Summary of the vaccines currently in clinical trials, adapted from the Tuberculosis Vaccine Initiative (137) and (127). 19

Table 2.1 Solutions added sequentially to the blotted membrane. 52

Table 2.2 Composition and dilution of antibodies used for surface and intracellular staining 59

Table 3.1 The experimental layout for MTB infection. 76

Table 3.2 E- value of mycobacterial proteins 81

Table 3.3 Immunopeptidomics and immunoinformatics characterisation of candidate antigens. 83

Table 4.1 The experimental layout of the six samples prepared previously for BCG infection, adapted from Bettencourt et al. (2020). 95

Table 4.2 Unique peptides that correspond to HLA-DR chains identified in silico or in vitro 98

Table 4.3 Reported values of peptide intensities (log_2) generated by MaxQuant and Progenesis 99

Table 5.1 Prediction of cleavage site and probability score after addition of IgGκ signal peptide 124

Table 5.2 Details of the ongoing in-vivo MTB-challenge experiments 152

LIST OF FIGURES

Figure 2.1 Visualisation of GFP expression under fluorescence microscope. 38

Figure 2.2 Visualisation of mCherry expression under fluorescence microscope. 53

Figure 2.3 Flow cytometric gating strategy for ICS. 60

Figure 3.1 Process of antigen identification. 63

Figure 3.2: The experimental layout of the samples used for the immunopeptidomics analysis. 65

Figure 3.3 Total numbers and distributions of peptides. 67

Figure 3.4 Prediction of peptide affinity against THP-1 HLA alleles. 69

Figure 3.5 Prediction of binding motifs of human peptides. 70

Figure 3.6 The effect of IFNγ on mycobacteria uptake and MHC-II. 73

Figure 3.7 BCG growth rate, counts and multiplicity of infection. 75

Figure 3.8 Distribution of peptides 77

Figure 3.9 Antigen selection process 78

Figure 3.10 First set of selected mycobacterial proteins 79

Figure 4.1 Up-regulation of surface expression of HLA-DR, -DP and -DQ. 97

Figure 4.2 Peptide peak intensities of HLA-DR alleles 100

Figure 4.3 Fold-change analysis 101

Figure 4.4 Peptide motifs and numbers taken from the immunopeptidomics data for individual HLA-DR alleles or trash clusters. 103

Figure 4.5 Analysis of fold-change and binding motifs. (A) 105

Figure 4.6 Prediction of HLA-DR*0101 and HLA-DR*1501 repertoires. 107

Figure 4.7 The effect of small molecules on levels of intracellular BCG. 109

Figure 4.8 The effect of Tubastatin A on MHC expression and intracellular BCG load. 110
Figure 5.1 Construction and confirmation of each antigen insert. 126
Figure 5.2 Immunisation layout and MGIA preparation. 128
Figure 5.3 TTD values of mycobacterial growth as measured by MGIA. 130
Figure 5.4 Detection of expressed antigens. 131
Figure 5.5 TTD values of mycobacterial growth by MGIA. 133
Figure 5.6 Intracellular cytokine staining in CD4+ T cells. 136
Figure 5.7 Intracellular cytokine staining for CD8+ T cells. 137
Figure 5.8 Cytokine secretion measured by ELISpot. 138
Figure 5.9 metE-specific antibody titres measured by ELISA. 142

LIST OF ABBREVIATIONS

AMI	antibody-mediated immunity
AS	absorbance summation
BAL	bronchoalveolar lavage
BCG	Bacille Calmette-Guérin
BSL3	biosafety level 3 laboratory
CAF01	cationic adjuvant formulation
CFUs	colony forming units
CIITA	class II transactivator
CLRs	c-type lectin receptors
CMI	cell-mediated immunity
CPI	correlations of protective immunity
CR	complement receptor
dBCG	of disseminated bcg infection
DCs	dendritic cells
DC-SIGN	dc-specific intercellular adhesion molecule-3 grabbing nonintegrin
DosR	dormancy survival regulator
ELISA	enzyme-linked immunosorbent assay
ELISpot	the ifnγ enzyme-linked immunospot
ET	endpoint titre
FcγRIII	specific fc receptors
GFP	green fluorescent protein
HDAC	histone deacetylase
HIV	human immunodeficiency virus
HLA	human leukocyte antigens
HNP	human neutrophil peptide
ICS	intracellular cytokine staining
IEDB	immune epitope database
IFNγ	interferon-gamma
Ig	immunoglobulin
IgGκ	immunoglobulin kappa
IGRA	ifnγ release assay
IL	interleukins
IP	immunoprecipitation
LC-MS-MS	tandem mass spectrometry
LTBI	latent tb infection
M1	pro-inflammatory macrophages
M2	anti-inflammatory macrophages
MAIT	mucosal-associated invariant t
MARCO	macrophage receptor with collagenous structure

MDR-TB	multidrug-resistant tb
MGIAs	mycobacterial growth inhibition assays
MGITs	mycobacterial growth indicator tubes
MHC	major histocompatibility complex
MHC-I	mhc class I
MHC-II	mhc class II
MOI	multiplicities of infection
MPS	mononuclear phagocyte system
MTB	*Mycobacterium tuberculosis*
MTBC	*Mycobacterium tuberculosis* complex
NC3Rs	national centre for replacement, refinement and reduction of animals in research
NCRs	natural cytotoxicity receptors
NHP	non-human primate
NK	natural killer
NKT	natural killer t cells
NLRs	nod-like receptors
NO	nitric oxide
OD	optical density
PBMCs	peripheral blood mononuclear cells
PBS	phosphate-buffered saline
PCR	polymerase chain reaction
PD-L1	programmed death ligand 1
POD	prevention of disease
POI	prevention of infection
POR	prevention of recurrence of tb
PPD	to tuberculin-purified protein derivative
PRRs	pattern recognition receptors
QFT	QuantiFERON tb gold in-tube test
RDs	regions of difference
ROS	reactive oxygen species
TB	tuberculosis
TCRs	t-cell receptors
Th1	cd4+ type-1 t helper cells
TLRs	toll-like receptors
TNFα	tumour necrosis factor-alpha
Tregs	regulatory t cells
TST	tuberculin skin tests
TTD	time to detection
WHO	world health organisation
WT	wild-type
αβ T cells	alpha beta t cells
γδ T cells	gamma delta (γδ) t cells

ACKNOWLEDGEMENTS

I was lucky enough to receive a full scholarship from King Khalid University, Saudi Arabia, to pursue a doctoral study at the University of Oxford, UK, and to be surrounded by wonderful people in both institutions.

First, I am incredibly grateful to my supervisors, who are among the significant figures in my life. Prof. Helen McShane, Dr. Nicola Ternette, Dr. Paulo Bettencourt and Dr. Iman Satti have provided invaluable advice and continuous support throughout my DPhil research. Their knowledge and vast expertise have inspired me throughout all the stages of my studies. I could not have undertaken this journey without all of you; many thanks.

Also, I would like to extend my sincere thanks to both Dr. Elena Stylianou for her consistent support and contribution while running animal experiments and Dr. Annalisa Nicastri for helping with the performance of immunopeptidomics experiments. Their input was critical and highly appreciated.

Further, I would like to thank the members of the TB group (Dr. Rachel Tanner, Marcellus Korompis, Shuailin Li and Marco Polo Peralta Alvarez) and antigen discovery group (Dr. Rebecca Doherty, Dr. Hanqing Liao and Dr. Robert Parker), who have been willing and enthusiastic to assist in any way, mainly when I performed extensive experiments, and they supported my research efforts.

My appreciation and thanks also go to Jennifer Yeulet for her outstanding efforts in organising all the meetings and liaising over administrative tasks.

Finally, words cannot express my gratitude to the most influential people in my life, my family. My prayers and great gratitude to my parents for their patience, wisdom and encouragement at all the stages of my life, and to my beloved wife (Thikra), who has endured my burdens, stood by me and supported me all the time to achieve my dreams. Thanks to them, my study was a fantastic journey.

Chapter 1

Introduction

1.1 Background

Since ancient times, tuberculosis (TB) has infected humans and caused significant morbidity and mortality worldwide. The control of TB was revolutionised by the discovery of the aetiological agent of TB, *Mycobacterium tuberculosis* (MTB), by Robert Koch in 1882 (1). A century ago, another significant breakthrough in the prevention of TB occurred with the development of the first TB vaccine, named the Bacille Calmette-Guérin (BCG) vaccine, by Albert Calmette and Jean-Marie Camille Guerin in 1921 (2). Since then, BCG has remained the only clinically used vaccine despite the variable levels of protection it provides (3) and the huge efforts that have been made to develop a more efficacious vaccine (4, 5), which are discussed later in this chapter.

TB was the first infectious disease to be declared a global emergency by the World Health Organisation (WHO), which occurred in 1993 (6). Since then, global efforts have led to a reduction in TB incidence of about 2% annually, but this disease is still considered a global health issue. According to the WHO's 2021 global TB report, TB was responsible for the death of 1.5 million people in 2020, 14% of whom were co-infected with human immunodeficiency virus (HIV); in the same year, nearly 10 million people became ill with TB, of whom 1.1 million were children (7). An individual with active TB is estimated to infect between five and 15 others over 12 months. If untreated, almost all HIV-positive people and approximately 45% of HIV-negative people with TB die. Additionally, the continuing spread of multidrug-resistant TB (MDR-TB) is of clinical concern, with over half a million cases of MDR-TB developing every year (8).

1.2 Immunopathogenesis of TB

Mycobacteria are aerobic, slow-growing bacteria with the ability to survive and replicate within phagocytes. They are rod-shaped bacilli (0.2–0.5 μm in width and 2–4 μm in length) and with cell walls rich in lipids (1, 9). Human TB can be caused by any member of the *Mycobacterium tuberculosis* complex (MTBC), but mainly by MTB and occasionally by *Mycobacterium africanum* and *Mycobacterium bovis* (10). TB is transmitted upon inhalation into the airways of aerosolised droplets that carry live mycobacteria. Invading mycobacteria are encountered by alveolar macrophages, which internalise them. Once internalised, MTB starts to release virulence factors, through the actions of which the bacteria can avert intracellular killing mechanisms, reside, replicate, and eventually evade the detection of immune cells. It is estimated that between 5% and 10% of those exposed to MTB develop active TB, while the rest clear the infection or contain the disease in the form of latent TB infection (LTBI) (11). According to a systematic review and meta-analysis, a quarter of the world's population is estimated to have LTBI (12), which can progress to active TB if carriers have compromised immune systems or as they age (13).

1.3 Natural immunity to TB

1.3.1 Innate immunity

Some infected people show no T-cell response or symptoms of TB. From this discovery, we can deduce that innate immune cells can clear TB before adaptive immune cells become involved. The mononuclear phagocyte system (MPS),

neutrophils and natural killer (NK) cells in innate immune cells play a central role in early defence mechanisms against TB. The MPS is composed of monocytes, macrophages, and dendritic cells (DCs), which share two phenotypes, high expression of pattern recognition receptors (PRRs) and efficient presentation of antigens (14). PRRs help immune cells to recognise mycobacteria as non-self-antigens and to initiate the immune response. Our understanding of the role of human immunity to MTB is based on inferences from studies of animal models of MTB infection and from analysis of human immune cells that are isolated from the blood or bronchoalveolar lavage (BAL) of infected people.

Macrophages recognise MTB initially via PRRs. These include nod-like receptors (NLRs), C-type lectin receptors (CLRs) and toll-like receptors (TLRs) (15). These receptors activate signalling pathways, which release various chemokines and cytokines, which in turn activate the recruitment and proliferation of immune cells (16, 17). The amounts of neutrophils, DCs and NK cells are found to increase up to 30-fold at the infection site (18). Upon *in vitro* infection of macrophages, mycobacteria have been reported to be phagocytosed by alveolar macrophages via complement receptor (CR) 4 (CR4) and by blood monocytes via CR1, CR3, and CR4 (19). Subsequently, macrophages employ multiple bactericidal processes to eliminate engulfed mycobacteria. These processes include phagosome-lysosome fusion (20), reaction with reactive oxygen species (ROS) (21), cathelicidin LL-37 expression (22), autophagy (23) and apoptosis (24).

Macrophages up-regulate and release specific cytokines and chemokines according to their pro-inflammatory (M1) or anti-inflammatory (M2) phenotypes. Polarisation into these phenotypes is triggered according to the virulence of

mycobacteria. For instance, macrophages infected with virulent MTB (H37Rv) differentiate into the M1 population, whereas avirulent MTB (H37Ra) induces M2 differentiation (25). M1 macrophages are characterised by efficient antigen presentation and are microbicidal, releasing specific proinflammatory cytokines such as the interleukins (IL) IL-1β, IL-6, IL-23 and tumour necrosis factor-alpha (TNFα) (26). However, it has been found that, over time, infected M1 macrophages undergo polarisation towards the M2 population, which is characterised by poor antigen presentation that leads to release of the anti-inflammatory cytokine IL-10 (27). Alveolar macrophages characterised by M2 phenotype are reported to present a niche for MTB proliferation (28). T cells play a central role in the subset polarisation of macrophages, as type-1 T helper (Th1) releases interferon-gamma (IFNγ), which induces the M1 macrophages, and Th2 releases IL-4, which induces the M2 macrophages (29).

Neutrophils are the most abundant innate cells found at the MTB infection site but are poorly understood, owing to their short-lived state and our inability to cryopreserve them (30). Neutrophils are recruited in response to the production of cytokines and inflammatory signals (TNF-α, IL-6, and IL-1β) when MTB escapes macrophage resistance and reaches the pulmonary interstitial tissue (31). In patients with active TB, blood neutrophil levels are higher than in healthy individuals; conversely, those with high levels of blood neutrophils have been reported to be less likely to develop TB (32). However, according to a whole-blood transcript signature analysis, which has been used to compare patients with TB and healthy subjects, neutrophils play a role in TB pathogenesis via expression-type-1 IFN-αβ (33). In this study, neutrophils isolated from TB patients were associated

with over-expression of type-1 IFN-αβ-inducible transcripts compared with the uninfected subjects, and the levels of over-expression were correlated with the severity of the disease. In a similar study, neutrophils isolated from TB patients were associated with expression of the programmed death ligand 1 (PD-L1) (34), which was reported to inhibit T-cell proliferation during MTB infection (35). Anti-mycobacterial effects of neutrophils involve respiratory burst and the release of cathelicidin LL-37 (36) and of human neutrophil peptide (HNP)-1 (37), which restrict mycobacterial replication. Although neutrophils are essential frontline antimicrobial cells, they may cause chronic inflammation and tissue damage as a result of their intensive response, which has been shown to facilitate MTB pathogenesis (38). The dual action of neutrophils poses a challenge to interpretation and correlation of their desirable functions against MTB infection.

NK cells mediate an innate immune response directly via the lysing of infected cells or indirectly by releasing cytokines, such as IFNγ. Natural cytotoxicity receptors (NCRs), e.g. NKp44, can recognise and bind to mycobacterial peptidoglycan (39). NKp46 can also bind to vimentin molecules, which are up-regulated upon H37Ra infection compared with uninfected monocytes. This binding causes cell lysis (40). This action can be reversed by the addition of anti-vimentin, which prevents NK cells from lysing infected cells. Upon analysis of a cohort study, patients with LTBI showed higher percentages of immune-effector cells, including NK cells, and greater rates of cytotoxic responses compared with those in healthy controls (41).

DCs mediate the interaction between innate and adaptive immune cells via antigen presentation (42). This vital function reveals the inhibitory role mediated by DCs

against TB, as evidenced by the experiment in which the depletion of DCs resulted in CD4+ T cells being unable to suppress MTB infection (43, 44). DCs recognise mycobacterial components, such as lipoarabinomannan, via the actions of DC-specific intercellular adhesion molecule-3 grabbing nonintegrin (DC-SIGN) (45). Upon phagocytosis of mycobacterial agents, DCs undergo a transformation from being highly phagocytic and poorly antigen-presenting cells (immature state) into less phagocytic and efficiently antigen-presenting cells (mature state). This transformation enables DCs to migrate into lymph nodes and prime naïve T cells (46). DCs devoid of the p40 subunit of IL-12, which is shared with IL-23, have been found to be unable to migrate and initiate cellular responses at lymph nodes, indicating the crucial role of IL-12 in facilitating migration (47). CD13, or aminopeptidase N, located on the cell surface, has been reported to be highly expressed on THP-1-derived DCs infected with heat-killed MTB, and able to bind to live mycobacteria (48). Additionally, the presence of CD13 may affect the T-cell response, as it is involved in major histocompatibility complex (MHC) peptide presentation by DCs (49). This involvement was observed when CD13 knock-out mice showed more activation of CD8+ T cells upon ovalbumin stimulation than wild-type (WT) mice (50). In this study, CD13KO DCs were distinguished by dysregulation of endocytic regulators such as p38MAPK and Akt, which indicated that CD13 was necessary for endocytic uptake.

Innate immune T cells can be divided into two main populations: gamma delta (γδ) T cells and unconventional alpha-beta (αβ) T cells. These cells can recognise antigens that are not presented by MHC molecules, i.e. non-peptidic antigens, which

are presented by the monomorphic MHC class Ib and MHC class-I-like molecules (51).

The γδ T cells account for between 0.5% and 16% of CD3+ lymphocytes in the circulation or peripheral lymphoid tissues (52). Sub-populations of γδ T cells are categorised based on the variable region of the T-cell receptors (TCRs); for example, the Vδ2+ subset forms 90% of γδ T cells in the circulation and is usually associated with Vγ9 (53). Another subset (Vδ2+ Vγ2+) has been found in macaque models to expand after BCG vaccination and to contribute to protection upon MTB challenge (54). Consistent with this, a study reported that individuals vaccinated with BCG showed activation and expansion of γδ T-cells, whereas unvaccinated people did not (55). The researchers also showed that stimulation of peripheral blood mononuclear cells (PBMCs) that had been taken from BCG-vaccinated individuals and but lacked γδ T cells resulted in poor stimulation of CD4+ and CD8+ T cells. This finding indicated that γδ T cells were involved in the proliferation of αβ T cells. It has been previously reported that γδ T cells function as antigen-presenting cells and are able to activate naïve αβ T cells through antigen presentation and co-stimulation (56).

Because γδ T cells express various types of PRRs, they can recognise a wide range of ligands and γδ TCR-restricted ligands, including MTB-derived phospho-antigens (57). Also, mycobacterial heat shock protein (hsp) 65 has been shown to be a ligand for γδ T cells in mice (58) and humans (59) When activated, γδ T cells produce certain cytokines, including TNF-α, IFNγ, and IL-17 (60). A study found that the maturation of DCs was mediated upon co-culturing with pre-activated γδ T cells via the release of TNF-α and IFNγ cytokines (61). Compared to mice or humans, cattle

have a larger number of circulating γδ T cells; they constitute up to 70% of blood lymphocytes in young animals and decrease as the animal ages to about 20% in adults (62). These cells play a crucial function in bovine immunity to pathogens, including bovine TB, which are an attractive target in vaccination strategies (63). Collectively, γδ T cells contribute to TB immunity as they interact directly with MTB and provide effector functions for other immune cells as they release cytokines and present mycobacterial antigens.

Unconventional αβ T cells are composed of two major subsets, mucosal-associated invariant T (MAIT) cells and invariant natural killer T (iNKT) cells. MAIT cells are tissue-resident cells that comprise 10-20% of the total T cells in the lungs (64). They recognise ligands bound to MHC-like molecule MR1, such as riboflavin, microbial-derived vitamin B2-based metabolites (65). When MAIT cells isolated from active TB patients were stimulated, they produced lower levels of IFNγ than did MAIT cells isolated from either those with LTBI or healthy individuals (65). In this study, down-regulation of the genes encoding for proinflammatory cytokines (IFNγ, TNF-α and IL-17F) was observed in MAIT cells taken from patients with active TB. Also, the frequency of production of MAIT cells was higher in individuals with LTBI than in individuals with active TB or in healthy subjects (66). In mice, aerosol infection with BCG vaccine resulted in a higher burden of mycobacteria in those animals that lacked MR1 compared with WT mice. These findings indicated the vital role of MAIT cells in early host defence against mycobacterial infection (67). Moreover, during chronic MTB infection, MAIT cells were found to exert therapeutic functions as they reduced mycobacterial loads when stimulated exogenously with a riboflavin metabolite (68).

The iNKT cells recognise glycolipids that are presented by CD1 molecules. Several studies have shown that iNKT cells inhibit MTB growth in infected macrophages due to their ability to release antimicrobial peptide granulysin and IFNγ (69-71). In mice, after MTB infection, Behar et al., (1999) found that animals that lacked CD1 receptors showed no difference in bacterial burden compared with the wild-type animals. In the same study, it was found that mice devoid of transporter associated with antigen processing (TAP) protein complex, which is essential for peptide presentation to MHC-I molecules, were more susceptible to infection and exhibited a higher bacterial burden than did control mice (72). However, when MTB-infected mice were administered external iNKT cells that had been obtained from naïve mice, the bacterial load was reduced in the lungs and spleens of recipient mice (69). It is possible that the absence of iNKT cells or their low number is not enough to offer protection against MTB infection but that when they are supplied in sufficient quantity, they provide protection (73). In humans, reports have been published that show different results regarding NKT-cell numbers in patients with TB. Some studies indicated that levels of NKT cells were significantly higher in patients with TB (74), contrary to others, which reported a decrease or no differences between patients with TB and healthy controls (75, 76). Such conflicting data provide no conclusive evidence on the contribution of iNKT cells to protection against pulmonary TB, which could be due to their relative scarcity.

1.3.2 **Adaptive immunity**

Adaptive immunity involves recruitment of immune cells to produce specific responses against mycobacteria in the form of mycobacteria-specific T cells and

antibodies (B cells) to augment the innate elimination of MTB infection. Since MTB resides and replicates intracellularly, mainstream attention has been on the study of cell-mediated immunity (CMI), with little focus on the role of B-cell- and antibody-mediated immunity (AMI) (77).

1.3.2.1 T-cell response

The importance of CMI to TB, which is mediated predominantly by a CD4+ T-cell response, has been manifested in HIV patients, who suffer from a reduction in CD4+ T-cell numbers and are at high risk of MTB infection or reactivation of LTBI (78, 79). Additionally, a significant dysfunction of mycobacteria-specific CD4+ T cells in HIV-positive individuals has been observed upon analysis of cytokines secreted by polyfunctional T cells, IFNγ, TNF-α, and IL-2, compared with HIV-negative individuals (80). In animal models, MTB growth was controlled in WT mice 20 days post-infection, whereas mice that lacked αβ T cells (CD4+) died after bacterial growth continued unchecked (81). Unlike B cells or γδ T cells, αβ T cells (CD4+ and CD8+) are primed and activated via recognition of antigenic peptides presented by MHC molecules (82). Antigen-presenting cells, particularly DCs, mediate the initiation of the T-cell response via the presentation of mycobacterial antigens on MHC molecules. CD4+ T cells recognise peptides that are presented by MHC class II (MHC-II), and CD8+ T cells recognise peptides presented by MHC class I (MHC-I).

In MTB infection, CD4+ T cells release more of the pivotal cytokine IFNγ than CD8+ T cells (cytotoxic T cells), which in part is due to the exposure of a wide array of mycobacterial antigens to CD4+ T cells (83). Consistently, upon analysis of human T-cell responses in people with LTBI, mycobacterial antigens have been recognised predominantly by CD4+ T cells (84). In mouse models, the control of MTB infection

has been shown to be reliant on IFNγ-dependent CD4+ T-cell response (85), but CD4+ T cell mediated resistance to infection was reported to occur independently of the presence of IFNγ, i.e. through nitric oxide (NO) production (86). This indicates that different subsets of CD4+ T cells are capable of activating bactericidal molecules, such as NO, independently of the IFNγ pathway. The subsets of CD4+ T cells include Th1, Th2, Th17, and regulatory T cells (Tregs), in which each subset is distinct in its functionality and production of cytokines.

Once CD4+ T cells have been primed, they migrate to the infection site to aid infected cells, particularly macrophages, to control MTB infection. The response of CD4+ T cells and their differentiation, to some extent, relies on the initial activation that takes place at the lymph nodes and, subsequently, on which cytokines are released in the milieu when the CD4+ T cells reach the site of infection (87, 88). Also, CD4+ T cells contribute to the cytotoxic effects of CD8+ T cells, as mice that lack CD4+ T cells have been shown to exhibit impaired cytotoxic abilities of CD8+ T cells despite the releases of cytokines (89). The risk of TB disease has been reported to be associated with the production of a subset of activated HLA-DR+ CD4+ T cells after BCG vaccination (90). This is consistent with studies that evaluated levels of circulating CD4+ T cells in patients with active TB. In these patients, HLA-DR expression by CD4+ T cells was considered as a marker of TB progression, as patients with active TB showed higher levels of HLA-DR+ CD4 T cells than did people with LTBI (91-94).

The two subsets of CD4+ T-helper cells (Th1 and Th17) play the central role as effector T cells in protection against TB (88). Upon activation, Th1 cells that are known as polyfunctional Th1 cells can stimulate action by macrophages and other immune cells by the simultaneous release of multiple cytokines (IFNγ, TNF-α and

IL-2) (95). Polyfunctional Th1 CD4+ T cells have been reported to be greater in number in people with LTBI and this increase occurs after the treatment of active infection (96), suggesting a protective role. Another study has shown the opposite; polyfunctional Th1 T cells were associated more with active TB than with LTBI (97). A study in South Africa found no correlation in terms of protection against TB upon analysis of the cytokine profile of mycobacteria-specific T cells and their incidence in newborns vaccinated with BCG (98). Such a discrepancy indicates the need to consider other immune mechanisms, which may be linked to protection (98, 99).

Th17 cells are special CD4+ T-helper cells that produce the proinflammatory cytokine IL-17. This cytokine can stimulate the production of various immune cells, including macrophages, DCs, and B and T cells. Interestingly, IL-17 has been reported to mediate potent immunity to a virulent clinical isolate of mycobacteria (CDC1551) but to play a non-essential role in immunity against the lab strain H37Rv (100). This study found that IL-17 was induced via the TLR-2 and IL-1β signalling pathway, as confirmed upon infection of mice devoid of IL-1β receptors with CDC1551 mycobacteria. The result was a significant reduction in the number of IL-17-producing T cells and uncontrolled mycobacterial growth. Analysis of peripheral blood indicated that IL-17 was produced by a specific subset of CD4+ T cells (>20%) in healthy individuals compared with people with active TB, who showed a lower incidence of the same subset (101). However, the Th17 subset that dually expressed IL-17 and IFNγ was reported to be associated with the severity of infection in patients with active TB (102). IL-17 and IFNγ are potent proinflammatory cytokines that aid in protective immunity to TB, but a prolonged proinflammatory response may exacerbate inflammation.

The contribution of CD8+ T cells to immunity against TB is attributed to two effector roles: the ability to produce proinflammatory cytokines, including IFNγ and TNF-α, and their cytotoxic effects. The latter role is mediated by the release of perforin (103) and granulysin (104), by which CD8+ T cells can kill infected macrophages and intracellular MTB, respectively. CD8+ T cells can recognise mycobacterial antigens presented by airway epithelial cells via MHC-I molecules (105). These cells first encounter invading MTB and become a niche for mycobacteria (106), indicating the unique role of CD8+ T cells in early host defence, particularly for cells that are restricted to MHC-I presentation.

1.3.2.2 Antibody response

Cumulative evidence indicates that AMI contributes to some extent to immunity against TB. A study has reported that antibodies in people with active TB show distinctive characteristics compared with antibodies in people with LTBI in terms of Fc receptor binding and glycosylation (107). A recent study showed that the total immunoglobulin (Ig) G that could be purified from plasma obtained after BCG vaccination mediated significantly the opsonisation of mycobacteria by macrophages, compared with the total IgG obtained prior to vaccination (108). This indicates a functional role for antibodies induced by BCG in the control of mycobacteria via phagocytosis. MVA85A was a vaccine that was tested as a possible booster for the BCG vaccine. During its phase IIB efficacy trial, an immune correlate of risk analysis of samples found that Ag85A-specific IgG was associated with a reduced risk of the development of TB in BCG-vaccinated infants (90). All these studies suggest the involvement of humoral responses against TB.

IgA1 and IgG have been found to inhibit and enhance MTB phagocytosis, respectively, in A549 human lung epithelial cells (109). IgG obtained from post-vaccination sera has also been reported to enhance MTB phagocytosis and subsequently reduce growth in macrophages of the human leukaemia monocytic cell line THP1 (110). Antibodies from people with LTBI have been found to enhance the microbicidal activity of internalised MTB compared with antibodies from patients with active TB (107). This microbicidal activity mediated by antibodies obtained from LTBI was attributed to their glycosylation patterns and selective binding to FcγRIII receptors.

1.3.3 **Granuloma**

In response to MTB infection, immune cells, including macrophages and B and T lymphocytes, aggregate at the infection site to form granulomas that contain MTB. However, MTB switches to a dormant state within lung granulomas to resist immune clearance. This process results in the development of LTBI (111). The risk of activation of LTBI to TB means that approximately 5-10% of latently infected people will develop TB within two years of infection and the risk for the rest increases over the rest of their lifetimes by 5% (112). Two mechanisms have been proposed to be associated with LTBI reactivation: dysfunction of CD4+ T cells and neutralisation of TNFα (113). Dysfunction of CD4+ T cells qualitatively and quantitatively is associated with the reactivation of LTBI, which is clearly seen after HIV infection, in which case MTB-specific CD4+ T cells are found to be depleted preferentially (78, 114). This enables the dissemination of MTB from granulomas. Similarly, the inhibition of TNFα by anti-TNF antibodies such as infliximab is

associated with an increased risk of LTBI reactivation (115-117). This inhibition has been reported to cause CD4+ T-cell deficits and disturbance of IFNγ production (118, 119).

1.4 Vaccines for TB

BCG remains the only licensed vaccine against TB, but it offers little to no protection against TB in older children and adults compared with newborns and infants, in whom it offers protective efficacy of 50-80% (120). Additionally, because it is a live mycobacterial vaccine, there is a high risk of disseminated BCG infection (dBCG) in immunocompromised children such as those who are HIV positive (121). Therefore, the Global Committee on Vaccine Safety (122) and the WHO (123) do not recommend the administration of BCG vaccine to HIV-infected or exposed infants. Due to these concerns, a new vaccine with higher rates of protective efficacy and safety is needed. In response to this, huge efforts have been devoted to the development of new strategies to produce TB vaccines.

Two main types are under consideration - whole organism BCG replacements, and subunit BCG boosters, which use a variety of delivery systems. These vaccines have been designed for use prophylactically or therapeutically according to the status of MTB exposure and TB progression as follows:

- in healthy individuals with no history of MTB exposure (IFNγ release assay (IGRA)-negative), vaccines are administered for the prevention of infection (POI) and/or prevention of disease (POD);
- in individuals with LTBI (who are IGRA-positive but have no symptoms), vaccines are given for POD;

- in individuals with a history of TB disease but who have been treated, vaccines are given for prevention of recurrence of TB (POR); and
- in individuals with active TB, therapeutic vaccines are administered (124, 125).

Two vaccines (VPM1002 and MTBVAC), which are live-attenuated, have been developed for infants and neonates, while all subunit vaccines have been investigated in adolescents and adults. A practical advantage of subunit vaccines is that they do not pose the safety and manufacturing concerns that whole-cell vaccines do (126).

Since I aim in my work to develop subunit vaccines, here I shed more light on this type. In 2012, the MVA85A vaccine was the first candidate TB vaccine to undergo clinical evaluation as a BCG-prime boost in infants (127). Since then, 14 candidate vaccines have passed through different phases of clinical trials (Table 1.1), but none has reached the market yet (124). More than 50% of the vaccines currently in clinical trials are subunit vaccines that were designed as adjuvant proteins (M72:ASO1, GamTBVac, H56:IC31, ID93:GLA-SE, and AEC/BC02) or viral vectored proteins (Ad5Ag85/MVA85A and TB/FLU-04L) (128). M72/AS01E is the most advanced subunit vaccine. It is composed of two fused MTB antigens (MTB32A and MTB39A) and is given with the AS01 adjuvant (129). Of subunit vaccines, M72/AS01E and H4:IC31 have been assessed for their protective efficacy (phase 2b). According to the final results, M72/AS01E confers 49.7% protection, i.e. it was found during the trial to prevent the development of active pulmonary TB by about 50% in IGRA-positive subjects (130). In IGRA-negative individuals, the H4:IC31

vaccine after trial was reported to provide protection of 34.2% (P=0.11), which was not significantly different from that offered by the placebo (P=0.16) and compared unfavourably with the 45.4% protection provided by the BCG (P=0.03). In these studies, the QuantiFERON TB Gold in-tube test (QFT) conversion was used to indicate the acquisition of MTB infection (131). The efficacy results for M72/AS01E and H4:IC31 vaccines could not be compared because they were tested in different ways: M72/AS01E was given to target the POD, which was evaluated through the analysis of bacteriologically confirmed pulmonary TB via polymerase chain reaction (PCR) assay and liquid culture of MTB; whereas H4:IC31 targeted the POI, which was assessed by testing MTB exposure via the use of the QFT. The other subunit vaccines have completed phase 1 trials with acceptable safety and immunogenicity profiles (132-136), except AEC/BC02 (ClinicalTrials.gov Identifier: NCT04239313) and TB/FLU-04L (ClinicalTrials.gov Identifier: NCT02501421).

Table 1.1 *Summary of the vaccines currently in clinical trials, adapted from the Tuberculosis Vaccine Initiative (137) and (127).*

Vaccine Type		Vaccine candidate	Composition	Indication	Clinical phase
Whole vaccines	**Live-attenuated**	VPM1002	Recombinant BCG expressing listeriolysin and deficient in urease	Prophylactic (infants & neonates)	Phase 3
				Prophylactic (adolescents & adults)	Phase 3
				Therapeutic	Phase 3
		MTBVAC	Attenuated MTB	Prophylactic (infants & neonates)	Phase 2a
				Prophylactic (adolescents & adults)	Phase 2a
		BCG	BCG	Prophylactic (adolescents & adults)	Phase 2b
	Dead/inactivated	MIP Immuvac	Heat-killed *Mycobacterium indicus pranii*	Prophylactic (adolescents & adults)	Phase 3
				Therapeutic	Phase 3
		M. vaccae (DAR-901)	Heat-killed *Mycobacterium vaccae*	Prophylactic (adolescents & adults)	Phase 3
		RUTI	Detoxified and fragmented *M. tuberculosis* cells	Therapeutic	Phase 2a

Vaccine Type		Vaccine candidate	Composition	Indication	Clinical phase
Subunit vaccines	**Adjuvanted protein(s)**	M72:ASO1	MTB32A and MTB39A adjuvanted with 3-O-desacyl-4'-monophosphoryl lipid A (MPL) and the saponin QS-21	Prophylactic (adolescents & adults)	Phase 2b
		GamTBVac	Ag85A, early secreted antigenic target (ESAT)-6 and culture filtrate protein (CFP)-10 as an adjuvant with diethylaminoethyl (DEAE)-dextran core and unmethylated cytosine-phosphate-guanine (CpG) oligodeoxynucleotides	Prophylactic (adolescents & adults)	Phase 2a
		H56:IC31	Ag85B, ESAT-6 and Rv2660c adjuvanted with 11-mer antibacterial peptide and a synthetic oligodeoxynucleotide (ODN1a)	Prophylactic (adolescents & adults)	Phase 2b
				Therapeutic	Phase 1
		ID93:GLA-SE	Rv2608, Rv3619, Rv3620 and Rv1813 adjuvanted with TLR4 agonist glucopyranosyl lipid (GLA) formulated in a squalene-in-water emulsion (SE)	Prophylactic (adolescents & adults)	Phase 2a
				Therapeutic	Phase 1
		AEC/BC02	Ag85A and ESAT-6 as an adjuvant with CpG DNA fragment and aluminium salt	Prophylactic (adolescents & adults)	Phase 1
	Viral vectored protein(s)	Ad5Ag85	Ag85A expressed by human adenovirus serotype 5 vector	Prophylactic (adolescents & adults)	Phase 1
		ChadOx1.85/MVA85A	Ag85A expressed by simian adenovirus vector and modified vaccinia Ankara virus vector	Prophylactic (adolescents & adults)	Phase 1
		TB/FLU-04L	Ag85A and ESAT-6 expressed by replication-deficient attenuated influenza virus mucosal vector	Prophylactic (adolescents & adults)	Phase 2a
				Therapeutic	Phase 2a

1.5 Novel antigen discovery

Unlike TB candidate vaccines, most licensed and clinically used vaccines have been developed and evaluated on the basis of induction of functional antibodies (138). This shows the main challenge that faces the development of effective vaccines for TB. Firstly, their efficacy does not rely significantly on antibody induction; secondly, there are no defined correlations of protective immunity (CPI) that can be utilised during vaccine evaluations. Moreover, mycobacteria express about 4000 proteins (139); identification and selection of protective antigens, therefore, requires massive effort. Only 13% of the total number of antigens with T-cell epitopes have been characterised, according to the immune epitope database (IEDB, accessed in Dec 2021), so about 87% of potential antigens remain unexplored.

Traditionally, the selection of candidate antigens has been undertaken by testing the T cell cytokine profile of the secreted or most expressed mycobacterial proteins through the use of IFNγ release assays based on animal or human samples exposed to MTB infection or BCG vaccination (140). This has led to the identification of several antigens, such as Ag85A (Rv3804c) (141), PepA (Rv0125) (142) and PPE18 (Rv1196) (143), which have been developed and tested in clinical trials as candidate TB vaccines. MVA85A was the first candidate vaccine to be evaluated in clinical trials. It was administered as a viral vector that expressed antigen Rv3804c (144). The leading subunit vaccine, M72/AS01, is composed of two fused antigens (Rv0125 and Rv1196), and when it was evaluated in a phase 2B efficacy trial in subjects with LTBI, it achieved 49.7% efficacy in the prevention of pulmonary TB (145).

Another approach to antigen discovery is based on metabolic and disease-stage-specific antigens. The aim is to identify those mycobacterial proteins associated with a particular stage of MTB infection, called latency-associated antigens (146, 147). When immune cells contain MTB infection, to ensure its survival, MTB adapts from a replicating to a non-replicating state (i.e. by entering dormancy or latency) via genes that are responsible for the activation of a dormancy survival regulator (DosR) (148, 149). This approach has inspired some researchers to identify 25 latency-associated antigens that are able to induce T-cell IFNγ responses. They have used PBMCs isolated from people with active TB and who showed positive tuberculin skin tests (TST+), as well as healthy controls (150). One of these 25 antigens (Rv1733c) was tested by another group, which reported that synthetic long peptides of Rv1733c conferred protection before and after MTB challenge (151). Also, several latency-associated antigens have been included in various multistage vaccines, such as A1D4 (152) and H56 (153). The latter vaccine is composed of one dormancy antigen (Rv2660c) and two secretory antigens (Rv1886c and Rv3875). It has been formulated with IC31 adjuvant. This vaccine has conferred protection in animal models (153, 154) and reached clinical trials (155, 156).

Advances in genomics and bioinformatics have elucidated how researchers are employing other strategies of antigen discovery, including comparative genomics and immunopeptidomics. The use of comparative genomic analysis enables the identification of regions of difference (RDs) between MTB and BCG strains, and has led to the identification of 11 RDs that are absent in all BCG strains (157). Several studies have been conducted to identify novel immunodominant antigens that are associated with RDs for vaccine developments (158, 159). In these

studies, IFNγ-secreting Th1-cell assays were used to determine potential antigens. The studies led to the identification of PPE68 (RD1), Rv2346c and Rv2347c (RD7), Rv3619 and Rv3620 (RD9) and Rv1966 (RD15) as vaccine candidates for preclinical evaluation.

In the proteomics field, liquid chromatography coupled with tandem mass spectrometry (LC-MS-MS) has revolutionised the quantification and identification of peptides and proteins (160). This system enables the ionisation and fragmentation of peptide sequences based on the mass-to-charge (m/z) ratio. In brief, the mass and the intensity of the ionised precursor peptides are measured (MS1 spectra). Then, the precursor ions are isolated sequentially using a mass filter (usually a quadrupole), and fragmented further in a collision cell to produce product ions, which are then also analysed to determine mass and intensity (MS2 spectra). The MS2 spectra contain the information of fragment masses of each peptide ion species, and therefore the full sequence of the parent peptide ion can be inferred from the information obtained (161, 162).

To measure quantitatively any differences in protein expression among samples, LC-MS/MS is employed to quantify proteins through the application of two main methods: isotope labelling (targeted proteomics) or label-free methods (untargeted proteomics) (163). In the quantification of labelled isotopes, predetermined, stable isotope-labelled peptides are included in the sample, either *in vivo* or *in vitro*. These labelled peptides are used as internal standards to quantify the amounts of specific proteins in the sample. The labelled peptides can be analysed using multiple reaction monitoring (MRM), which involves the detection and quantitation of specific transitions between precursor and fragment ions (164). In contrast, in

label-free analysis, the intensity of the signal from the precursor ion and the chromatographic elution profile is used to compare relative differences in abundance between different conditions. In precursor ion, intensity-based quantification, the maximal peptide intensity or the area under the peptide elution curve defines the relative abundance of the peptide ion, whereas in spectral counting, the number of acquired MS2 spectra for the specific precursor, which correlates with the size of the area under the elution curve, is used to estimate the relative abundance of the peptide in the sample (165). The regarding relative parent protein abundance for determination of regulatory protein abundance ratios between different experimental conditions can then be estimated by summing (or, less common, averaging) either peptide intensities from each ion originating from the parent protein sequence, or the number of MS2 spectra acquired for each peptide derived from the parent protein. These data can then also be used to rank the proteins within a sample by relative abundance, estimating which proteins are most and least abundant in a given sample.

For identification, the raw data obtained from MS/MS spectra can be interrogated to identify peptide sequences via two approaches: a database search or *de novo* sequencing (166). In a database search, experimental MS/MS spectra are compared with theoretical mass spectra that are stored in a database of known peptides or proteins. This enables the identification of peptides or proteins that match the experimental spectra. *De novo* sequencing involves the reconstruction of the amino acid sequence of a peptide from the fragment ions in its MS/MS spectrum without the use of a database. This method is useful to identify novel or unknown peptides that are not present in a database. The accuracy and sensitivity of peptide identification have been enhanced as a result of the combination of the two

approaches in one research tool, such as Peaks DB (167). For each peptide, the similarities between the experimental spectrum and the theoretical spectra are calculated for each peptide-spectrum match (PSM) (168). The PSM scores are used to rank identified peptides and assign a confidence level to each match; the higher the score, the higher the level of confidence. However, to control the number of false discoveries, a decoy database is involved in the analysis to estimate a false discovery rate (FDR). The choice of where to set the FDR threshold is important in order to balance the trade-off between maintaining accurate PSM assignments and minimising the number of false-positive PSMs included in the final list of identifications.

Immunopeptidomics technique offers direct identification of peptides presented by MHC molecules, which enables the discovery of T-cell pathogenic and non-pathogenic epitopes that are associated with various diseases (169, 170). In cancer, the identification of tumour-associated peptides (neoantigens) has facilitated the development of T-cell-based immunotherapy (171, 172). For example, in one study, 41 peptides were identified upon analysis of glioblastoma samples, and the three that occurred most frequently showed specific CD8+ T-cell responses *in vitro* (173). In another study, mutated peptides were identified from tumour specimens taken from patients with melanoma, and when these peptides were tested, the immunogenicity of four of them induced neoantigen-specific T-cell responses (174). For infectious diseases, immunopeptidomics has been employed to identify *Chlamydia*-derived peptides presented by infected mouse DCs (175). In this study, 14 peptides were identified that represented nine *Chlamydia* proteins. These peptides induced IFNγ secretion by CD4+ T cells that had been isolated from

immunised mice, compared with naïve CD4+ T cells. Also, autologous DCs pulsed with identified peptides were found to provide protection *in vivo* against *Chlamydia* infection. Another research group has applied the same approach: they infected mouse DCs with *Salmonella enterica*, which resulted in the identification of 23 and 87 *Salmonella*-derived peptides associated with MHC classes I and II respectively (176). Twelve of these peptides were further evaluated through application of the IFNγ enzyme-linked immunospot (ELISpot) assay, which employed CD4+ T cells from mice infected with *Salmonella.* Four of them induced strong responses compared with the controls.

In the context of TB, Flyer et al. were the first group to employ immunopeptidomics to identify peptides derived from a human cell line infected with mycobacteria (177). They identified several mycobacterial peptides that were associated with HLA-A molecules and which represented three mycobacterial proteins (iniB, hsp65 and glfT2). Since then, several studies have used the same approach and have identified further mycobacterial proteins associated to MHC molecules (178). Upon employment of the immunopeptidomics approach, our group selected three mycobacterial proteins (glfT2, fas, and iniB) and delivered them by viral vectors in a murine aerosol MTB challenge model. Upon evaluation of protective efficacy, the combination of the three antigens showed better protection in the BCG-boost group than did BCG alone (169).

The development of effective vaccines that target T-cell immunity requires the identification of antigens that are robustly presented by MHC molecules, as they are responsible for the presentation of antigens to T cells. However, MHC molecules are highly polymorphic, and each variant presents peptide antigens with different

sequence features. Therefore, different individuals can present different MHC-presented peptide patterns. To overcome the diversity of MHC alleles and ensure that a vaccine can elicit a strong T-cell response in a maximal population, various computational tools are used to predict antigens that will be presented by the most frequently observed MHC alleles. These tools include the NetMHCIIpan server, which has been trained on data obtained from immunopeptidomics (through the use of eluted ligands) combined with MHC-II binding affinity. The use of this server results in more accurate MHC-II peptide prediction for the mapping of CD4+ T-cell epitopes (179). Candidate antigens can be prioritised based on their content of epitopes against the most frequently occurring HLA alleles for *in vivo* evaluation to determine their protective efficacy.

1.6 MHC structure and function

MHC-I presents short peptides (8 to 11 amino acids long) derived endogenously to CD8+ T cells, whereas MHC-II presents longer peptides (10-20 amino acids in length) derived exogenously to CD4+ T cells (170). Unlike MHC-I, MHC-II has a groove with open ends, which enables it to accommodate longer peptides that may extend beyond the groove (180). Structurally, three 'classic' genes (HLA-A, HLA-B, and HLA-C) encode the main subunit (heavy chain) of MHC-I, forming the groove (binding site) for the loading of peptides, whereas the groove of MHC-II is formed jointly as heterodimers of two chains (α and β) encoded by three pairs of genes HLA-DPA1/HLA-DPB1, HLA-DQA1/HLA-DQB1 and HLA-DRA1/HLA-DRB1, and the corresponding DRB3, 4 and 5 genes (180). All HLA genes are inherited together as a group of genes from each parent, so each individual carries two haplotypes, either

homozygous or heterozygous (181). In theory, an individual may inherit and express up to six different forms of MHC-I and up to 12 combinations of MHC-II (182, 183). The β chain of all HLA-II molecules (DR, DP and DQ) and the α chain of DP and DQ are polymorphic. In contrast, the α chain of DR is monomorphic (structurally invariant) and able to pair with any β chain of DRB variants (184).

The sequence of peptides responsible for binding to the groove is called the anchor residue, and the unbound sequence is called the flanking residue. The anchor residue is usually nine amino acids long, but four main positions at the binding site (P1, P4, P6, and P9) determine the association (185). Because the level of polymorphism in the HLA loci is very high, the binding site of the MHC groove is highly diverse. This diversity enables certain HLA alleles to bind preferentially to certain peptide sequences, which maximises their opportunity to recognise diverse pathogen-derived peptides (186).

The molecular expression of MHC is regulated primarily by the class II transactivator (CIITA). The transcription of the CIITA gene is driven by three independent promoters (pI, pIII and pIV) (187). As an example of their roles, pI is responsible for promotion of CIITA in macrophages and DCs. The degree of MHC transcription primarily determines the amount of MHC synthesis and expression on the cell surface (188). Several factors have been shown to influence this transcription, one of which is the signalling that results from toll-like receptors and cytokines, such as IFNγ and IL-10 (189). MTB has been shown to employ different strategies, including suppression of MHC expression and presentation to evade the T cell response (190). Measuring the differential expression of HLA-II proteins and their relative abundance between different conditions is important for

understanding the role of HLA-II alleles in response to infections. However, due to high sequence similarity among HLA-II alleles, mass spectrometry is a powerful tool that can be used to measure their protein levels in a sample accurately by identifying and quantifying the unique peptide(s) representing the allele of interest. In this thesis, I employed LC-MS/MS to quantitate HLA-DR alleles expressed by THP-1 cells via a label-free analysis approach (Chapter 4).

1.7 Animal models

After novel candidate vaccines have been identified, their safety, immunogenicity and protective efficacy are evaluated in animal models. For TB, there is no validated animal model that enables the transition from preclinical to clinical evaluation, and the prediction of protection in humans is poorly correlated with the protection obtained in laboratory animals (191). Three main experimental animal groups are used for the preclinical evaluation of candidate vaccines against TB: small and large mammalian, and invertebrate models (192). The animals most commonly utilised for TB vaccine studies are mice, which are useful for early screening of novel candidate antigens because they are easily handled and are inexpensive. Another advantage of using mice (inbred strains) is that potential genetic factors can be excluded that could otherwise confound the readouts. This enables standardisation between research groups and the performance of reproducible experiments (193, 194). However, it should be noted that mice are not natural hosts of MTB and their immune systems are different to those of humans (192). Moreover, our group has reported that BALB/c and C57BL/6 mice provide variable protection upon vaccination with the same regimen, which involved the boosting of BCG-primed

responses with ChAdOx1.PPE15 (195). That is why the mouse is used as the first of three evaluation models (mouse, guinea pig/rabbit, and non-human primate (NHP) for preclinical studies of any novel TB vaccine. Researchers generally agree that data consistency should be seen between the three models, particularly concerning the evaluation of protective efficacy (196). In order to evaluate protective efficacy, mice are vaccinated first with tested candidate vaccines, and then inoculated with MTB intranasally or by aerosol (*in-vivo* challenge). To be classed as protective, candidate vaccines should reduce the number of MTB colony forming units (CFUs) in the lungs by 0.7 log10 minimum compared with the naïve group, as this reduction can be achieved upon BCG vaccination (193).

1.8 Mycobacterial growth inhibition assays (MGIAs)

MGIAs offer an alternative approach to *in-vivo* challenges for the evaluation of the protective efficacy of a vaccine candidate (197). MGIAs have been employed for preclinical assessment in mice (198-200), cattle (201) and NHPs (202), as well as in clinical trials (203, 204). Principally, the challenge takes place *ex vivo;* immune cells (e.g. PBMCs or splenocytes) are inoculated with a virulent or avirulent mycobacterial strain, and protective efficacy is measured based on differences generated by the immune cells to limit the growth of mycobacteria between vaccinated and unvaccinated samples (205). MGIAs are an efficient tool to screen for protective mycobacterial antigens. Such screening requires 3-5 million splenocytes per subject, so the use of *ex-vivo* techniques offers researchers more options to perform immunogenicity assays that can be correlated with protection (197, 206). Additionally, since the challenge takes place *ex vivo,* MGIAs support the

goals of the National Centre for Replacement, Refinement and Reduction of Animals in Research (NC3Rs) (207). In two matched experiments, the results from the MGIA that used BCG as a challenging agent were comparable with those from in vivo MTB challenge when BCG-vaccinated mice were compared with naïve mice (200). This suggests that the MGIA (ex vivo challenge) can be used as an alternative assay to the in vivo MTB challenge model. In humans, the capacity of whole blood samples from people with active TB, LTBI and healthy people was tested through the use of MGIA. BCG and MTB were found to exhibit comparable results ex vivo, which suggested that BCG could be used as a surrogate for MTB (208). A study examined whether MGIA could discriminate between splenocytes from mice that lacked IFNγ and WT mice (206). In this study, splenocytes from IFNγ-deficient mice showed greater mycobacterial growth than did the cells obtained from the WT animals, which indicated that the MGIA could be utilised to understand the immune mechanisms involved in the control of mycobacterial growth. The assay for use with lung cells was adapted for use in mice, and the MGIA results for cells obtained from the BCG-immunised mouse lungs showed a reduction in mycobacterial growth compared with the naïve mice. This method would be useful in the study of the protection afforded by BCG in a primary TB-infected organ (209). Collectively, MGIAs are a robust tool for the preclinical and clinical evaluation of TB vaccine candidates and they offer advantages of time- and cost-efficiency.

Early screening of candidate vaccines relies on testing the ability of an antigen to elicit an immune response (immunogenicity), which is an important factor in the determination of its potential as a vaccine. However, an antigen that confers immunogenicity may not provide protection against infection; this must be confirmed through the use of an *in vivo* challenge model. Many mycobacterial

antigens have been reported to be immunogenic (210). For example, 94 mycobacterial proteins were tested in the development of new anti-TB vaccines (211). Of these, 68 proteins were found to induce a positive IFNγ response in cells from people with LTBI but not in those from healthy volunteers; 48 of these proteins, which induced the highest IFNγ levels, were selected for *in vivo* MTB challenge in mice. Only six of them were found to reduce the bacterial load (CFU) effectively in the lungs (>0.3 log10), and 12 showed modest CFU reduction (0.1–0.3 log10) compared with naïve mice. These results suggest that, although many proteins may elicit an IFNγ response (and can therefore be said to be immunogenic proteins), they may not be protective and thus may not be suitable as vaccine candidates.

Given that no immune correlates have been established that can be used to predict protection against MTB infection, it is reasonable to start the screening of novel candidate antigens with an evaluation of their protective immunity regardless of cytokine profiles. Since the protective efficacy is determined by the reduction in bacterial load, rather than by measuring immunological markers, MGIAs can be used to predict protective immunity through the measurement of the ability of the host immune cells, such as PBMCs or splenocytes, to control mycobacterial growth when they are co-cultured *ex vivo* (212). In a mouse model, optimised MGIA has been shown to discriminate significantly between unvaccinated and BCG-vaccinated groups, which therefore enables the screening of potential antigens and selection of the protective one (205). Therefore, I employed an MGIA tool to evaluate the protection provided by the candidate mycobacterial proteins (hisD, metE and mmpL12). Then, I selected the most promising candidate for further evaluation, which included immunogenicity.

1.9 Thesis aims

Through the work performed for this PhD, I aimed to identify, select, and evaluate novel mycobacterial proteins with a broad HLA coverage that provided protection in preclinical model systems. To achieve this aim, three objectives were proposed, as outlined below.

1. To identify mycobacterial proteins derived from BCG and MTB *in vitro* through the use of an immunopeptidomics and bioinformatics approach.
2. To screen identified mycobacterial proteins *in silico* through the use of an immunoinformatics tools to prioritise identified mycobacterial proteins.
3. To evaluate the protective efficacy of the selected candidates *in vivo* by application of MGIAs.

To meet the first objective, immunopeptidomics technology has become a robust way to discover MHC-bound mycobacterial proteins. This is because MTB infection is caused by an intracellular pathogen, mediated mainly by cellular immunity, which in turn relies on MHC presentation. To meet the second objective, I employed immunoinformatics tools to shortlist the identified mycobacterial proteins rationally, based on a selection of mycobacterial proteins that provided a broader binding onto the most frequently occurring HLA alleles across populations. For this, I used the netMHCIIpan prediction server (179). To fulfil the third objective, I utilised MGIA, which has become a powerful tool for the evaluation of the protective efficacy of candidate vaccines at preclinical and clinical stages.

Chapter 2

Materials and Methods

2.1 Reagents and solutions

All individual reagents that were used in this project are mentioned in this method section. Working solutions and buffers that were used were prepared as explained here.

- **Lysis buffer** (immunopeptidomics): 1% octylphenoxy poly(ethyleneoxy)ethanol (IGEPAL), 100mM tris(hydroxymethyl) aminomethane buffer (tris), pH 8.0, 300mM NaCl
- **Beads washing buffer**: 50mM borate, 50mM KCl pH 8.0.
- **Washing buffer 1:** 50mM tris, pH 8.0, 150mM NaCl, 5mM ethylenediaminetetraacetic acid (EDTA).
- **Washing buffer 2:** 50mM tris, pH 8.0, 400mM NaCl.
- **Washing buffer 3:** 50mM tris, pH 8.0.
- **Elution solution:** 10% acetic acid.
- **Loading buffer:** 0.1% trifluoroacetic acid (TFA), 1% acetonitrile in ultra-grade (Milli-Q) water.
- **Buffer A:** 0.1% TFA in water.
- **Buffer B:** 0.1% TFA, 60% acetonitrile in water.
- **LC-MS-MS loading buffer:** 0.1% TFA in ultra-grade water.
- **Tris solution (0.4M):** 12.1g tris base dissolved in 200ml Milli-Q H_2O, pH adjusted to 7.8 with 6M HCl and the total volume was brought to 250ml with Milli-Q H_2O.
- **Urea-tris buffer (6M):** 2g urea, 1.25ml 0.4M tris buffer and the total volume was brought to 5ml with Milli-Q H_2O.
- **Reducing solution:** 31mg dithiothreitol (DTT) dissolved in 750µl Milli-Q H_2O + 250µl 0.4M tris buffer.
- **Alkylating solution:** 37mg iodoacetamide dissolved in 750µl Milli-Q H_2O + 250µl 0.4M tris buffer.
- **Protein solubilisation solution:** 6M urea, 100 mM tris-HCl pH 7.4, and 5 mM DTT.

- **Trypsin solution (0.2µg/µl):** 75µl Milli-Q H_2O + 25 µl 0.4M tris buffer (both ice-cold) and 20µg modified trypsin (Promega).
- **Ammonium-chloride-potassium (ACK) lysis buffer:** 8.29g NH4Cl, 1g *KHCO3*, 37.2mg Na2-EDTA in deuterated (d)H_2O, pH 7.2-7.4 adjusted with 1M HCl.
- **Solid growth medium for mycobacteria:** 19.7g Middlebrook 7H10 agar base, 5ml glycerol, 900ml dH20 + 100ml oleic albumin dextrose catalase (OADC) after autoclaving and cooling below 55°C.
- **Liquid growth medium for mycobacteria:** 4.7g Middlebrook 7H09 agar base, 2ml glycerol, 900ml dH20 + 0.05% tyloxapol, 100ml OADC after autoclaving and cooling below 55°C.
- **Cryopreservation medium:** 90% foetal calf serum (FCS) with 10% dimethyl sulphoxide (DMSO).
- **ELISpot colour development buffer**: 5ml deionised water, 200µl of 25x buffer, 50µl reagent A and 50µl reagent B.
- **Flow cytometry staining (FACS) buffer:** (2% foetal calf serum (FCS) in phosphate-buffered saline (PBS) or 1% bovine serum albumin (BSA) in PBS)
- **Complete medium:** Roswell Park Memorial Institute 1640 (RPMI-1640) medium supplemented with 10% filtered, heat-inactivated FCS, 2mM L-glutamine, and 100units/ml (U/ml) penicillin and streptomycin sulphate (pen-strep).
- **Infection medium (antibiotic free):** RPMI 1640 supplemented with 10% filtered, heat-inactivated FCS, 2mM L-glutamine.
- **ELISpot stimulation medium:** Dulbecco's modified Eagle medium supplemented with 10% filtered, heat-inactivated FCS, 2mM L-glutamine, and 100U/ml penicillin.
- **MGIA supplement medium** (800µl/tube from premixed solution): PANTA antibiotics (polymyxin B, amphotericin B, nalidixic acid, trimethoprim and azlocillin) + OADC enrichment broth, one bottle each.
- **DNA digestion buffer:** 2µl restriction enzyme 10x buffer, 0.2µl acetylated BSA (10µg/µl) and a 1µl DNA sample (1µg/µl) mixed, to which was added 1µl restriction enzyme + nuclease-free dH_2O to bring the total volume to 20µl.

- **Tris base, acetic acid, EDTA (TAE) buffer, made at 50x quantity:** 242g tris base dissolved in 750ml dH_2O, 57.1ml glacial acetic acid, 100ml 0.5M EDTA and dH_2O were mixed to bring the total volume to 1l.
- **Radioimmunoprecipitation (RIPA) lysis buffer system:** 1ml 1x lysis buffer, 10µl protease inhibitor cocktail in DMSO and 500µl (100mM) sodium orthovanadate in water.
- **1x iBind™ Flex solution:** 10ml iBind™ Flex 5x buffer, 500µl iBind™ Flex 100x additive and 39.5ml distilled water.
- **5-bromo-4-chloro-3-indolyl phosphate (BCIP)/nitro blue tetrazolium (NBT) solution:** one tablet of BCIP/NBT dissolved in 10ml deionised water.

2.2 Cell culture and *in-vitro* infection

2.2.1 THP-1 cells

The human leukaemia monocytic cell line THP-1 was obtained from the American Type Culture Collection. THP-1 cells were cultured in a complete RPMI-1640 medium (R0883-500ML, Sigma-Aldrich) at 37°C and 5% CO_2. Cells were subcultured when the cell density reached 1 x 10^6/ml for up to three months or until passage 25 had been completed (213). The frozen stock was prepared by harvesting cells (centrifuge at 150*g* for 5 min). Cells were resuspended in cold complete RPMI-1640 medium with 10% Dimethyl sulfoxide (D2650-100ML, Sigma-Aldrich) to obtain ~5 x 10^6/ml, transferred into cryovials, placed into a freezing box and stored at -80˚C overnight. Cryovials were transferred to liquid nitrogen.

2.2.2 **BCG and MTB culture and freezing**

BCG-GFP, which expressed green fluorescent protein (GFP) with resistance to hygromycin, was kindly provided by Dr Rajko Reljic from St George's University of London. BCG-GFP was cultured in Middlebrook's 7H9 broth (BD Biosciences, UK) containing 50μg/ml hygromycin (Merck Life Science UK Limited), at 37ºC, in aerobic conditions, on a shaker at 200rpm. MTB-GFP was cultured as BCG but without shaking. To remove large clumps, mycobacteria were centrifuged at 300*g* for 2 min; the supernatant was collected and sonication was performed for 10 min in a water bath. I found that the best procedure was to perform sonication over 10 cycles and to place the vial containing BCG in the sonication bath for 30 seconds and then on ice for 30 seconds during each cycle (Figure 2.1). This method allowed for a greater degree of clump dissociation. BCG or MTB were used when their growth reached the middle of the exponential phase, which could be assessed through the use of optical density (OD); the required OD was approximately 0.6, where an OD of 0.1 was equivalent to ~$1x10^7$ bacilli/ml. The frozen stocks were prepared by harvesting BCG or MTB (centrifuged at 3,000*g* for 10 min) and resuspending in 20% glycerol in PBS.

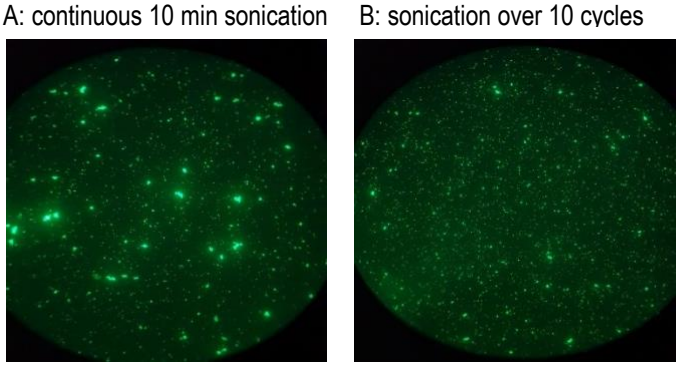


Figure 2.1 Visualisation of GFP expression under fluorescence microscope.
BCG-GFP underwent different techniques to optimise single-cell suspension. After performance of continuous 10 min sonication (A) and sonication over 10 cycles (B), 10ul of each were placed on slides and the images were captured at 10x lens magnification.

2.2.3 **Infection of THP-1 cells with MTB for immunopeptidomics**

For *in vitro* infection with MTB, 3 x 10^8 THP-1 cells were differentiated into macrophage-like cells by stimulation with 20nM Phorbol 12-Myristate Acetate (PMA, Sigma-Aldrich, UK) overnight, and then were treated with cytokines: 50ng/ml IFNγ (Immuno Tools, Germany) and 1μg/ml anti-IL10 (BD Biosciences, UK) for a day before infection. When MTB growth reached the exponential phase, the MTB was centrifuged at 3,000*g* for 10 min and washed in PBS. Then, the bacteria were resuspended in an antibiotic-free medium and clumps were removed. On the infection day, THP-1 cells were washed and infected with MTB-GFP at an MOI of five. After 4 hours of exposure, THP-1 cells were washed with PBS three times to remove MTB and resuspended in a fresh antibiotic-free medium. After 24 hours, cells were harvested, pelleted by centrifugation and stored at -20˚C.

2.2.4 **Removal of MTB from the lysate**

The cell pellet was lysed with 2x lysis buffer, supplemented with complete™ protease inhibitor cocktail (Roche) for 30 min on ice with shaking every 10 min. Lysates were centrifuged at 500*g* for 10 min to remove nuclei. The supernatant was filtered twice with centrifugal filters (0.22 µm pore size, hydrophilic PVDF, 0.5 mL, Millipore) at 2000*g* for 5 min. The filtrate was transferred into a fresh 15 ml Falcon tube for IP. This protocol was validated for bacteriological sterility before immunopeptidomics experiments were conducted.

2.2.5 **Flow cytometry**

THP-1 cells were differentiated into macrophages using 50ng/ml PMA over two days (169). Macrophages were harvested using a cell scraper and stained with antibodies specific for human HLA-DP (1:50; clone B721; Leinco Technologies, USA), HLA-DQ (1:50; clone Tu169) and HLA-R (1:100; clone L243, both from BioLegend, USA), or stained with antibodies specific for pan-MHC-I and pan-MHC-II (1:100; both from Miltenyi Biotec, Germany) for 30 min at 4˚C. After washing the cells with FACS buffer (PBS, 1% BSA), the cells were acquired through the use of an LSR-II flow cytometer and data were analysed through the use of FlowJo® software (BD Biosciences).

2.2.6 **Quantification of mycobacteria**

The CFU assay was performed to quantify cultured BCG after infection of macrophages in various experiments. THP-1 cells were differentiated into macrophages through the use of 50ng/ml PMA over two days. Differentiated THP-1 cells were treated with different agents (IFNγ at 50ng/ml, Metformin at 2mM, Entinostat at 1uM and Tubastatin A at 1uM; Alfa Aesar) one day before infection and CFUs were enumerated immediately post-infection. The exposure time of BCG was 4 hours with an MOI of 10. After infection, cells were washed twice with PBS and lysed to release intracellular bacteria. Three serial dilutions from each sample were plated in duplicate on Middlebrook 7H11 agar plates supplemented with OADC. After a week of incubation at 37°C, CFU were counted. Enumeration of CFU was conducted under the microscope (fluorescence microscopy; Leica DMI3000);

mycobacterial colonies could be seen under the microscope on agar plates (Middlebrook 7H10) at 5x or 10x magnification, 5-7 days after incubation (214).

2.3 MS-based immunopeptidomics and proteomics

2.3.1 IP of peptide-MHC complex

For BCG-related IP, two antibodies were cross-linked to Protein A Sepharose beads with the use of dimethyl pimelimidate (Sigma). B721 antibody was used to complex and precipitate HLA-DP molecules, followed by IVA12 antibody to complex and precipitate HLA-DR, -DP or -DQ molecules (1mg each per $1x10^8$ cells). Lysates were incubated overnight with each antibody (bound to beads). Beads were subsequently washed with 10 column volumes of 1x150 mM NaCl, 5 mM EDTA in 50 mM Tris, 1x150 mM NaCl in 50 mM Tris, 1x450 mM NaCl in 50 mM Tris and 50 mM Tris buffer without salt. Peptides bound to the HLA molecules were dissociated upon mild acid elution with 5ml 10% acetic acid to denature α and β subunits of MHC molecules. The dissociated peptides were purified from MHC molecules through the use of HPLC (reversed phase monolith column (RP-1S) 4.6x50mm, Thermo Fisher Scientific). HPLC fractions that contained eluted peptides were collected, concentrated and stored at -20°C. The same protocol was applied to MTB IP with some modifications as follows. The IP order was B721 (HLA-DP), IVA12 (pan-MHC-II) and W632 (pan-MHC-I). A volume of 2ml of Sepharose beads was used for 5mg antibody per sample. Each sample was incubated with antibodies twice (first incubation overnight and second incubation for an hour).

2.3.2 **Purification of HLA peptides**

RP-HPLC was used to separate the peptides from the HLA complexes. Briefly, samples were injected into a column (4.6x50mm ProSwift RP-1S, Thermo Fisher Scientific) and eluted for 10 minutes at a buffer gradient of 2% to 35% buffer B (0.1% TFA in acetonitrile) and at a flow rate of 1000µl/min through the use of the Ultimate 3000 HPLC system (Thermo Fisher Scientific). Odd and even fractions that did not contain ß2-microglobulin were combined as two final fractions. Samples were dried, re-suspended in 20ul of loading buffer (0.1% TFA, 1% acetonitrile) and stored at −20°C before MS analysis.

2.3.3 **MS and data analysis**

Peptides were analysed through the use of nano-LC-MS-MS in an Ultimate 3000 RSLCnano System (PepMap C18 column, 2µm particle size, 75µm × 50cm; Thermo Fisher Scientific) coupled with an Orbitrap Fusion Lumos Tribrid (Thermo Fisher Scientific) or a Q Exactive HF-X mass spectrometer (Thermo Fisher Scientific). Peptides were separated by applying a 60-min linear gradient from 3% to 25% acetonitrile in 5% DMSO/0.1% formic acid in water for HLA-I peptides, while a linear gradient from 3% to 30% acetonitrile was applied for HLA-II peptides at a flow rate of 250nl/min. For samples to be analysed through the use of the Orbitrap Fusion Lumos Tribrid mass spectrometer, the acquisition was performed at a resolution of 120,000 for full MS (300-1500 mass/charge number of ions (m/z) scan range) at an automatic gain control (AGC) target of 400,000. Precursor peptides were selected in a top-speed, 2s cycle time and at an isolation width of 1.2 atomic mass units (amu), over an accumulation time of 120ms. MS-MS resolution

was set at 30,000 at an AGC target of 300,000 and high-energy collisional dissociation (HCD) was used to fragment precursor ions (28V collision energy for peptides in a charge state of 2-4 and 32V for singly charged precursor ions). For samples analysed through the use of the QExactive HFX mass spectrometer, the acquisition was performed at a resolution of 120,000 for full MS (320-1600m/z scan range) at an AGC target of 300,000. The 20 most intense precursor ions were selected for fragmentation at an isolation width of 1.6 amu for 120ms, resulting in a 2.5s cycle time. MS2 resolution was set at 60,000 at an AGC target of 50,000 and used HCD for the fragmentation at a collision energy setting of 25V.

2.3.4 **Data analysis for immunopeptidomics**

MS data were analysed using Peaks V8 and V10 (Bioinformatics Solutions) by matching the spectra to the proteome of humans and BCG (Pasteur 1173P2) or MTB (H37Rv) (both imported from the UniProt database) to determine peptide spectrum matches (PSMs). Once analysed, identified peptides and corresponding proteins were exported from Peaks software with a minimum score threshold of -10logP=15. To achieve PSM, the exported data (Excel format) were analysed further to determine the mycobacterial peptides and mycobacterial proteins as follows:

- all human peptides/proteins were excluded;
- any mycobacterial peptides/proteins presented in the control sample were excluded from the infected samples; and
- the mycobacterial peptides/proteins that were defined in the infected samples were analysed further.

2.3.5 **MHC protein digestion and peptide purification**

Tubes containing dried MHC proteins were resuspended in 50ul 6M urea buffer and mixed by vortexing and sonication, 5 min each. A volume of 10ul of DTT, 20mM, solution (reducing reagent to convert disulphide bonds into free sulfhydryl groups) for 30 min, followed by addition of 2.5ul 5mM iodoacetamide solution (an alkylating reagent that reacts with free sulfhydryl groups of cysteine residues to form S-carboxyamidomethyl-cysteine, to maximise trypsin access to cleavage sites within the protein) in the dark at room temperature (RT). The mixture was diluted with 250µl Milli-Q H_2O to obtain a urea concentration of 2M. Next, 1ul (0.2µg/µl) of trypsin was added (1:50 enzyme:protein ratio), and the solution was mixed and incubated overnight at 37°C. The next day, C18 columns (Waters Oasis SPE kit) were attached to a vacuum manifold to clean the samples. The eluted peptides were dried through the use of a Vacufuge plus Centrifuge Concentrator (Eppendorf). Purified dry peptides were resuspended in loading buffer (solution A) for MS acquisition.

2.3.6 **Data analysis for quantitative proteomics**

Quantitative analysis of the raw data (MS-MS spectra) was performed through the use of MaxQuant or Progenesis QI software (Waters), at the default search settings. For MaxQuant, variable modifications regarding amino-acid residues (N-terminal acetylation, oxidation, and fixed modification of carbamidomethyl cysteine) were included. The human proteomic sequences were utilised, including for HLA proteins expressed by THP-1 cells. Proteins and peptides with a false discovery rate (FDR) of <1% were selected. The exported data (Excel files) were analysed manually, during which relative quantification was determined for unique

peptide(s) that represented single MHC chain proteins. Label-free quantification (LFQ) intensity values were used. For Progenesis, label-free quantification was performed upon using chromatographic alignment, a scalar factor normalization of all proteins over three steps to all protein and determination of individual peptide ion abundances. When samples aligned according to retention time on Progenesis, the database search was performed using Peaks, where default search settings were applied (N-terminal acetylation, oxidation, and fixed modification of carbamidomethyl cysteine). Then, files were uploaded again on Progenesis. Further analysis was performed on exported data (Excel files) to determine relative quantitation using unique peptide(s) per MHC chain protein.

2.4 *In silico* analysis and computational tools

2.4.1 T-cell MHC-II prediction

To map CD4+ T-cell epitopes, MHC-II binding peptides present in identified mycobacterial proteins were predicted through the use of the NetMHCIIpan server online (https://services.healthtech.dtu.dk/) set at the default settings, for a peptide length of 15-mer, and the binding affinity thresholds (1% and 5%) were used to define strong and weak binders respectively. The prediction was performed against 27 human HLA alleles (DRB1*0101, DRB1*0301, DRB1*0401, DRB1*0405, DRB1*0701, DRB1*0802, DRB1*0901, DRB1*1101, DRB1*1201, DRB1*1302, DRB1*1501, DRB3*0101, DRB3*0202, DRB4*0101, DRB5*0101, DQA1*0501/DQB1*0201, DQA1*0501/DQB1*0301, DQA1*0301/DQB1*0302, DQA1*0401/DQB1*0402, DQA1*0101/DQB1*0501, DQA1*0102/DQB1*0602, DPA1*0201/DPB1*0101, DPA1*0103/DPB1*0201, DPA1*0103/DPB1*0401,

DPA1*0301/DPB1*0402, DPA1*0201/DPB1*0501 and DPA1*0201/DPB1*1401) and eight mouse MHC alleles (H-2-D^d, H-2-D^b, H-2-K^d, H-2-L^d, H-2-Ia^d, H-2-IE^d, H-2-K^b and H-2-IA^b) that represented the CB6F1 mouse strain. Mycobacterial proteins with a broad repertoire of epitopes covering all human and mouse alleles were selected.

2.4.2 **Non-homologous protein identification**

To determine non-homologous mycobacterial proteins to the human proteome, each mycobacterial protein sequence was analysed through the use of the Vaxign server (https://violinet.org/vaxign/) to find similarities with any human protein. The BLAST protein database was used to calculate the homology between sequences represented by E-value; smaller E-value scores indicated higher similarity.

2.4.3 **Peptide yield after trypsin digestion**

The server PeptideCutter (https://web.expasy.org/peptide_cutter/) was used to predict the unique peptides that were likely to be present in MHC protein that had been expressed by THP-1 HLA alleles. The protein sequences were uploaded, and trypsin was selected as the protease enzyme. The query sequences were exported (Excel files) and analysed manually to exclude overlapping sequences.

2.5 Plasmid amplification and purification

2.5.1 Escherichia coli transformation

Competent *Escherichia coli* bacteria were thawed on ice. An aliquot of 5µl of DNA (~100ng) was added to 30-40µl of competent bacteria in a microtube and the solution was mixed gently by flicking the bottom of the tube. To facilitate the transfection, the tube was incubated on ice for 20-30 min, after which it was placed in a 42°C water bath for ~45s (to achieve heat-shock transformation), and then on ice for 2 min. An aliquot of 500µl Luria broth (LB) or super-optimal broth with catabolite repression (SOC) outgrowth medium (New England Biolabs) was added to the bacteria and incubated with shaking for 45 min at 37°C. Meanwhile, LB agar plates containing carbenicillin antibiotic as a selective marker were prepared. A sample of 10µl was used for bacterial plating, while 20µl was used for bacterial plating that employed the streak-plate technique to generate visible, isolated colonies. A single colony was picked up and inoculated in a starter culture of 10ml LB medium that contained carbenicillin (1:1000) in a 50ml Falcon tube and was incubated for about 8h at 37°C with vigorous shaking (280-300rpm). The bacteria from the starter culture was diluted at 1:500 into fresh LB medium that contained carbenicillin and incubated at 37°C for 16-18h with vigorous shaking (the volume of the flask was four times larger than the volume of the culture). The bacteria were harvested the following day by centrifugation of the overnight LB culture at 4000*g* for 15 min and removal of the supernatant (the pellets can be frozen at -20°C at this stage).

2.5.2 **Plasmid purification**

All the following buffers were previously prepared by the manufacturer (PureLink™ HiPure Expi Plasmid Gigaprep Kit - Thermo Fisher Scientific). An aliquot of 125ml resuspension buffer was mixed with RNase A. The mixture was divided over the five bottles (25ml each), added to the pellets, and vortexed until the bacterial pellets became completely homogeneous. Then all were compiled into one bottle. A 125ml aliquot of lysis buffer was added slowly. The combination was mixed gently by inversion of the bottle until the lysate mixture was homogeneous, after which it was incubated for 5 min (no vortexing or incubation for more than 5 min). A 125ml aliquot of precipitation buffer was added and mixed gently through inversion of the bottle until the mixture was homogeneous and precipitation occurred (proteins, cellular debris, genomic DNA). To remove unwanted fluffy white precipitate, the lysate was centrifuged at ≥20,000*g* for 20 min at 4°C. The supernatant containing plasmid DNA was poured into the prepared lysate filtration cartridge and attached to a 1000ml receiver flask for further clearing. A vacuum (−600mbar to −800mbar) was applied. The clear flow-through was collected in the flask. Wash buffer (50ml) was added to the filtration cartridge, and the vacuum was applied until all the liquid had been drained into the flask that contained the previous filtrate. Endotoxin removal buffer (30 ml) was added to the flask and the solution was mixed by inversion of the bottle ten times. Equilibration buffer (100ml) was added to a DNA-binding cartridge that was attached to a fresh 1000ml receiver flask, and the vacuum was applied until all the liquid had been drained. The filtrate containing the plasmids was loaded into the equilibrated DNA-binding cartridge, and the vacuum was applied until all the liquid had passed into another fresh flask. Wash buffer

(275ml in total) was added in two aliquots to a DNA-binding cartridge, and the vacuum was applied until all the liquid had drained. The binding cartridge that contained the DNA was connected to a fresh 250ml receiver flask. Endotoxin-free elution buffer (100ml, pre-warmed to ~45°C was added to the binding cartridge, and the vacuum was applied until 50% of the liquid had passed through; at this point, the vacuum was turned off for 2 min, then reapplied until all the liquid had drained entirely into the receiver flask. The purified plasmid DNA was precipitated through the addition of isopropanol at a ratio of 70% isopropanol to the total volume of the eluate (e.g., 100ml eluate required the addition of 70ml isopropanol) followed by centrifugation at >12,000*g* for 30 min at 4°C. The supernatant was discarded carefully. The DNA pellet was collected in several 2ml sterile endotoxin/DNase-free tubes and washed with 70% ethanol in fresh tubes. The tubes were centrifuged at >12,000*g* for 10 min at 4°C, and the ethanol was removed without disturbance of the DNA pellets, which were left to dry in air (~15 min). Subsequently, the pellets were resuspended in endotoxin/DNase-free water and stored at -20°C after the DNA concentrations had been measured through the use of a NanoDrop™ One/OneC Microvolume UV-Vis Spectrophotometer (Thermo Fisher Scientific.

2.6 Confirmation of inserts and expression

2.6.1 Agarose gel electrophoresis

To confirm the size of inserts that were required, agarose gel electrophoresis was performed. DNA digestion buffer was prepared on ice in 0.5ml tubes. The buffer was mixed gently through pipetting and centrifugation for a few seconds at maximum

speed in a microcentrifuge, after which the tubes were incubated at the enzyme's optimum temperature for 5-15 minutes. Meanwhile, 1% agarose gel was prepared, and 10µl of 10,000x SYBR Safe stain was added, with a gentle swirling motion, to the agarose solutions when the temperature reached approximately 50°C. The mixture was poured onto a sealed gel tray to a depth of ~1.5cm after the appropriate comb had been placed, and it was left to cool for about 15-20 min at RT. Once solidified, the comb was removed, and the gel was placed into a gel tank filled with 1x TAE buffer (enough to cover the gel). Subsequently, the digested DNA, mixed with the loading dye (25ul sample + 5ul 6x loading dye) and 5ul DNA ladder, were loaded into the wells as specified in the tank instructions. The lid was placed on the gel tank, and the electrode contacts were seated correctly and plugged into a power pack. The gel was run at 100V for about 50 minutes. The gel was placed onto a suitable tray for carriage to the gel imager (the Gel Doc EZ System; Bio-Rad).

2.6.2 **Western blotting**

To confirm that the inserted mycobacterial proteins had been expressed by pDNA3.1 plasmid extracellularly, 293T cells were seeded in six-well plates and incubated at 37°C with CO_2 until they reached a confluency of 70-80%, after which they were transfected with 1ug of each plasmid at a w/w ratio of 1:3 (DNA:transfecting reagent, polyethyleneimine (PEI),) in RPMI medium only for 2-3 hours. Next, they were washed with PBS and incubated in complete RPMI medium for 48 hours. The supernatants and/or cell pellets were collected and suspended in 0.5ml RIPA lysis buffer over ice for 10-20 min (mixed gently every 3-5 min). Cell lysates were centrifuged at 500*g* for 10 min. Aliquots of 13ul from each sample

(supernatant and cell lysate) were each mixed with 5ul of lithium dodecyl sulphate sample buffer (4x) and 2ul of reducing agent (10x) and vortexed and incubated at 90°C for 10 min. Meanwhile, the chamber and protein gel were assembled and filled with 1x running buffer (Thermo Fisher Scientific). Prestained protein marker (5ul) and 20ul from each sample were loaded into specified wells and run at 180V for 50 min. The chamber was disassembled, and the gel was obtained carefully. After preparation of the transfer pack, the gel was placed on the membrane (anode stack) and covered by a cathode stack. The locked cassette was inserted into the Trans-Blot Turbo Transfer System (Bio-Rad) and set up for the transfer. Then, the membrane was blocked with 5% skimmed milk in PBS that contained 0.05% Tween 20 for 2 hours. After this, it was washed three times. The blotted membrane was left on a container of 1x iBind™ Flex solution (Life Technologies Ltd). The iBind™ card was rinsed in dH_2O and placed on the stage of the iBind™ Flex western device. An aliquot of 10ml 1x iBind™ was pipetted across the flow region, and an additional 2ml 1x iBind™ over the membrane region. The blotted membrane was placed where the protein side faced the iBind™ card and high molecular weight protein region toward the wells (multi-strip insert). The lid was closed, and the solutions were added sequentially to the wells according to Table 1. The next day, the membrane was washed in dH_2O and immersed in BCIP/NBT solution until protein bands developed, after which they were washed with tap water to stop the reaction and left to dry at RT.

Table 2.1 *Solutions added sequentially to the blotted membrane.*

Solutions	Volume
Row 1: primary antibody	2ml (anti-his-tag antibodies 1:200; BioLegend)
Row 2: 1x iBind™ Flex	2ml
Row 3: secondary antibody	2ml anti-mouse IgG (whole molecule)-alkaline phosphatase 1:2000 (Sigma)
Row 4: 1x iBind™ Flex	6ml

2.6.3 **Flow cytometry**

To confirm that the inserted antigens had been expressed by pDNA3.1 plasmid intracellularly, human embryonic kidney cells (293T) were seeded in six-well plates and incubated at 37°C with CO_2 until they reached a confluency of 70-80%. After the plasmid DNA had been optimised to the PEI (Alfa Aesar) ratio, cells were transfected with 1ug of each plasmid at a 1:3 DNA:PEI w/w ratio in RPMI medium only for 2-3 hours (Figure 2.2). This was followed by washing with PBS and incubated in complete RPMI medium for 24 hours. Cells were collected through the use of 0.5ml trypsin (Invitrogen, USA), resuspended in 100µl 4% paraformaldehyde in PBS and incubated for 10 minutes at RT. Subsequently, cells were washed (centrifugation at 300*g* for 10 min) in 2% BSA/PBS. After the last wash, cells were permeabilised with 100µl 0.1% saponin in PBS for 10 minutes at RT and then centrifuged at 300*g* for 10 min. Cells were resuspended in a 100µl solution of PE-anti-his-tag antibody (1:50; BioLegend) in 0.1% saponin/PBS and incubated for 30 min. After two washes with 0.1% saponin/PBS, cells were resuspended in 100µl 2% BSA/PBS and run on an LSRII™ with FACSDiva™ software (BD Biosciences) and the exported data were analysed through the use of FlowJo® software (BD Biosciences).

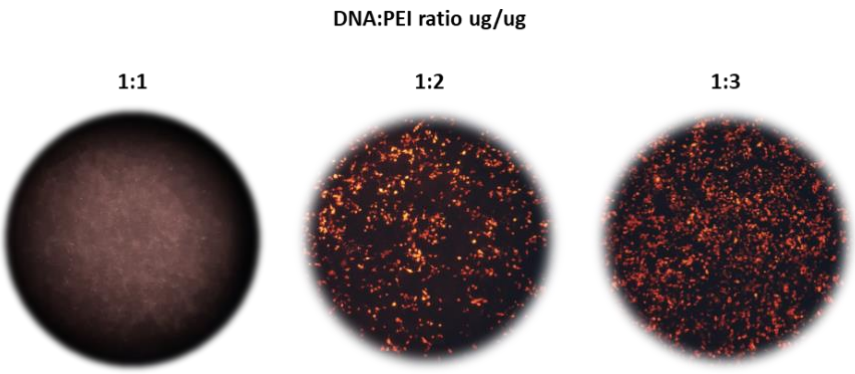


Figure 2.2 ***Visualisation of mCherry expression under fluorescence microscope.***
HEK293T cells were transfected with different ratios of plasmid-expressing mCherry and PEI (DNA:PEI; ug/ug) to optimise the transfection efficiency. One day after transfection, the cells were imaged directly while in culture plates, at 10x lens magnification.

2.7 Animal experiments

All animal work was conducted under authorised project and personal licences at the Functional Genetics Facility (University of Oxford) in compliance with the UK Animal (Scientific Procedures) Act of 1986.

2.7.1 **CB6F1 Mice**

All mice used in this project were female and designated specific-pathogen-free CB6F1 mice purchased from Charles River UK Ltd, ranging in age from 6-9 weeks. The mice were housed in groups of four to six mice per ventilated cage. All immunisation procedures, intradermal and intramuscular, were undertaken under inhalational anaesthesia using isoflurane.

2.7.2 **Immunisation**

For the first experiments, CB6F1 mice were randomly divided into six groups (eight mice in each) and vaccinated as follows: one group was vaccinated with BCG Pasteur ($3.5x10^5$cfu/mouse) intradermally once; four groups were vaccinated with plasmid DNA (hisD, metE, mmpL12 or PPE15; 100ug/100ul PBS/mouse) separately, three times at two-week intervals; and one naïve group was left unvaccinated. Mouse spleens and blood were collected two weeks after the final vaccination.

In the second experiment, CB6F1 mice were randomly divided into five groups (eight mice in each) and vaccinated as follows: one group was vaccinated with BCG intradermally once; three groups were vaccinated with metE antigen (metE alone (1ug/100ul PBS/mouse), metE-DNA (100ug/100ul PBS/mouse) and metE with adjuvant (1ug/100ul/mouse) in a dose prepared with 1:1 ratio with adjuvant system AddaS03™ (InvivoGen), separately three times at three-week intervals; and one group (naïve) was left unvaccinated. Mouse spleens and blood were collected three weeks after the final vaccination.

2.7.3 **MGIA**

To obtain single-cell suspensions of splenocytes, spleens were mashed in a six-well plate using the rubber plunger of a 20ml sterile syringe. The dissociated spleen cells were rinsed constantly with PBS and transferred to a 50ml Falcon tube through a 70uM cell strainer placed over the tube. The PBS was discarded (to achieve this, the tubes were centrifuged at 350*g* for 5 min), and cells were resuspended in 3ml ACK buffer for 5 min (maximum) to lyse the red blood cells. After this, RPMI-MGIA was

added until the mixture measured 35ml. After centrifugation at 350*g* for 5 min, cells were resuspended in 2ml RPMI-MGIA and adjusted to obtain $3x10^6$ or $5x10^6$ splenocytes in a final volume of 600µl RPMI-MGIA when co-cultured with BCG in 48-well tissue-culture plates; BCG was added to cells at ratios of 1:5000 and 1:7000. All plates were incubated for 96 hours at 37°C with CO_2.

All the well contents were collected in 2ml screw-cap tubes and centrifuged at 12,000rpm for 10 minutes. During this time, 500µl sterile water was added to each well to lyse any adherent cells. Supernatants were discarded carefully without disturbing the pellet. Water containing lysate was transferred into the corresponding 2ml screw-cap tubes. Tubes were pulse-vortexed to disrupt the pellet and to cause mixing with the lysate, and the whole volume was transferred to BACTEC MGITs supplemented with PANTA antibiotics and OADC enrichment broth (Becton Dickinson, UK).

2.7.4 **Enzyme-linked immunosorbent assay (ELISA)**

Blood samples were collected from the mice hearts into empty 2ml screw-cap tubes during the takedowns and stored at 4°C overnight. Tubes were centrifuged at 2000*g* for 10 min at 4°C. Serum was collected and stored at -20°C for antibody titration.

ELISA was used to measure the amounts of metE-specific antibodies that were present in the mouse sera. Maxisorp 96-well plates (Thermo Fisher Scientific) were coated with 2.5µg/ml recombinant metE in 50µl PBS in order to detect total IgG, IgM and IgG subclasses (IgG1, IgG2a, IgG2b and IgG2c), and were incubated overnight at RT. The plates were washed six times with PBS/Tween-20 (Sigma-Aldrich) and blocked with 200µl of casein blocking buffer (Fisher Scientific UK Ltd)

for 1-2 hours at RT. The blocking solutions were discarded, and sera were prepared at an initial dilution of 1:100 in the blocking buffer. Sera were serially diluted (four-fold) for endpoint titre (ET) and absorbance summation (AS) methods. Aliquots of 50µl were added in duplicate for each dilution and incubated for 2 hours at RT. Following washing, anti-mouse secondary antibodies conjugated to alkaline phosphatase (IgG, IgG1, IgG2a, IgG2b and IgM; all from BioRad) were diluted at a ratio of 1:3000, and 50ul of these solutions were added to the corresponding plates and incubated for 1 hour at RT. After washing, 100µl of development buffer (1mg/ml of a 4-nitrophenylphosphate tablet (Sigma-Aldrich)) diluted in diethanolamine buffer (Thermo Fisher Scientific) was added. The reaction was developed at RT, and optical density (OD) was measured at 405nm (Gen5 software) using a spectrophotometer (BioTeK Microplate Reader). The mean of the data for blank wells was subtracted from sample means to obtain adjusted ODs.

2.7.5 **Enzyme-linked immunospot (ELISpot)**

Splenocytes were prepared as mentioned in section 2.7.3. ELISpot was used to measure the amounts of cytokine secreted upon metE stimulation. MultiScreen-IP filter plates (Millipore) were coated separately with 50µl (10ug/ml in PBS) of anti-mouse antibody to IFNγ, IL-2, IL-4 or IL-17 (all from Mabtech) and stored at 4°C overnight. After the coating buffer had been discarded (by flicking the plates) and the plates had been washed six times with PBS, the reactions on the plates were blocked with 200µl of complete media for a minimum of 2 hours at 37°C. The blocking buffer was discarded, and 50ul of the solutions, which contained 2.5×10^5 splenocytes, were added to all wells, and then 50µl of complete media (for a

negative control) or diluted metE (10μg/ml) was added according to the layout. Following overnight incubation at 37°C and in 5% CO_2, the plates were washed six times with PBS 0.05% Tween 20. They were incubated for 2 hours at RT after the addition of 50μl/well of biotinylated goat anti-mouse IgG (Mabtech) diluted at a ratio of 1:1000 in PBS. After they had been washed six times with PBS 0.05% Tween 20, streptavidin-ALP (Mabtech) was diluted at a ratio of 1:1000 in PBS and 50μl of this solution was added to each well. Then the wells were incubated for an hour at RT. Aliquots of 50ul/well of colour development buffer (AP Conjugate sub kit, BioRad) were added to the wells, which were incubated for 5-10 min at RT until colour developed (visible spots); the reaction was stopped by washing the plates under running tap water. When the plates were dry, spots were counted with the application of an ELISpot reader (AID Germany, software version 5.0). Results were reported as numbers of spot-forming units (SFU) per $1x10^6$ cell after the mean SFU counts for the unstimulated cells had been subtracted from the mean SFU counts for antigen-stimulated wells.

2.7.6 **Intracellular cytokine staining**

Splenocytes were prepared as explained in section 2.7.3. One million cells/well were stimulated with 10μg/ml metE protein (all groups), 10μg/ml tuberculin-purified protein derivative (PPD) (BCG vaccinated group), or with a complete RPMI-1640 medium only for unstimulated negative controls in 96-well U-bottom plates. Stimulation took place in the presence of anti-CD28 (1 μg/ml) and anti-CD49d (1 μg/ml), both from BioLegend Inc. Plates were incubated for 2 hours at 37°C in 5% CO_2, after which 1μl/ml of GolgiPlug (BD Biosciences) was added and the plates

were incubated again for 4-6 hours at 37°C in 5% CO_2. After this, they were incubated overnight at 4°C. In the following day, cells were centrifuged at 300*g* for 5 min at 4°C and washed with PBS. Aliquots of 10ul of PBS were added to unstained wells and 10ul amounts of live/dead (1:200, Invitrogen, UK) were added to the rest of the wells for 10 min. Then, 40ul of antibody-cocktail 1 (Table 2.2) for surface staining was added directly (no wash) and the solutions were incubated for 30 min at 4°C. Plates were then washed through the addition of 150ul BSA/PBS, after which the solutions were centrifuged for 5 min at 300*g*, and the supernatant was discarded. Cells were incubated with 100ul Cytofix/Cytoperm solution (BD Biosciences) for 10 min and then permeabilised with 100ul of 1/10 (diluted in water) Perm/Wash solution (BD Biosciences) before intracellular cytokine staining (ICS) was pursued. Cytofix/Cytoperm solutions were discarded, and cells were washed with 150ul Perm/Wash solution. They were centrifuged again at 300*g* for 8 min at 4°C. Cells were stained for intracellular marking with 40ul antibody-cocktail 2 (Table 1) prepared in Perm/Wash solution. The mixtures were incubated for 30 min at 4°C, after which 150ul aliquots of Perm/Wash solution were added and the mixtures centrifuged. Then, the plates were washed twice with Perm/Wash solution and then with PBS/BSA solution. Finally, cells were resuspended in 80ul PBS/BSA solution and analysed through the use of an LSR-II™ with FACSDiva™ software (BD Biosciences). The exported data were analysed through the application of FlowJo® software (BD Biosciences) following application of the gating strategy (Figure 4).

Table 2.2 *Composition and dilution of antibodies used for surface and intracellular staining*

Staining	**Antibody cocktail**	**Dilution**
Surface-cocktail 1	FC blocker	1:50
	PE-CF594 rat anti-mouse CD45R (eBioscience)	1:300
	TCR beta antibody, eFluor TM 450 (H57-597), (eBioscience)	1:100
	Brilliant Violet 650(TM) anti-mouse CD4 (BioLegend Inc)	1:100
	CD8a antibody, APC-eFluor TM 780 (53-6.7), (eBioscience)	1:300
Intracellular-cocktail 2	IFNγ antibody, APC (XMG1.2), (eBioscience)	1:200
	TNFα antibody, Alexa Fluor 488 (MP6-XT22), (eBioscience)	1:200
	IL-2 antibody, PE-cyanine7 (JES6-5H4), (eBioscience)	1:200
	IL-17A antibody, PE (eBio17B7), (eBioscience)	1:200

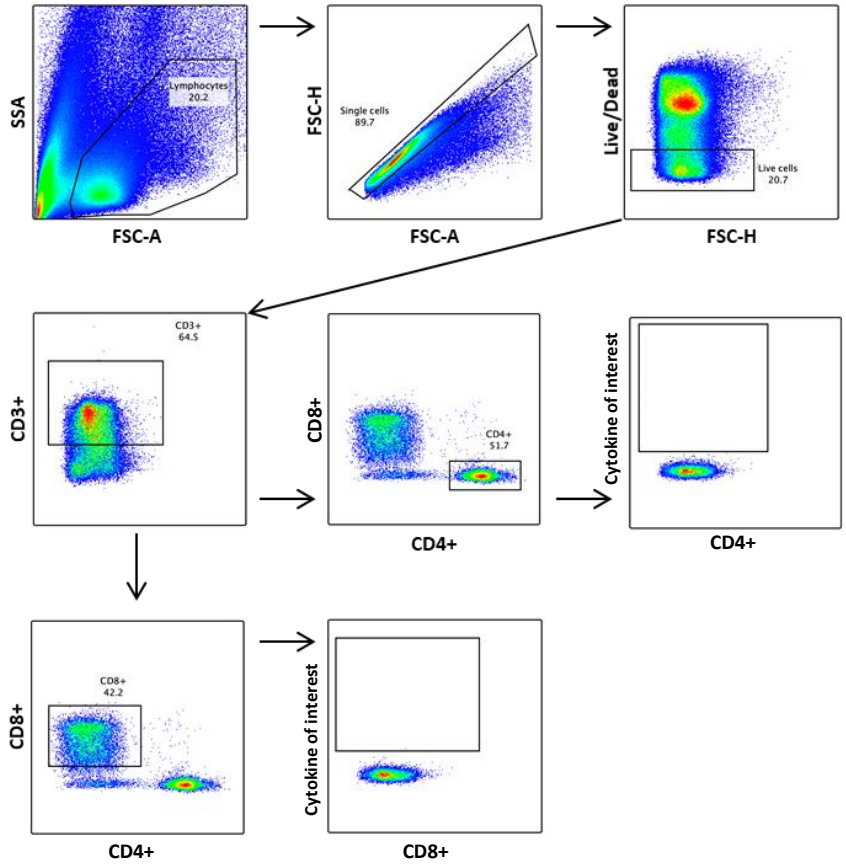


Figure 2.3 Flow cytometric gating strategy for ICS.

After gating the lymphocyte population based on forward scatter (FSC) and side scatter (SSC), singlets were gated, from which live cells were identified. Then, the CD3+ population was gated, from which CD4+ and CD8+ cells were identified. The signals of cytokine expressions (INFγ, TNFα, IL-2 and IL-17) were determined from CD4+ and CD8+ populations separately.

2.8 Statistical analyses

All statistical analysis was performed on GraphPad Prism version 8. The Mann-Whitney test was used to compare two groups, and the Kruskal-Wallis test with Dunn's multiple comparison post-test was used for multiple-group comparisons. The P value was considered significant at $P < 0.05$.

Chapter 3

Identification of *Mycobacterial* antigens presented by MHC molecules

3.1 Introduction

Understanding the pathogen-host interaction aids antigen discovery and the development of an effective subunit vaccine for TB. As mentioned earlier, T cells have been shown to play a central role in the control of MTB infection, according to data from human (78, 79) and animal studies (81, 85). Naïve T cells are primed by DCs via peptides that are derived from pathogens and present in the MHC. This priming enables the recognition by antigen-specific T cells of infected cells that display pathogen-specific peptides. MHC-I and MHC-II proteins are encoded by HLA genes, which in humans are located on chromosome 6. The genes for MHC-1 proteins comprise three classical subclasses (HLA-A, HLA-B and HLA-C); for MHC-II, they comprise three other classical subclasses, HLA-DP, HLA-DQ and HLA-DR. Once encoded, MHC proteins are assembled within the cells in which peptide fragments are loaded to be recognised by T cells. Epitopes restricted by CD8 T cells are presented by MHC-I proteins, which can accommodate peptides of lengths of between eight and 12 amino acids, whereas MHC-II molecules display CD4+ T-cell epitopes that are usually of 12-30 amino acids in length.

The identification and selection of protective antigens for preclinical evaluation is a daunting task because MTB encodes for approximately 4,000 proteins and the alleles of MHC molecules are extremely genetically variable among individuals. Identification of MHC-binding peptides is an essential step in the identification of antigens that are expressed by an intracellular pathogen and detected by the host's immune response. Immunopeptidomics is used to identify a repertoire of peptides bound to MHC molecules on infected immune cells, from which precursor proteins

can be identified, which can then be screened to determine the protective antigens. Also, the availability of specific antibodies that are used during immunoprecipitation (IP) to bind selectively to a subclass of interest offers the advantage that the researcher can determine which peptides are associated with which subclasses of HLA molecules. The workflow of immunopeptidomics starts with the lysing of infected cells and IP of peptide-MHC complex. Then, bound peptides are dissociated and separated from MHC molecules. Finally, isolated peptides are analysed through the use of LC/MS-MS or LC-MS2, as shown in Figure 3.1.

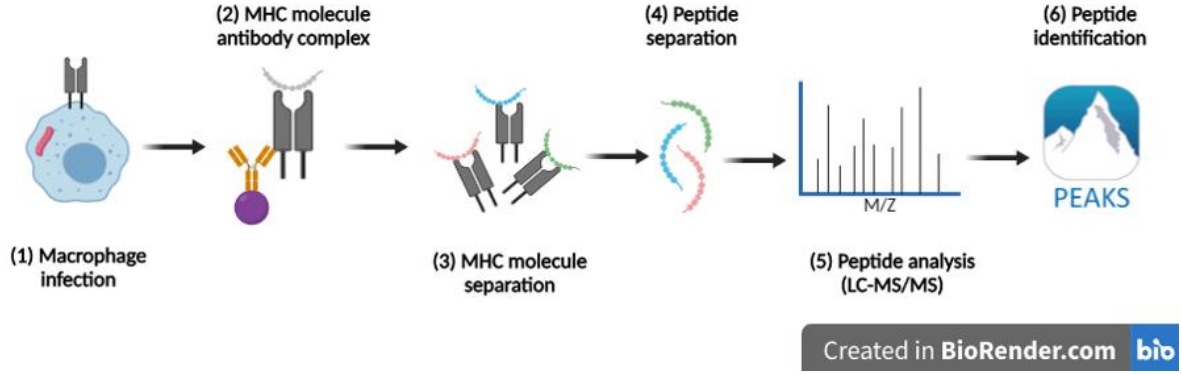


***Figure 3.1* Process of antigen identification.**

(1) Monocyte-derived macrophages (THP-1 cells) are infected with mycobacteria. (2) One day after infection, cells are harvested and lysed for IP using the antibody of interest. (3) The MHC-peptide complex is separated from the antibody and bound peptides are dissociated by acid elution. (4) Peptides are separated from MHC molecules by use of high-performance liquid chromatography (HPLC). (5) HPLC fractions containing eluted peptides are run through LC-MS-MS. (6) Mass fragment spectra are analysed with the use of Peaks software (version 10).

3.2 Aims of the work described in this chapter

The main work of the work presented in this chapter is outlined in Figure 3.2, which aims to:

1. Identify BCG-derived proteins associated with HLA-DP and -DQ.
2. Identify MTB-derived proteins associated with HLA-DP, -DQ and -DR and HLA-I.
3. Prioritise mycobacterial proteins using immunopeptidomics and immunoinformatics tools.

To address the first aim, I used the cell lysate that had been used in earlier work conducted by our group to isolate HLA-DP and -DQ. Briefly, the differentiated THP-1 cells were prepared in six different treatment and infection conditions (169). Regarding treatment conditions, samples 1, 2 and 3 were left untreated, while samples 4, 5 and 6 were treated with IFNγ and anti-IL-10 to combat mycobacterial inhibitory effects on MHC presentation (169, 215, 216). Regarding infection conditions, samples 1 and 4 were left uninfected, samples 2 and 5 were infected with heat-killed BCG, and samples 3 and 6 were infected with live BCG. This system was chosen because macrophages have been reported to process HK-MTB more rapidly and present more peptides than live MTB (217). The cells were then subjected to immunoprecipitation using two antibodies: anti-HLA-DR (L243) and anti-MHC-I (W6/32). As a result, 70 unique mycobacterial proteins were identified from all infected samples (169). Since THP-1 cells express HLA-DP and -DQ, they would remain in the cell lysate. Therefore, I continued the immunopeptidomics work using two additional antibodies, B721 and IVA12, to immunoprecipitate the HLA-DP and -DQ, respectively.

For the second aim, I optimised the model for MTB infection and prepared new samples using differentiated THP-1 cells under strict biosafety protocols (Figure 3.2). For the third aim, all the identified mycobacterial proteins that had been derived from BCG and MTB were combined into a single set for antigen selection. This set underwent *in silico* analysis to shortlist the top candidate antigens.

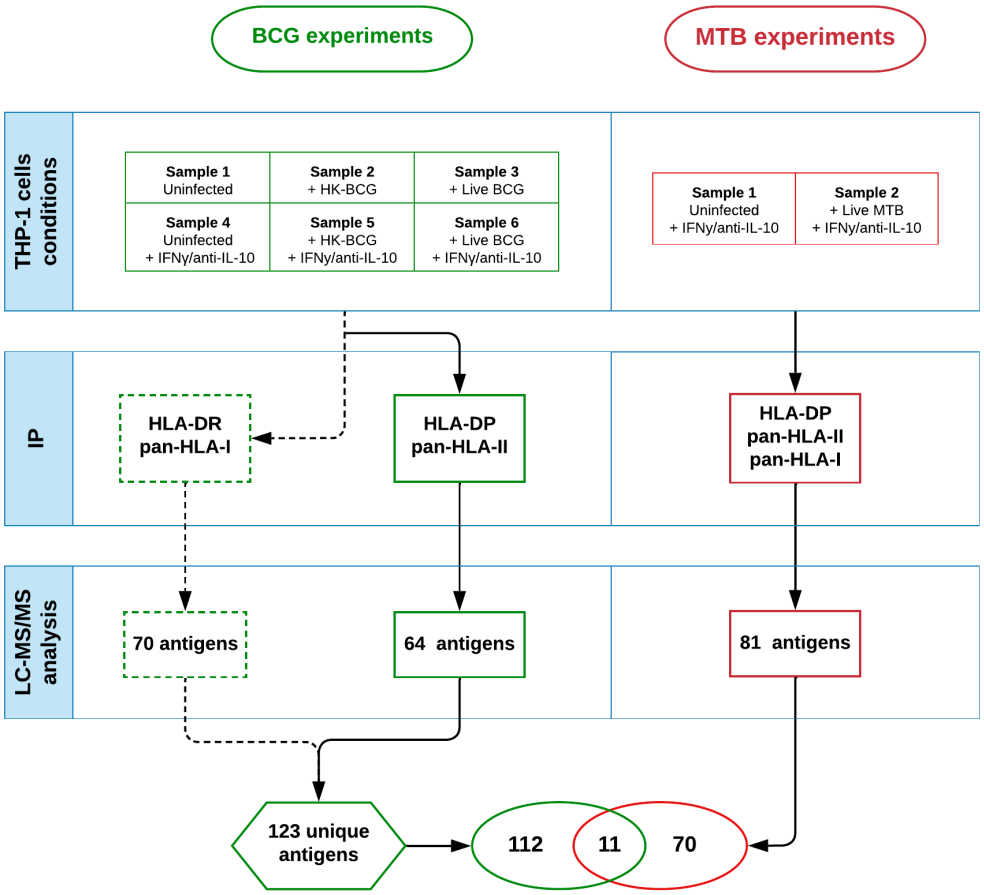


Figure 3.2: The experimental layout of the samples used for the immunopeptidomics analysis.

In the BCG experiments, all samples (six conditions) had been prepared previously by Bettencourt et al. (2020) and subjected to immunoprecipitation (IP) through the use of two antibodies, L243 and W6/32, to isolate HLA-DR and HLA-I, respectively. This experiment resulted in the identification of 76 unique antigens (dotted arrows and squares). The same samples (lysates) underwent IP with two different antibodies, B271 and IVA12, to isolate HLA-DP and -DQ, respectively. This led to identification of 64 antigens. For the MTB experiments, two samples were prepared and subjected to sequential IP with the use of three antibodies to isolate HLA-DP, DR/DQ and HLA-II. The result was the identification of 81 antigens.

3.3 Results

3.3.1 Profiling identified MHC peptides

To identify peptides associated with HLA-DP and -DQ, I utilised the frozen cell lysates from BCG experiments (six samples), which underwent two successive IP procedures. In the first IP procedure, I used a DP-specific antibody (B721) to isolate HLA-DP molecules. In the second, I used a pan-class II antibody (IVA12) to isolate HLA-DQ molecules. It is important to note that the use of the pan-class II antibody (IVA12) may also pull-down other class II molecules that are present in the cell lysate besides HLA-DQ. Peptides were dissociated from HLA complex components, purified and analysed through the use of LC-MS2 (details of process described in Chapter Two). The mass fragment spectra were de-novo sequenced and mapped against the human and BCG proteome databases (imported from UniProt) through the use of Peaks Studio software. Identified peptides were exported at a threshold score of $-10\log P=15$ to maintain the confidence of peptide spectrum matches (PSMs). A total of 39 and 34 unique BCG peptides were identified, associated with DP and DQ molecules, respectively. These represented 64 proteins (Figure 3.2, A and B, and Appendix Table 7.1). I observed that the total number of identified peptides was higher in samples treated with IFNγ compared with untreated samples. As expected, the distribution of the overall lengths of the peptides was indicative of MHC-II, as the majority of identified peptides were of lengths between 13 and 17 amino acids in both MHC isotypes (Figure 3.2, C and D). However, a high percentage of 9-mer long peptides were seen in the data associated with HLA-DP, which could be a characteristic of the HLA-I peptides as a result of co-immunoprecipitated contaminants.

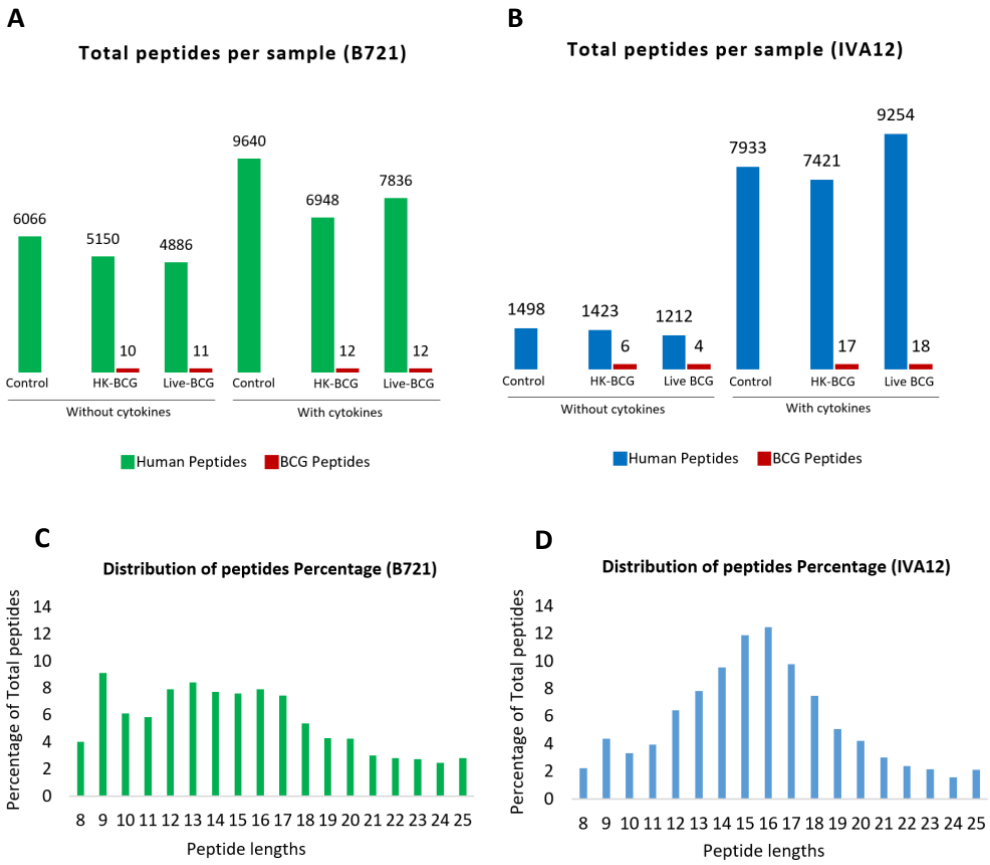


***Figure 3.3* Total numbers and distributions of peptides.**

A and B show the total numbers of peptides per sample. The numbers against bars indicate the total peptides per sample (human and BCG). Samples 1, 2 and 3 contained no cytokines, whereas samples 4, 5 and 6 were dosed with IFNγ and anti-IL-10 two days before infection. C and D show the distributions of peptide lengths from eight to 25 amino acids as percentages. The peptides resulted from HLA-DP and HLA-DQ IP. All analyses based on the data exported from Peaks software.

3.3.2 **Prediction of binding motifs**

The HLA-II molecules present in the BCG experiments (six samples) were isolated through the application of sequential IP in the following order: HLA-DR, HLA-DP and HLA-DQ. L243 and B721 antibodies were used to bind specifically to HLA-DR and HLA-DP, respectively. However, for HLA-DQ, the pan-class II antibody IVA12 was used. IVA12 can bind to all class II molecules, including HLA-DP, -DQ, and -DR. Because IVA12 antibodies are pan-HLA-II, it was unclear whether the identified peptides that resulted from the IVA12 antibody IP were associated mainly with HLA-DQ or with other isotypes that were still present. To confirm with which isotypes the identified peptides were associated, I used 5751 unique peptides (12-18 amino acids long), which represent the majority of peptides (Figure 3.3 D), for prediction analysis that involved use of the NetMHCIIpan server. When they were predicted against HLA alleles of THP-1 cells (DRB1*0101; DRB1*1501; DRB5*0101; DQA1*0102-DQ1B*10105; and DQA1*0102-DQB1*0206), most of the peptides were found to be associated with DR alleles and a few peptides were found to be associated with HLA-DQ alleles. This result was unexpected. Additionally, there were a few peptides that were assigned to HLA-DP alleles. The effect of IFNγ on boosting the presentation of peptides was seen across all HLA-II alleles to variable degrees when compared with untreated and treated samples (Figure 3.4).

Consistently, when I used the GibbsCluster 2.0 server to predict the peptide-binding motifs of each set of peptides associated with each allele (from previous step). These predictions enabled the visualisation of sequence logos of binding cores, as described by Andreatta, Alvarez and Nielsen (2017). When I compared the predicted binding motifs with the reference binding motifs provided by

NetMHCIIpan. Also, the performance of Gibbs clustering analysis revealed that binding motifs of predicted peptides restricted to DR, DP and DQ alleles were aligned with reference binding motifs. This finding indicated that the majority of peptides that were identified from the IVA12 experiment were associated with HLA-DRB alleles (Figure 3.5).

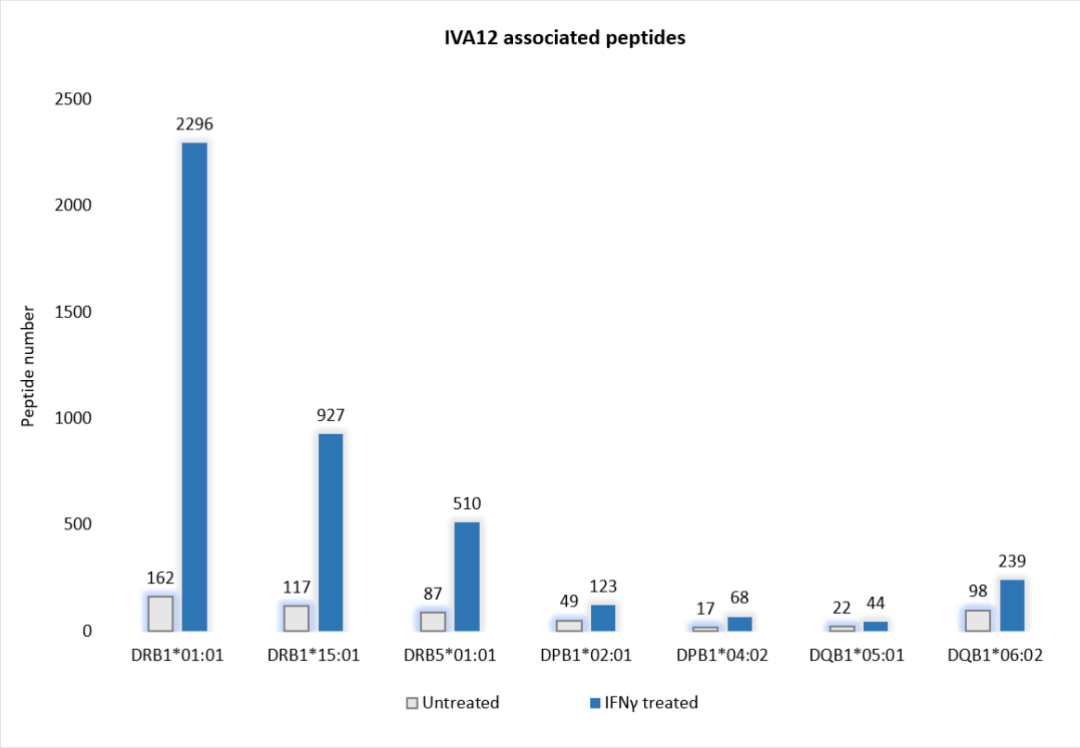


Figure 3.4 Prediction of peptide affinity against THP-1 HLA alleles.

Peptides of length 12-18 obtained from an IVA12 IP process were analysed to predict their binding affinity to the THP-1 HLA alleles. The predicted peptides were compiled by IFNγ treatment condition. The prediction analysis was undertaken by the NetMHCIIpan server.

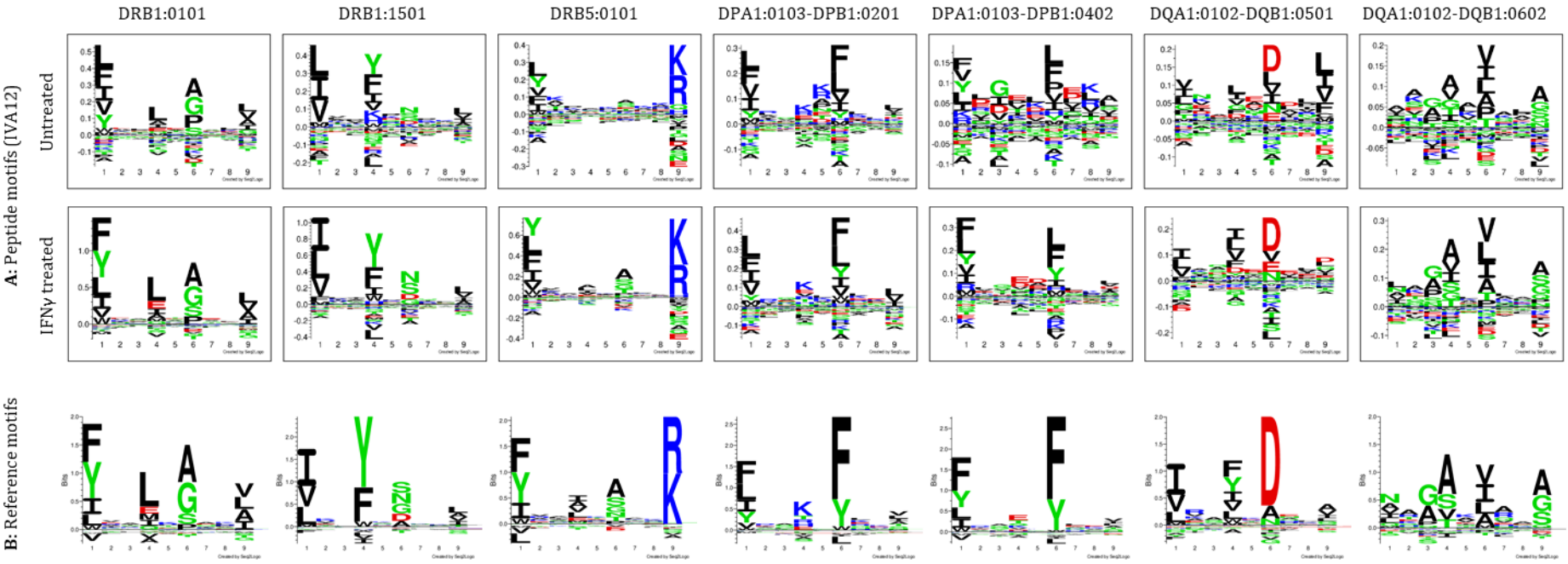


Figure 3.5 Prediction of binding motifs of human peptides.

Panel A shows the binding motifs of the predicted peptides identified from samples associated with IVA12 antibodies which were grouped based on the treatment of IFNγ. Panel B shows the reference binding motifs (obtained from e NetMHCII motif viewer) of HLA-DR HLA-DP and HLA-DQ. All predicted binding motifs of human peptides were generated by the GibbsCluster server.
Amino acid key: acidic [DE]; basic [HKR]; hydrophobic [ACFILMPVW]; neutral [GNQSTY].

3.3.3 Optimisation of MTB macrophage-infected model

The workability of the *in vitro* model of BCG-infected macrophages motivated me to use MTB as an infectious agent to identify MTB-derived peptides through the use of the immunopeptidomics approach. However, any experiment that involves the use of MTB must be conducted under comprehensive and strict biosafety measures, including the use of a biosafety level 3 laboratory (BSL3). Any sample exposed to MTB that is to be investigated further outside the BSL3 must be fully decontaminated of MTB. As a result, I optimised further the *in-vitro* model regarding the optimal time for IFNγ treatment and I introduced a decontamination step so that I could transfer the samples for immunopeptidomics analysis. I decided to limit the sample number to two, one control and one infected, to minimise the number of samples that would be used in the BSL3 facility, as I had to infect $3x10^8$ THP-1 macrophages per condition, which required the use of six large-cell-type culture flasks ($150cm^2$).

3.3.3.1 Optimisation of the time-point of IFN*γ* treatment

As described, I found that the pre-treatment of samples with IFN*γ* increased the numbers of identified peptides, particularly those associated with HLA-DR. This finding was supported by previous results, which showed that treatment of macrophages with IFN*γ* induced the expression of MHC-II (169, 218). However, IFNγ has been reported to inhibit bacterial uptake *in vivo* and *in vitro* (219), which may lead to a decrease in bacterial peptide yield in the context of MHC presentation. Therefore, I explored the effect of IFN*γ* on mycobacterial uptake to determine the optimal time-point of pre-infection treatment. Determination of this optimal point

could enhance MHC-II expression while it would barely affect mycobacterial uptake.

After THP-1 macrophages had been treated with IFNγ 72, 48 and 24 hours before infection, the cells were harvested for phagocytosis analysis. It was found that the presence of IFNγ reduced phagocytosis of MTB-GFP and BCG-GFP in a time-based manner (Figure 3.5, A and B). Also, I tested whether treatment with IFNγ after infection would enhance MHC expression. I observed that treatment with IFNγ pre-infection enhanced MHC-II expression better than it did post-infection (Figure 3.5, C). Therefore, I decided to treat cells with IFNγ 24 hours before infection to minimise the inhibitory effect on phagocytosis and to preserve peptide presentation.

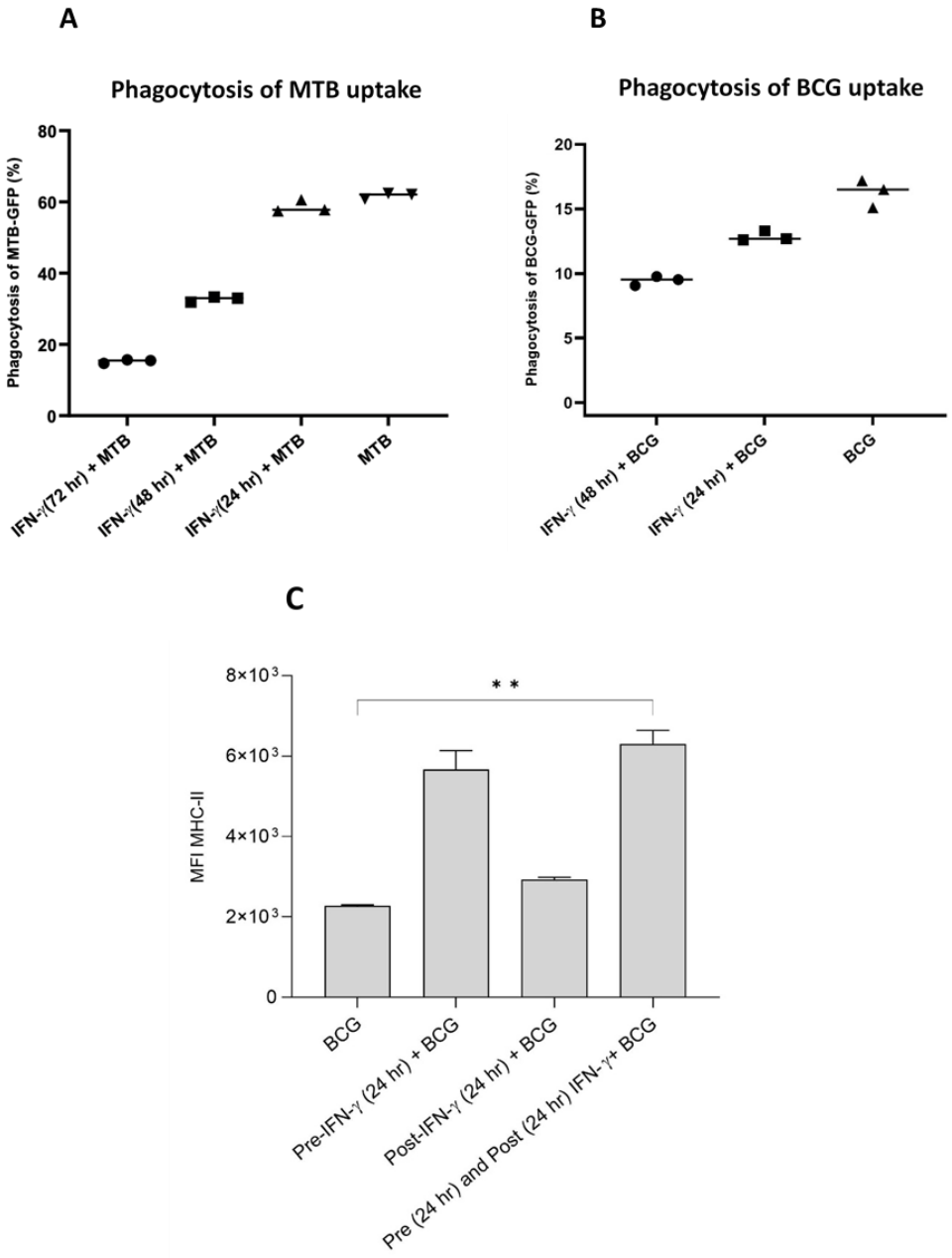


Figure 3.6 The effect of IFNγ on mycobacteria uptake and MHC-II.

THP-1 macrophages were treated with IFNγ (50ng/ml) 72 hours, 48 hours and 24 hours before infection in triplicate. Cells were infected with MTB (panel A) or BCG (panel B) for four hours. Cells were washed three times with phosphate-buffered saline (PBS) to remove extracellular bacteria. Cells were harvested and fixed to be run through flow cytometry. Panel C shows the effect of IFNγ treatment on MHC-II expression upon BCG infection.

3.3.3.2 Determination of the exponential phase of mycobacterial growth and multiplicity of infection

After I had determined the optimal time-point for IFNγ treatment, I monitored the mycobacterial growth curve to determine the log phase, in which the exponential (log) increase would take place to produce a balanced number of single cells. At this stage, I used BCG as a surrogate for MTB, since both strains are known to exhibit similar average cell division rates of 18-24 hours (220). This procedure would avoid the requirement to use the BSL3 for MTB experimentation. After inoculation of BCG into a fresh medium, the log phase was observed to occur from day four to day six and was followed by the stationary phase (Figure 3.6, A). To estimate the number of viable cells that were produced during the log phase, I normalised any optical density (OD) readings to an OD of 0.1 and enumerated the CFUs accordingly through the use of Agar plates, which were equivalent to $\sim 1x10^7$ cells per ml (Figure 3.6, B). Finally, I compared two different multiplicities of infection (MOI) of 1:1 and 10:1 (CFU:cell) *in vitro* through the use of THP-1 macrophages (Figure 3.6, C). Upon reviewing this data, I decided to perform the MTB infection with an MOI of 5-10.

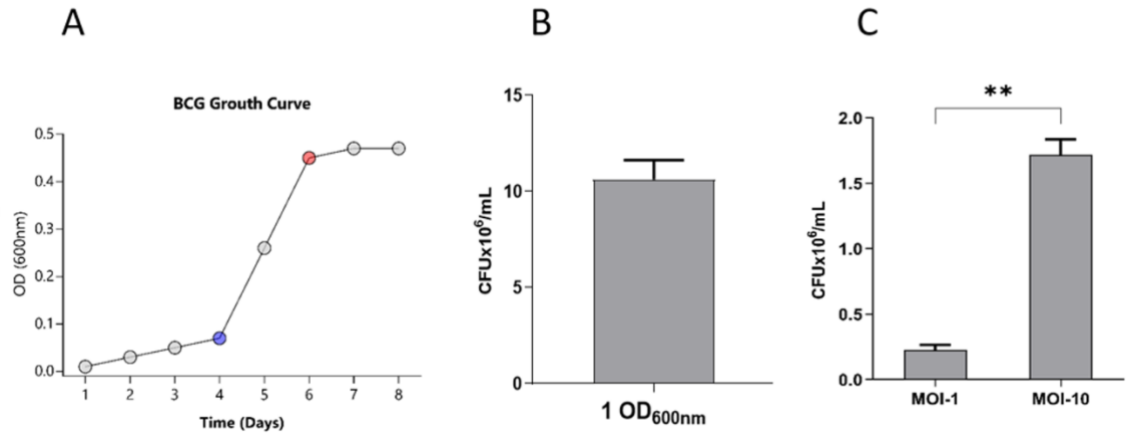


***Figure 3.7* BCG growth rate, counts and multiplicity of infection.**

*A: the BCG growth curve shows that the log phase occurred between days four and six. B the colony-forming unit (CFU) count, based on an optical density (OD) of 1.0. C: differentiated THP-1 cells were infected with different multiplicities of infection (MOI) and CFUs were enumerated one day post-infection. The infection (four hours exposure) was performed in triplicate at MOIs of one and 10. The CFU values are expressed as means ± standard deviation. The Mann Whitney test was used to compare CFU counts, **p <0.01.*

3.3.3.3 Validation of sterility test for MTB

I validated a sterilisation method that I could use to remove samples from the BSL3 facilities. This involved subjecting the contaminated samples to membrane filtration (0.22uM) twice (221). To verify the sterility of the filtrates, the BACTEC MGIT 960 system was used to detect MTB rapidly and accurately (222). No mycobacterial growth was detected in the filtered samples, whereas the unfiltered controls registered positive after 56 days.

3.3.4 Profiling identified MHC peptides upon MTB-infected macrophages

I performed *in-vitro* experiments using MTB according to the schematic layout shown in Table 3.2. About $3x10^8$ THP-1 macrophages were treated with IFNγ for 24

hours and infected with MTB at an MOI of five. Cell lysates were filtered twice and subjected to sequential IP through the use, first, of a DP-specific antibody (B721), followed by the use of a pan-class II antibody (IVA12) and finally a pan-class I antibody (W632). Peptides were eluted, purified and analysed through the application of LC-MS2. I analysed the mass fragment spectra with the use of Peaks software against a database of human and MTB proteomes (both imported from the UniProt database). Once analysed, the identified peptides were exported at a threshold score of – 10logP=15 to maintain the quality of PSMs. Most peptides were between 13 and 17 amino acids long for MHC-II (Figure 3.7, A-D) and nine long for MHC-I (Figure 3.7, E and F). Then, after I had applied filtration criteria (provided in the method section), I identified 87 non-redundant MTB peptides, which represented 81 unique proteins (Appendix Table 7.2).

Table 3.1 *The experimental layout for MTB infection.*

Control	**Live MTB**	
Sample 1	Sample 2	With IFNγ and anti-IL-10

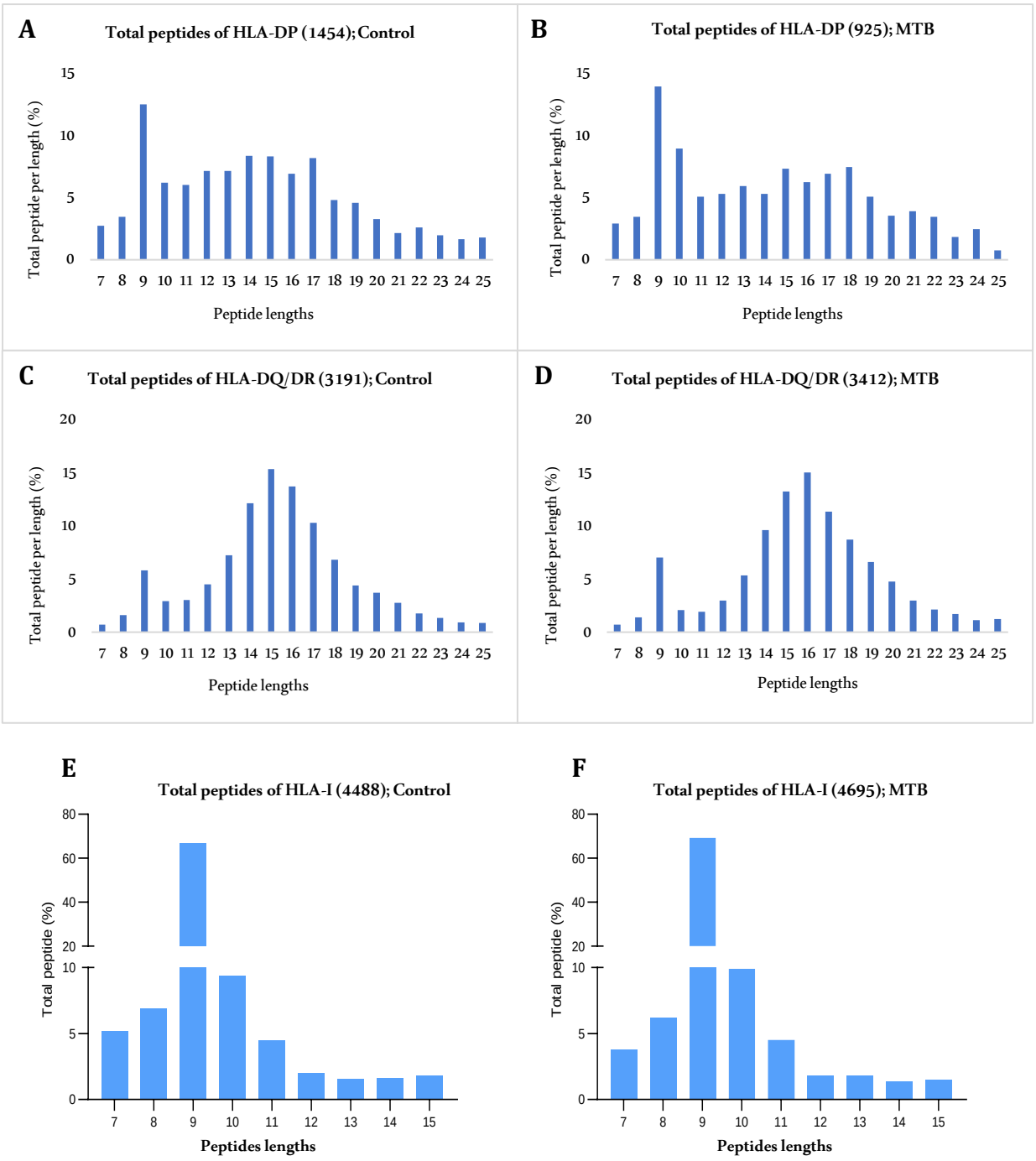


***Figure 3.8* Distribution of peptides.**

The distribution of peptides that were of lengths 7- 25 amino acids and which resulted from HLA-DP (A and B), HLA-DR and DQ (C and D) and MHC-I (E and F) are shown as percentages. The numbers in brackets indicate the total numbers of identified peptides.

3.3.5 Selection and prioritisation of candidate antigens

As depicted in Figure 3.2, the total number of mycobacterial proteins that derived from BCG and MTB was 193, including 11 shared proteins (groS, hisD, Rv0426c (BCG_0465c), Rv2164c (BCG_2181c) Rv3239c (BCG_3788), Rv3776 (BCG_3838), nrp, PE_PGRS48, PE_PGRS53, PE1 and ppsD). Determination of the potential protective candidates among the total of 193 unique proteins would have required a huge amount of time and effort. Therefore, I devised an approach through which candidate antigens could be selected rationally based on immunopeptidomics and immunoinformatics tools, Figure 3.9.

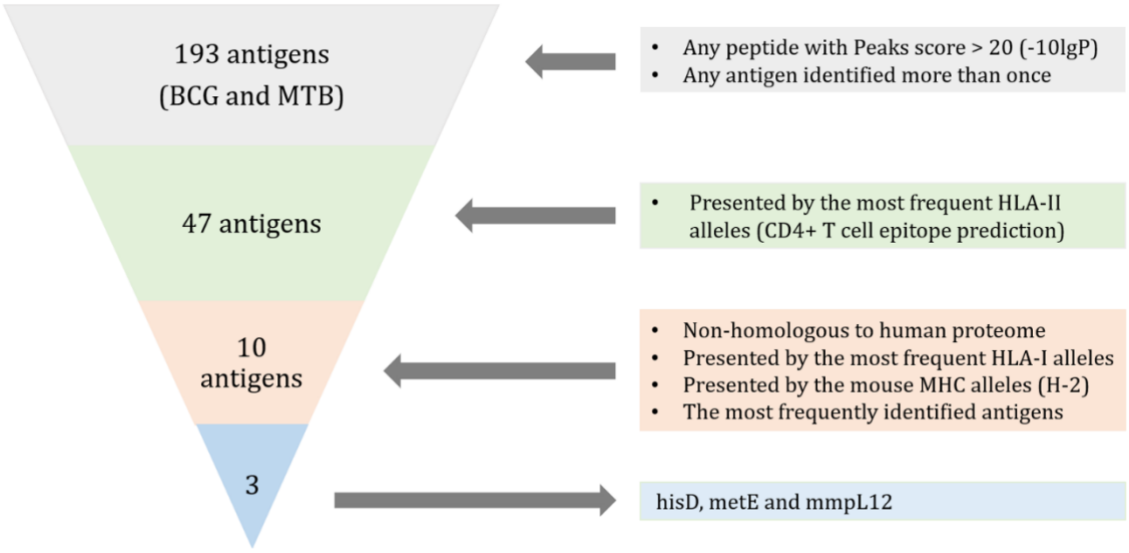


Figure 3.9 Antigen selection process

The selection criteria were applied in three main steps. Firstly, mycobacterial proteins with a peptide Peaks score greater than 20 or that were identified more than once were selected; this process resulted in a set of 47 antigens. Secondly, after HLA-II coverage had been predicted through the use of the most frequent alleles, the antigens with full coverage were selected; this process resulted in 10 candidates. Finally, from the 10 antigens, the most frequently identified, non-homologous antigens that were presented by the frequent HLA-I alleles were selected. This method led to a final list of three candidate antigens: hisD, metE and mmpL12.

3.3.5.1 Peaks-score-based selection

Each identified peptide was assigned a Peaks score (-10logP), which indicated the quality of the match between the *de-novo* sequencing peptide (peptide reconstruction based on MS-MS spectrum and the peptide mass) and the database peptide (reference peptide). A Peaks score of 20 is equivalent to a P-value of 0.01, so the higher the value of -10logP, the greater the significant match and confidence (167, 223). Therefore, I selected the mycobacterial proteins with a peptide Peaks score greater than 20, which resulted in more accuracy as the average false discovery rate (FDR) was 0.85% for BCG peptides and 1.38% for MTB peptides. This selection criterion resulted in a set of 47 proteins, 24 of which are from BCG, 18 from MTB, and five were shared across both, Figure 3.10 and Appendix Table 7.3.

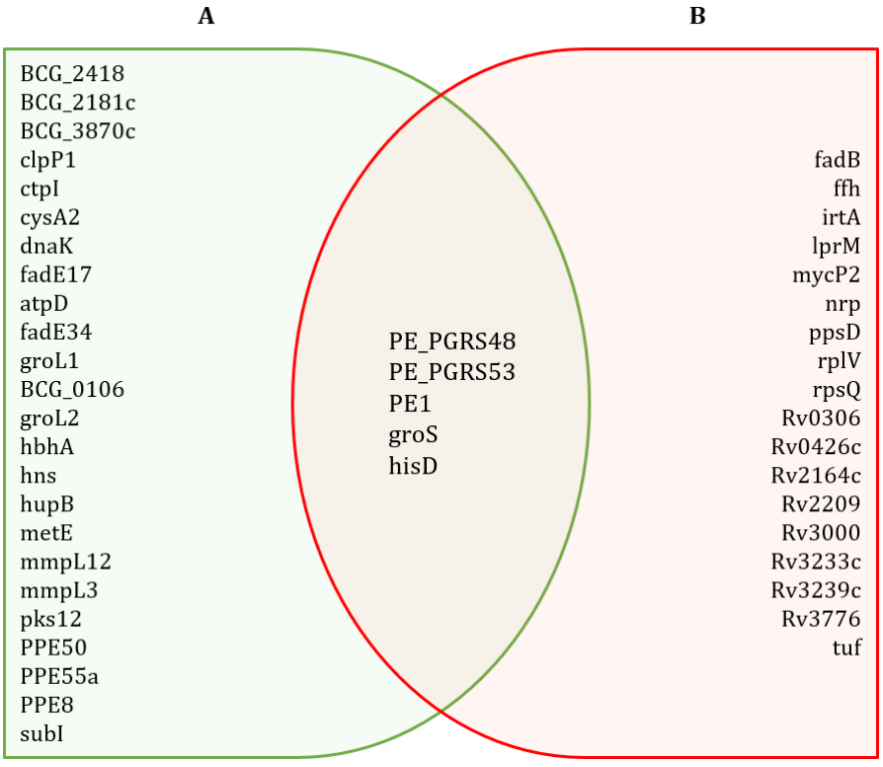


Figure 3.10 First set of selected mycobacterial proteins
Panel A shows the proteins derived from BCG and Panel B shows proteins derived from MTB. Additionally, there are 5 shared proteins.

3.3.5.2 MHC allele-coverage-based selection

Despite the wide diversity of HLA alleles, some alleles are more commonly seen than others. According to the IEDB, there is a set of 27 HLA-II supertype alleles from the HLA-DR, -DP, and -DQ loci, providing more than 98% of population coverage worldwide (224). Targeting the supertype alleles is an effective strategy for selecting antigen candidates with broad MHC presentation in the majority of the populations. Therefore, each of the 47 protein sequences was analysed with the use of the NetMHCIIpan server to predict those that were likely to contain MHC-II binding peptides (Appendix Table 7.4 and Table 7.5). I used the server's default percentile rank, which is a specific threshold to classify the peptide binding affinity level, where 1% was used to identify strong binders, and 5% was used to identify weak binders. Mycobacterial proteins with a broad repertoire (strong and weak binders) that covered all 27 alleles were selected. This process resulted in selection of ten candidate antigens: BCG_2418, BCG_3870c, fadE17, fadE34, hisD, metE, mmpL12, mmpL3, Rv3239c and Rv3776.

3.3.5.3 Homology-based selection

A non-self-antigen with a high degree of sequence similarity to human proteins could cause an autoimmune response (225) or might not elicit a desirable immune response, as the immune system may not recognize the antigen as foreign and therefore not mount an immune response against it. Therefore, I excluded any mycobacterial proteins that contained sequences similar to those of the human proteome from further consideration as potential vaccine candidates. To accomplish I utilized a bioinformatics tool the Vaxign server (226), which relies on the Basic Local Alignment Search Tool (BLAST) protein database to calculate the homology between sequences in terms of the Expect value (E-value). The E-value indicates the level of similarity of the

sequences and the likelihood that the match is due to random chance, i.e., the lower the E-value, the more likely it is that the match is significant. Statistically, any match with an E-value below 10-6 is considered significant (227, 228). Therefore, the mycobacterial proteins fadE17 and fadE34 were excluded because they contain sequences that are homologous to human proteins, Table 3.2.

Table 3.2 *E- value of mycobacterial proteins*

Antigen		**Length**	**E-value**
1	BCG_2418	642	0.27
2	BCG_3870c	637	1.0
3	fadE17	409	$2x10^{-28}$ homologous to the human acyl-CoA dehydrogenase enzyme
4	fadE34	711	$3x10^{-18}$ homologous to the human isovaleryl-CoA dehydrogenase enzyme
5	hisD	438	6.6
6	metE	759	1.9
7	mmpL12	1107	0.39
8	mmpL3	944	No hits found
9	Rv3239c	1048	$2x10^{-11}$
10	Rv3776	519	No hits found

3.3.5.4 The candidate antigens

I added a further tier to select from within the final set of top candidates: the prediction of CD8+ T-cell epitope repertoires. I used the NetMHCpan server to predict MHC_I binding peptides through the use of a set of MHC_I alleles with >97% coverage across the populations (229) (Appendix Table 7.6). Also, the prediction of mouse MHC (H-2) was included, as these candidates were to be evaluated in the mouse model, using the NetMHCpan server (Appendix Table 7.7). Three potential antigens (hisD, metE, and mmpL12) were selected for protective efficacy

evaluation, as they were found to be conserved in BCG and MTB strains, provide broad HLA coverage (class I and II) across the population and are considered non-homologous to the human proteome (Table 3.3). The construction, preparation and evaluation of these antigens are discussed in detail in Chapter 5.

Table 3.3 *Immunopeptidomics and immunoinformatics characterisation of candidate antigens.*

Antigen	Immunopeptidomics					Immunoinformatics				
	Length	Identified peptide (mass spec)	Length	Peaks score (-10lgP)	Sample source	HLA hit (THP-1 alleles)		HLA-I and HLA-II coverage (%)	Mouse MHC coverage (%)	Protein homology (human)
						HLA	%Rank*			
hisD	438	KDVSGHVIT	10	20.04	HK-BCG infection (B721; HLA-DP)	HLA-C-0303	21.71	100	100	Non-homologous
		RVGIDAEAGPT RVGIDAEAGPT	11 11	19.9 19.71	Live BCG infection (L243; HLA-DR) Live MTB infection (W6/32; HLA-I)	HLA-C-0303	29.58			
metE	759	DTNYHYLVPEIGPS DTNYHYLVPEIGPS DTNYHYLVPEIGPS	14	46.86 25.94 31.61	HK-BCG infection (IVA12; pan-HLA-II) Live BCG infection (IVA12; pan-HLA-II) HK-BCG infection (L243; HLA-DR)	DRB1-0101	0.40	100	100	Non-homologous
mmpL12	1107	AGCTLLIR	8	24.98	Live BCG infection (W6/32; pan-HLA-I)	HLA-C-0303	33.83	100	100	Non-homologous
		KALMSIGKVITASAAT	16	16.7	Live BCG infection (IVA12; pan-HLA-II)	DQA10102-DQB10602	6.40			
		KLIENLRADT	10	15.17	HK-BCG infection ((IVA12; pan-HLA-II)	HLA-A-0201	4.37			

* %Rank <20 indicates good binder

3.4 Discussion

As there is an urgent need for an effective vaccine against TB, I employed immunopeptidomics and immunoinformatics to identify novel antigens for consideration as candidate subunit vaccines. By using infected macrophages as *in-vitro* models of TB, followed by mass spectrometric analysis to identify mycobacterial peptides presented by MHC molecules, I have identified 64 and 81 proteins derived from BCG and MTB, respectively. These proteins were prioritised *in silico* through the use of immunoinformatics tools, resulting in a list of potential candidate antigens.

To provide cellular immunity, TB vaccines should induce the production of memory T cells that mediate a fast immune response upon infection and the killing of the infected cells (230). However, a lack of knowledge among vaccine researchers regarding which antigens may be presented by infected cells with potential to induce protective T-cell responses, has posed challenges in the development of protective vaccines against intracellular pathogens, including TB (231). Since T cells are activated via the presentation of MHC molecules, immunopeptidomics has facilitated the identification of T-cell antigens that may be presented by MHC molecules. The application of immunopeptidomics for the discovery of novel TB antigens is rather limited compared with its use of tumour antigens (178). In this regard, a few groups have implemented immunopeptidomics since 2002 to identify novel antigens in the context of MHC peptide presentation.

In humans, active TB disease is caused by inhalation of aerosolised MTB, which is encountered and phagocytosed by alveolar macrophages. Once phagocytosed, a macrophage either eliminates the bacilli or provides a niche for the residence of

persistent mycobacteria. My model of macrophages infected with BCG or MTB mimics to some degree the natural infection and enables the identification of MHC-associated mycobacterial peptides that are produced as a result of the interaction between internalised mycobacteria and macrophages. The THP-1 cell line is widely used as an alternative to primary human macrophages to study immune responses to MTB infection *in vitro,* because it exhibits similar reactions in terms of bacterial uptake, cytokine profiles (IFNγ, IL-1β and TNF-α) and CFU load post-infection (232, 233). The identification of protective antigens that are expressed during early interaction between MTB and macrophages is a key to the development of novel vaccine candidates. The use of MS provides direct identification of mycobacterial peptides that are presented by MHC molecules after *in-vitro* MTB infection, from which precursor mycobacterial proteins can be identified.

A limitation of identifying MHC-associated peptides is that peptides with low binding affinities may not be detected because they dissociate during the processing of samples before their elution and purification (234). Also, MS analysis requires a large number of cells as starting material, because MHC complexes must first be purified from whole-cell proteomes, and the associated peptides further purified for LC-MS analysis. However, the use of the THP-1 cell line, in this case, addressed this issue and enabled the achievement of the amount of interest, which was in the range of ~6 x10^8 MTB-infected cells. Additionally, the THP-1 cell line is homogeneous; its proliferation can be maintained for up to 25 passages and usage does not require ethical approval (235). Moreover, utilisation of a cell line as a starting material enabled the expansion of the range of identified peptides compared with the range that would be produced in *in-vivo* models that employed mice. For example, in one study, from splenocytes isolated from MTB-infected mice,

only four MHC-I-associated MTB unique peptides were identified (236), whereas 37 peptides restricted to MHC-I were identified from my model of THP-1 macrophages infected with MTB.

I observed during the BCG experiments that samples treated with IFNγ and anti-IL-10 antibodies produced higher yields of immunopeptidome compared with the amounts produced during use of untreated samples (Figure 2, A and B). MTB employs various mechanisms to evade host immunosurveillance by T cells, including inhibition of MHC-II expression and presentation (237). The inhibitory effects were reported as a result of interference with IFNγ pathways via down-regulation of class II transactivator (CIITA) (238, 239) and up-regulation of histone deacetylase (HDAC) (240). Another IFNγ-independent mechanism was reported via induction of IL-10, which was found to inhibit the expression of cathepsin S and thus processing of MHC antigens (190, 215). Therefore, I treated the THP-1 macrophages with IFNγ and anti-IL-10 antibodies one day before I infected them with MTB to enhance MHC processing and presentation of mycobacterial peptides. In line with my observation that mycobacterial uptake decreased upon prolonged (>24h) treatment with IFNγ before infection, a study reported that, upon viral infection, IFNγ inhibited the capacity of alveolar macrophages phagocytose pneumococcal bacteria (241). These researchers found that IFNγ caused down-regulation of a class A scavenger receptor, the macrophage receptor with collagenous structure (MARCO), which mediates uptake of unopsonised bacteria. It was unclear whether prolonged stimulation with IFNγ at the site of infection would reduce rates of mycobacterial uptake and clearance. The presence of IFNγ clearly enhanced the number of peptides that were identified as associated with HLA-DR alleles compared with those linked with DP or DQ. After peptides from IVA12 IP

samples had been stratified according to their binding affinity to THP-1 HLA-II alleles, most of the peptides were found to be associated with HLA-DR subtypes (Figure 3). This stratification was confirmed by visualisation of the sequence logos of peptide binding motifs, which were compared with the logos of the reference binding motifs (Figure 4). Taken together, it was found that pre-treatment of macrophages with IFNγ enhanced the presentation of peptides associated with HLA-DR predominantly, which raised a question about this selective effect. In a follow-up experiment, I investigated the up-regulation effect of IFNγ on each HLA-II subtype. I observed that HLA-DR was the most up-regulated subtype (more detail is given in Chapter 4). In this regard, a study has reported that treatment of breast cancer cells with IFNγ enhanced the number and diversity of antigens that were presented by MHC-I and MHC-II (242). So, because the presence of IFNγ improves the yield of the immunopeptidome, its use may enable the identification of less abundant peptides.

The successful identification of new antigens derived from BCG inspired me to use a virulent MTB strain (H37Rv) in my *in vitro* infection model to identify MTB antigens. BCG exhibits a high degree of similarity in its DNA sequence (>99.9%) with MTB and has been used experimentally and clinically as a proxy for MTB in drug and vaccine screening (243-245). However, a comparative genomic analysis of the two bacteria has revealed that 14 RDs are absent in all BCG strains compared with MTB H37Rv (246). Another analytical study has reported that 133 genes are absent from BCG compared with MTB due to RDs (185), and among these, genes that express antigenic proteins containing 433 T-cell epitopes have been validated empirically (247). For example, Rv3879 is encoded within RD1 and has been reported to be a T-cell antigen as it has been recognised in MTB-infected people

(248) and cattle (249) compared with BCG-vaccinated subjects. It is of note that the expression of certain genes of intracellular MTB (e.g. in infected macrophages) is different from that in MTB grown extracellularly (liquid medium) (250). This could explain why my MTB experiments did not lead to the identification of certain mycobacterial proteins known to be highly expressed during MTB growth, including ESAT-6 and Ag85B. Nevertheless, 81 antigens in the context of MHC were identified. When I compared proteins derived from BCG and MTB, I found 11 shared mycobacterial proteins, three of which were identified by the same nested peptide sequences, groS (NGEEYLILSARDVLA), hisD (RVGIDAEAGPT) and PE1 (TTYTLEYDG).

Classical approaches are commonly employed for the initial assessment of candidate antigens of interest. One such is the investigation of IFNγ-secreting T cells *in vitro* from samples exposed to MTB infection or BCG vaccination to identify immunogenic antigens (251). However, to screen for many antigens, such an approach requires the expenditure of considerable effort and time. Additionally, IFNγ does not represent a reliable correlate of protection (98), and CD4+ T cells have been shown to mediate IFNγ-independent immunity against TB (252).

The utilisation of immunoinformatics tools has facilitated the selection of candidate antigens for vaccine evaluation irrespective of cytokine profiles. Because MHC-II molecules mediate the activation of CD4+ T cells, the rationale for the selection relies on the mapping of T-cell epitopes through the application of prediction analysis *in silico*. During the COVID-19 pandemic, it was found that computer-based mapping of T-cell epitopes generated data with high confidence in less time than experimental methods (253). I employed *in-silico* tools to prioritise candidate antigens based on the prediction of T-cell epitope repertoires that could bind to

given HLA alleles. Peptide-MHC binding is a selective association due to the high polymorphism of HLA alleles, which leads to the preference of alleles for the distinct binding of a set of peptide sequences (called motifs). *In-silico* analysis enabled me to tackle this crucial issue of heterogeneity of HLA across the population via the inclusion of a reference set of 27 common HLA-II alleles (across DP, DQ and DR) in the general population for the prediction of peptide-MHC binding (224). Limiting the prediction of T-cell epitopes to the reference HLA alleles may introduce bias; nevertheless, utilisation of these alleles is a sensible and efficient solution (84) and has been used not only for TB (251) but for other pathogenic diseases, such as leishmaniosis (254), malaria (255), Dengue fever (256) influenza (257) and COVID-19 (258). Among other prediction tools, the outperformance of the NetMHCIIpan server is well recognised and benchmarked, as it has been trained on two integrated datasets, binding affinity generated in vitro and eluted ligands generated by MS (179, 259). The use of the latter dataset enhanced the prediction power, as the ligands resulted from the natural processing and presentation of the peptide on MHC molecules.

The primary selection criterion was to define the mycobacterial proteins that were predicted to be rich in CD4+ T-cell epitopes, because of the essential role of CD4+ T lymphocytes in the provision of immunity against TB and their role in the enhancement of effector functions and memory development of both B cells (260) and CD8+ T cells (261). Nevertheless, I used the most common HLA-I alleles to map the presence of CD8+ epitopes for the top eight candidate antigens (Appendix Table 5) to broaden population coverage and cover CD8+ immunity (229). The consideration of antibody response was implicit upon the prediction of CD4+ T-cell epitopes, since B cells are antigen-presenting cells and interaction with CD4+ T cells

has been shown to enhance the development of B cells, both plasma and memory, and the generation of mature antibodies (262). Moreover, the antigens selected for protective evaluation were designed to be expressed in the host as a whole protein, as this would offer maximum opportunity to induce both cellular and humoral responses.

Three mycobacterial proteins (hisD, metE and mmpL12) were selected for the initial evaluation of protective efficacy through the use of the MGIA tool (Chapter 5). These proteins are present in both BCG and MTB strains and, to the best of my knowledge, their immunogenicity and protective efficacy have not been investigated previously. The protein hisD (Rv1599) is essential for MTB growth *in vitro* (263) and *in vivo* (264), and has been selected in a study of 50 antigens as a target for new anti-TB drugs (265). Immune cells can mediate histidine degradation as a mechanism to limit the proliferation of MTB. However, MTB has been found to counteract this by synthesising its own histidine through the hisD enzyme (264). When two-dimensional, capillary high-performance LC coupled with MS (2DLC/MS) was used in a study, metE protein was detected in three subcellular localisations (cytosol, cell wall, and cell membrane) (266) and the culture filtrate (267). The essential nature of metE for MTB growth is controversial; one study reported the identification of metE among non-essential genes for MTB growth *in vitro* (268), while other studies have shown it to be crucial for MTB growth *in vitro* (263, 269, 270). Regarding mmpL12, despite being reported as a non-essential protein, it was ranked as a protective antigen in a study that employed the reverse vaccinology approach. In that study, 82 antigens involved in MTB virulence or latency, or that belonged to previously identified immunogenic protein families,

were screened. Consistent with my prediction, mmpL12 provided the greatest number of MHC-II epitopes (271).

3.5 Conclusion and future work

My research combined two approaches (immunopeptidomics and immunoinformatics) to identify and prioritise novel antigens for the development of subunit vaccines against TB. First, I identified mycobacterial peptides that were presented on MHC alleles of THP-1 cells; then I predicted the presentation of mycobacterial proteins that have been identified on the most common human MHC alleles that could be used to develop candidate vaccines with wide population coverage. An interesting finding was that IFNγ enhanced the total number of identified peptides associated selectively with HLA-DR. This observation is investigated further in Chapter 4. Among the top candidates, three mycobacterial proteins (hisD, metE and mmpL12) were selected for evaluation of their protection and immunogenicity, and this part of my study is described in Chapter 5. The combined approaches could be implemented for other pathogens against which a T-cell response is considered protective, and in cases in which accounting for the diversity of HLA alleles is important.

Chapter 4

Effect of IFNγ and small agents on MHC molecules

4.1 Introduction

As mentioned earlier, two primary classes of MHC molecules are found in humans, MHC-I and MHC-II and the MHC-II peptide-binding site (the groove) is formed jointly as heterodimers of two chains (α and β), encoded by two pairs of genes (180). There are three subtypes of MHC-II proteins encoded by human leukocyte antigens (HLA) genes, HLA-DP, HLA-DQ and HLA-DR. Because the level of polymorphism in the HLA loci is very high, the MHC groove is highly diverse. This diversity makes certain HLA alleles bind preferentially to specific peptide sequences (186).

MTB has been shown to employ different strategies, including suppression of MHC expression and presentation to evade the T cell response (190). For example, MTB mediates HDAC expression, such as HDAC6, which can inhibit HLA-DR expression when the cells are stimulated with IFN-γ. Studies have shown that suppressing HDAC activity in infected THP-1 cells can restore HLA-DR expression (240, 272). Targeting HDAC by Tubastatin A, selectively inhibiting HDAC6 has been shown to enhance immunity against MTB infection via suppression of IL-10 expression (272). The induction of IL-10 cathepsin S from removing the invariant (Ii) chain, which prevents MHC molecules from loading antigenic peptides. (190). As a result, immature MHC molecules (occupied by the Ii chain) are accumulated intracellularly and transported to be expressed on the cell surface. By inhibiting HDAC6, Tubastatin A can reduce the expression of IL-10 and enhance antigen processing and presentation.

Accumulated evidence for the existence of certain HLA alleles associated with susceptibility or resistance to TB disease has been reported in the literature (273). For example, HLA DRB1*01:01 was associated with TB protection according to a genome-wide association study (GWAS) (274), whereas the DRB1*1501 allele was linked with increased risk of TB (275, 276). Moreover, another study reported that the HLA-DRB1*15 allele was correlated with low mycobacterial antibody responses (277). Interestingly, in countries with high TB rates (Brazil, China, India, Russia, and South Africa), HLA-DRB1*15 was reported to be among the most frequently distributed alleles at up to 80% coverage (278). These findings suggest that MTB might target specific HLA-DRB1 alleles to restrict antigen presentation so that induction of a protective immune response is inhibited.

I observed that pre-treatment with IFNγ enhanced the number of identified peptides associated with HLA-DR compared to those associated with HLA-DP and HLA-DQ in THP-1 cells. This raises a question regarding the up-regulation effect of IFNγ on each HLA-II subtype (DP, DQ and DR) of THP-1 cells. The flow cytometric results (Figure 4.1) showed that HLA-DR was the most up-regulated subtype, supporting the immunopeptidomics data. However, as THP-1 cells express three HLA-DRB1 alleles (DRB10101, DRB11501 and DRB5*0101) and there is no available antibody that can target each allele specifically, I used a label-free quantitative proteomics approach using mass spectrometry to investigate the degree of expression of each HLA-DR allele upon IFN-γ treatment and mycobacterial infection. I used the cell lysates from immunopeptidomics experiments that resulted from the IVA12 IP process. The fractions that contained the MHC-II subunit proteins (α- and β chains) were collected and stored after the IP

process. I utilised these fractions to analyse the HLA-DR proteins present in all samples (Table 4.1). This approach allowed you to quantify the levels of HLA-DR alleles and investigate how they were affected by the treatment and infection.

Table 4.1 *The experimental layout of the six samples prepared previously for BCG infection, adapted from Bettencourt et al. (2020).*

Control	**HK BCG**	**Live BCG**	
Sample 1	Sample 2	Sample 3	**Without treatment**
Sample 4	Sample 5	Sample 6	**With IFNγ and anti-IL-10**

4.2 Aims of the work described in this chapter

In the work described in this chapter, I aimed to:

- explore the up-regulation effect of IFNγ on HLA-DP, -DQ and -DR through the application of flow cytometry;
- explore the up-regulation effect of IFNγ the down-regulation effect of BCG infection on the quantity of HLA-DR alleles (DRB1*0101, DRB1*1501 and DRB5*0101) through the use of MS;
- screen the identified mycobacterial peptides to discover their binding affinity with HLA-DR alleles (DRB1*0101, DRB1*1501 and DRB5*0101) through the use of an *in-silico* prediction method (netMHCIIpan); and similarly,
- explore the effect of Tubastatin A on the on the expression of HLA molecules.

4.3 Results

4.3.1 HLA expression upon IFNγ treatment

The variability in the expression levels of surface HLA-II isotypes (DR, -DQ, -DP) has been reported previously (279, 280). To see the up-regulation effect of IFNγ on each HLA-II isotype expressed by THP-1 cells, I treated the differentiated THP-1 cells with IFNγ for two days and measured the expression levels by flow cytometry. Without exposure to IFNγ, the surface expressions of the three HLA-II isotypes were comparable in THP-1 cells. However, after two-day exposure to IFNγ, the surface expression of DR molecules showed maximal up-regulation, with about a 48-fold increase compared with the untreated cells (Figure 4.1, A and D). The surface expression of the DP and DQ isotypes underwent modest up-regulation upon IFNγ treatment of about 6.4- and 3.6-fold increases, respectively (Figure 4.1, B-D).

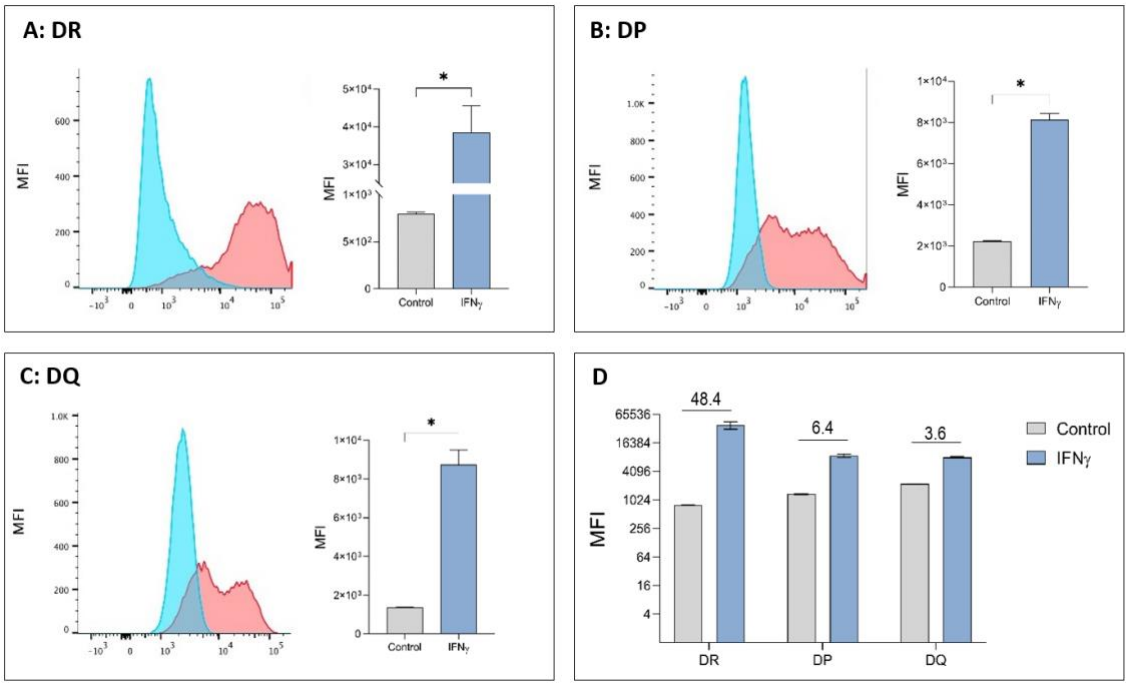


***Figure 4.1* Up-regulation of surface expression of HLA-DR, -DP and -DQ.**
THP-1 cells were treated with 50ng recombinant IFNγ for two days and the expression levels were measured through the use of flow cytometry. Panels A, B and C show the up-regulation effects of IFNγ on HLA-DR, -DP and -DQ respectively compared with the controls. Untreated samples (blue histograms) and IFNγ-treated samples (pink histograms) represent one sample. Mean fluorescence intensity (MFI) was used for fold-change calculations as shown by the numbers between bars, panel D.

4.3.2 Identification of unique peptides that represent HLA-DR chains

The significant up-regulation of HLA-DR leads to consideration of the differential expression among DR alleles of THP-1 cells (DRB1*0101, DRB1*1501 and DRB5*0101) upon IFNγ treatment and BCG infection. To investigate this matter, I analysed the samples that had been used for immunopeptidomics and which represented all required conditions (Table 4.1). But because human MHC proteins are similar to a level of about 70% (281), I firstly identified the unique peptides that were derived from proteolytic HLA proteins and which represented a single allele

using only *in-silico* tools. I employed the PeptideCutter server to predict the peptide fragments that would be produced during trypsin digestion. I filtered out all overlapping peptides, selected those that were unique, and compared them with the MS results (Table 4.2).

Table 4.2 *Unique peptides that correspond to HLA-DR chains identified in silico or in vitro*

Trypsin			
HLA-II allele	*In silico* (PeptideCutter)	*In vitro* (MaxQuant)	*In vitro* (Progenesis)
DRA1*0101	LEEFGR EDHLFR SNAAER ANLEIMTK EPNVLICFIDK FTPPVVNVTWLR VEHWGLDEPLLK FASFEAQGALANIAVDK NGKPVTTGVSETVFLPR FHYLPFLPSTEDVYDCR	ANLEIMTK EPNVLICFIDK VEHWGLDEPLLK FASFEAQGALANIAVDK FASFEAQGALANIAVDKANLEIMTK NGKPVTTGVSETVFLPR	ANLEIMTK EPNVLICFIDK FASFEAQGALANIAVDK FASFEAQGALANIAVDKANLEIMTK FHYLPFLPSTEDVYDCR NGKPVTTGVSETVFLPR VEHWGLDEPLLK
DRB1*0101	FLWQLK DLLEQR NGQEEK CIYNQEESVR FECHFFNGTER	CIYNQEESVR	AVTELGRPDAEYWNSQKDLLEQRR CIYNQEESVR
DRB1*1501	FLWQPK DILEQAR FDSDVGEFR WFLNGQEEK ECHFFNGTER YFYNQEESVR HNYGVVESFTVQR	YFYNQEESVR AVTELGRPDAEYWNSQKDILEQAR	DILEQAR HNYGVVESFTVQR YFYNQEESVR
DRB5*0101	FLQQDK DFLEDR NSQEEK VTVYPAR LPGGSYMAK AQSESAQSK DIYNQEEDLR YECHFFNGTER GHSGLHPTGLVS TQTLQHHNLLVCSVNGFYPGSIEVR	DIYNQEEDLRFDSDVGEYR TQTLQHHNLLVCSVNGFYPGSIEVR	DFLEDRR DIYNQEEDLR DIYNQEEDLRFDSDVGEYR TQTLQHHNLLVCSVNGFYPGSIEVR VTVYPAR

For the quantification, the workflow began with the subjection of HLA proteins (collected after the IVA12 IP process) to enzymatic digestion (trypsin) followed by the analysis of the digested peptide fragments by MS. The abundance of peptides was determined through the measurement of the intensity of the signal for the

peptide ions as recorded by MS. The intensity of the peptide ion signal, together with the number of peptides identified in the sample, can be used as a proxy to determine the relative abundance of the corresponding protein in the sample (282). Once analysed, I used two pieces of quantitative label-free proteomics software, MaxQuant and Progenesis, to process the raw MS-MS data.

Then, I analysed comparatively the unique peptides that had been identified in all samples. At this stage, I employed Progenesis for this task, as this enabled the use of better MS-MS spectra than did MaxQuant, which had generated some missing values (Table 4.3). This observation had been reported previously during a study in which the performance of commonly used software, including MaxQuant and Progenesis, had been evaluated. It was reported that the number of missing values generated by Progenesis was significantly lower than that generated by MaxQuant (283).

Table 4.3 *Reported values of peptide intensities (log_2) generated by MaxQuant and Progenesis*

Software	Allele	Untreated			Treated (IFNγ and anti-IL-10)		
		Sample 1 Uninfected	Sample 2 HK-BCG	Sample 3 Live BCG	Sample 4 Uninfected	Sample 5 HK-BCG	Sample 6 Live BCG
MaxQuant	DRA1*0101	21.45	24.29	24.77	28.66	28.81	28.92
	DRB1*0101	No value	No value	23.4	No value	No value	26.04
	DRB1*1501	24.44	24.96	24.59	26.47	27.72	27.6
	DRB5*0101	No value	23.52	No value	No value	29.02	No value
Progenesis	DRA1*0101	14.36	15.7	15.74	19.65	20.26	20.15
	DRB1*0101	17.4	18.06	18.72	19	19.59	18.92
	DRB1*1501	16.42	17.38	15.1	19.88	20.76	20.81
	DRB5*0101	15.1	15.74	15.28	19.33	19.15	18.86

4.3.3 **Quantification of α or β chains of HLA-DR alleles by use of MS**

Generally, peak intensities for the selected unique peptides showed that IFNγ treatment induced up-regulation of all HLA-DR alleles to various degrees, irrespective of BCG infection (Figure 4,2). Interestingly, without IFNγ treatment, DRB1*0101 was dominantly expressed compared with DRB1*1501 and DRB5*0101. Also, DRB1*1501 was inhibited upon live BCG infection in the absence of IFNγ treatment. In contrast, when treated with IFNγ, DRB1*1501 and DRB5*0101 were up-regulated more than DRB1*0101, and in this case, DRB1*0101 and DRB5*0101 were inhibited by BCG infection (Figure 4.2).

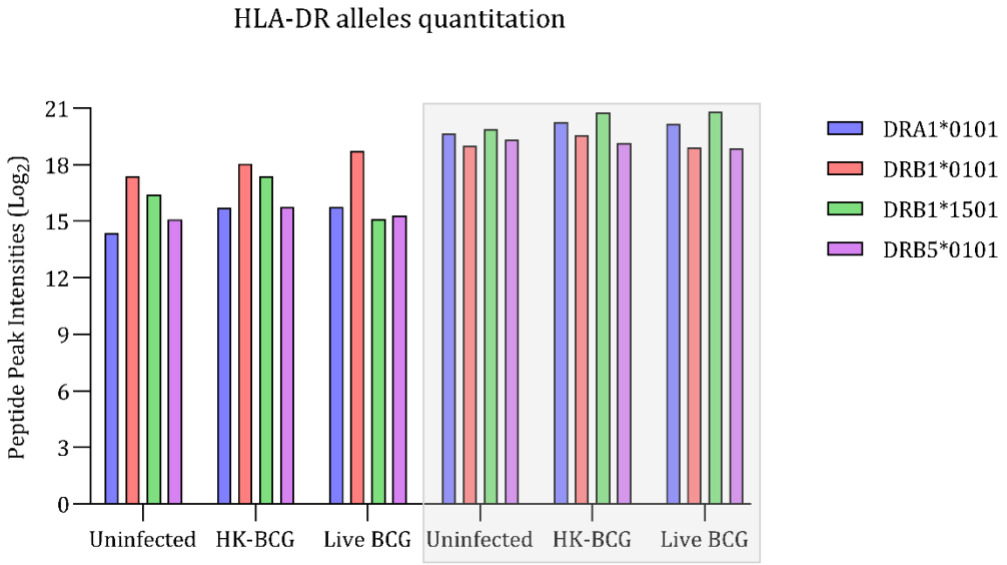


***Figure 4.2* Peptide peak intensities of HLA-DR alleles.**

Peptide peak intensities were generated through analysis of MS-MS spectra by Progenesis (Table 4.3). Each bar represents a or β chains of HLA-DR alleles according to the shown ligands. The x-axis shows the experimental conditions across samples. The shadow area indicates the treated samples with IFNγ and anti-IL-10.

4.3.4 **Comparisons of each HLA-DR chain across experimental conditions**

To estimate the expression patterns of each DR chain (α and β chains) across the experimental conditions (IFNγ treatment and BCG infection), I calculated the fold-change in amounts of chains expressed between relevant samples (sample 1 versus sample 4, sample 2 versus sample 5 and sample 3 versus sample 6). I observed that the fold-change of DRA1 and DRB1*0101 showed a decreasing trend upon infection, whereas levels of DRB1*1501 and DRB5*0101 increased or remained unchanged (Figure 4.3). For DRA1, the fold change between the untreated sample (S1) and IFNγ-treated sample (S4) was 39, which decreased with HK-BCG and live BCG infection to 23.5 and 21.3, respectively. I also saw this trend for DRB1*0101 and DRB5*0101, as infection with HK-BCG or live BCG caused a reduction in the fold change. Interestingly, DRB1*1501 seemed not to be inhibited by BCG infection; on the contrary, its level was increased upon infection, particularly by live BCG.

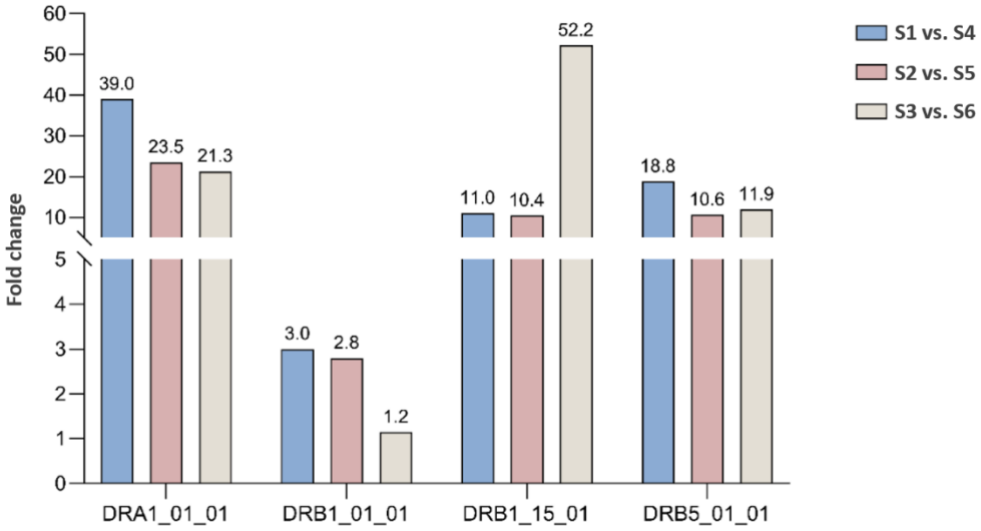


***Figure 4.3* Fold-change analysis.**

Changes in amounts of each HLA-DR chain expressed across experimental conditions were compared in terms of fold-change. Each bar represents the fold-change in peptide intensities. S1: sample 1 (no IFNγ and no BCG), S2: sample 2 (no IFNγ and HK-BCG), S3: sample 3 (no IFNγ and live BCG), S4: sample 4 (IFNγ and no BCG), S5: sample 5 (IFNγ and HK-BCG), and S6: sample 6 (IFNγ and live BCG).

4.3.5 **Analysis of human immunopeptidome (BCG experiments)**

The quantitative analysis of HLA-DR molecules inspired me to analyse the immunopeptidomics data to see the numbers of peptides that were associated with each DR allele. However, the immunopeptidomics data were complex because all HLA-DR molecules had been immunoprecipitated together, regardless of allelic variation. This caused difficulties in the definition of which peptide set was associated with which allele. The cutting-edge prediction tool, MHCMotifDecon, can be used to analyse eluted peptides individually to determine which HLA molecule is most likely to be bound (284). I employed this tool to analyse the immunopeptidomics data collected from the same samples that had been used for quantification. In agreement with the previous observations, the up-regulation effect of IFNγ treatment was observed on all MHC-II molecules. However, the number of peptides assigned to DRB1*0101 was higher than that assigned to DRB1*1501 and to DRB5*0101 across all the experimental conditions (Figure 4.4). Surprisingly, regardless of allele, the numbers of peptides were increased upon BCG infection in all the samples that were infected compared with uninfected samples except for sample 3, which showed a decrease in peptide number (Figure 4.4). The binding motifs of DR alleles that were generated by prediction analysis were similar to the reference motifs of each allele. Generally, they were characterised by four binding anchors with different preferences for amino acids (allele-specific anchors). For example, acidic amino acids characterised DRB1*0101 and DRB1*1501 at positions four and six, respectively, whereas basic amino acids characterised DRB5*0101 at position nine.

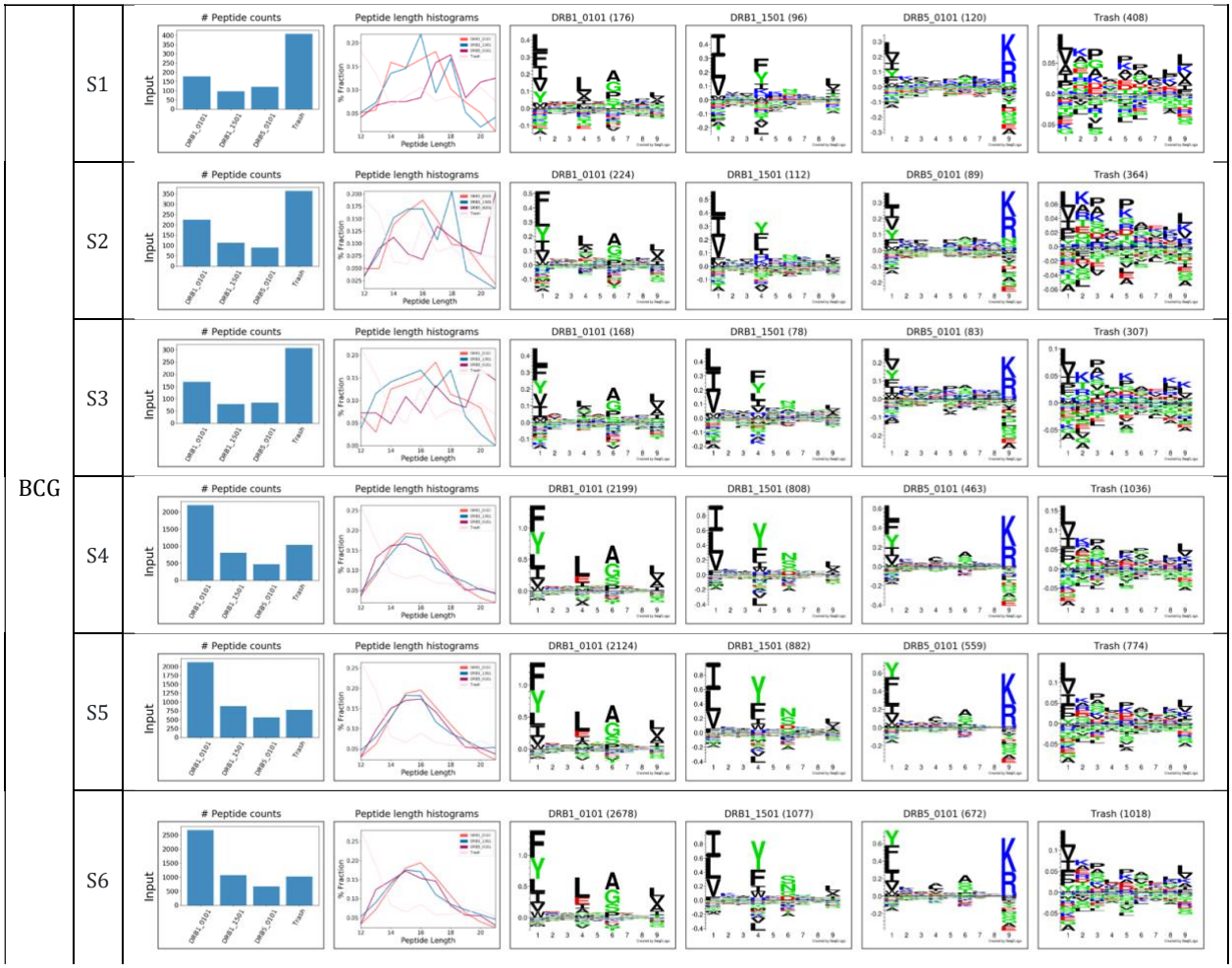


***Figure 4.4* Peptide motifs and numbers taken from the immunopeptidomics data for individual HLA-DR alleles or trash clusters.**

All identified peptides of lengths 12-25 amino acids were used for the analysis, considering a percentile rank score >20% (trash bin 20% by default). Peptide counts, length distribution and binding motifs per allele or trash are shown for each condition. S1: sample 1 (no IFNγ and no BCG), S2: sample 2 (no IFNγ and HK-BCG), S3: sample 3 (no IFNγ and live BCG), S4: sample 4 (IFNγ and no BCG), S5: sample 5 (IFNγ and HK-BCG), S6: sample 6 (IFNγ and live BCG).

4.3.6 Quantification of HLA proteins and analysis of human immunopeptidome (MTB experiments)

As described in Chapter 1, I performed an *in-vitro* TB model experiment that involved the use of differentiated THP-1 cells (two conditions): the two samples received IFNγ, after which one of them was infected with live MTB, and the other was left uninfected. After IP process, the fractions that contained HLA proteins were analysed as explained in section 2.2. I observed a decrease in the DRB1*0101 (4.6-fold decrease) and DRB1*1501 (4-fold decrease) but not DRB5*0101 upon MTB infection (Figure 4.5, A). I also analysed the human immunopeptidome to discover the contribution of each allele to the identified peptide repertoire. When the peptides were assigned according to their binding affinity, there was an increase in the number of peptides associated with DRB1*1501 and DRB5*0101 upon MTB infection compared with uninfected samples, and the number of peptides assigned to DRB1*0101 did not change upon infection (Figure 4.5, B). The discrepancy between the quantitative and predicted results for the DRB1*01:01 allele could be because there was a bias in the prediction towards this allele, or because the DRB1*1501 and DRB5*0101 proteins were expressed but not loaded with peptides as DRB*10101. This discrepancy was also observed in the previous results (Figure 4.4).

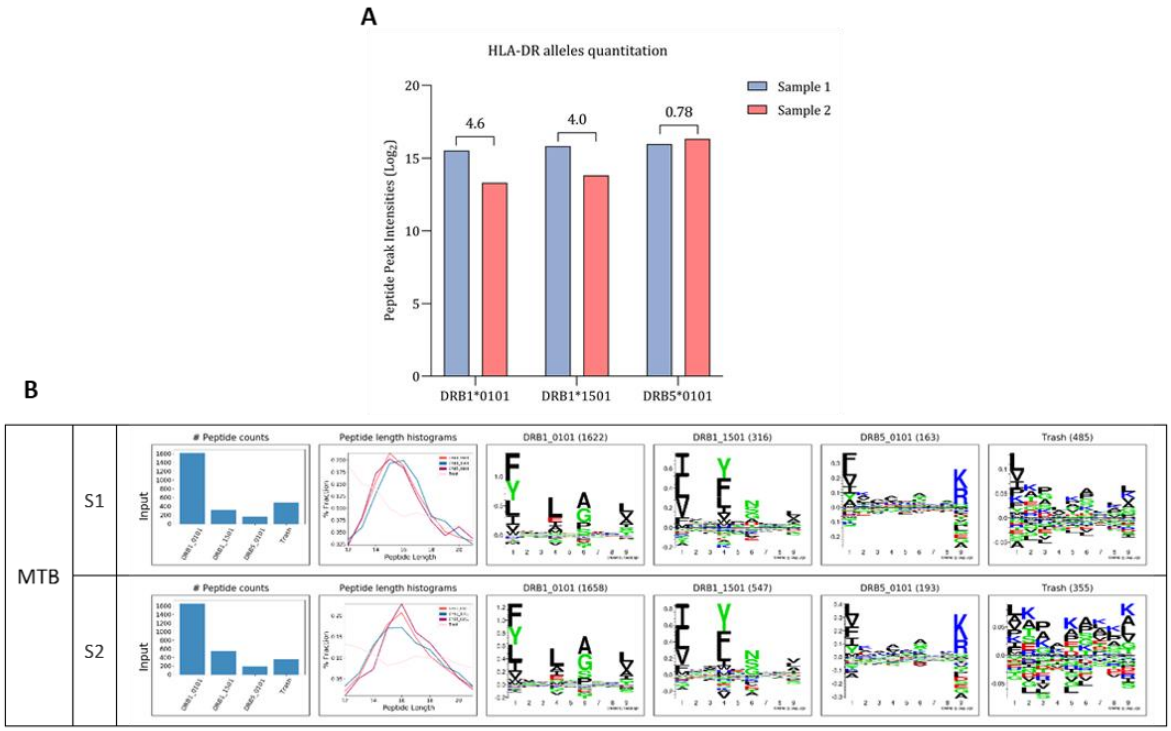


***Figure 4.5* Analysis of fold-change and binding motifs. (A)**

Comparisons of changes in amounts each HLA-DR chain expressed across experimental conditions were performed in terms of fold-change. Each bar represents peptide peak intensities of each β chain of HLA-DR alleles across samples. The fold-change was calculated between both samples for each HLA-DRB1 chain. Peptide peak intensities were generated through analysis of MS-MS spectra by Progenesis. (B) Peptide counts, length distribution and binding motifs per HLA-DRB1 allele or trash are shown for each condition with a percentile rank score >20% (trash bin 20% by default). S1: sample 1 (IFNγ and no MTB), S2: sample 2 (IFNγ and MTB).

4.3.7 **Prediction of binding affinity through the use of whole antigen sequences**

My preliminary data suggested that IFNγ treatment and MTB infection influenced the expression of HLA-DR alleles differentially. These changes could favour MTB infection, but the underlying mechanisms are poorly understood. Several studies have shown that MTB successfully evades T-cell recognition by perturbing antigen processing and presentation (190, 285, 286). Given that the number of peptides predicted to be associated with the DRB1*0101 allele was higher than the numbers of those assigned to DRB1*1501 and DRB5*0101, I assumed that MTB could evade MHC by targeting DR alleles that were more likely to present their antigens. To test this, I predicted the most likely DR allele to which mycobacterial peptides (previously identified Appendix Tables 7.1 and 7.2) would bind. Interestingly, 55% of peptides were assigned as ligands for DRB1*0101, compared with about 24.3% and 20.7% assigned as ligands for DRB1*1501 and DRB5*0101, respectively. To expand this further to the whole sequence of mycobacterial antigens, I compared the number of peptides that were likely to be presented by DRB1*0101 and DRB1*1501. Surprisingly, 76% of the tested antigens (47 antigens, Tables 7.4 and 7.5) were predicted to contain more peptides for DRB1*0101 than DRB1*1501 (Figure 4.6). This finding indicated that the DRB1*0101 allele was more promiscuous than DRB1*1501 or that MTB antigens had fewer peptide repertoires for DRB1*1501. This could explain the association between the risk of development of TB and the presence of the DRB1*1501 allele (273).

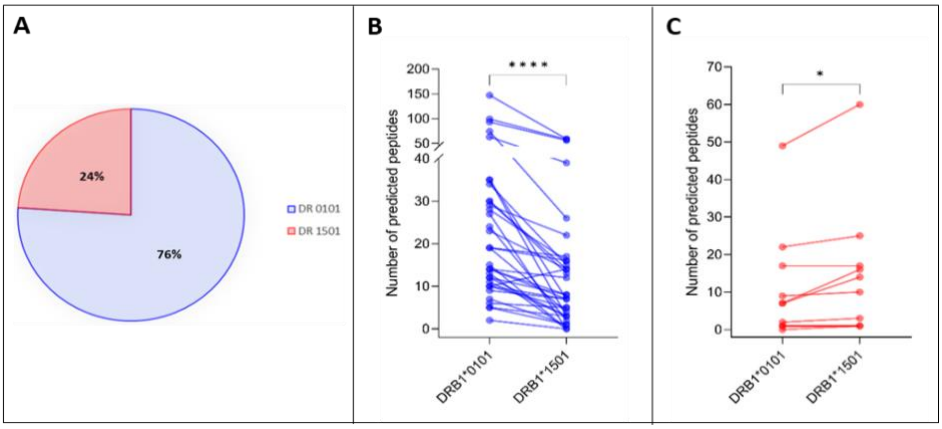


Figure 4.6* Prediction of HLA-DR*0101 and HLA-DR*1501 repertoires.
*Prediction data for 47 antigens were analysed to compare peptide repertoires for HLA-DR*0101 and HLA-DR*1501. (A): pie chart shows the percentage of antigens with a higher repertoire to HLA-DR*0101 (blue) and HLA-DR*1501 (red). (B): a comparison of peptide repertoires of HLA-DR*0101 and HLA-DR*1501 for each antigen from the 76% sector. (C): a comparison of peptide repertoires of HLA-DR*0101 and HLA-DR*1501 for each antigen from the 24% sector. All predictions were performed through the application of the NetMHCIIpan server.*

4.3.8 **Effect of small molecules on HLA expression**

I explored the effects of certain pharmacological agents on the expression of MHC molecules. Histone deacetylase inhibitors (HDACIs), such as Tubastatin A, selectively inhibit HDAC6 and have been shown to enhance immunity against MTB infection via suppression of IL-10 expression (272). Metformin (used to control hyperglycaemia) has been suggested as an adjunct therapy for TB due to its ability to boost the immune response against MTB infection via facilitation of phagosome-lysosome fusion and ROS production (287). However, neither agent has been investigated regarding MHC presentation of mycobacterial antigen. I also studied Entinostat (which selectively inhibits HDAC 1 and 3) to explore the effect of other HDACs (288). I hypothesised that boosting the intracellular killing of mycobacteria

by these agents could enhance the diversity and numbers of antigenic peptides presented on MHC molecules. To test this hypothesis, I sought to study the killing effects that would be mediated by test agents on intercellular BCG through the use of CFU assays. Once confirmed, I planned to evaluate the expression of MHC molecules of infected macrophages that had been treated with each agent. Finally, I aimed to identify mycobacterial peptides through the use of immunopeptidomics. However, I could not complete this experiment due to the onset of the COVID-19 pandemic.

I initially performed phagocytosis assays to determine the effect of each agent on BCG uptake by macrophages to avoid confounding during comparison of CFU counts post-infection. The confounding effect would be that a reduction in mycobacterial uptake would lead to fewer CFU counts. THP-1 macrophages were treated with each agent one day before BCG infection. The CFU assay was performed immediately post-infection (t0) to evaluate the effect of each agent on BCG uptake, and again one day post-infection to determine the impact of the agents on intracellular BCG burden. Regarding BCG uptake, the presence of Metformin and Entinostat reduced phagocytosis of BCG significantly ($P<0.05$), whereas IFNγ and Tubastatin A had no significant effect on phagocytosis compared with the controls (Figure 4.7, A). Next, I compared the CFU counts for each agent at the two time points (t0 versus t24) to determine their ability to control levels of intracellular BCG. CFU counts were enumerated one-day post-infection and compared with the CFU counts at t0 (Figure 4.7, B). Only Metformin and Tubastatin A showed a significant CFU reduction with P values of $P=0.002$ and $P=0.015$, respectively.

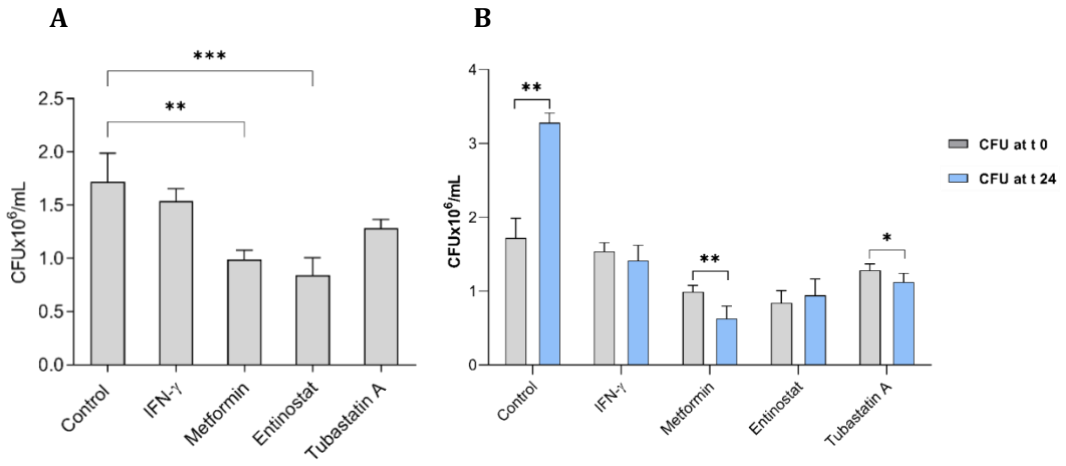


Figure 4.7 The effect of small molecules on levels of intracellular BCG.

*Colony-forming unit (CFU) assays were used to determine survival of intracellular BCG in macrophage-differentiated THP-1 cells. (A): differentiated THP-1 cells were treated with different agents (IFN**γ** at 50ng, Metformin at 2mM, Entinostat at 1uM and Tubastatin A at 1uM) one day before infection and CFUs were enumerated immediately post-infection (t0). (B): differentiated THP-1 cells were treated with the same agents after infection and CFUs were enumerated 24h post-infection (t24). Each infection (4hrs exposure) was performed in triplicate at an MOI of 10 (10 bacilli per cell). The CFU values are expressed as means ± standard deviation. A Kruskal-Wallis test with Dunn's multiple comparison post-test was used to show significant difference between each group compared with the controls. A Mann Whitney test was used to compare CFU counts between both time-points of each agent, *P<0.05 and **P<0.01.*

4.3.9 **Effect of Tubastatin A on HLA expression**

Since Tubastatin A did not inhibit mycobacterial uptake and aided in the control of levels of intracellular BCG, I explored the effect of Tubastatin A on MHC expression in the context of BCG infection, through the use of flow cytometry. I observed that MHC-I expression was increased upon co-exposure to BCG and IFNγ but not with Tubastatin A, whereas MHC-II expression was decreased upon co-exposure to BCG and IFNγ but not with Tubastatin A. This indicates that Tubastatin A prevents the inhibitory effects of BCG infection on MHC-II expression. Because I used BCG that expressed green

fluorescent protein (GFP), I assessed the intracellular load of BCG-GFP upon IFNγ and Tubastatin A treatment. Tubastatin A was found to reduce intracellular growth of BCG significantly compared with untreated cells (Figure 4.8).

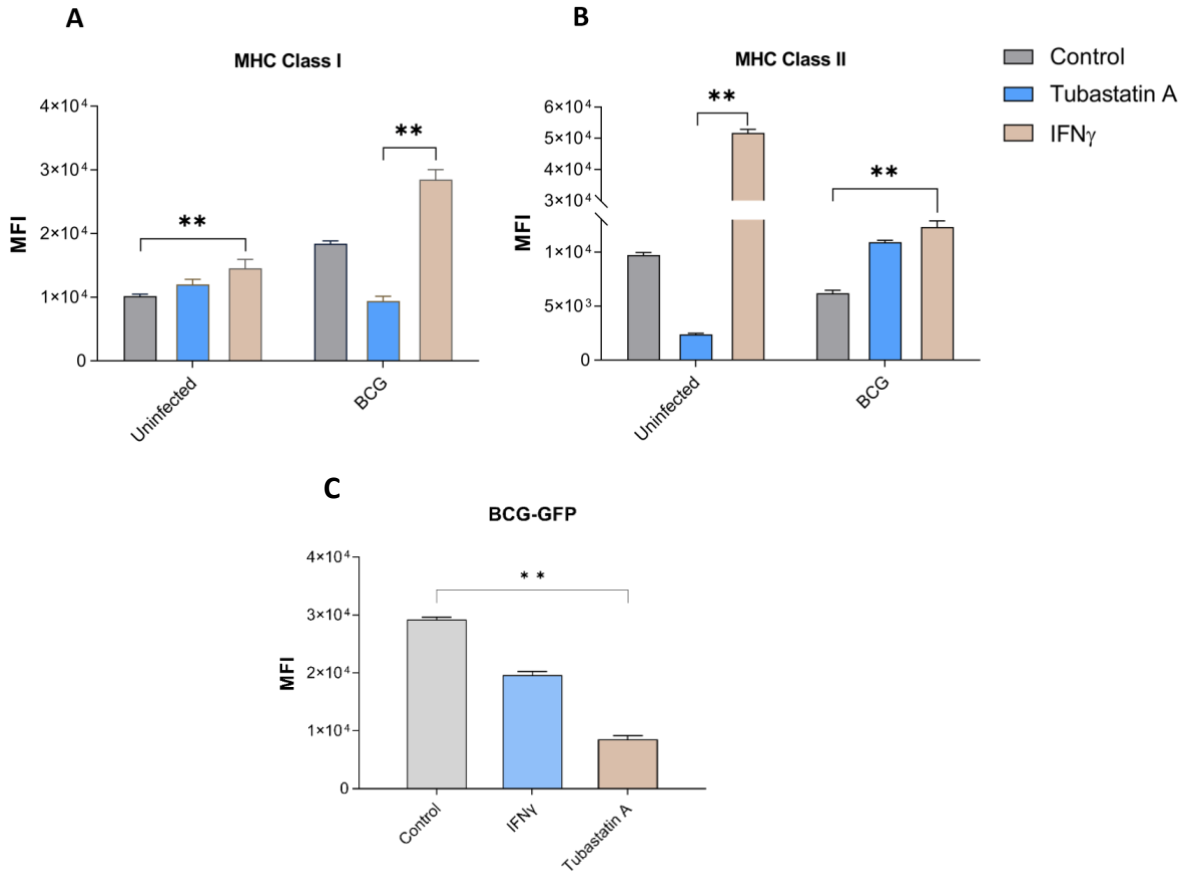


***Figure 4.8* The effect of Tubastatin A on MHC expression and intracellular BCG load.** *Differentiated THP-1 cells were treated with different agents (IFN$\boldsymbol{\gamma}$ at 50ng and Tubastatin A at 1uM) one day post-infection. A and B: the surface expression of MHC-I and MHC -II, respectively. C: the different levels of expression of intracellular BCG-GFP. Each infection (4hrs exposure) was performed in triplicate at an MOI of 10 (10 bacilli per cell). MFI values are expressed as means ± standard deviation. A Kruskal-Wallis test with Dunn's multiple comparison post-test was used to show significant differences among groups compared with the controls. *P<0.05 and **P<0.01.*

4.4 Discussion

The work described in this chapter aimed to assess the levels of HLA-DR allele-specific expression quantitatively in the context of IFNγ treatment and BCG infection, and to explore the effect of small molecules on antigen presentation. Using MS-based quantitative proteomics, I measured the differential expression of HLA-DR alleles (HLA-DRB1*0101, -DRB1*1501 and -DRB5*0101) by THP-1 cells across experimental conditions. I observed that the expression of each allele was different upon IFNγ exposure and mycobacterial infection. DRB1*0101 was expressed dominantly in the absence of IFNγ stimulation compared with DRB1*1501 and DRB5*0101; contrarily, DRB1*1501 and DRB5*0101 were up-regulated more than DRB1*0101 upon IFNγ treatment. I also observed that the fold-change in expression of DRA1 and DRB1*0101 showed a decreasing trend upon BCG infection, whereas levels of DRB1*1501 and DRB5*0101 increased or remained unchanged. The quantitative analysis of the immunopeptidomics data produced different results from those predicted, as the numbers of peptides associated with DRB1*0101 were found to be higher than those with DRB1*1501 and DRB5*0101 in all conditions. These findings warrant further investigations to determine whether mycobacteria can selectively inhibit and/or avoid presentation by specific DR alleles.

I found that Tubastatin A was a promising agent to prevent the inhibitory effect of mycobacterial infection on MHC-II expression; its presence restored HLA-II expression and controlled levels of intracellular BCG compared with the control but caused a decrease in MHC-I expression.

Classical methods for quantification of HLA-II proteins include western blot, immunohistochemistry and flow cytometry (289). Although these methods are useful for the assessment of different levels of expression among HLA-II subtypes (-DR, DP and DQ), they cannot be used to distinguish among the variant alleles of the same HLA-II subtype (e.g. HLA-DRB1*0101 and -DRB1*1501) that are expressed by the same cells or individual. Moreover, due to the high similarity and diversity of the HLA-II variants, there is a lack of specific antibodies for alleles of interest. Additionally, immunopeptidome data are complex as they are usually generated from the IP of multiple HLA alleles with the use of pan-antibodies. This poses a significant challenge in the definition of allele-restricted peptides. The software MHCMotifDecon was developed to determine which peptides were most likely to bind to a specific HLA allele and to generate sequence logos accordingly (290). Use of this software enables the determination of the contribution of each HLA-DR allele to the total peptide repertoire and the visualisation of peptide binding motifs, which can be compared with the reference binding motifs of a given allele. In all experiments, HLA-DRB1*0101 showed the greatest contribution to the immunopeptidomics data, followed by DRB1*1501 and DRB5*0101, regardless of IFNγ treatment or BCG infection.

Advances in MS-based quantitative proteomics enable the accurate quantification of targeted proteins (291). Quantification of allele-specific protein levels can be achieved when the unique proteolytic sequence(s) that represent the allele of interest is identified. To the best of my knowledge, only one study has employed the MS technique to quantify HLA-II protein levels (292). This study identified three peptides (VEHWGLDKPLLK, VEHWGLDQPLLK and VEHWGLDEPLLK) that resulted from trypsin digestion. Each represents the α-chains of HLA-DQA1, -DPA1 and -

DRA1, respectively, used for MS quantification. However, the researchers did not consider the β-chain of HLA-DR alleles, as the aim was to quantify the total numbers of α-chains of each HLA-II type (DR. DP and DQ) and to compare their abundance. In my experiments, I developed an approach to predict all potential proteotypic peptides *in silico* to aid in the selection of unique peptides that corresponded to the tested alleles. Once the HLA protein had been digested *in vitro*, liquid chromatography was a powerful tool for the individual separation of fragment peptides, so that precise analysis of cell-specific HLA-DR proteins could be achieved by the use of MS-MS.

Even though the levels of DRB1*1501 and DRB5*0101 were higher than that of DRB1*0101, the prediction results showed that more than 50% of peptides were expected to be associated with DRB1*0101. The disagreement in the results can be explained by the observations reported during the prediction analysis, in which the DRB1*0101 allele was found to have a greater contribution to the total immunopeptidome than DRB1*1501 in other cell lines, which express DRB1*0101 and/or DRB1*1501 (179). This suggested that the DRB1*0101 allele might have a greater binding capacity to a wide range of peptides, which could explain the discrepancy between the predictive and quantitative analyses. If this was the case, it would be important to investigate why DRB1*0101 could bind more peptides than could other alleles, particularly in the context of mycobacterial antigen presentation.

Although all HLA-II alleles are closely linked and can be inherited as extended haplotypes, their expressions are tightly controlled by CIITA and share highly conserved regulatory elements called the SXY box or an enhanceosome (293). It is unclear how a specific allele is preferentially expressed and whether this

preferencing mechanism occurs transcriptionally or post-transcriptionally. My preliminary data indicated that DR alleles were expressed differently according to stimulatory or inhibitory factors. In line with this, a study reported that in individuals with the HLA-DR15 haplotype (who expressed both DRB1*1501 and DRB5*0101), mRNA levels for DRB5*0101 were expressed more than those for DRB1*1501 in monocytes, B cells and DCs obtained from the peripheral blood mononuclear cells (294). However, when the allele-specific antibody was used in this same study, flow cytometry data showed that surface expression of the DRB1*1501 molecule was higher than that of DRB5*0101 in monocytes and DCs. This finding indicated that mRNA levels were not correlated with the surface protein levels (295). This may be due to the interference of post-translational processes during HLA molecule synthesis or during transit to the cell membrane. Earlier studies had reported the induction of a specific HLA-DRB1 allele. For example, the surface expression of HLA-DRB1*1501 was shown to be up-regulated selectively by vitamin D3 treatment compared with HLA-DRB1*07 (296). This selective induction was related to the vitamin D response element in the HLA-DRB1 promoter region, which was shown to be responsive and conserved in HLA-DRB1*1501 haplotypes. Environmental factors, such as mycobacterial infection and the presence of vitamin D, may influence the genetic regulation of specific HLA-DR alleles.

It is worth noting that HLA-DRB1*1501 is considered a strong genetic risk factor for multiple sclerosis (297). Differential methylations of HLA-DRB1 genes in heterozygote DRB1*1501 carriers have been shown to lead to different surface expressions of HLA-DR alleles (298). In this study, hypomethylation at the DRB1*1501 allele was shown to be associated with higher expression of this allele

compared with hypermethylation in the other alleles, such as DRB1*0101, in the same individuals (298). This clearly indicates that epigenetic modifications can modify HLA-II expression according to the type of methylation and the influenced allele within the loci of HLA-ll genes. In this regard, MTB infection has been shown to exploit epigenetic modifications by causing methylation to suppress genes involved in antigen presentation, such as CIITA promoters (299, 300).

Modification of the post-transitional process of MHC molecules can alter the amount of MHC surface expression. It has been shown that MTB releases urease enzymes in infected cells, which increases alkalinity due to elevated levels of carbon dioxide and ammonia and therefore leads to sequestration of MHC-II molecules in the endocytic compartment and subsequent decreases in rates of surface expression of MHC-II (285, 301). MTB also causes inhibition of surface MHC-II expression via induction of IL-10 (286, 302-304), which in turn mediates inhibitory effects in two ways post-translationally; IL-10 reduces the rates of transport of newly synthesised MHC-II molecules to the cell surface, and promotes the recycling of MHC-II molecules that are anchored to the cell surface (305). A mechanism by which MTB can induce IL-10 is mediated by the up-regulation of HDAC6 in infected macrophages; in studies, the levels of IL-10 protein and mRNA were found to be significantly reduced in cells that lacked HDAC6 (272, 306). To explain this, I hypothesise that modulation of HDAC6 may restore surface expression of HLA-II that has been inhibited by MTB infection and enhance antigen presentation (240, 307-309). Tubastatin A, a selective HDAC6 inhibitor, has been shown to control MTB (H37Rva) infection in mouse lungs, and this effect has been shown to be correlated with IL-10 suppression (310). My preliminary data showed that Tubastatin A enhanced surface expression of MHC-II but not MHC-I upon BCG

infection and it controlled intracellular bacterial growth in macrophages. However, the opposite action has been observed in melanoma cell lines, in which levels of MHC-I and tumour antigens were increased compared with those of MHC-II upon treatment of HDAC6 inhibition (311). These findings indicated that HDAC6 could mediate differential immunomodulatory effects according to cell type.

Contrary to what has been observed previously concerning the inhibitory effect of HDAC6, a recent study showed that high HDAC6 expression was the phenotypical feature of monocyte-derived macrophages obtained from TB resistors (people who display no reactivity to a tuberculin skin test or IFNγ release assays despite persistent exposure to MTB infection) compared with expression data for those with latent MTB infection or active TB, or healthy subjects (312). High rates of HDAC6 expression are associated with high levels of pro-inflammatory cytokines (TNF-α, IL-1β, and IL-6) and the acidification of vacuoles that harbour MTB. These conditions have been found to lead to controlled bacterial growth. One possible explanation for such inconsistent findings is that HDAC6 expression may have a vital role in the boosting of early innate immunity, which is sufficient to clear the MTB infection (313) without the involvement of T-cell responses, but that when MTB resists that innate immunity, HDAC6 expression is harnessed to decrease antigen presentation by MHC molecules.

The current data show certain limitations due to missing samples and values. For BCG-related quantitation experiments, I used samples that had been generated from the second IP through the use of the pan-HLA-II antibody (IVA12). Previously the samples had undergone the first IP with the use of an HLA-DR-specific antib

ody (L243), but the fractions that were supposed to contain HLA-DR protein chains were missing. This result may have altered the overall quantified level of HLA-DR alleles, but the data I obtained showed interesting findings that merit further investigation. For consistency, I used the immunopeptidomics data that had been generated by IVA12 antibodies for subsequent analysis, including the peptide binding prediction against HLA-DR alleles. Also, regarding MTB-related quantitation experiments, no sequence of the alpha chain was identified during the analysis of the MS-MS data by either MaxQuant or Progenesis for reasons that are unclear. These valuable data are essential in the assessment and interpretation of HLA-DR expression levels.

4.5 Conclusions

The quantitative analysis demonstrated differential expression levels of HLA-DR alleles upon IFNγ and BCG exposure. Despite the high similarity and diversity of the HLA-II alleles, MS-based quantitative proteomics offered a powerful tool to quantify specific HLA-DR alleles accurately. Employment of *in silico* tools, such as to identify unique peptides that corresponded to a specific allele that used or predicted peptide affinity, facilitated data analysis and interpretation. The current data showed that without IFNγ treatment, DRB1*0101 was dominantly expressed compared to DRB1*1501 and DRB5*0101. In contrast, when treated with IFNγ, DRB1*1501 was up-regulated more than DRB1*0101. Compared to uninfected samples, the levels of HLA-DRA1 and -DRB1*0101 showed a decreasing trend upon infection, whereas levels of DRB1*1501 and DRB5*0101 increased or remained unchanged. Also, the data suggested that DRB1*0101 allele displayed a greater

repertoire for different binding peptides than the DRB1*1501 allele. The targeting of HDAC6 by Tubastatin A could reverse the inhibition of surface MHC-II presentation caused by mycobacterial infection, but the role of HDAC6 in immunity against TB disease should be investigated further. My hypothesis is that mycobacteria could avert presentation to the DRB1*1501 allele; however, confirmation of this hypothesis requires additional research.

4.6 Ongoing and Future work

I plan to perform two experiments to explore two main points regarding the interaction between BCG infection and MHC expression and antigen presentation.

1. To see whether BCG infection may influence the surface expression of DRB1*0101 and DRB1*1501 alleles differentially, I plan to use two lymphoblastoid cell lines: one is the heterozygote-encoding DRB1*0101/0103 line, and the other is a homozygote-encoding DRB1*1501 line. The surface expression of both alleles will be measured by flow cytometry upon BCG infection. B-lymphocytes exhibit the phagocytic activity of mycobacteria and antigen processing and presentation (314, 315), and the use of homozygous cell lines enables a detailed analysis of the effect of infection on each allele. Although DRB1*0103 and DRB1*0101 differ by three amino acids, they have similar binding motifs, which means that they exhibit similar peptide binding specificities and are likely to bind similar peptides.
2. To see whether BCG antigens may undergo presentation preferentially by DRB1*0101 or DRB1*1501 alleles, I plan to transfect THP-1 DRB1 knockout cells with plasmids that express DRB1*0101 and DRB1*1501 separately. Having validated surface expression, I will infect them, in addition to wild-type THP-1 cells, with BCG. The immunopeptidome of each condition will be analysed through the use of LC-MS-MS.

This work is beyond the scope of my DPhil thesis, but I hope to complete it and include the data in publications that arise from my thesis.

Chapter 5

Evaluation of protective effects of candidate antigens

5.1 Introduction

The WHO has established its end TB strategy and has named 2035 as a target to eliminate TB globally by reducing mortality rates by 95% and TB incidence by 90% (316). To achieve this target, intensified research is necessary to develop new tools to control TB worldwide. These include the drawing up of effective vaccine strategies to protect individuals from developing active TB when they are infected with MTB and after the exposure to prevent reactivation of active TB from a state of LTBI (317). The only available vaccine (BCG) protects against extra-pulmonary TB, including tuberculous meningitis and miliary TB, but offers inadequate protection against pulmonary TB. The pulmonary system is the primary target through which MTB is transmitted. The BCG shows variable efficacy against pulmonary TB, from 0% to 80% (120, 318). BCG protection declines after vaccination but with variable periods. According to a review, the BCG vaccine may display protective efficacy for 10-15 years after vaccination (319). However, some studies have reported longer periods, of protection of 20 years (320) and up to 60 years (321). This limited longevity of protection poses a significant challenge for people with LTBI, particularly adolescents and adults who account for 90% of LTBI cases and face progression of the disease to active TB (322). Therefore, effective boosters and lifelong vaccines are urgently needed.

The foremost aim of all TB vaccine developers is to induce long-life protection against MTB infection (323). However, due to the complexity of the interaction between MTB infection and host immunity, researchers have found it challenging to correlate protective immunity to defined immunological markers (324). This difficulty limits the identification of potential protective antigens and the prediction

of protection levels that candidate vaccines might provide (325). Cell-mediated immunity, particularly that offered by CD4+ T cells, has been the focus of attention in the development of new TB vaccines, as they play a central role in the containment of MTB infection (325-327). The method of their immune responses to TB is undetermined; however, many studies have shown associations between CD4+ T-cell subsets, including Th1 cells (328) and Th17 cells (329), as well as CD8+ T cells, and protection against TB (330, 331). No specific T-cell subset has been correlated with protection against TB. Still, the induction of heterogeneous effector cells, such as CD4+ T cells and CD8+ T cells (332), and functional antibodies is a target for the development of a successful vaccine (99, 328). Researchers have also realised that induction of IFNγ alone is not a reliable marker for the prediction of protective immunity mediated by T cells. Even polyfunctional CD4+ T cells (Th1) that are able to express two or three proinflammatory cytokines (IFNγ, IL-2, and TNFα) simultaneously, have been reported not to be correlated with protection (99). Therefore, I employed MGIAs as tools to evaluate the protection provided by the candidate antigens (hisD, metE and mmpL12). Then, I selected the most promising candidate for further evaluation, which included immunogenicity and *in-vivo* MTB challenge.

5.2 Aims of the work described in this chapter

In the work described in this chapter, I aimed to:

- evaluate the protection provided by the selected antigens (administered as a DNA vaccine) through the use of an MGIA as a surrogate for *in-vivo* MTB challenge;
- evaluate the protection provided by best candidate (metE antigen) through the use of an MGIA metE delivered through two different platforms, DNA and adjuvant protein vaccines; and to
- evaluate the immunogenicity of metE through the use of enzyme-linked immunosorbent assay (ELISA), enzyme-linked immunosorbent spot (ELISpot) and intracellular cytokine staining (ICS).

5.3 Results

5.3.1 Construction of candidate antigens as DNA vaccines

I sought to test the candidate antigens (hisD, metE and mmpL12) through the use of a DNA plasmid platform. At this stage, the protein PPE15 (195), which has been shown to provide protection in mice(195) was included in the evaluation as a positive control. The gene sequence of each antigen was obtained from the Mycobrowser database (https://mycobrowser.epfl.ch/) for incorporation into mammalian expression plasmids (pcDNA3.1). I added a signal peptide (METDTLLLWVLLLWVPGSTGD, derived from the immunoglobulin kappa (IgGκ)) at the N-terminus of each antigen to enhance the secretion of the expressed antigen extracellularly by the host cells (333, 334). To verify this, I predicted the secretion of each antigen *in silico* through the use of the SignalP-5.0 server (335), which can be used to predict the presence of signal peptides with their cleavage sites and cleavage probability score (a score close to 1 indicates high probability) (Table 5.1). I also added a his-tag at the C-terminus to facilitate detection and confirmation of expression *in vitro*.

Table 5.1 *Prediction of cleavage site and probability score after addition of IgGκ signal peptide*

Protein	Cleavage site	Cleavage probability
hisD	Between positions 20 and 21	0.979
metE	Between positions 20 and 21	0.981
mmpL12	Between positions 20 and 21	0.416
PPE15	Between positions 20 and 21	0.978

5.3.2 Confirmation of correctly sized inserts and plasmid expressions *in vitro*

The gene of each antigen was codon-optimised to enhance the expression by the host (336). It was designed by Biomatik. Initially, I used *E. coli* to amplify the plasmids at a miniprep scale to confirm the correct size of each insert using agarose gel electrophoresis and the *in-vitro* expression of each plasmid with the use of HEK293T cells (Figure 5.1). Once confirmed, I successfully obtained an average of 10mg of each plasmid upon gigapere amplification, which required the overnight culturing of two litres of bacteria. Although HEK293T cells were transfected with the same amount of plasmid DNA of each antigen (1ug each), the expression varied among antigens: metE>hisD>PPE15>mmpL12 (Figure 5.1, C).

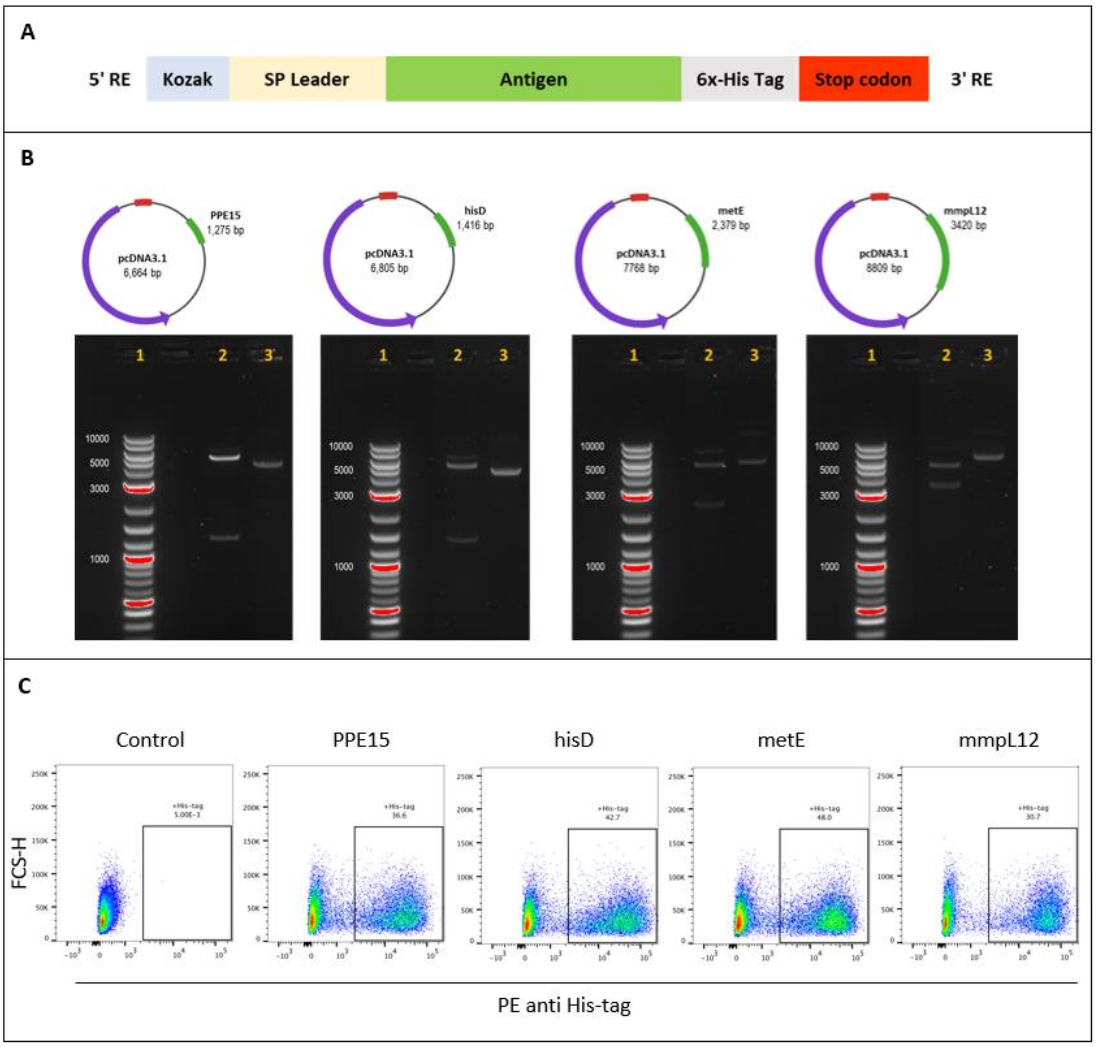


***Figure 5.1* Construction and confirmation of each antigen insert.**

Panel A depicts the construction of antigen inserts. Kozak and signal peptides were added at the N-terminii and polyhistidine tags (6x-his tag) and stop codon were added at the C-terminii. Panel B shows the products of the restriction digest (lane 2) and the intact plasmids (lane 3) for each antigen. Lane 1 shows the DNA ladder. Panel C shows the expressions of each protein antigen upon transfection of HEK293T cells with each plasmid.

5.3.3 **Antigen Evaluation using MGIA**

I screened the protective efficacy of the candidate antigens by monitoring their ability to inhibit mycobacterial growth *ex vivo,* through the application of an MGIA (198-200). I used the CB6F1 mice strain, derived from female BALB/c and male

C57BL/6 mice, since they express more diverse MHC-II alleles (I-A^b, I-A^d, I-E^d). There were six groups of mice (eight mice in each) altogether. Four were vaccinated with each antigen in the form of plasmid DNA intramuscularly three times every two weeks; one group was immunised with the BCG vaccine intradermally once, and one group remained unimmunised (naïve) (Figure 5.2). Two weeks after the final vaccination (week 6), mouse spleens were harvested and processed for MGIA. A total of $3x10^6$ and $5x10^6$ splenocytes were infected with one inoculation of BCG (~500 CFU). The greatest discrepancy in inhibitory effects between cells taken from unvaccinated and BCG-vaccinated mice was observed after an incubation period of four days (205). Therefore, after four days of incubation, supernatants and cell lysates were transferred into mycobacterial growth indicator tubes (MGITs) and incubated in the BACTEC MGIT system until the time to detection (TTD) registered positive. Principally, mycobacterial growth is monitored hourly according to oxygen consumption, and prompt recording of positivity (a low TTD) indicates rapid growth.

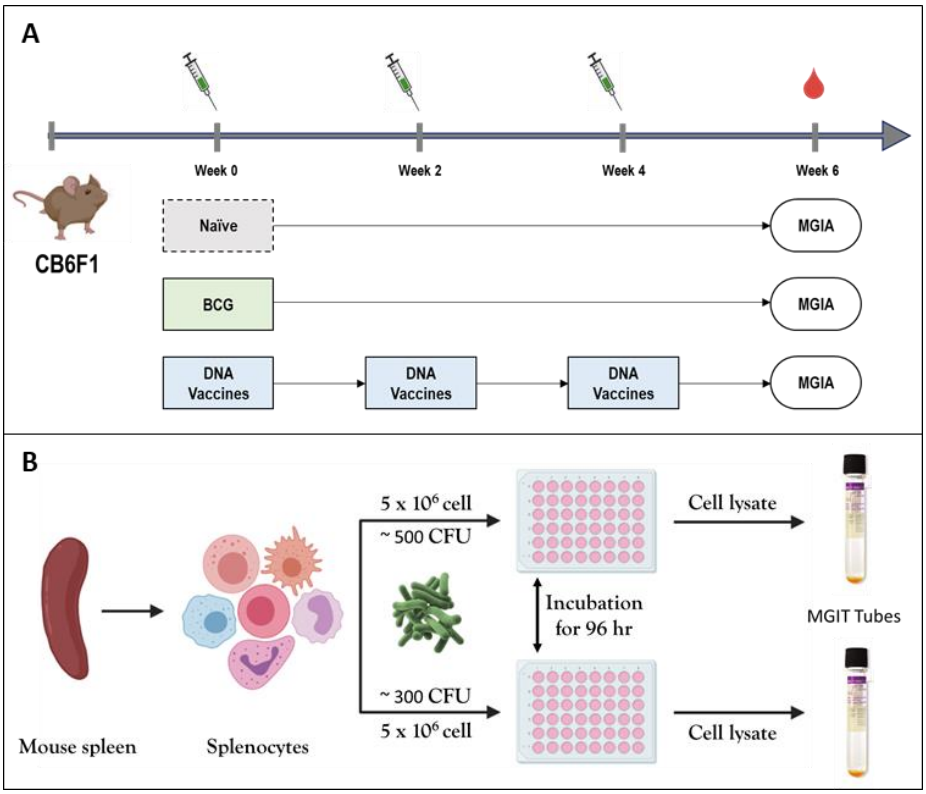


***Figure 5.2* Immunisation layout and MGIA preparation.**

Panel A shows the mouse immunisation time points. CB6F1 mice were separated randomly into six groups (eight mice in each). One group was vaccinated intradermally with BCG once, four groups to be tested regarding antigens were vaccinated with plasmid DNA three times at two-week intervals, and one group was left unvaccinated. Panel B shows the layout of the MGIA assay, in which splenocytes were infected with ~500 CFU of BCG, incubated for 96 hours and transferred to the BACTEC MGIT system until time to detection (TTD) became positive.

5.3.4 **Vaccination with metE inhibited mycobacterial growth**

There was a significant difference in TTD between the naïve and BCG groups in both cell concentrations ($3x10^6$ and $5x10^6$ splenocytes), with a mean difference of 18.6h ($P < 0.0375$) and 28.2h ($P < 0.0002$), respectively. This result indicated the robustness of the MGIA to discriminate between immunised and unimmunised animals (Figure 5.3, A and B). Vaccination with metE inhibited mycobacterial growth compared with the naïve group, with a TTD mean difference of 22.7h ($P < 0.0057$) for $3x10^6$ splenocytes and a TTD mean difference of 25h ($P < 0.0017$) for $5x10^6$ splenocytes (Figure 5.3, A and B). The mmpL12 also induced inhibition of mycobacterial growth in the $5x10^6$ splenocyte set only (TTD mean difference = 18.2h; $P < 0.045$) (Figure 5.3, B). The splenocytes of the animals vaccinated with PPE15 and hisD showed no significant inhibition of mycobacterial growth (Figure 5.3, A and B).

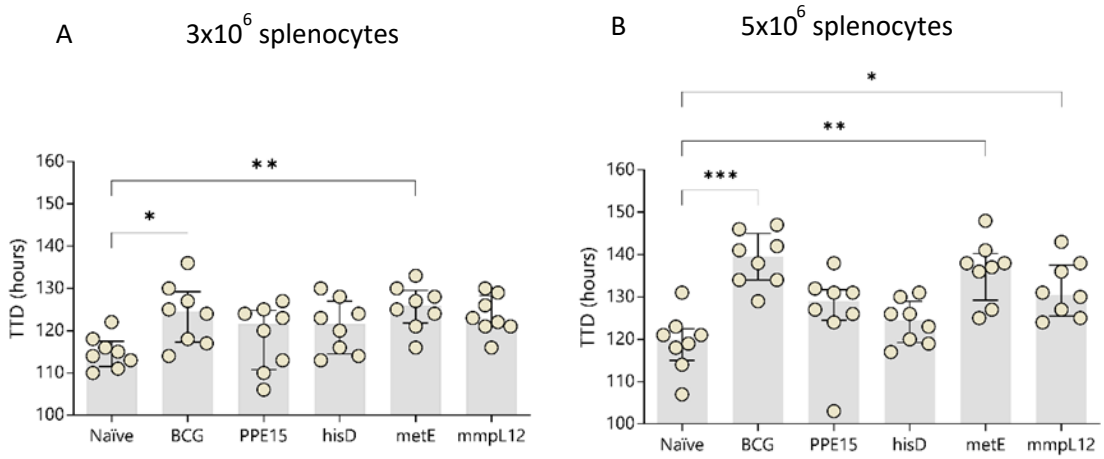


***Figure 5.3* TTD values of mycobacterial growth as measured by MGIA.**

*TTD values were produced from BCG co-cultured with mouse splenocytes that numbered 3x10⁶ (A) and 5x10⁶ (B). The splenocytes were obtained from unimmunised mice (naïve) and mice immunised with BCG, PPE15, hisD, metE and mmpL12 (each antigen was given as a DNA vaccine of 100ug). Once the TTD registered positive, statistical analysis was performed to calculate the statistical significance of the results. Plotted circles represent individual mice, lines represent median data, and whiskers denote the interquartile ranges (IQR). A Kruskal-Wallis test with a Dunn's multiple comparisons test was used to show significant differences in comparison with the control (naïve). * indicates a P value of <0.05, ** indicates a P value of <0.01, and *** indicates a P value of <0.001.*

5.3.5 **Exploring antigen secretion**

Given that PPE15 has been shown to be protective in mice (195), and I confirmed its expression *in vitro*, I thought the expressed PPE15 had not been secreted extracellularly after immunisation. To verify this, I transfected HEK293T cells with each plasmid DNA of the tested antigens and collected the supernatants and cell lysates for Western blot analysis. Unexpectedly, only metE was detected in the supernatants and the cell lysates, whereas the PPE15, hisD and mmpL12 were detected in the cell lysates only. This result indicated that they had been expressed intracellularly without undergoing a secretory pathway (Figure 5.4).

I conducted an analysis to predict the presence of transmembrane domains (TMDs) in the tested antigens through the use of the DeepTMHMM server (https://dtu.biolib.com/DeepTMHMM). TMDs are regions of a protein that span the cell membrane, and they may affect protein localisation and secretion. The mmpL12 protein was found to contain 12 transmembrane helices, which could explain its presence in the supernatant. However, hisD and PPE15 do not have TMDs but were expressed intracellularly. This suggests that the presence of SP or absence of TMDs are not the only determinants of protein secretion.

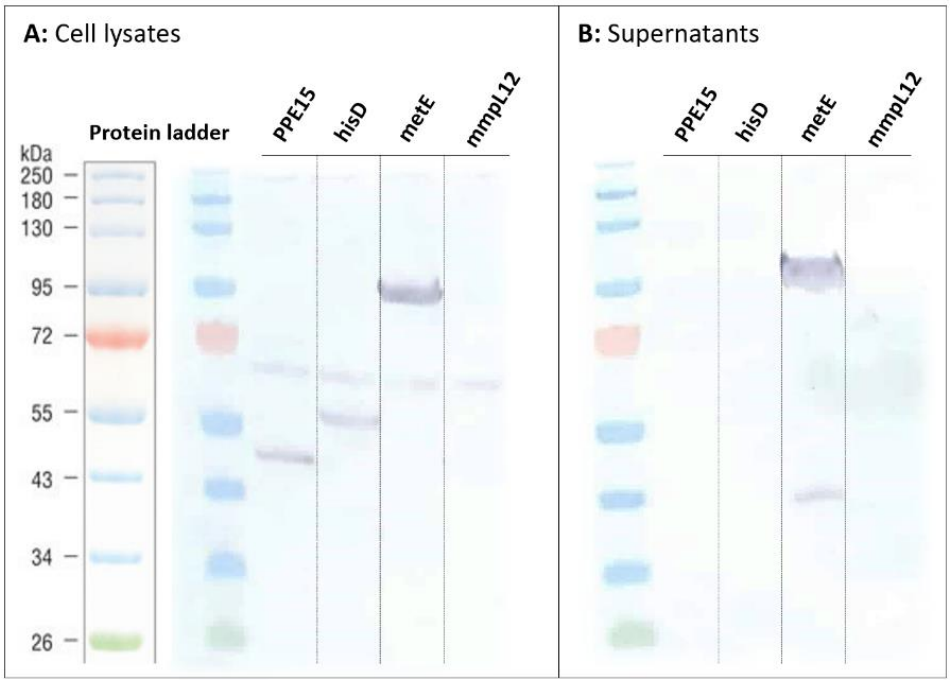


***Figure 5.4* Detection of expressed antigens.**
24 hours after transfection of HEK293T cells, antigen expression was detected through use of Western blot analysis in cell lysates (A) and supernatants (B) with the use of an anti-his tag antibody. Each lane was labelled according to the loaded sample for each antigen.

5.3.6 **Vaccination with metE conferred protection**

I selected metE as a candidate antigen for further investigations. This antigen was administered as a DNA vaccine (to confirm the earlier MGIA findings) and as a protein-adjuvant formulation. I included an adjuvant protein platform due to the better immunogenicity profiles of these formulations in humans compared with the profile of DNA vaccines (337, 338). I selected AS03 as the adjuvant; this is an oil-in-water emulsion composed of squalene, α-tocopherol and polysorbate 80 (339) that is approved by the European Commission and the US Food and Drug Administration for human application (340). A total of 1ug of purified metE protein (produced by BiologicsCorp) was mixed with AddaS03 (an adjuvant that is biosimilar to AS03 supplied by InvivoGen) for mice vaccination. Splenocytes were collected at the end of the experiment for MGIA and immunogenicity tests. This experiment was modified compared with the previous experiment; vaccination was given at three-week intervals instead of two, and two sets of $5x10^6$ splenocytes were co-cultured with two inoculations of BCG separately (~500 and 300 CFU). I chose to use $5x10^6$ splenocytes as this amount allowed for better discrimination between groups and therefore detection of differences among vaccines. Two BCG dilutions were chosen in order to determine which dilution would enable me to see a greater difference between the control and BCG groups. Vaccination of mouse groups with metE (either in the form of plasmid DNA or as a protein with AddaS03 adjuvant) conferred protection compared with unvaccinated mice (Figure 5.5 A and B). In high BCG inoculation (500 CFU), only adjuvanted metE induced significant inhibition of mycobacterial growth.

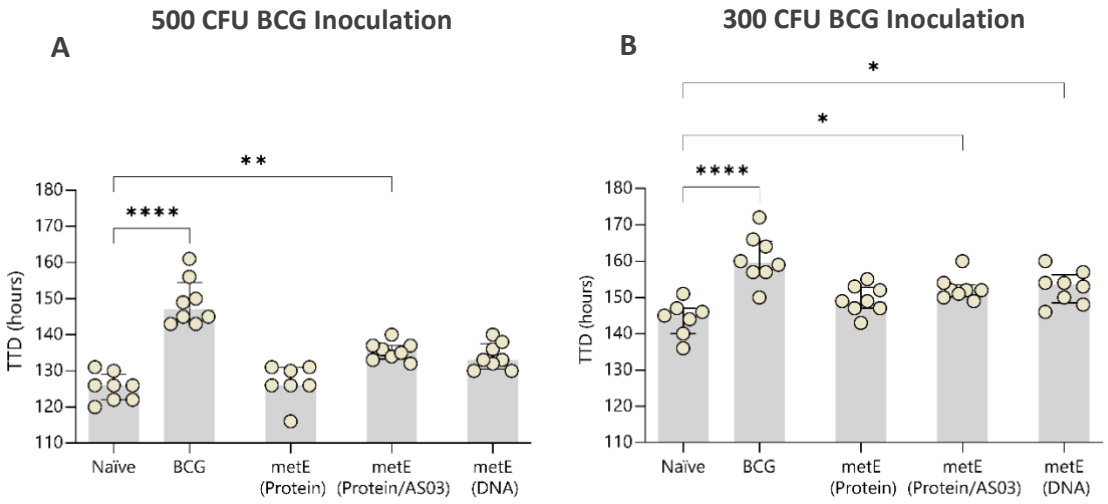


Figure 5.5 TTD values of mycobacterial growth by MGIA.

*TTD values were produced from experiments in which BCG was co-cultured with mouse splenocytes of 5x10^6 inoculated with ~500 CFU of BCG (A) and ~300 CFU of BCG (B). The splenocytes were obtained from unimmunised mice (naïve) and mice immunised with BCG, metE (1ug), metE-AddaS03 (1ug) or metE-DNA (100ug). Plotted circles represent individual mice, lines represent median, and whiskers denote the IQR. A Kruskal-Wallis test with a Dunn's multiple-comparisons test were used to show significant differences in comparison with the control (naïve); * indicates a P value of <0.05, ** indicates a P value of <0.01, and *** indicates a P value of <0.001.*

5.3.7 **Assessment of T cell responses induced by metE vaccinations**

Next, I assessed both cellular and humoral responses that were induced by metE antigen alone and in different formulations. To investigate the cellular responses, I used ICS and ELISpot to assess CD4+ and CD8+ cytokine release upon metE protein stimulation.

In response to metE stimulation, CD4+ T cells obtained from the metE-AddaS03 group released IL-2, TNFα and IL-17 at greater levels than did the naïve control group (Figure 5.6 B). The metE-DNA group released IFNγ, TNFα and IL-2 at significantly greater levels compared with the unvaccinated control group. The BCG group showed a significant expression of IFNγ, TNFα, IL-2 and IL-17 in response to tuberculin-purified protein derivative (PPD) stimulation but not in response to metE protein (Figure 5.6, B). The results of the metE vaccination showed the presence of polyfunctional T cell populations. In the metE-AddaS03 group, a 2-functional population of CD4+ cells (IL-2+/TNF-α+) was detected, while metE-DNA immunization resulted in the induction of two different populations of functional CD4+ cells (IFN-γ+/IL-2+/TNF-α+ and IL-2+/TNF-α+) (Figure 5.6, C).

When CD8+ T cells were stimulated, they did not produce any detectable levels of cytokines in any of the groups (Figure 5.7). This could be because the assay was performed using cells that had been cryopreserved, which could have reduced the level of antigen-specific T-cell responses (341, 342).

Because metE-AddaS03 did not induce IFNγ upon stimulation with metE protein, I tested whether metE-AddaS03 vaccination elicited a Th2-skewed metE-specific response. To test this, I measured by ELISpot IL-4 cytokine secretion that followed

stimulation with metE protein. To confirm the absence of IFNγ responses, I also measured levels of IFNγ using ELISpot as it is a more sensitive assay than ICS. In parallel, TNFα and IL-17 were also measured through the use of ELISpot to confirm the trends identified when ICS was used.

Levels of IL-4 were significantly higher in the metE-AddaS03 group than in the naïve group and there was no detectable IL-4 in any of the other groups (Figure 5.8, D). As had been shown in the ICS experiments, IFNγ was present only in the metE-DNA and BCG groups.

The above data were generated through the use of frozen splenocytes and metE protein, rather than overlapping peptides, as the first attempt at the experiment, using fresh splenocytes and overlapping peptides, failed.

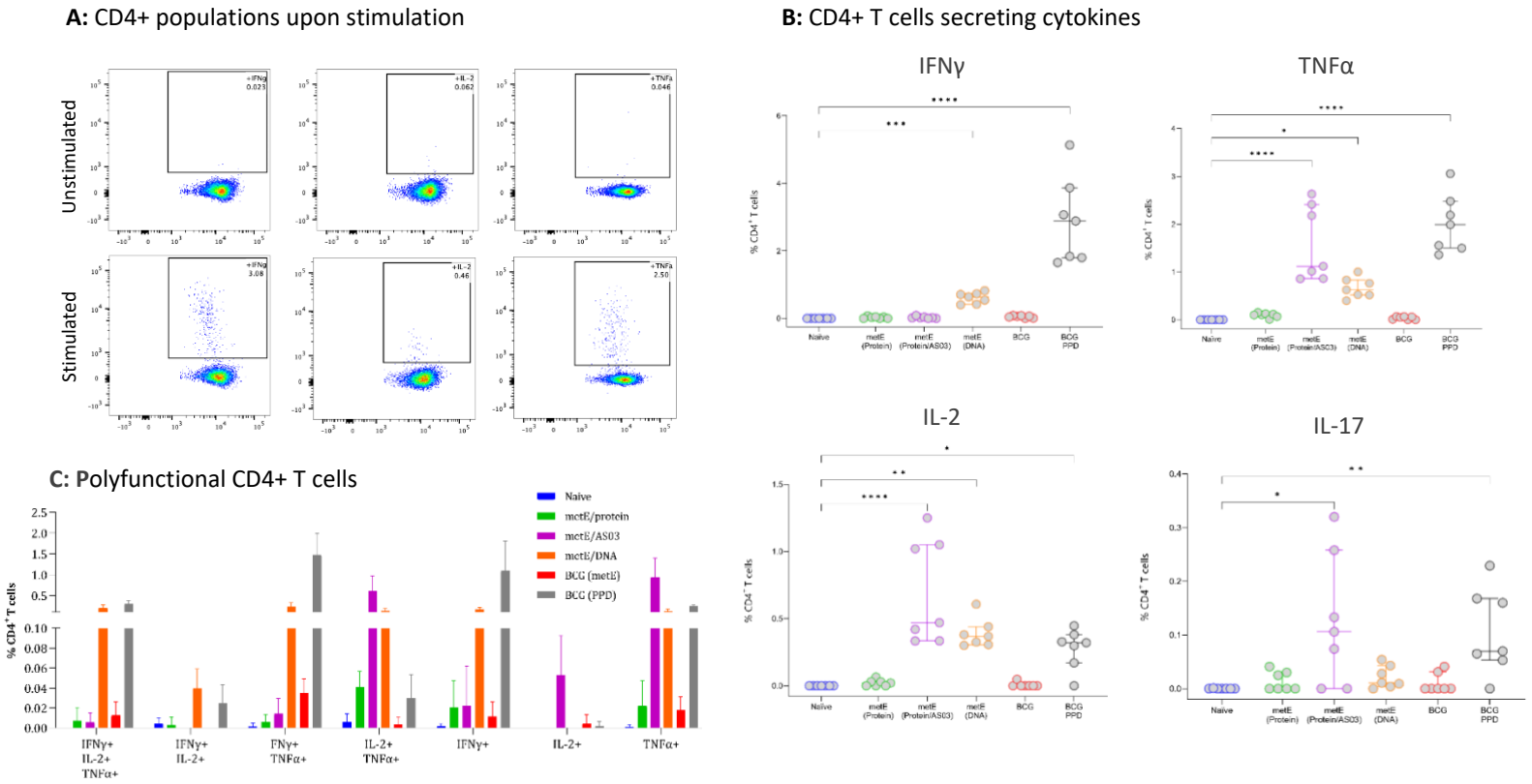


Figure 5.6 Intracellular cytokine staining in CD4+ T cells.

*Mouse splenocytes (10^6) were stained for CD4+ surface markers and ICSs (IFNγ, TNFα, IL-2 and IL-17) after overnight stimulation with metE protein. A: Representative of flow cytometric analysis of CD4+ T cells stimulated with either medium or metE protein. B: The percentage of cytokine production by CD4+ T cells was calculated for each cytokine. C: The detection of polyfunctional CD4+ T cells upon vaccination (characterized by their ability to produce multiple cytokine). Plotted circles represent individual mice, lines represent medians, and whiskers denote the IQR. A Kruskal-Wallis test with a Dunn's multiple comparisons test was used to show significant differences in comparison with the control (naïve): * indicates a P value of <0.05, ** indicates a P value of <0.01, *** indicates a P value of <0.001, and **** indicates a P value of <0.0001.*

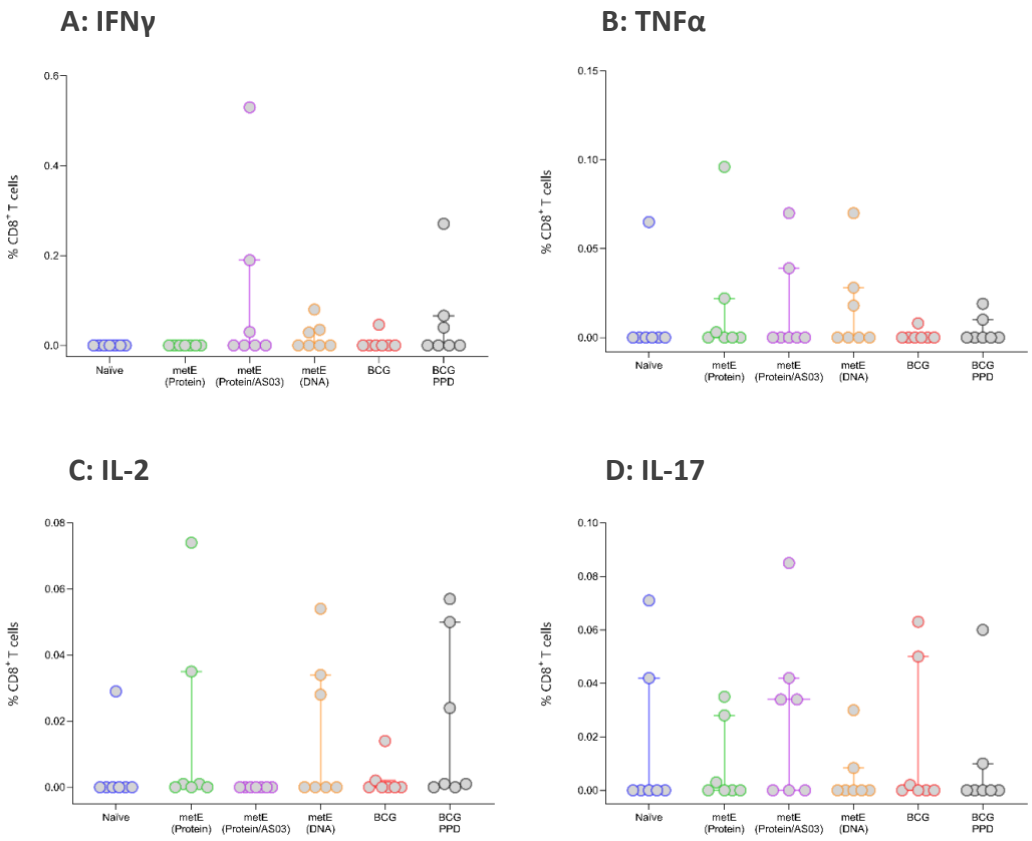


Figure 5.7 Intracellular cytokine staining for CD8+ T cells.

Mouse splenocytes (10^6) were stained for CD8+ surface markers and intracellular cytokines (IFNγ, TNFα, IL-2 and IL-17) after overnight stimulation with metE protein. The percentage of cytokine production by CD8+ T cells was calculated for IFNγ (A), TNFα (B), IL-2 (C) and IL-17 (D). Plotted circles represent individual mice, lines represent medians, and whiskers denote IQRs. A Kruskal-Wallis test with a Dunn's multiple comparisons test was used to show significant differences in comparison with the control (naïve). All P values were non-significant.

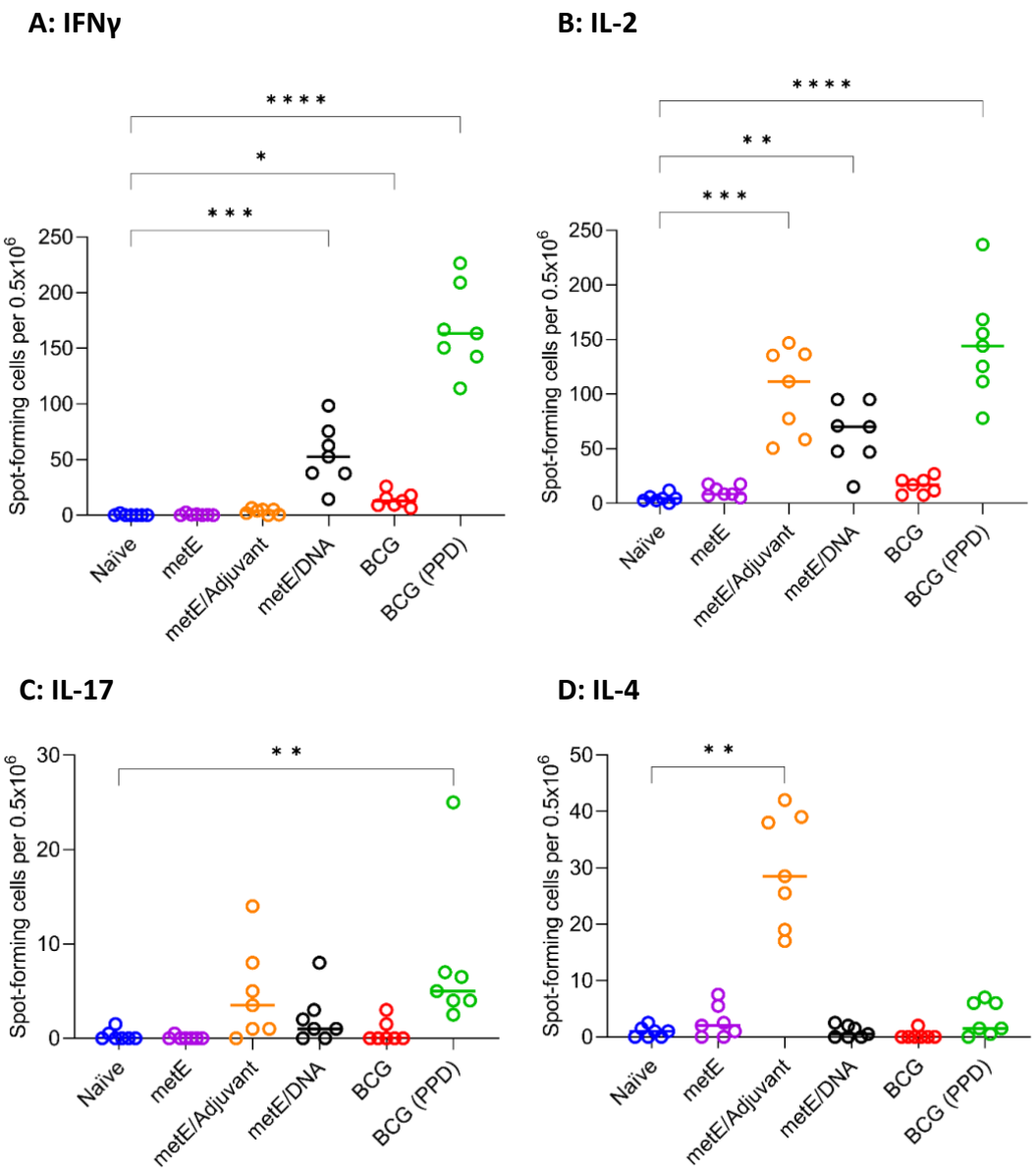


***Figure 5.8* Cytokine secretion measured by ELISpot.**

*2.5 x 10^5 splenocytes were stimulated with metE protein overnight. ELISpot was used to measure the secretion of IFNγ (A), IL-2 (B), IL-17 (C) and IL-4 (D). Plotted circles represent the number of spots produced by individual mice, lines represent medians. A Kruskal-Wallis test with a Dunn's multiple comparisons test was used to show significant differences in comparison with the control (naïve): * indicates a P value of <0.05, ** indicates a P value of <0.01, and *** indicates a P value of <0.001.*

5.3.8 **Assessment of antibody responses induced by metE vaccinations**

Next, I assessed the responses of metE-specific antibodies, which were IgM, total IgG and IgG subclasses (IgG1, IgG2a, IgG2b and IgG2c), obtained from the sera of vaccinated mice three weeks after the final vaccination. ELISA was used to detect antigen-specific antibodies.

IgM responses that were metE-specific were detectable only in the metE-AddaS03 group, whereas both metE-AddaS03 and metE-DNA induced metE-specific responses to IgG (Figure 9, A and B). BCG and metE protein alone did not produce any metE-specific antibodies (Figure 5.9, A and B). Therefore, I opted to compare the levels of antibody responses between metE-AddaS03 and metE-DNA.

When compared, the level of metE-specific antibody that was induced by metE-AddaS03 was significantly higher than that induced by metE-DNA for IgM, total IgG and IgG1. In the absence of a standard curve, the readout of ELISA (OD) can only reflect the amount of antigen-specific antibodies based on the intensity of the colour generated. However, the serial dilutions approach can be used to compare the concentration of antibodies between different samples. Because I did not have a standard curve for metE antigen, I used endpoint titre (ET) and absorbance summation (AS) methods (343) to compare the antibody concentration between metE-AddaS03 and metE-DNA samples. The ET was determined through selection of the first reading (and corresponding dilution) that was observed above 0.2OD, which is an arbitrary absorbance cut-off value (343, 344). When determined, the average ET of metE-AddaS03 sera (which corresponded to 1/102400 dilution) was a 16-fold higher titre than the average ET of metE-AddaS03 sera (which corresponded to 1/1600 dilution), as shown in Figure 5.9 E. Use of the AS method

enabled the statistical comparison of antibody concentrations among different groups without a standard curve via summation of absorbance values (OD) of all dilutions of each sample to obtain a final value that represented that sample (343, 345-347). Comparison of all the final values between metE-AddaS03 and metE-DNA groups showed that the anti-metE antibody concentration that was induced by the metE-AddaS03 vaccine was significantly higher ($P<0.0001$; unpaired t-test) than that induced by the metE-DNA vaccine (Figure 5.9, F).

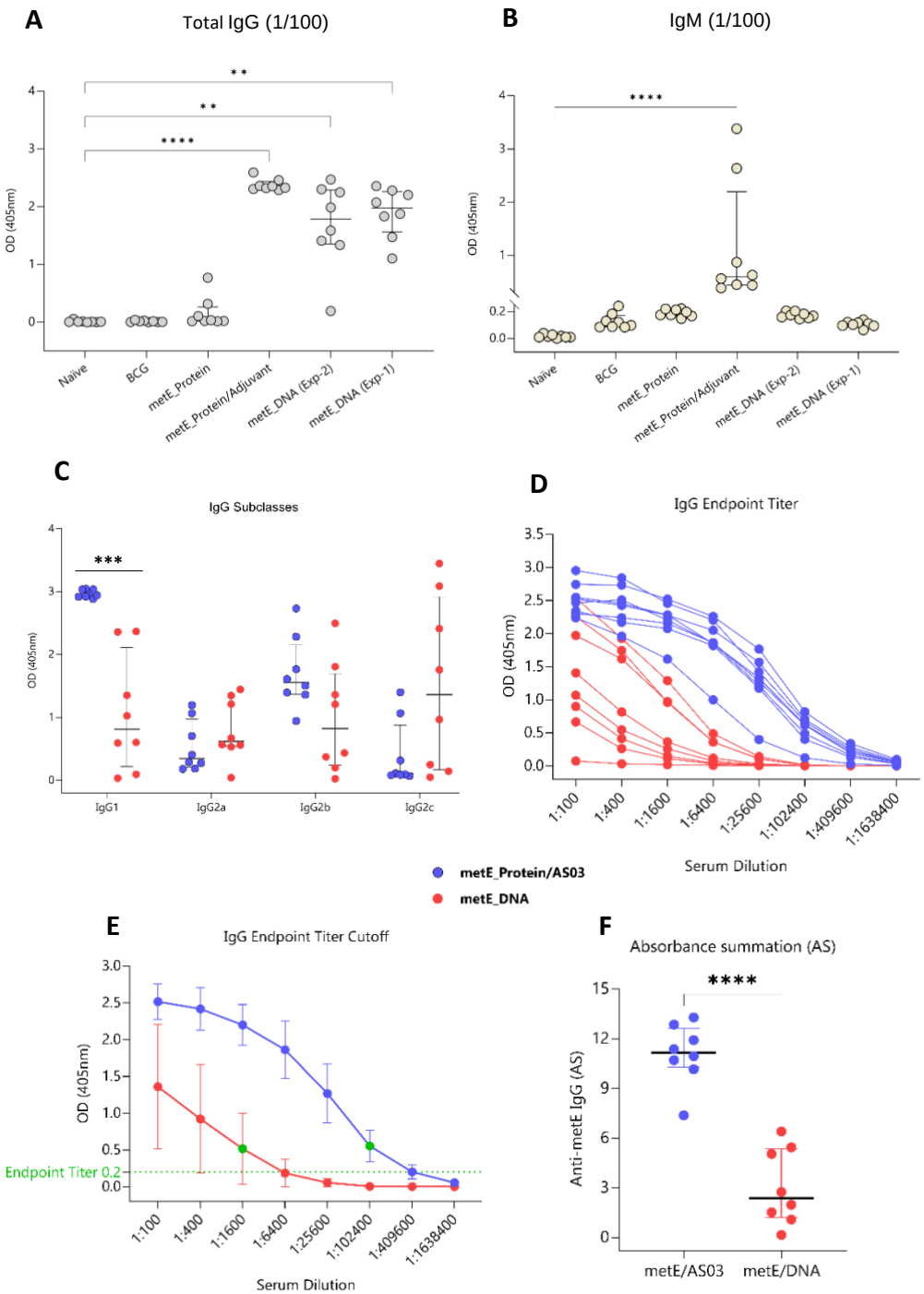

A
Total IgG (1/100)
OD (405nm)
Naive
BCG
metE_Protein
metE_Protein/Adjuvant
metE_DNA (Exp-2)
metE_DNA (Exp-1)
B
IgM (1/100)
C
IgG Subclasses
IgG1
IgG2a
IgG2b
IgG2c
D
IgG Endpoint Titer
Serum Dilution
metE_Protein/AS03
metE_DNA
E
IgG Endpoint Titer Cutoff
Endpoint Titer 0.2
F
Absorbance summation (AS)
Anti-metE IgG (AS)
metE/AS03
metE/DNA

Figure 5.9 **metE-specific antibody titres measured by ELISA.**

*Sera were obtained three weeks after the final vaccination for all groups. Panels (A) and (B) show metE-specific IgG and IgM antibodies respectively among all groups. Panel (C) shows the comparison between IgG subclasses induced by metE-AddaS03 and metE-DNA vaccines. Panel (D) shows the absorbance of serial dilutions of sera obtained from metE-AddaS03 and metE-DNA groups. Panel (E) shows the average titres (± standard deviation) and defined ET dilution (green dot). In panel (F), each dot represents the final value obtained from the absorbance sum of all dilutions (shown in panel D), which was used to calculate the AS to compare total IgG concentrations between metE-AddaS03 and metE-DNA groups. A Kruskal-Wallis test with a Dunn's multiple comparisons test was used to show significant differences for multiple comparisons in panels (A) and (B); and an unpaired t test was used to compare two groups in panels (C) and (F). * indicates a P value of <0.05, ** indicates a P value of <0.01, and *** indicates a P value of <0.001.*

5.4 Discussion

I used immunopeptidomics and immunoinformatics approaches to identify and select candidate antigens for screening. Three antigens (hisD, metE, and mmpL12) were evaluated for their protection in mice through the use of the MGIA, an *ex-vivo* surrogate of an MTB challenge. The mouse groups that were vaccinated with metE (either plasmid DNA or protein in an adjuvant with AddaS03) displayed significantly higher levels of protection compared with unvaccinated mice. Vaccination with metE-DNA induced polyfunctional CD4+ T cells to express IFNγ, TNFα, and IL-2, whereas metE-AddaS03 elicited a range of CD4+ T cells that expressed TNFα, IL-2, IL-4, and IL-17. Both metE-DNA and metE-AddaS03 vaccines significantly induced the production of IgG antibodies compared with the naïve group; when compared, the antibody concentration that was induced by the metE-AddaS03 vaccine was 16-fold higher than the concentration induced by the metE-DNA vaccine. The current work showed that the metE antigen was a novel candidate vaccine for TB that merited further evaluation.

Many attempts have been made to develop an effective subunit vaccine as a booster for the BCG vaccine or as a replacement (i.e., prime vaccine) in cases in which BCG use is contraindicated. However, the selection of which antigen(s) should be preclinically evaluated from among more than 4000 that are found in MTB is challenging, particularly in the absence of immune correlates of protection. Moreover, no animal model can mimic human MTB infection, and humans cannot be employed as MTB infection guinea pigs due to ethical considerations (348). I used a rational approach that involved a combination of immunopeptidomics and immunoinformatics analysis, and which enabled me to determine potential

candidates for initial evaluation. Through this approach, I identified antigens that are presented naturally by human immune cells infected with mycobacteria and selected the top T-cell epitope-rich antigens (hisD, metE, and mmpL12).

I utilised the MGIA tool because it offers a robust alternative assay for early assessment of candidate vaccines in the absence of established immunity to protection. This assay reflects the ability of a wide range of inoculated immune cells, such as splenocytes, to inhibit the growth of mycobacteria. It provides an unbiased readout of the overall immune response without the need for pre-selection of either a specific group of cells or cytokine(s) (197). The MGIA has been utilised across various animal models, including mice (198, 200, 205), NHP (349), and humans (203, 350). Correlation of the outcome of the *ex-vivo* challenge (MGIA) with the result of MTB challenges in animal models would raise the level of confidence during the use of human samples because the challenge of immune cells, even with MTB, takes place *ex vivo* (203). In a study that used an NHP model, it has been shown that MGIA can be used as a reliable surrogate for vaccine-induced protection against TB. The protection provided by BCG was measured by the MGIA and the total pathology score and lung CFU were calculated following *in vivo* MTB challenge. The study found a correlation between the MGIA and *in vivo* challenge results concerning bacterial load and protection (349). Currently, I am undertaking an *in-vivo* MTB challenge in mice to assess the protection offered by the metE vaccines.

A DNA vaccine platform is a practical choice for early screening of novel antigens due to its simple production, high stability and efficiency in mouse models (351). Also, DNA vaccination has been shown to induce production of Th1 CD4+ cells and CD8+ T cells, as well as antibodies, which are required to build immunity against MTB infection (352). Therefore, I formulated the candidate antigens (hisD, metE

and mmpL12) and PPE15 as DNA vaccines. When tested by MGIA, the metE DNA vaccine significantly inhibited mycobacterial growth compared with cells from unvaccinated animals. Unexpectedly, the PPE15 antigen did not inhibit mycobacterial growth significantly, despite being shown to be protective. One explanation could that the signal peptide failed to guide the expressed antigen on the secretion pathway. This seems a possible explanation because, when I tested this through the use of Western blotting, I found that metE was the only antigen secreted in the supernatant. Inclusion of signal peptides, such as IgGκ and tissue plasminogen activator (tPA), has been shown to enhance immunogenicity and protection of secreted antigens in cases in which the secretion of the expressed antigen outside myocytes increases the opportunity for it to be exposed to and recognised by immune cells, particularly DCs and B cells. Such secretion results in increased amounts of CD4+ T cells and antibody titres compared with cases in which the antigen is unsecreted (353, 354). For example, the addition of IgGκ signal peptide to adenovirus vectors that expressed malaria antigen was shown to increase antibody avidity and levels of CD4+ T-cell cytokines (IFNγ and IL-2) compared with a vector that lacked the signal peptide (333). Also, when tPA signal peptide was added into a DNA vaccine that encoded the antigen Ag85A or into the modified vaccinia virus Ankara (MVA)-based vaccine that expressed Ag85B-TB10.4, the tPA increased the cellular and humoral responses significantly compared with expressed antigen without secretion (355, 356). Because the SignalP-5.0 server exhibited higher cleavage probability scores after the addition of IgGκ than it did upon tPA inclusion, I selected the IgGκ signal peptide for mouse vaccination experiments. The prediction provided by the SignalP-5.0 server should

be verified *in vitro,* and it is possible that certain antigens may require the presence of a specific signal peptide to facilitate their secretion.

The first DNA vaccine that expressed mycobacterial antigen was used in 1996. Since then, the DNA vaccine platform has been employed to screen candidate antigens in animal models. All the antigens included in current subunit vaccines that are undergoing clinical trials, except for ID93 vaccine (211, 357), were tested initially as DNA vaccines during preclinical evaluation (e.g., Ag85, ESAT6, and MTB32) (358, 359). However, no DNA vaccine against TB has completed testing in a clinical trial. GX-70 was the only DNA vaccine that reached phase one of a clinical trial but it was withdrawn five months after the trial began (337).

Although DNA vaccines are efficient to a great extent in animal models, they have been associated with variable immunogenicity when tested in humans for various infectious diseases (360). For example, participants in a trial of a DNA vaccine against human immunodeficiency virus type 1 showed insignificant immune responses but acceptable safety results upon vaccination (361). Malaria and hepatitis B DNA vaccines have been reported to induce protective CD8+ T-cell and antibody responses, respectively, in humans (362, 363). However, the vaccines against both diseases that succeeded in clinical trials (e.g., RTS/S vaccines for malaria) or were granted approval (e.g., Engerix-B and HB-Vax II for hepatitis B) were recombinant antigen protein(s) with adjuvants. Collectively, DNA vaccines must be improved further for use in humans but remain an excellent platform in animal models for the screening of candidate vaccines due to their aforementioned advantages. Therefore, I sought, through the second set of MGIA experiments, to test the metE antigen as a recombinant protein that could perform as a suitable delivery platform for human vaccination.

Recombinant protein-based vaccines require the addition of adjuvants to elicit desirable immune responses. AS03 is one of the most successfully used adjuvants in clinical trials and has been approved for use in influenza vaccines, e.g. Pandemrix and Prepandrix. It has been shown to induce innate and adaptive immune responses in terms of administered antigens in animal models (364-367) and humans (368-371). These studies showed that antigen-specific CD4+ T cells and antibodies were induced when the tested vaccine used AS03 as an adjuvant. I observed that metE-DNA vaccine induced polyfunctional Th1 CD4+ T cells that were characterised by three cytokines (IFNγ, TNFα and IL-2) but that administration of the metE-AddaS03 vaccine led to the production of a wide range of cytokines, including TNFα and IL-2 (Th1), IL-4 (Th4) and IL-17 (Th17). Although IFNγ was not detected, the metE-AddaS03 group was able to inhibit mycobacterial growth significantly, which finding indicated the ability of CD4+ T cells to control infection independently of IFNγ production. Previously, CD4+ T cells have been shown to mediate cytokine-independent control of MTB infection *in vivo* (86, 252). However, due to the importance of IFNγ in immunity against MTB infection, characterisation of the IFNγ response has been a part of the immunogenicity assessment for every TB vaccine that has reached clinical trials. Previously, the immunogenicity of BCG or candidate TB vaccines has been assessed through measurement of the production of cytokines, particularly IFNγ secretion (331), but researchers have realised that induction of IFNγ alone is not a reliable marker to predict protective immunity mediated by T cells. Therefore, the inclusion of different cytokines, such as TNFα, IL-2 and IL-17, should be considered for the screening and evaluation of novel candidates (372).

The number of multifunctional CD4+ T cells that are produced by vaccination is the most widely used indicative measurement of a vaccine's protective response against TB in mouse models and clinical trials. In mice, several studies have shown that the level of production of multifunctional CD4+ cells that is induced by tested vaccines is strongly associated with protection when the animals are challenged with MTB (357, 373-379). In contrast, other studies have shown no correlation between the induction of multifunctional CD4+ T cells and protection (380-382). The same scenario has been seen in humans; the induction of multifunctional CD4+ cells in BCG-vaccinated infants is not correlated with protective immunity against MTB infection (98). However, in one study, PBMCs obtained from infants who had been vaccinated with BCG were found to inhibit mycobacterial growth *ex vivo,* and this inhibition was reported to be correlated with the production of multifunctional CD4+ T cells that expressed IFNγ, IL-2, and TNFα (383). Despite the inconsistency among these studies, which can cause difficulty when trying to establish immune correlates of protection, CD4+ T cells have been found to play an essential role against MTB infection. However, further studies are required to discover methods other than cytokine release assays in which their protective markers can be characterised.

In the work performed for this thesis, the metE-AddaS03 vaccine induced IL-17 signals when the cells were restimulated. Th17 cells have been shown to play a vital role in vaccine-induced protection in MTB-challenged animal models (384-387). However, according to the data obtained during clinical trials of six anti-TB vaccines and during tests of BCG, the expression of IL-17 is minimal or undetected across these vaccines (388). It is unclear whether Th17 cells play a minor role in the human immune response or whether, during the trials, IL-17 was not detected because the

vaccines were designed to target Th1 mainly. The potency of the cationic adjuvant formulation (CAF01) of the vaccines was demonstrated in the induction of a Th17 response in mice in addition to the induction of Th1 (389, 390). However, unexpectedly, CAF01 did not produce a significant Th17 response when administered to human subjects as an adjuvant of the H1 subunit vaccine (391). This finding indicates that an adjuvant may target distinct cell types, depending on the species.

A study was carried out to compare the antigen-specific T-cell responses that were elicited by a number of different vaccines (MVA85A, AERAS-402, H1:IC31, H56:IC31, M72/AS01, ID93/GLA-SE, and BCG) (388). Generally, every vaccine elicited antigen-specific CD4+ T-cell responses that were characterised by the production of Th1 cytokines, but the numbers of Th1 cells produced was the most distinguishable factor among the tested vaccines. While all vaccines exhibited similar cytokine profiles, M72/AS01 was shown to produce a stronger memory CD4+ T-cell response than the other vaccines. Given that M72/AS01 provided ~50% efficacy according to the final report (130) and induced the highest memory CD4+ response according to the comparative study, the amount produced and the durable response of CD4+ T cells could be a reliable indicator of protection rather than measurement of the phenotype of cytokine-expressing CD4+ T cells (392). I observed that IL-4 CD4+ T cells, which characterised the Th2 phenotype, were induced upon administration of the AddaS03 adjuvant with metE. Therefore, AS01 was included in the *in-vivo* challenge experiment, which is currently ongoing. This inclusion aims to induce Th1-biased CD4+ T cells predominantly.

When I measured the antibody response, I observed that metE-DNA and metE-AddaS03 vaccines induced high amounts of total IgG titres. At low dilution (1:100),

it is impossible to estimate antibody concentrations and to compare results statistically, particularly in the absence of a standard for metE antigen. However, when I used the ET and AS methods (343), I found that the metE-AddaS03 vaccine induced a significantly higher level of antibodies than did the metE-DNA vaccine, and this result was attributed to the adjuvant. When I analysed IgG subclasses, anti-metE IgG1 titres were induced significantly among other subclasses. Similarly, in a mouse study, in which different adjuvants were formulated with the ID93 vaccine, IgG1 antibodies were found to be induced significantly across all groups with comparable titres (393). However, these researchers did not report the IL-4 response. An earlier report suggested that IL-4-dependent T cells were required for the production of IgG1 antibodies (394), and this finding could explain the high IgG1 titres as the metE-AddaS03 but not the metE-DNA vaccine. In mice, it has been reported that a high titre of IgG1 indicates a Th2 response, whereas the presence of IgG2a indicates a Th1 response (395). This is in line with the phenotypes of Th2 and Th1 cells that were induced by metE-adjuvant and metE-DNA, respectively.

In humans, the most promising subunit vaccine, M72/AS01, not only elicited potent T-cell responses but also induced the production of IgG antibodies to the M72 antigen and remained durable for three years. These findings suggested that this strong response was correlated with protection (396). Also, in a study in which correlates of risk were analysed based on the cohort of infants who participated in the MVA85A efficacy trial, an association between the presence of Ag85A-specific IgG antibodies and a reduced risk of development of TB was observed (90). These studies highlight the crucial contribution of antibody responses in the provision of protection and the reduction of the risk of developing TB.

5.5 Research limitations

This work had certain limitations. I did not include an adjuvant group as an additional control during animal vaccination. Such inclusion would have been useful to assess the impact of the adjuvant on the immunogenicity level generated by the metE antigen. However, I have adjuvant-control groups in the *in vivo* MTB challenge experiments that I am currently conducting. Another limitation was the use of a single dose of protein in the experiments. The performance of protein-dose-escalation experiments may have helped with the selection of the most effective dose. I chose to use 1ug, as this amount was within the average range of the amounts used by other researchers in mouse TB vaccine experiments.

5.6 Conclusions

With the employment of immunopeptidomics and immunoinformatics methods, I successfully identified and selected candidate antigens for preclinical evaluation. Of three tested antigens, metE exhibited promising data in a mouse model. When given as a DNA or adjuvant protein vaccine, metE was found to inhibit mycobacterial growth significantly *ex vivo* and to elicit antigen-specific CD4+ T-cell and antibody responses. The metE-DNA vaccine was distinct in the generation of Th1-cell phenotypes (IFNγ, TNFα, IL-2) and IgG antibodies, whereas the metE-AddaS03 vaccine induced a range of CD4+ T cells that expressed TNFα, IL-2, IL-4, and IL-17 in addition to high titres of IgM and IgG antibodies. The metE antigen warrants further development for inclusion in a subunit vaccine to tackle TB, particularly as it has recently been reported as an immunogenic protein detected in multidrug-resistant TB (397).

5.7 Ongoing and future work

To verify the protective effect of metE, I have initiated an *in-vivo* MTB challenge experiment that employs three formulations of metE (metE-DNA, metE-AS01 and metE-AddaS03) (Table 2). Two adjuvant-control groups are included as a negative control to exclude any 'adjuvant-protective' effects. In parallel, I am conducting an immunogenicity experiment to compare the immune responses induced by the promising AS01 adjuvant with those induced by the AS03 adjuvant. Cellular and humoral responses will be correlated with the efficacy data from the challenge experiment. The final data analysis should be completed in December 2022. Upon completion, I will write a paper on these findings for publication.

Table 5.2 *Details of the ongoing in-vivo MTB-challenge experiments.*

Mouse strain	CB6F1
Mice per group	8
- Vaccination group - Route of administration and at what interval	- Naïve
	- BCG ID, given once
	- AS01 only - IM, three times every two weeks
	- AS03 only - IM, three times every two weeks
	- metE-DNA - IM, three times every two weeks
	- metE-AS01 - IM, three times every two weeks
	- metE-AS03 - IM, three times every two weeks
- Challenge - Route of administration and at what interval	- MTB (H37Rv) - IN, four weeks after the final vaccination
- Takedown - Targeted organs	- Four weeks after the challenge - Lungs and spleens
Readout	CFU

Chapter 6

Overall conclusions and future work

6.1 Summary of main findings of work described in Chapter 3

It is very challenging to identify protective antigens among approximately 4000 mycobacterial proteins that are present in MTB, in the absence of immunological correlates of protection and optimal animal models of TB. Therefore, as a first step in the identification, I employed human macrophages (differentiated THP-1 cells) as an *in-vitro* model of TB. This model mimicked, to a high degree, the natural interaction between the mycobacteria and the host, as the macrophages are the niche cells in which MTB survives and replicates.

Because MTB is an intracellular pathogen, cellular immunity plays a vital role in the control of MTB infection. So, to identify mycobacterial antigens that might mediate T-cell responses, I employed MS-based immunopeptidomics to identify MHC-bound peptides. This approach enabled me to identify naturally processed mycobacterial peptides that were presented by MHC molecules on infected macrophages. I identified 64 and 81 antigens derived from BCG and MTB, respectively. Two challenges arose at this stage: first, the selection of antigen(s) through the use of a classical method. An example of such a method is the measurement of the release of IFNγ upon restimulation of cells from mice or humans who have been exposed to mycobacteria. This method is both expensive and time-consuming to accomplish. Second, since MHC genes are highly polymorphic in humans, the immunopeptidomics data lacked diversity, as the peptides were identified based on MHC alleles that were expressed by THP-1 cells only. I utilised immunoinformatics tools to address these challenges. I retrieved the whole sequence of identified antigens from the UniProt database and subjected them to prediction analysis. Through this analysis, I aimed to select those antigens that contained a large

repertoire of CD4+ T-cell epitopes that were presented using a set of 27 MHC-II alleles that are most frequently seen in humans, in order to maximise population coverage. As a result, I was able to target cellular immunity and take into account HLA allele variability during prioritisation of the candidate antigens. This approach could be applied to other pathogenic diseases to develop a candidate vaccine that targeted T-cell response with a broad HLA-allele coverage.

6.1.1 **Future work**

Improvements in sensitivity and resolution of mass spectrometers have led to the ability to identify MHC-bound peptides with the use of just a low number of cells. For example, the previous protocol required the presence in a sample of 3 x 10^8 cells in order to identify mycobacterial peptides, but with current advanced spectrometers, it is possible to analyse samples that contain 10-fold fewer cells. This enables researchers to include more conditions and explore the mycobacterial immunopeptidome accordingly. For example, macrophages can be infected at different time points or other antigen-presenting cells, such as DCs, can be included. Also, human macrophages derived from PBMCs can be utilised to perform *in vitro* MTB infection.

6.2 Summary of main findings of work described in Chapter 4

During immunopeptidomics analysis, I observed that the presence of IFNγ enhanced the total number of identified peptides that were associated with HLA-DR more than those with HLA-DQ or with HLA-DP. IFNγ is a potent inducer of MHC-

II up-regulation, but does it affect each HLA subtype (HLA-DR, -DQ and -DP) equally? When I explored the surface expression of these HLA subtypes through the use of flow cytometry, for which THP-1 macrophages were treated for 48hrs, expression of HLA-DR was found to be up-regulated predominantly at a rate that was about 45 times that of untreated cells, whereas HLA-DP and -DQ showed modest up-regulation of about a six-fold increase. This finding raised another question regarding the effect of IFNγ on HLA-DR alleles expressed by THP-1 cells: are they expressed at the same level or differentially? I explored this question through the use of MS to quantify MHC-DR proteins for each allele (HLA-DRB1*0101, -DRB1*1501 and HLA-DRB5*0101). During immunopeptidomics experiments, I retained the fractions that contained α- and β-chains of the MHC complex, which were enriched as they had resulted from IP. I aimed to quantify the amounts of HLA-DR alleles in the context of IFNγ treatment and BCG infection.

I summarised the main observations as follows:

- IFNγ was found to enhance the expression and the total number of identified peptides associated with HLA-DR significantly compared to HLA-DQ and HLA-DP.
- Without IFNγ treatment, DRB1*0101 was dominantly expressed compared to DRB1*1501 and DRB5*0101.
- Upon IFNγ treatment, DRB1*1501 was up-regulated more than DRB1*0101.
- The levels of HLA-DRA1 and DRB1*0101 showed a decreasing trend upon infection, whereas levels of DRB1*1501 and DRB5*0101 increased or remained unchanged.

- Prediction analysis of the immunopeptidomics data showed that the DRB1*0101 accounted for a higher number of assigned peptides than did either DRB1*1501 or DRB5*0101.
- When the mycobacterial peptides were predicted according to their binding affinity, 55% of peptides were assigned as ligands for DRB1*0101, compared with about 24.3% and 20.7% assigned as ligands for DRB1*1501 and DRB5*0101, respectively.
- When the whole sequence was analysed, 76% of the tested antigens (47 antigens) were predicted to contain more peptides for DRB1*0101 than DRB1*1501.

I also utilised human immunopeptidomics data to discover the level of contribution of each DR allele to the total immunopeptidome and the contribution trends in the context of IFNγ treatment and BCG infection. To perform this experiment, the identified peptides were assigned to each allele based on their binding affinity through the use of a prediction tool called NetMHCIIpan. This analysis showed that the numbers of peptides associated with DRB1*1501 and DRB5*0101 were increased upon mycobacterial infection. This finding was in agreement with the quantitative results, which showed that HLA-DRB1*1501 and -DRB5*0101 levels were not affected by infection compared with HLA-DRB1*0101. However, the quantitation data and prediction results showed opposite trends for HLA-DRB1*0101.

Then, I tested whether the HLA-DRB1*1501 and HLA-DRB1*0101 could display different levels of peptide repertoire. When I mapped 45 antigens, 75% of them contained a higher level of repertoire for HLA-DRB1*0101 than for HLA-

DRB1*1501. Although this finding was based on a limited number of antigens, it indicated that mycobacterial antigens might have evolved to avert presentation by HLA-DRB1*1501, which could explain why HLA-DRB1*0101 was inhibited during infection compared with HLA-DRB1*1501.

Despite the high levels of similarity and diversity of the MHC-II alleles, MS-based quantitative proteomics provides a powerful tool to quantify specific HLA-allele-specific expression. These observations indicate that DR-alleles undergo differential expression, and that mycobacterial infection could selectively interfere with that. Considering the several reports which show an association between HLA-DRB1*1501 and TB susceptibility, I speculate mycobacteria may avoid T cell recognition via inhibit HLA-DRB1*0101 allele and avoid being presented to the DRB1*1501 allele.

6.2.1 **Ongoing work**

Currently, I am undertaking two main experiments to explore the interactions between BCG infection and the expression and presentation of HLA-DRB1*0101 and HLA-DRB1*1501.

1. Mycobacterial infection may influence the surface expression of HLA-DRB1*0101 and -DRB1*1501 alleles differentially. To investigate this, I am using two lymphoblastoid cell lines: one is a heterozygote-encoding DRB1*01:01/01:03 line, and the other is a homozygote-encoding HLA-DRB1*15:01 line. These cell lines will be used to discover the effect of mycobacterial infection on the surface expression of each allele with analysis through flow cytometry.

2. I aim to find out the contribution level of HLA-DRB1*0101 and -DRB1*1501 alleles in presentation of mycobacterial antigens. Because we have THP-1 cells that lack DRB1 alleles, I plan to transfect these cells with plasmids that express HLA-DRB1*01:01 and -DRB1*15:01 separately. Once the surface expression of each allele has been validated, I will infect them and wild-type THP-1 cells with mycobacteria. Then, I will analyse the immunopeptidome of each group with the use of LC-MS-MS.

6.2.2 **Future work**

To expand on the observation that HLA-DRB1*0101 is predicted to present more mycobacterial peptides than HLA-DRB1*15:01, an unbiased *in-silico* analysis of the whole proteome of mycobacteria can be undertaken to map all MTB antigens against HLA-DRB1*01:01 and -DRB1*15:01 and to discover the different levels of peptide repertoire for each allele. If there is a significant difference between the two, this work can be translated to *in-vivo* evaluation with the use of HLA-DR transgenic mice to discover the effect of these alleles on TB disease susceptibility, the priming of T cells and protection levels. In this regard, two groups of transgenic mice can be generated to express HLA-DRB1*01:01 and -DRB1*15:01 separately, and immunogenicity and protective efficacy can be assessed in comparison with a wild type.

6.3 Summary of main findings of work described in Chapter 5

As mentioned, when there are no immunological markers of protection that can be used to identify protective antigens, the best way to assess candidate antigens is to measure their ability to provide significant protection. The use of MGIA enables the evaluation of vaccine-induced protection by measurement of the ability of immune cells to inhibit mycobacterial growth *ex vivo*. This assay was utilised not only as a surrogate for *in vivo* challenge with MTB but also served as a functional correlate of protection (350). Therefore, initially, I employed MGIA to screen the selected antigens (hisD, metE, and mmpL12). It was found that metE conferred protection, as the mouse groups that were vaccinated with metE antigen (either as DNA or adjuvant protein vaccines) inhibited mycobacterial growth significantly compared with the unvaccinated group. Depending on the vaccination platforms, different immunogenicity outcomes were obtained; the metE-DNA vaccine-elicited Th1 cytokines (IFNγ, TNFα, and IL-2), whereas the metE-AddaS03 vaccine induced production of mixed Th1 and Th2 responses characterised by TNFα, IL-2 and IL-4. Both metE-DNA and metE-AddaS03 vaccines significantly induced the production of IgG antibodies compared with the naïve and BCG-vaccinated groups, but when they were compared with each other, the antibody concentrations that were induced by the metE-AddaS03 vaccine were 16-fold greater than the concentrations induced by the metE-DNA vaccine. The current work showed that the metE antigen is an immunogenic and protective antigen that warrants further evaluation.

6.3.1 **Ongoing work**

To verify the protective effect results that were obtained through MGIA of the metE antigen, I am currently performing *in-vivo* MTB challenge experiments in mice. I have included AS01 adjuvant to induce a Th1-biased immune response to metE, because it was found that AS03 adjuvant shifted the immune response towards Th2 cells. In parallel, I am performing an immunogenicity experiment to compare the different immune responses, in terms of T cells and antibody titres, which are induced by AS01 and AS03 when formulated with metE antigen. This will enable me to correlate cellular and humoral responses with the efficacy data from the challenge experiment.

6.3.2 **Future work**

The following is a list of proposed experiments to further characterise the metE antigen.

- Optimisation of the metE antigen dose is important to determine the dose that is effective below 1ug, as certain antigens have been shown to be more immunogenic and protective when given at a low dose (398).
- The protective effect of metE antigen must be evaluated when delivered through different systems, such as viral vector and mRNA, as these platforms are safe and effective in humans.
- Similarly, the protective effect of metE antigen must be evaluated when administered through different vaccination regimens, such as during use as a booster for BCG.

- The protective effect of metE antigen must also be evaluated according to the route of administration, such as intranasal to induce local immunity, since MTB primarily affects the lungs.
- The protective effect of metE antigen must be investigated when it is combined with other protective antigens such as PPE15.

Chapter 7

Appendix

7.1 Identified BCG peptides

Appendix Table 7.1 *Identified BCG peptides and corresponding proteins.*

Number	Peptide	Peaks score (-10lgP)	Length	Gene	Protein	Accession
IP: B721 Sample 2: HK-BCG						
1	KAAPAKKAAPAK	18.16	12	hbhA	Heparin-binding hemagglutinin	A1KFU9
2	KDVSGHVITL	20.04	10	hisD	Histidinol dehydrogenase	A0A0H3M564
3	KHRGLSFL	21.91	8	fadE17	Probable acyl-CoA dehydrogenase	A0A0H3M7B4
4	KKAPAKASET	16.93	10	rplV	50S ribosomal protein L22	A1KGI7
5	KVVVVGGGT	18.63	9	cysG	Possible multifunctional enzyme siroheme synthase cysG	A0A0H3M9R7
6	TGSMHDLLMSNFFA	16.95	14	pgi	Glucose-6-phosphate isomerase	A1KH80
7	TTYTLEYDG	15.96	9	PE1	PE family protein	A0A0H3M9W4
8	TVRCVSGTVEL	23	11	BCG_2418	Uncharacterized protein	A0A0H3MCK0
9	VLSLLGMVLLMLGTGRL	15.24	17	BCG_3867c	Probable conserved transmembrane protein	A0A0H3MFQ9
10	WDNGTTHD	32.83	8	ctpI	Probable cation-transporter atpase I	A0A0H3M0P5
IP: B721 Sample 3: live BCG						
1	APQLGRWKWHDPWVHASLLA	16.03	20	fbpD	Secreted MPT51/MPB51 antigen protein	A0A0H3MA34
2	CAAVCTGCVAVVLAPVSLA	17.67	19	BCG_0349	Possible conserved exported protein	A0A0H3M181
3	DFDGAADAGFTAPATTL	15.04	17	PPE55a	PPE Family protein [first part]	A0A0H3M8U0
4	ELATSRRPDHLHGLATQL	18.74	18	BCG_1984	Uncharacterized protein	A0A0H3MEB3|A0A0H3M474
5	KATMRISA	17.58	8	treZa	Maltooligosyltrehalose trehalohydrolase TreZ	A0A0H3MAJ3
6	KHRGLSFL	25.07	8	fadE17	Probable acyl-CoA dehydrogenase	A0A0H3M7B4
7	LLARRPVVH	15.45	9	BCG_3268c	Probable conserved transmembrane transport protein	A0A0H3MAR2|A0A0H3MBW3
8	LRHRIRFGA	15.53	9	BCG_0944	Probable monooxygenase	A0A0H3M920
9	TVAIQNKAI	19.57	9	BCG_3870c	Galactofuranosyl transferase	A0A0H3MAQ2
10	TVRCVSGTVEL	17.4	11	BCG_2418	Uncharacterized protein	A0A0H3MCK0
11	VAGPVPVAGHLT	15.62	12	BCG_0616c	Uncharacterized protein	A0A0H3MAR4
IP: B721 Sample 5: + IFNγ / anti-IL-10 + HK-BCG						
1	ADIAIQAEQFAVIKK	45.19	15	clpP1	ATP-dependent Clp protease proteolytic subunit	A0A0H3M791
2	ELATSRRPDHLHGLATQL	16.24	18	BCG_1984	Uncharacterized protein	A0A0H3MEB3|A0A0H3M474
3	EVDEDTSAYD	21.33	10	cysA2	Sulfurtransferase	A0A0H3MB67|A0A0H3M8T4
4	EVNSARIYAGA	19.71	11	PPE13	PPE family protein	A0A0H3M4M6
5	FVRSRPELKLPDLELIFAP	16.86	19	BCG_1338	Probable dehydrogenase FAD flavoprotein gmc oxidoreductase	A0A0H3M4G4

6	IKYNGEEYLIL	17.65	11	groS	10 kDa chaperonin	A1KPA9
7	KFARITLGT	15.67	9	nuoG	NADH-quinone oxidoreductase	A0A0H3MAH2
8	KPADGVPPPPLNTKLPEDPPP	15.87	21	BCG_2181c	Probable conserved proline rich membrane protein	A0A0H3MBV1
9	LATLFGDGVLRPLPV	16.09	15	pks12	Probable polyketide synthase pks12	A0A0H3M7L7
10	SAVTAGLCRALAR	15.36	13	cobQ	Cobyric acid synthase	A1KF76
11	TGFYNTGDVNT	16.08	11	PPE8	PPE family protein	A0A0H3M207
12	TLRLPLDV	18.38	8	BCG_1012	Possible magnesium chelatase	A0A0H3M4V4
IP: B721 **Sample 6: + IFNγ / anti-IL-10 + live BCG**						
1	ADIAIQAEQFAVIKK	31.37	15	clpP1	ATP-dependent Clp protease proteolytic subunit	A0A0H3M791|A0A0H3M791_MYCBP
2	AILRLPLT	18.71	8	BCG_2874	Uncharacterized protein	A0A0H3MGJ6
3	APTNHAGV	19.78	8	BCG_2590	Conserved hypothetical alanine and leucine rich protein	A0A0H3MCX2
4	AVDPTVRVQ	19.56	9	BCG_0467c	Uncharacterized protein	A0A0H3MAG6
5	FGTFQLTMFGVGATI	15.53	15	rocE	Probable cationic amino acid transport integral membrane protein rocE	A0A0H3M616
6	GFYNTGSYNTGGFN	16.03	14	PPE8	PPE family protein	A0A0H3M207
7	KAAPAKKAAPAK	22.72	12	hbhA	Heparin-binding hemagglutinin	A1KFU9
8	KAAQVATTLT	15.05	10	BCG_3311	Nucleoside triphosphate pyrophosphatase	A1KNT4
9	KPAKAAKPAL	18.22	10	BCG_3557c	Conserved hypothetical mce associated alanine and valine rich protein	A0A0H3M9N5
10	LLIDRLSVQ	17.05	9	BCG_2206c	Uncharacterized protein	A0A0H3M6M1
11	TALLQLLSA	16.52	9	BCG_1349c	Uncharacterized protein	A0A0H3M4H3
IP: IVA12 **Sample 2: HK-BCG**						
1	KKAAPAKKAAPAK	23.04	13	hbhA	Heparin-binding hemagglutinin	A1KFU9
2	PGDMPGGTAAADAAHTED	16.92	18	grpE	Protein GrpE	A1KFH3
3	TADQRVLAIRLTNGSSLLISKSLKP	16.35	25	mprB	Signal transduction histidine-protein kinase/phosphatase MprB	A1KHB8
4	TFSGLLDRFGRGKGCDICKPVVAS	17.42	24	nirB	Probable nitrite reductase	A0A0H3M1Q9
5	WDNGTTHD	24.84	8	ctpI	Probable cation-transporter atpase I ctpI	A0A0H3M0P5
IP: IVA12 **Sample 3: live BCG**						
1	KALMSIGKVITASAAT	16.7	16	mmpL12	Probable conserved transmembrane transport protein mmpL12	A0A0H3M689
2	KAPAKKAATKAPAKK	18.28	15	hupB	Probable DNA-binding protein HU homolog hupB	A0A0H3M7X4
3	KATLMSALTL	15.44	10	mmpL3	Conserved transmembrane transport protein mmpL3	A0A0H3M2S6
4	KPLVRHTVHT	19.84	10	nrp	Probable peptide synthetase nrp	A0A0H3M1C1
IP: IVA12 **Sample 5: + IFNγ / anti-IL-10 + HK-BCG**						
1	AQTGVYEDLLAAGVADPVK	67.66	19	groL2	60 kDa chaperonin 2	A1KFR2
2	DDLLRPGI	16.4	8	subI	Probable sulfate-binding lipoprotein subI	A0A0H3MFF9
3	DNQPSVQIQVYQGEREIAAHNKL	57.14	23	dnaK	Chaperone protein DnaK	A1KFH2

4	DPFEDLGAQLVK	45.44	12	groL1	60 kDa chaperonin 1	A1KPA8
5	DTNYHYLVPEIGPS	46.86	14	metE	5-methyltetrahydropteroyltriglutamate--homocysteine methyltransferase	A1KHS4
6	FLKFIATEIFP	18.69	11	mmaA2	Methoxy mycolic acid synthase 2 mmaA2	A0A0H3M233
7	FRDEQGQDVLL	21.4	11	atpD	ATP synthase subunit beta	A1KI98
8	GLTGIIMRATI	15.23	11	BCG_3852	Putative oxidoreductase	A0A0H3MC09
9	IAGRFGLLD	16.45	9	mmpL9a	Probable conserved transmembrane transport protein mmpL9a	A0A0H3M636
10	KLIENLRADT	15.17	10	mmpL12	Probable conserved transmembrane transport protein mmpL12	A0A0H3M689
11	LQDMAILTGGQVIS	34.93	14	groL2	60 kDa chaperonin 2	A1KFR2
12	NGEEYLILSARDVLA	60.72	15	groS	10 kDa chaperonin	A1KPA9
13	SPPDNTIRAFRDEVLAA	15.87	17	cysA2	Sulfurtransferase	A0A0H3MB67|A0A0H3M8T4
14	TGVYEDLLAAGVADPVK	60.75	17	groL2	60 kDa chaperonin 2	A1KFR2
15	WDNGTTHD	28.9	8	ctpI	Probable cation-transporter atpase I ctpI	A0A0H3M0P5
16	YLILSARDVLA	35.95	11	groS	10 kDa chaperonin	A1KPA9
IP: IVA12 **Sample 6: + IFNγ / anti-IL-10 + live BCG**						
1	ANRAELKALIASNLLGQNT	44.17	19	PPE50	PPE family protein	A0A0H3M8U4
2	AQTGVYEDLLAAGVADPVK	76.47	19	groL2	60 kDa chaperonin 2	A1KFR2
3	DDLLRPGI	23.71	8	subI	Probable sulfate-binding lipoprotein subI	A0A0H3MFF9
4	DTNYHYLVPEIGPS	25.94	14	metE	5-methyltetrahydropteroyltriglutamate--homocysteine methyltransferase	A1KHS4
5	GGAGGAGGWLIGQSGSTGGGGAGG	15.25	24	PE_PGRS48	PE-PGRS family protein	A0A0H3M9S3
6	GTTTYSSTAQHSA	19.16	13	BCG_2720	Probable conserved transmembrane alanine and leucine rich protein	A0A0H3MD69
7	KPEDRYASAG	15.01	10	pknH	Probable transmembrane serine/threonine-protein kinase H pknH	A0A0H3M9Y5
8	LAIDVSDPRVI	16.35	11	BCG_3198	Probable short-chain dehydrogenase/reductase	A0A0H3MHA8
9	LQDMAILTGGQVIS	39.74	14	groL2	60 kDa chaperonin 2	A1KFR2
10	LRTLRDDPADAEVASHKLL	15.73	19	proS	Proline--tRNA ligase	A1KMI8
11	NGEEYLILSARDVL	25.25	14	groS	10 kDa chaperonin	A1KPA9
12	NGEEYLILSARDVLA	68.19	15	groS	10 kDa chaperonin	A1KPA9
13	PGIPFGAA	21.71	8	BCG_0106	Probable aminotransferase	A0A0H3M786
14	TIAMLETAGLWG	16.49	12	BCG_1796	Possible sulfite oxidase	A0A0H3MDW2
15	WPAPYGRG	15.47	8	fadE34	Probable acyl-CoA dehydrogenase fadE34	A0A0H3MIH3
16	YLILSARDVLA	35.2	11	groS	10 kDa chaperonin	A1KPA9

7.2 Identified MTB peptides

Appendix Table 7.2 *Identified MTB peptides and corresponding proteins.*

Number	Peptide	Peaks score (-10lgP)	Length	Gene	Protein	Accession
IP: B721 Sample 2: + IFNγ / anti-IL-10 + live MTB						
1	AAPKNDLSWHDCT	15.04	13	Rv2672	Possible secreted protease	P71969
2	AGTWVKAVAGIRLALSLGFRVRVA	16.67	24	moeX	Possible molybdopterin biosynthesis protein MoeX	O33183
3	APGAVDPAGLRAQLAQRLPGYLVP	15.37	24	nrp	Phenyloxazoline synthase MbtB	Q10896
4	ARAKARKAKAPK	18.44	12	Rv2164c	Probable conserved proline rich membrane protein	O06213
5	ETRLDMSIPAP	17.82	11	dnaX	DNA polymerase III subunit gamma/tau	P9WNT9
6	KAPAGGTGGAGGDGGAGGKG	15.93	20	PE_PGRS56	PE-PGRS family protein PE_PGRS56	Q6MWW7
7	KLGAVAVPINTRLAAP	15.81	16	fadD13	Long-chain-fatty-acid--CoA ligase FadD13	P9WQ37
8	KPFELMELDLDGP	15.31	13	adhD	Putative alcohol dehydrogenase D	P9WQB9
9	RAKARKAKAPK	24.62	11	Rv2164c	Probable conserved proline rich membrane protein	O06213
10	RLAIADDLAF	17.38	10	Rv2282c	Uncharacterized HTH-type transcriptional regulator	P9WMF3
11	RPDRIVVGEVRGAEVVDLLAAL	16.6	22	Rv3659c	Putative conjugal transfer protein	P9WMT3
12	TPHTEFEGQVYILSKDEGG	24.54	19	tuf	Elongation factor Tu	P9WNN1
13	TTYTLEYDG	17.24	9	PE1	PE family protein PE1	Q79G06
14	TVGPARATFR	15.88	10	helZ	Probable helicase HelZ	I6YCF3
15	VGMPAPA	18.3	7	pssA	CDP-diacylglycerol--serine O-phosphatidyltransferase	P9WPG1
16	VTPVKPGTPGEPTPITPVTPPVAP	15.65	24	espK	ESX-1 secretion-associated protein EspK	P9WJC1
IP: IVA12 Sample 2: + IFNγ / anti-IL-10 + live MTB						
1	AIEKTFAAI	16.52	9	Rv1488	Uncharacterized protein	P9WPR9
2	AQTGVYEDLLAAGVADPVK	50.03	19	groEL2	Heat shock protein 65	P9WPE7
3	DAGGTYQPHPAEAVVE	38.99	16	fadB	3-hydroxyacyl-CoA dehydrogenase	O53872
4	DMAILTGGQVISEE	27.16	14	groEL2	Heat shock protein 65	P9WPE7
5	DMAILTGGQVISEEVG	22.7	16	groEL2	Heat shock protein 65	P9WPE7
6	EDALWRWMTAAALVRPRGAG	15.13	20	priA	Probable primosomal protein N	P9WMQ9
7	ESLQEVARAAGLQ	19.93	13	fadD9	Carboxylic acid reductase	Q50631
8	EVTRELQAL	18.66	9	pks17	Probable polyketide synthase Pks17	O06585
9	FFKAYVVN	15.22	8	mce3C	Mce-family protein Mce3C	O53969
10	FGLTQNVYLVFAAT	15.58	14	Rv2723	Uncharacterized membrane protein	P9WG93
11	GGLGNRGGAGGAGGAGGVGG	18.72	20	PE_PGRS21	PE-PGRS family protein PE_PGRS21	Q79FT0
12	GTGGAGGAGGLGGHGGAGGLLIGNG	16.88	25	PE_PGRS48	PE-PGRS family protein	Q6MX26
13	GVDPLTAIRY	25.37	10	Rv3000	Possible conserved transmembrane protein	I6X5Z8
14	GVGGAGGQGGLLFGDGGNGGA	15.57	21	PE_PGRS58	PE-PGRS family protein PE_PGRS58	I6XHM5

Number	Peptide	Peaks score (-10lgP)	Length	Gene	Protein	Accession
15	GYDFLPGTTVN	15.28	11	fadA3	Probable beta-ketoacyl CoA thiolase FadA3	O53422
16	KAAPRVAKAAKAAPKK	20.5	16	rpsQ	30S ribosomal protein S17	P9WH51
17	KAVSKAARAK	15.7	10	secE	Protein translocase subunit SecE	P9WGN7
18	KPAEEGDVVGASEPDAK	15.74	17	rplQ	50S ribosomal protein L17	P9WHD3
19	KSKGAKGKSGKK	21.3	12	ffh	Signal recognition particle protein	P9WGD7
20	KTPVSRMRPTRCCCPAAP	16.13	18	Rv2251	Possible flavoprotein	L0TBR2
21	LAQQGFFKG	15.39	9	ppiB	Probable peptidyl-prolyl cis-trans isomerase B	P9WHW1
22	LTILLACSAIDTSSAAALL	15.09	19	Rv0235c	Probable conserved transmembrane protein	P96418
23	NAVVVKPVPPSAVVVGVPGQVIGQ	16.33	24	cysE	Serine acetyltransferase	P95231
24	NGEEYLILSARDVL	30.61	14	groS	Co-chaperonin GroES	P9WPE5
25	NGEEYLILSARDVLA	31.38	15	groS	Co-chaperonin GroES	P9WPE5
26	PLKQIAFNSGLEPGVVAEKVRNLP	16.3	24	groEL2	Heat shock protein 65	P9WPE7
27	PMFEAPGRITELITSFIEE	16.95	19	Rv3338	AB hydrolase-1 domain-containing protein	O53388
28	PVLVYLTIT	24.54	9	irtA	Mycobactin import ATP-binding/permease protein IrtA	P9WQJ9
29	QALTAGAGAYAFAEAA	17.11	16	PE_PGRS53	PE-PGRS family protein PE_PGRS53	Q6MWW9
30	TLISAGAVEY	15.67	10	mltG	Endolytic murein transglycosylase	I6XEK6
31	VPAISLPLAQSADGMPVGMML	15.75	21	amiC	Putative amidase AmiC	P9WQ95
32	WPQPAQP	16.87	7	Rv0926c	DAP_DH_C domain-containing protein	I6WZS8
33	WVQEYLEATARLDAL	16.5	15	Rv1894c	NMO domain-containing protein	O07738
34	YSFVVLLIT	17.47	9	qcrB	Cytochrome bc1 complex cytochrome b subunit	P9WP37
IP: W6/32 Sample 2: + IFNγ / anti-IL-10 + live MTB						
1	AAKKAPARK	20.38	9	hbs	Possible histone-like protein Hns	I6YHB0
2	AGKVLRI	16.61	7	lppZ	Probable conserved lipoprotein LppZ	I6Y293
3	ALAIGAI	19.01	7	Rv0426c	Possible transmembrane protein	P96272
4	AVAAPTG	16.52	7	MmpL13b	Probable conserved transmembrane transport protein MmpL13b	O06546
5	ELLSRAHQL	15.28	9	Rv0024	Secreted protein P60-related protein	P71594
6	FIRITDETL	25.85	9	Rv0306	Oxidoreductase	O07233
7	GFAEIAL	15.13	7	ppsD	Phenolphthiocerol/phthiocerol polyketide synthase subunit D	P9WQE3
8	IAINLRGAW	16.72	9	Rv1941	Probable short-chain type dehydrogenase/reductase	I6XZC4
9	IAQKHATI	17.68	8	Rv2209	Uncharacterized protein	P9WLI3
10	IAVGKLAL	15.43	8	mez	Putative malate oxidoreductase	P9WK25
11	IEIGAGV	18.4	7	Rv0161	Possible oxidoreductase	O07406
12	IGPTHTL	15.5	7	Rv3776	Uncharacterized protein	P72042
13	LAARLPLAY	17.2	9	Rv1204c	AAA domain-containing protein	O05305
14	LAGELKAAGDDY	15.95	12	Rv1260	Uncharacterized protein	P9WM51
15	LENVRPLA	16.57	8	Rv3239c	Probable conserved transmembrane transport protein	O05884
16	LFAGDLLFI	15.49	9	Rv0939	Possible bifunctional enzyme	O86346
17	LGGAGVFAV	15.59	9	SugI	Probable sugar-transport integral membrane protein SugI	L0TDU1
18	LVTDDLIEY	17.4	9	Rv3359	Possible oxidoreductase	O50388

Number	Peptide	Peaks score (-10lgP)	Length	Gene	Protein	Accession
19	MIGAGIFAAL	16.34	10	Rv1999c	Uncharacterized transporter	P9WQM3
20	PRDWHQVTVVSSPSWFSDY	24.33	19	mycP2	Mycosin-2	O05458
21	QLMLRPVL	18.07	8	Rv0998	Acetyltransferase Pat	O05581
22	RVGIDAEAGPT	19.71	11	hisD	Histidinol dehydrogenase	P9WNW9
23	SDAAHDMVSSCA	16.6	12	Rv2488c	Probable transcriptional regulatory protein	O53213
24	SHGSAYPSTEQ	18.71	11	lprM	Possible Mce-family lipoprotein LprM	O53971
25	SHGSAYPSTEQT	23.59	12	lprM	Possible Mce-family lipoprotein LprM	O53971
26	TAQNVIDASV	16.91	10	Rv3365c	Conserved protein	Q93IG6
27	TLAAFLWAL	16.32	9	lhr	Probable ATP-dependent helicase Lhr	P96901
28	TLADGTVLGYD	17.01	11	Rv0688	Ferredoxin reductase	P95034
29	TLSGLAPATL	20.12	10	Rv3233c	Possible triacylglycerol synthase	O05878
30	TPKKMIAA	17.83	8	rplD	50S ribosomal protein L4	P9WH85
31	TTDLLYEVD	15.82	9	Rv3472	Conserved protein	I6YG83
32	TVAFPKPSV	15.46	9	Rv1320c	Uncharacterized protein	P9WQ29
33	TVELDEPLV	15.8	9	dlaT	Dihydrolipoyllysine-residue acetyltransferase	P9WIS7
34	TVHGKCGSLTL	15.44	11	manA	mannose-6-phosphate isomerase	O05898
35	VHADAAPA	17.24	8	Rv2642	mannose-6-phosphate isomerase	O05898
36	VIHVVADASAL	20.11	11	Rv2209	Uncharacterized protein	P9WLI3
37	VLAVVIIGVL	17.06	10	Rv0544c	Possible conserved transmembrane protein	O06410

7.3 Prioritisation of identified antigens

7.3.1 Characterisation of identified peptides

Appendix Table 7.3 *Immunopeptidomics and immunoinformatics information of each selected antigens.*
Key: SB = strong binder; WB = week binder and BH = best hit.

Peptide	Source of peptide	Peaks score -10lgP	Length	HLA Hit (THP-1 alleles)	Predicted affinity (IC50)	Bind level	Antigen	Length	HLA-II Coverage %
AQTGVYEDLLAAGVADPVK	BCG live infection (sample 3/6)	76.47	19	HLA-DRB1*01:01	120.1	SB	groL2	540	96.3
AQTGVYEDLLAAGVADPVK	MTB live infection	50.03							
AQTGVYEDLLAAGVADPVK	BCG live infection (Bettencourt et al, 2020)	35.11							
AQTGVYEDLLAAGVADPVK	BCG HK infection (sample 2/5)	67.66							
DMAILTGGQVISEE	MTB live infection	27.16	14	DRB1*01:01	125.93	WB			
				DQA1*01:02/DQB1*06:02	681.57	WB			
DMAILTGGQVISEEVG	MTB live infection	22.7	16	DQA1*01:02/DQB1*06:02	325.4	WB			
DPYEKIGAELVK	BCG HK infection (Bettencourt et al, 2020)	68.08	12	DRB1*01:01	168.26	SB			
				DRB5*01:01	3330.13	WB			
				DQA1*01:01/DQB1*05:01	10620.69	WB			
DPYEKIGAELVKEVA	BCG HK infection (Bettencourt et al, 2020)	46.93	15	DRB1*01:01	19.32	SB			
				DRB5*01:01	505.81	WB			
				DQA1*01:01/DQB1*05:01	5015.64	WB			
				DPA1*01:03/DPB1*02:01	921.1	WB			
				DPA1*01:03/DPB1*04:01	3112.14	WB			
DPYEKIGAELVKEVAK	BCG HK infection (Bettencourt et al, 2020)	49.14	16	DRB1*01:01	43.46	SB			
				DRB5*01:01	978.14	WB			
				DQA1*01:01/DQB1*05:01	3929.4	WB			

				DPA1*01:03/DPB1*02:01	835.56	WB			
				DPA1*01:03/DPB1*04:01	2733.5	WB			
EDPYEKIGAELVKE	BCG HK infection (Bettencourt et al, 2020)	45.4	14	DRB1*01:01	50.68	SB			
				DRB1*15:01	53.51	WB			
				DRB5*01:01	29.36	SB			
				DQA1*01:01/DQB1*05:01	6440.5	SB			
				DPA1*01:03/DPB1*02:01	2652.36	WB			
				DPA1*01:03/DPB1*04:01	6429.98	WB			
LEDPYEKIGAELVKE	BCG HK infection (Bettencourt et al, 2020)	30.75	15	DRB1*01:01	27.8	SB			
				DRB1*15:01	2452.01	WB			
				DRB5*01:01	728.03	SB			
				DQA1*01:01/DQB1*05:01	7059.76	SB			
				DPA1*01:03/DPB1*02:01	2136.74	WB			
				DPA1*01:03/DPB1*04:01	5702.38	WB			
LQDMAILTGGQVIS	BCG live infection (sample 3/6)	39.74	14	DRB1*01:01	38.05	SB			
				DRB1*15:01	547.02	WB			
LQDMAILTGGQVIS	BCG HK infection (sample 2/5)	34.93							
TGVYEDLLAAGVADPVK	BCG HK infection (sample 2/5)	60.75	17	DRB1*01:01	83.16	SB			
NGEEYLILSARDVL	BCG live infection (sample 3/6)	25.25	14	DRB1*01:01	10.11	SB			
				DRB1*15:01	454.15	WB			
NGEEYLILSARDVL	MTB live infection	30.61		DRB5*01:01	310.26	WB			
				DQA1*01:01/DQB1*05:01	1434.35	WB			
NGEEYLILSARDVLA	BCG live infection (sample 3/6)	68.19	15	DRB1*01:01	4.11	SB			
NGEEYLILSARDVLA	BCG live infection (Bettencourt et al, 2020)	68.22		DRB1*15:01	113.16	WB	**groS**	100	88.8
NGEEYLILSARDVLA	MTB live infection	31.38		DRB5*01:01	70.36	WB			
NGEEYLILSARDVLA	BCG HK infection (sample 2/5)	60.72		DQA1*01:01/DQB1*05:01	499.3	WB			
YLILSARDVLA	BCG live infection (sample 3/6)	35.2							
YLILSARDVLA	BCG live infection (Bettencourt et al, 2020)	41.23	11	HLA-B*15:11	13797.22	BH			
YLILSARDVLA	BCG HK infection (sample 2/5)	35.95							
DNQPSVQIQVYQGEREIAAHNKL	BCG HK infection (sample 2/5)	57.14	23	DRB1*01:01	137.46	SB	**dnaK**	625	100
				DQA1*01:02/DQB1*06:02	1280.6	WB			

DTNYHYLVPEIGPS DTNYHYLVPEIGPS DTNYHYLVPEIGPS	BCG HK infection (sample 2/5) BCG live infection (sample 3/6) BCG HK infection (Bettencourt et al, 2020)	46.86 25.94 31.61	14	DRB1*01:01 DRB5*01:01 DQA1*01:01/DQB1*05:01 DQA1*01:02/DQB1*06:02 DPA1*01:03/DPB1*02:01 DPA1*01:03/DPB1*04:01	64.01 1742.68 785.74 2328.59 3676.84 7054.19	SB WB WB WB WB SW	**metE**	759	100
DPFEDLGAQLVK	BCG HK infection (sample 2/5)	45.44	12	DRB1*01:01 DQA1*01:01/DQB1*05:01	168.09 3918.83	SB WB	**groL1**	539	100
ADIAIQAEQFAVIKK ADIAIQAEQFAVIKK	BCG HK infection (sample 2/5) BCG live infection (sample 3/6)	45.19 31.37	15	DQA1*01:01/DQB1*05:01 DPA1*01:03/DPB1*02:01 DPA1*01:03/DPB1*04:01	168.09 3918.83	SB WB	**clpP1**	200	88.9
ANRAELKALIASNLLGQNT ANRAELKALIASNLLGQNT	BCG live infection (sample 3/6) BCG live infection (Bettencourt et al, 2020)	44.17 39.94	19	DRB1*01:01	11.35	SB	**PPE50**	381	92.6
DAGGTYQPHPAEAVVE	MTB live infection	38.99	16	DRB1*01:01 DRB1*15:01 DRB5*01:01 DPA1*01:03/DPB1*02:01 DPA1*01:03/DPB1*04:01	318.75 4512.01 2976.13 3385.79 9408.99	WB WB WB WB WB	**fadB**	720	100
WDNGTTHD	BCG HK infection (sample 2/5)	32.83	8	HLA-B*15:11	41372.39	BH	**ctpI**	1,625	100
LAASLLSRV	BCG HK infection (Bettencourt et al, 2020)	28.16	9	HLA-C*03:03	560.92	BH	**BCG_3870c**	637	100
TVAIQNKAI	BCG live infection (sample 3/6)	19.57	9	HLA-C*03:03	2537.49	BH			
FIRITDETL	MTB live infection	25.85	9	HLA-C*03:03	409.85	WB	**Rv0306 (BCG_0346)**	223	81.5
GVDPLTAIRY	MTB live infection	25.37	10	HLA-A*02:01	10557.66	BH	**Rv3000 (BCG_3022)**	219	85.2
KHRGLSFL KHRGLSFL	BCG live infection (sample 3/6) BCG HK infection (sample 2/5)	25.07 21.91	8	HLA-C*03:03	20813.90	BH	**fadE17**	409	100
AGCTLLIR	BCG live infection (Bettencourt et al, 2020)	24.98	8	HLA-C*03:03	41825.10	BH	**mmpL12**	1,107	100
KALMSIGKVITASAAT	BCG live infection (sample 3/6)	16.7	16	DQA1*01:02/DQB1*06:02	164.68	WB			
KLIENLRADT	BCG HK infection (sample 2/5)	15.17	10	HLA-C*03:03	28331.79	BH			
RAKARKAKAPK	MTB live infection	24.62	11	HLA-C*03:03	27278.95	BH	**Rv2164c (BCG_2181c)**	384	70.4

TPHTEFEGQVYILSKDEGG	MTB live infection	24.54	19	DPA1*01:03/DPB1*02:01 DPA1*01:03/DPB1*04:01		BH	**tuf**	396	100
PVLVYLTIT	MTB live infection	24.54	9	HLA-C*03:03	39196.13	BH	**irtA (BCG_1410)**	859	100
PRDWHQVTVVSSPSWFSDY	MTB live infection	24.33	19	DQA1*01:01/DQB1*05:01	290.19	BH	**mycP2 (BCG_3941c)**	550	100
DDLLRPGI DDLLRPGI	BCG live infection (sample 3/6) BCG HK infection (sample 2/5)	23.71 16.4	8	HLA-A*02:01	35559.24	BH	**subI**	356	100
SHGSAYPSTEQT	MTB live infection	23.59	12	DQA1*01:01/DQB1*05:01	12863.86	BH	**lprM (Rv1970)**	377	85.2
KKAAPAKKAAPAK	BCG HK infection (sample 2/5)	23.04	13	DRB5*01:01	10003.21	BH	**hbhA**	199	74
KKAAAKKAPAKKAAAKK	BCG live infection (Bettencourt et al, 2020)	28.56	17	DRB5*01:01	390.08	BH			
KAPAKKAAAKKVTQK	BCG HK infection (Bettencourt et al, 2020)	24.92	15	HLA-DRB1*01:01	292.87	WB			
KAPAKKAAAK	BCG HK infection (Bettencourt et al, 2020)	21.26	10	HLA-C*03:03	24882.07	BH			
KAAPAKKAAPAK KAAPAKKAAPAK	BCG live infection (sample 3/6) BCG HK infection (sample 2/5)	22.72 18.16	12	DRB5*01:01	16067.89	BH			
AKKAAPAKKAAPAKKAAAKK	BCG live infection (Bettencourt et al, 2020)	17.73	20	DRB5*01:01	175.16	BH			
AAAKKAPAKKAAAKK	BCG live infection (Bettencourt et al, 2020)	17.24	15	DRB5*01:01	555.08	BH			
TVRCVSGTVEL TVRCVSGTVEL	BCG HK infection (sample 2/5) BCG live infection (sample 3/6)	23 17.4	11	HLA-C*03:03	1437.83	BH	**BCG_2418**	642	100
PGIPFGAA	BCG live infection (sample 3/6)	21.71	8	HLA-C*03:03	31060.9	BH	**BCG_0106**	390	96.3
FRDEQGQDVLL	BCG HK infection (sample 2/5)	21.4	11	HLA-C*03:03	2751.98	BH	**atpD**	486	96.3
EVDEDTSAYD	BCG HK infection (sample 2/5)	21.33	10	HLA-C*03:03	36141.06	BH	**cysA2**	277	96.3
KSKGAKGKSGKK	MTB live infection	21.3	12	DRB5*01:01	15270.06	BH	**ffh (BCG_2937c)**	525	92.6
KAPAKKAPAKASETSAAKGGS	BCG live infection (Bettencourt et al, 2020)	21.12	21	HLA- DQA1*01:02/DQB1*06:02	2283.41	WB	**rplV**	197	100
KKAPAKASET	BCG HK infection (sample 2/5)	16.93	10	HLA-C*03:03	35367.39	BH			
PAKKAAAKAPA	BCG live infection (Bettencourt et al, 2020)	16.31	11	HLA-C*03:03	26265.23	BH			
KAAPRVAKAAKAAPKK	MTB live infection	20.5	16	DRB1*01:01 DRB5*01:01	235 177.59	WB WB	**rpsQ (BCG_0760)**	136	74

				DQA1*01:02/DQB1*06:02 DPA1*01:03/DPB1*04:01	637.87 9396.07	WB WB			
AAKKAPARK	MTB live infection	20.38	9	HLA-C*03:03	28178.94	BH	**hbs (BCG_3915)**	134	37
TLSGLAPATL	MTB live infection	20.12	10	HLA-A*02:01 HLA-C*03:03	146.63 442.10	WB	**Rv3233c (BCG_3263c)**	469	100
VIHVVADASAL	MTB live infection	20.11	11	HLA-C*03:03	321.29	WB	**Rv2209 (BCG_2119)**	550	96.3
KDVSGHVITL	BCG HK infection (sample 2/5)	20.04	10	HLA-C*03:03	4429.97	BH	**hisD**	438	92.6
RVGIDAEAGPT RVGIDAEAGPT	BCG live infection (Bettencourt et al, 2020) MTB live infection	19.9 19.71	11	HLA-A*02:01	26550.96	BH			
RLGVDLAEV	BCG live infection (Bettencourt et al, 2020)	19.13	9	HLA-A*02:01	34.40	SB	**fadE34**	711	100
WPAPYGRG	BCG live infection (sample 3/6)	15.47	8	HLA-B*15:11	19466.69	BH			
EINSARLYV	BCG HK infection (Bettencourt et al, 2020)	18.25	9	HLA-A*02:01	9195.62	BH	**PPE8**	3,507	100
ITNVSIPAI	BCG HK infection (Bettencourt et al, 2020)	16.41	9	HLA-C*03:03	1989.19	BH			
TGFYNTGDVNT	BCG HK infection (sample 2/5)	16.08	11	HLA-C*03:03	28026.9	BH			
GFYNTGSYNTGGFN	BCG live infection (sample 3/6)	16.03	14	DRB1*01:01	1588.84	BH			
GDYEGLWGL	BCG live infection (Bettencourt et al, 2020)	17.95	9	HLA-A*02:01	1989.19	BH	**PPE55a**	2,096	89
DFDGAADAGFTAPATTL	BCG live infection (sample 3/6)	15.04	17	DQA1*01:01/DQB1*05:01	969.87	BH			
VTVNATPD	BCG live infection (Bettencourt et al, 2020)	16.06	8	HLA-C*03:03	25842.4	BH	**pks12**	4,151	100
LATLFGDGVLRPLPV	BCG HK infection (sample 2/5)	16.09	15	DQA1*01:01/DQB1*05:01	112.44	BH			
RTLFRVPF	BCG HK infection (Bettencourt et al, 2020)	15.38	8	HLA-C*03:03	2443.19	BH	**mmpL3**	944	100
KATLMSALTL	BCG live infection (sample 3/6)	15.44	10	HLA-C*03:03	33.85	SB			
PAKKAAAKRPATKAPAKKATARR	BCG HK infection (Bettencourt et al, 2020)	15.36	23	DRB5*01:01	528.46	BH	**hupB**	205	74
KAPAKKAATKAPAKK	BCG live infection (sample 3/6)	18.28	15	DRB5*01:01	467.6	BH			
ALAIGAI	MTB live infection	19.01	7	-	-	-	**Rv0426c (BCG_0465c)**	147	33.3
PVKAKLAPVP	BCG HK infection (Bettencourt et al, 2020)	17.37	10	HLA-A*02:01	40489.28	BH			
ARAKARKAKAPK	MTB live infection	18.44	12	DRB5*01:01	7415.61	BH	**Rv2164c (BCG_2181c)**	384	70.4
KPADGVPPPPLNTKLPEDPPP	BCG HK infection (sample 2/5)	15.87	21	DQA1*01:01/DQB1*05:01	9336.58	BH			
LENVRPLA	MTB live infection	16.57	8	HLA-A*02:01	31060.9	BH	**Rv3239c (BCG_3268c)**	1048	100
KPNPIGVGLME	BCG HK infection (Bettencourt et al, 2020)	16.32	11	HLA-C*03:03	32610.74	BH			

IGPTHTL	MTB live infection	15.5	7	-	-	-	**Rv3776 (BCG_3838)**	519	92.6
APLLAELIRGGAALSRVRHPGD	BCG HK infection (Bettencourt et al, 2020)	16.23	22	DRB1*01:01	33.94	SB			
APGAVDPAGLRAQLAQRLPGYLVP	MTB live infection	15.37	24	DRB1*01:01 DRB1*15:01 DQA1*01:02/DQB1*06:02	26.9 48.3 22.1	SB WB WB	**nrp**	2,512	100
KPLVRHTVHT	BCG live infection (sample 3/6)	19.84	10	HLA-C*03:03	31569.21	BH			
GTGGAGGAGGLGGHGGAGGLLIGNG	MTB live infection	16.88	25	DRB1*01:01	3540.48	BH	**PE_PGRS48**	597	59.3
GGAGGAGGWLIGQSGSTGGGGAGG	BCG live infection (sample 3/6)	15.25	24	DRB1*01:01	786.73	BH			
QALTAGAGAYAFAEAA	MTB live infection	17.11	16	DRB1*01:01 DQA1*01:02/DQB1*06:02	32.5 34.5	WB SB	**PE_PGRS53**	1,372	85.2
GTGGNASATGT	BCG HK infection (Bettencourt et al, 2020)	19.84	11	HLA-A*02:01	31398.89	BH			
TTYTLEYDG	MTB live infection	17.24	9	HLA-A*02:01	28026.9	BH	**PE1**	588	100
TTYTLEYDG	BCG HK infection (sample 2/5)	15.96	9						
GFAEIAL	MTB live infection	15.13	7	-	-	-	**ppsD**	1,827	100
GPAFAALS	BCG live infection (Bettencourt et al, 2020)	16.51	8	HLA-B*15:11	27006.72	BH			

7.3.2 **Prediction of HLA-DR peptides**

Appendix Table 7.4 *Number of predicted peptides for of the selected antigens against human HLA alleles.*
Key: SB = strong binder; WB = week binder.

	Allele DR-	B1_0101		B1_0301		B1_0401		B1_0405		B1_0701		B1_0802		B1_0901		B1_1101		B1_1201		B1_1302		B1_1501		B3_0101		B3_0202		B4_0101		B5_0101	
#	Gene	SB	WB	SB	WB	SB	WB	SB	WB	SB	WB	SB	WB	SB	WB	SB	WB	SB	WB	SB	WB	SB	WB	SB	WB	SB	WB	SB	WB	SB	WB
1	groL2	27	61	15	55	14	71	9	48	19	60	11	46	28	62	5	44	8	66	8	69	0	45	22	50	10	64	21	84	6	69
2	groS	5	5	4	11	2	8	4	9	0	13	0	4	1	7	0	2	4	9	3	8	3	13	3	12	4	9	4	10	2	11
3	dnaK	10	54	30	96	27	72	6	69	9	48	21	65	12	63	16	49	7	45	26	65	7	47	36	76	17	69	36	105	14	62
4	metE	29	90	23	88	14	94	10	79	26	89	24	48	30	115	20	44	10	85	11	63	22	62	30	83	10	88	26	88	27	72
5	groL1	12	68	24	57	16	64	14	52	23	51	1	42	27	57	3	37	7	56	15	56	3	50	31	66	14	71	24	65	7	43
6	clpP1	12	28	4	8	0	24	4	24	3	21	0	23	12	23	3	14	4	24	4	13	8	8	0	24	8	19	10	30	3	16
7	PPE50	34	45	1	14	14	41	4	35	5	32	5	39	15	45	6	25	5	39	4	19	15	34	10	14	9	35	2	30	9	28
8	fadB	30	66	17	44	17	84	12	63	20	60	26	78	35	85	22	91	10	65	22	64	14	58	7	51	13	72	22	80	21	78
9	ctpI	74	201	40	153	26	183	8	134	46	182	20	169	83	193	16	139	39	165	18	130	26	144	41	150	11	171	59	164	53	169
10	BCG_3870c	14	55	15	42	16	60	7	58	12	48	3	54	12	65	4	55	14	30	4	64	12	41	19	49	14	55	24	83	10	51
11	Rv0306 (BCG_0346)	13	21	13	23	2	17	9	20	6	26	5	23	10	30	2	23	1	35	4	9	0	21	0	23	0	19	3	20	6	32
12	Rv3000 (BCG_3022)	7	28	8	16	0	15	2	8	1	14	3	14	0	13	9	11	13	25	4	19	1	13	5	20	1	15	0	28	2	14
13	fadE17	7	45	9	34	19	29	6	30	8	30	9	38	9	43	2	40	13	39	2	41	14	27	2	25	2	43	14	24	6	38
14	mmpL12	22	144	10	84	22	107	19	87	7	102	21	108	18	99	26	97	27	120	10	92	25	112	15	57	5	73	22	125	29	77
15	Rv2164c (BCG_2181c)	1	20	6	15	5	16	2	13	0	24	2	15	2	22	3	15	0	7	0	16	1	9	0	21	0	27	1	13	8	10
16	tuf	5	34	14	40	17	42	17	37	7	36	20	56	7	46	17	51	9	47	16	40	1	21	9	51	18	43	25	68	1	43
17	irtA (BCG_1410)	30	88	36	85	25	75	20	55	23	81	17	85	35	95	23	81	18	90	24	88	13	68	42	79	18	82	27	98	14	76
18	mycP2 (BCG_3941c)	24	58	2	28	8	64	7	40	16	63	10	57	44	67	11	32	8	28	9	45	2	49	4	19	16	66	8	51	2	39
19	subI	23	43	6	28	7	46	9	43	12	55	9	31	17	71	5	27	7	27	8	31	14	38	16	20	7	33	5	50	15	49

20	lprM (Rv1970)	14	35	11	34	6	43	15	37	15	32	4	28	16	36	3	27	8	36	5	28	7	31	3	46	9	44	17	37	9	22
21	hbhA	2	21	2	16	2	16	0	17	0	19	2	17	2	24	3	17	2	15	2	6	0	7	1	13	0	9	0	22	0	26
22	BCG_2418	9	43	9	51	11	49	17	37	17	46	9	35	14	49	9	36	4	30	7	35	7	44	9	41	4	51	17	55	10	58
23	BCG_0106	10	54	0	49	8	37	9	37	17	45	12	38	22	54	12	40	6	55	15	45	5	46	3	52	20	28	4	58	14	39
24	atpD	19	53	10	35	8	47	21	51	14	57	7	31	18	53	11	27	15	38	7	46	16	36	10	51	0	45	14	42	10	41
25	cysA2	7	24	13	38	7	42	4	31	0	17	1	13	4	17	2	9	2	10	1	15	16	19	12	42	2	28	13	27	8	22
26	ffh (BCG_2937c)	11	55	20	54	4	36	0	34	12	40	2	30	13	51	8	32	6	46	13	27	3	35	14	34	0	34	15	47	20	58
27	rplV	6	18	8	10	6	14	4	14	6	24	8	28	7	15	8	18	2	10	5	20	5	17	3	8	7	14	6	18	5	27
28	rpsQ (BCG_0760)	2	10	0	19	0	5	0	2	7	9	4	11	6	15	4	18	4	15	6	14	3	10	0	10	0	14	9	15	2	21
29	hbs (BCG_3915)	0	4	0	10	4	5	0	4	0	6	2	8	0	3	1	7	0	2	8	4	0	2	0	5	8	4	4	8	0	2
30	Rv3233c (BCG_3263c)	17	65	9	38	12	42	13	40	19	68	11	45	18	66	8	34	11	51	16	50	17	43	8	43	15	43	15	52	7	42
31	Rv2209 (BCG_2119)	14	46	18	33	8	35	16	25	18	41	3	27	16	53	4	20	2	29	4	35	8	35	10	37	6	40	4	36	5	30
32	hisD	19	46	0	40	15	41	7	32	21	49	17	31	30	53	12	25	13	47	12	45	17	47	0	40	7	40	21	54	9	47
33	fadE34	35	104	26	72	15	77	11	62	16	84	8	56	43	86	3	48	21	64	12	48	3	63	30	63	13	69	24	88	16	73
34	PPE8	99	456	28	108	136	493	29	314	118	385	20	154	140	550	8	117	29	115	20	150	58	257	73	201	91	456	29	143	6	163
35	PPE55a	49	243	38	84	48	189	4	138	50	211	4	77	77	268	0	45	48	98	20	145	60	182	40	138	36	196	40	132	5	76
36	pks12	147	520	100	415	99	494	87	345	101	460	84	339	149	609	85	293	91	364	45	325	59	406	111	400	47	411	171	444	114	382
37	mmpL3	10	109	19	92	11	61	10	41	10	106	17	52	9	112	13	48	17	78	11	59	14	72	21	77	14	91	14	74	14	62
38	hupB	1	12	3	15	4	2	3	4	5	30	9	29	8	18	11	28	2	10	2	33	1	13	0	4	0	11	0	11	8	20
39	Rv0426c (BCG_0465c)	0	2	0	2	1	6	0	4	0	6	2	14	0	5	3	11	0	1	0	3	1	10	0	3	0	3	1	6	0	3
40	Rv2164c (BCG_2181c)	1	20	6	15	5	16	2	13	0	24	2	15	2	22	3	15	0	6	0	16	1	9	0	21	0	27	1	13	8	10
41	Rv3239c (BCG_3268c)	35	129	13	75	14	73	7	77	19	77	22	103	20	112	24	89	22	87	17	79	7	112	10	54	8	80	24	86	27	90
42	Rv3776 (BCG_3838)	9	39	8	48	7	23	4	23	10	34	4	30	7	38	6	20	2	31	7	26	10	36	11	24	6	32	5	33	2	28
43	nrp	93	298	46	289	49	260	42	237	67	259	42	201	81	282	41	177	40	270	38	210	56	248	74	260	27	250	72	287	49	204
44	PE_PGRS48	15	37	0	2	16	24	6	21	4	31	11	12	20	38	2	15	1	18	0	9	0	19	0	9	14	36	4	25	0	19
45	PE_PGRS53	19	46	3	17	21	49	9	29	14	31	16	16	27	43	6	18	7	14	4	13	4	26	4	31	20	46	7	25	11	24
46	PE1	28	89	4	28	20	87	19	72	32	88	6	42	50	86	5	19	27	58	11	59	16	70	9	66	27	79	14	76	6	50
47	ppsD	63	208	42	214	49	190	58	146	41	199	30	186	58	231	35	183	17	189	40	175	39	137	71	164	35	178	67	214	44	181

7.3.3 **Prediction of HLA-DP and HLA-DQ peptides**

Appendix Table 7.5 *Number of predicted peptides of the selected antigens against human HLA alleles.*
Key: SB = strong binder; WB = week binder.

	Allele	DPA10103-DPB10201		DPA10103-DPB10401		DPA10201-DPB10101		DPA10201-DPB10501		DPA10201-DPB11401		DPA10301-DPB10402		DQA10101-DQB10501		DQA10102-DQB10602		DQA10301-DQB10302		DQA10401-DQB10402		DQA10501-DQB10201		DQA10501-DQB10301	
#	Gene	SB	WB	SB	WB	SB	WB	SB	WB	SB	WB	SB	WB	SB	WB	SB	WB	SB	WB	SB	WB	SB	WB	SB	WB
1	groL2	5	33	5	41	10	49	9	56	20	80	13	51	4	36	40	92	31	86	38	82	46	85	38	99
2	groS	8	9	7	5	6	10	4	9	3	12	6	10	2	11	6	5	4	14	5	10	4	22	8	11
3	dnaK	12	35	15	37	12	48	16	50	22	76	14	47	14	60	47	92	29	87	31	88	18	88	40	71
4	metE	8	54	11	60	8	72	13	66	51	105	7	64	28	81	37	100	48	121	52	119	50	109	53	141
5	groL1	3	26	10	26	10	36	11	25	23	72	14	34	10	32	39	104	33	115	31	93	34	86	30	132
6	clpP1	11	18	12	21	17	20	11	18	8	24	11	24	9	28	4	13	17	23	16	19	15	27	14	25
7	PPE50	0	7	1	15	1	15	0	12	18	48	2	18	7	24	49	82	12	68	22	69	12	51	27	97
8	fadB	24	51	19	58	17	68	17	74	18	83	20	72	12	82	34	75	35	82	29	89	33	84	53	128
9	ctpI	2	68	4	72	13	105	18	102	129	216	11	85	23	150	139	317	74	292	93	290	94	281	181	313
10	BCG_3870c	14	45	7	39	5	47	9	38	17	75	6	45	22	70	13	59	22	58	27	61	23	68	23	65
11	Rv0306 (BCG_0346)	2	14	0	25	2	34	10	25	14	34	0	32	5	31	6	10	4	40	12	25	2	36	7	22
12	Rv3000 (BCG_3022)	5	8	5	7	4	14	2	14	22	19	5	14	0	4	2	25	3	14	3	7	6	16	4	18
13	fadE17	11	39	16	34	20	24	18	24	21	50	15	35	12	20	18	49	10	31	15	36	11	28	28	53
14	mmpL12	16	61	20	47	12	58	22	74	36	97	14	46	33	70	31	131	24	87	16	83	26	73	22	136
15	Rv2164c (BCG_2181c)	0	9	0	12	3	10	5	19	24	55	2	5	0	12	10	28	6	28	6	26	4	23	20	47
16	tuf	13	30	14	39	13	39	7	44	6	60	11	40	3	40	21	44	8	72	19	50	20	63	13	54
17	irtA (BCG_1410)	10	73	7	68	9	85	12	79	35	100	9	68	33	56	19	112	48	110	55	107	31	102	52	117
18	mycP2 (BCG_3941c)	6	19	8	22	6	23	4	20	36	57	4	21	4	39	32	104	15	91	20	83	18	84	72	113

19	subI	4	14	7	15	7	26	12	26	15	54	8	19	12	49	21	50	19	64	21	59	17	57	22	73
20	lprM (Rv1970)	0	12	2	21	0	20	0	11	7	25	0	19	7	42	6	33	9	44	9	44	5	40	3	37
21	hbhA	4	5	4	7	4	6	6	15	19	41	5	10	5	7	4	39	0	18	3	19	1	15	3	22
22	BCG_2418	8	61	5	59	3	51	4	57	21	59	4	55	15	56	11	50	20	57	30	69	13	63	14	54
23	BCG_0106	9	31	10	28	10	33	3	45	24	39	8	37	8	47	16	51	18	59	12	74	16	45	26	57
24	atpD	9	40	6	49	5	57	15	36	17	30	6	60	19	53	5	35	21	60	16	53	9	67	15	61
25	cysA2	11	26	8	27	9	28	9	22	8	16	8	25	12	25	4	24	13	28	12	33	17	19	1	27
26	ffh (BCG_2937c)	4	33	3	31	2	51	13	40	10	76	6	32	10	31	24	62	16	67	18	56	12	57	23	71
27	rplV	4	12	4	10	3	12	6	28	33	54	2	10	2	11	20	46	10	25	10	31	11	12	14	39
28	rpsQ (BCG_0760)	4	9	0	15	1	17	8	17	13	28	0	20	1	13	3	29	7	15	9	18	12	11	14	24
29	hbs (BCG_3915)	0	0	0	1	0	0	0	3	6	19	0	1	4	3	16	19	4	9	1	21	0	5	4	34
30	Rv3233c (BCG_3263c)	8	27	8	30	9	25	9	48	19	43	12	34	13	50	19	81	18	35	14	45	9	55	12	77
31	Rv2209 (BCG_2119)	6	28	0	29	3	24	5	18	38	57	1	22	22	34	13	69	23	57	34	58	14	58	23	80
32	hisD	1	31	1	34	2	40	7	30	27	63	9	35	16	43	39	92	26	92	22	92	23	64	28	102
33	fadE34	7	34	11	37	8	58	4	59	46	98	9	56	7	52	51	74	44	99	53	90	37	112	57	123
34	PPE8	32	191	42	104	42	113	9	51	20	92	36	145	16	178	103	486	35	249	49	242	71	336	323	845
35	PPE55a	0	73	5	74	7	75	0	22	18	64	3	90	24	123	112	265	46	175	62	142	57	241	232	480
36	pks12	47	231	63	229	59	254	62	271	144	498	56	258	87	410	265	676	200	629	226	600	196	617	392	853
37	mmpL3	16	65	15	68	13	60	14	48	43	79	18	58	10	71	26	115	19	80	19	79	17	91	39	135
38	hupB	0	6	0	9	0	11	7	48	42	62	0	8	2	6	7	30	6	12	8	26	6	9	13	20
39	Rv0426c (BCG_0465c)	0	4	0	0	0	0	0	0	10	23	0	1	8	5	16	31	2	20	6	27	2	30	40	21
40	Rv2164c (BCG_2181c)	0	9	0	12	3	10	5	19	24	55	2	5	0	12	10	28	6	28	6	26	4	23	20	47
41	Rv3239c (BCG_3268c)	19	109	21	81	19	79	21	72	25	153	28	79	9	91	60	123	24	122	34	117	21	118	72	158
42	Rv3776 (BCG_3838)	3	29	0	20	3	20	7	31	28	62	0	17	22	29	14	54	14	59	16	57	11	46	25	60
43	nrp	26	204	39	192	30	208	35	212	100	297	34	213	74	226	67	296	96	319	71	319	65	310	104	325
44	PE_PGRS48	2	7	0	5	0	4	0	0	2	20	0	5	0	12	30	67	14	37	12	42	13	39	47	187
45	PE_PGRS53	2	16	0	15	0	7	0	6	14	18	0	19	9	16	43	177	24	75	25	78	20	62	132	355
46	PE1	4	33	8	49	11	54	1	23	7	45	6	62	15	77	41	84	22	84	28	69	29	67	42	116
47	ppsD	28	132	46	122	47	134	51	136	86	221	44	144	24	173	69	283	89	307	88	259	82	274	116	327

7.3.4 **Prediction of H2 peptides**

Appendix Table 7.6 *Number of predicted peptides of the selected antigens against mouse MHC alleles.*
Key: SB = strong binder; WB = week binder.

#	Antigen	BALB/c										C57BL/6					
		Class I						Class II				Class I				Class II	
		H-2-D^{d}		H-2-K^{d}		H-2-L^{d}		H-2-Ia^{d}		H-2-IE^{d}		H-2-D^{b}		H-2-K^{b}		H-2-IA^{b}	
		SB	WB	SB	WB	SB	WB	SB	WB	SB	WB	SB	WB	SB	WB	SB	WB
1	groL2	6	2	0	5	0	1	44	107	3	65	3	8	0	4	16	64
2	groS	1	0	0	0	0	0	8	17	0	5	1	2	1	0	1	13
3	dnaK	3	14	1	5	1	8	47	106	9	69	2	6	0	4	14	75
4	metE	7	9	5	15	7	12	32	122	11	78	4	12	2	15	37	118
5	groL1	4	4	1	2	2	3	35	114	6	50	5	5	0	6	13	50
6	clpP1	0	3	1	7	0	1	1	28	2	24	3	5	0	4	13	28
7	PPE50	2	4	3	5	1	4	51	85	2	24	4	10	2	4	36	79
8	fadB	3	12	1	7	6	7	31	102	13	73	6	10	4	9	13	105
9	ctpI	9	37	5	28	8	21	99	342	11	129	10	31	2	19	81	300
10	BCG_3870c	4	12	5	11	5	22	15	79	10	72	4	12	3	10	30	68
11	Rv0306 (BCG_0346)	2	4	1	1	0	6	12	15	6	22	3	2	2	3	22	15
12	Rv3000 (BCG_3022)	0	5	1	3	0	6	3	19	2	9	1	7	3	7	1	13
13	fadE17	6	11	3	4	2	7	5	44	4	40	2	4	0	9	10	52
14	mmpL12	4	17	8	18	8	25	10	138	19	96	20	19	9	30	51	85
15	Rv2164c (BCG_2181c)	4	10	0	3	7	12	16	47	4	19	1	4	0	2	39	62
16	tuf	4	4	1	6	3	9	20	68	12	51	0	6	0	5	8	53
17	irtA (BCG_1410)	7	16	4	13	12	20	28	129	11	87	4	12	10	18	55	110
18	mycP2 (BCG_3941c)	4	12	4	7	7	16	32	81	0	36	9	14	4	9	47	136
19	subI	2	11	0	6	4	11	20	68	15	37	3	2	1	10	29	60
20	lprM (Rv1970)	4	8	1	3	3	5	7	37	6	22	2	4	0	8	5	36
21	hbhA	0	0	1	1	0	0	11	49	3	23	0	3	0	2	2	22

22	BCG_2418	5	14	5	12	6	15	11	58	6	56	5	7	5	10	11	56
23	BCG_0106	1	6	2	8	1	16	30	40	16	36	1	5	2	10	29	65
24	atpD	4	13	3	9	2	5	3	43	12	27	4	4	3	5	14	49
25	cysA2	3	2	0	4	1	7	2	24	2	20	1	5	0	5	12	21
26	ffh (BCG_2937c)	3	9	0	5	3	6	35	72	10	35	2	3	1	6	14	61
27	rplV	1	4	0	0	1	1	34	50	9	42	0	2	0	2	13	41
28	rpsQ (BCG_0760)	0	3	0	1	0	0	12	32	10	15	1	3	1	2	7	21
29	hns (BCG_3915)	0	0	0	2	4	2	11	30	1	17	0	2	1	2	11	32
30	Rv3233c (BCG_3263c)	1	8	5	9	3	10	18	76	9	48	5	9	7	13	8	54
31	Rv2209 (BCG_2119)	6	11	1	8	6	7	23	71	3	25	2	10	2	10	17	81
32	hisD	5	8	5	4	2	7	45	105	9	30	4	4	1	9	16	96
33	fadE34	4	9	3	10	3	8	61	92	6	49	4	9	4	9	33	105
34	PPE8	41	96	34	77	17	89	26	253	2	90	43	76	17	63	264	649
35	PPE55a	27	41	10	29	20	56	54	169	0	42	24	59	7	34	135	350
36	pks12	36	86	17	42	31	64	258	706	56	335	26	72	24	60	175	656
37	mmpL3	7	20	6	20	6	16	40	107	9	66	8	24	7	37	29	127
38	hupB	1	1	0	0	0	1	16	35	18	59	0	1	0	1	2	26
39	Rv0426c (BCG_0465c)	0	1	0	2	0	0	17	27	0	9	0	1	0	0	0	43
40	Rv2164c (BCG_2181c)	4	10	0	3	7	12	16	47	4	19	1	4	0	2	39	62
41	Rv3239c (BCG_3268c)	9	30	5	13	9	19	35	142	22	73	13	23	8	31	51	124
42	Rv3776 (BCG_3838)	5	11	1	6	4	8	18	69	5	28	1	11	1	11	21	69
43	nrp	13	41	8	40	17	43	76	307	25	180	15	35	9	52	54	306
44	PE_PGRS48	4	15	3	6	1	6	27	62	0	9	4	4	0	3	19	65
45	PE_PGRS53	4	31	1	7	0	4	34	104	3	26	5	3	0	6	27	116
46	PE1	8	18	6	14	16	21	23	84	4	34	6	22	5	16	43	91
47	ppsD	16	40	8	30	5	23	86	295	32	168	12	26	9	24	89	254

7.3.5 **Prediction of HLA-I peptides**

Appendix Table 7.7 *Number of predicted peptides of the top selected antigens against human HLA alleles.*
Key: SB = strong binder; WB = week binder.

	BCG_2418		BCG_3870c		hisD		metE		mmpL12		mmpL3		Rv3239c (BCG_3268c)		Rv3776 (BCG_3838)	
HLA-A01:01	14	44	13	42	1	11	5	20	2	15	6	23	4	16	2	6
HLA-A02:01	15	41	9	39	1	17	14	24	28	43	23	33	19	42	7	11
HLA-A02:03	14	42	14	36	5	23	21	26	34	58	20	43	25	45	7	17
HLA-A02:06	11	39	14	32	10	23	18	38	32	86	28	50	26	59	7	20
HLA-A03:01	7	25	9	38	0	7	6	10	2	20	10	18	11	22	4	11
HLA-A11:01	7	24	10	50	1	10	5	19	5	19	15	19	12	25	6	11
HLA-A23:01	13	44	5	38	2	6	5	16	9	25	7	34	7	20	1	7
HLA-A24:02	14	51	5	40	2	5	6	16	8	26	9	29	8	16	1	5
HLA-A26:01	12	58	16	31	8	11	16	29	15	45	13	27	8	32	3	14
HLA-A30:01	8	29	10	16	5	13	6	37	11	25	16	42	21	37	11	17
HLA-A30:02	15	49	11	37	3	8	9	10	8	19	8	19	8	18	3	8
HLA-A31:01	12	53	16	58	5	8	12	18	8	21	14	29	24	36	14	14
HLA-A32:01	18	51	12	38	6	7	9	26	17	64	21	41	14	39	11	13
HLA-A33:01	17	77	23	56	6	8	14	18	17	18	12	33	17	35	7	20
HLA-A68:01	20	34	20	39	4	8	10	19	10	20	12	22	16	30	6	11
HLA-A68:02	10	44	13	31	16	22	22	39	29	70	21	52	25	51	4	19
HLA-B07:02	9	14	11	23	6	14	11	38	15	35	16	39	19	50	7	23
HLA-B08:01	6	20	9	30	4	13	8	34	14	46	17	40	11	42	7	17
HLA-B15:01	8	20	10	10	7	5	8	11	15	38	15	22	6	25	6	5
HLA-B35:01	8	28	16	23	9	13	11	31	13	42	15	39	17	34	5	13
HLA-B40:01	6	18	7	13	1	9	3	19	6	23	3	14	6	23	2	12

HLA-B44:02	14	14	5	17	1	7	4	21	8	22	3	18	5	18	3	10
HLA-B44:03	12	16	4	17	0	10	5	18	8	20	3	18	5	18	3	9
HLA-B51:01	11	21	13	24	10	20	13	22	18	57	25	43	30	37	5	14
HLA-B53:01	11	24	12	28	3	12	16	14	11	31	13	30	19	26	5	14
HLA-B57:01	9	15	8	14	2	5	3	13	9	17	10	16	7	22	3	13
HLA-B58:01	12	15	9	13	3	5	8	12	10	28	12	26	10	22	5	12

References

1. Caws M, Marais B, Heemskerk D, Farrar J. Tuberculosis in adults and children: Springer Nature; 2015.
2. Luca S, Mihaescu T. History of BCG vaccine. Maedica. 2013;8(1):53-8.
3. Mangtani P, Abubakar I, Ariti C, Beynon R, Pimpin L, Fine PE, et al. Protection by BCG vaccine against tuberculosis: a systematic review of randomized controlled trials. Clinical infectious diseases. 2014;58(4):470-80.
4. Sable SB, Posey JE, Scriba TJ. Tuberculosis Vaccine Development: Progress in Clinical Evaluation. Clinical Microbiology Reviews. 2019;33(1):e00100-19.
5. McShane H. Insights and challenges in tuberculosis vaccine development. Lancet Respiratory medicine. 2019;7.
6. Programme WGT. TB : a global emergency, WHO report on the TB epidemic. World Health Organization; 1994. Report No.: WHO/TB/94.177.
7. Organisation WH. Global tuberculosis report 2021. WHO; 2021.
8. World Health O. BCG vaccine: WHO position paper, February 2018 - Recommendations. Vaccine. 2018;36(24):3408-10.
9. Wurie FB, Lawn SD, Booth H, Sonnenberg P, Hayward AC. Bioaerosol production by patients with tuberculosis during normal tidal breathing: implications for transmission risk. Thorax. 2016;71(6):549-54.
10. Heemskerk D, Caws M, Marais B, Farrar J. Epidemiology. Tuberculosis in Adults and Children. Cham: Springer International Publishing; 2015. p. 1-7.
11. Dheda K, Gumbo T, Maartens G, Dooley KE, McNerney R, Murray M, et al. The epidemiology, pathogenesis, transmission, diagnosis, and management of multidrug-resistant, extensively drug-resistant, and incurable tuberculosis. The lancet Respiratory medicine. 2017;5(4):291-360.
12. Cohen A, Mathiasen VD, Schön T, Wejse C. The global prevalence of latent tuberculosis: a systematic review and meta-analysis. European Respiratory Journal. 2019;54(3).
13. Shah M, Dorman SE. Latent Tuberculosis Infection. New England Journal of Medicine. 2021;385(24):2271-80.
14. Pahari S, Kaur G, Negi S, Aqdas M, Das DK, Bashir H, et al. Reinforcing the functionality of mononuclear phagocyte system to control tuberculosis. Frontiers in immunology. 2018;9:193.
15. Killick KE, Ní Cheallaigh C, O'Farrelly C, Hokamp K, MacHugh DE, Harris J. Receptor-mediated recognition of mycobacterial pathogens. Cellular microbiology. 2013;15(9):1484-95.
16. Stamm CE, Collins AC, Shiloh MU. Sensing of M ycobacterium tuberculosis and consequences to both host and bacillus. Immunological reviews. 2015;264(1):204-19.
17. Weiss G, Schaible UE. Macrophage defense mechanisms against intracellular bacteria. Immunological reviews. 2015;264(1):182-203.
18. Abebe F. Immunological basis of early clearance of Mycobacterium tuberculosis infection: the role of natural killer cells. Clinical & Experimental Immunology. 2021;204(1):32-40.
19. Hirsch CS, Ellner JJ, Russell DG, Rich EA. Complement receptor-mediated uptake and tumor necrosis factor-alpha-mediated growth inhibition of Mycobacterium

tuberculosis by human alveolar macrophages. The Journal of Immunology. 1994;152(2):743-53.
20. Desjardins M. Biogenesis of phagolysosomes: the ‘kiss and run’hypothesis. Trends in cell biology. 1995;5(5):183-6.
21. Khan TA, Kalsoom K, Iqbal A, Asif H, Rahman H, Farooq SO, et al. A novel missense mutation in the NADPH binding domain of CYBB abolishes the NADPH oxidase activity in a male patient with increased susceptibility to infections. Microbial pathogenesis. 2016;100:163-9.
22. Rivas-Santiago B, Hernandez-Pando R, Carranza C, Juarez E, Contreras JL, Aguilar-Leon D, et al. Expression of cathelicidin LL-37 during Mycobacterium tuberculosis infection in human alveolar macrophages, monocytes, neutrophils, and epithelial cells. Infection and immunity. 2008;76(3):935-41.
23. Gutierrez MG, Master SS, Singh SB, Taylor GA, Colombo MI, Deretic V. Autophagy is a defense mechanism inhibiting BCG and Mycobacterium tuberculosis survival in infected macrophages. Cell. 2004;119(6):753-66.
24. Behar S, Martin C, Booty M, Nishimura T, Zhao X, Gan H, et al. Apoptosis is an innate defense function of macrophages against Mycobacterium tuberculosis. Mucosal immunology. 2011;4(3):279-87.
25. Ferluga J, Yasmin H, Al-Ahdal MN, Bhakta S, Kishore U. Natural and trained innate immunity against Mycobacterium tuberculosis. Immunobiology. 2020;225(3):151951.
26. Khan A, Singh VK, Hunter RL, Jagannath C. Macrophage heterogeneity and plasticity in tuberculosis. Journal of leukocyte biology. 2019;106(2):275-82.
27. Refai A, Gritli S, Barbouche M-R, Essafi M. Mycobacterium tuberculosis virulent factor ESAT-6 drives macrophage differentiation toward the pro-inflammatory M1 phenotype and subsequently switches it to the anti-inflammatory M2 phenotype. Frontiers in cellular and infection microbiology. 2018;8:327.
28. Russell DG, Huang L, VanderVen BC. Immunometabolism at the interface between macrophages and pathogens. Nature Reviews Immunology. 2019;19(5):291-304.
29. Shapouri-Moghaddam A, Mohammadian S, Vazini H, Taghadosi M, Esmaeili SA, Mardani F, et al. Macrophage plasticity, polarization, and function in health and disease. Journal of cellular physiology. 2018;233(9):6425-40.
30. Lowe DM, Redford PS, Wilkinson RJ, O’Garra A, Martineau AR. Neutrophils in tuberculosis: friend or foe? Trends in immunology. 2012;33(1):14-25.
31. Kroon EE, Coussens AK, Kinnear C, Orlova M, Möller M, Seeger A, et al. Neutrophils: innate effectors of TB resistance? Frontiers in immunology. 2018;9:2637.
32. Martineau AR, Newton SM, Wilkinson KA, Kampmann B, Hall BM, Nawroly N, et al. Neutrophil-mediated innate immune resistance to mycobacteria. The Journal of clinical investigation. 2007;117(7):1988-94.
33. Berry MP, Graham CM, McNab FW, Xu Z, Bloch SA, Oni T, et al. An interferon-inducible neutrophil-driven blood transcriptional signature in human tuberculosis. Nature. 2010;466(7309):973-7.
34. McNab FW, Berry MP, Graham CM, Bloch SA, Oni T, Wilkinson KA, et al. Programmed death ligand 1 is over-expressed by neutrophils in the blood of patients with active tuberculosis. European journal of immunology. 2011;41(7):1941-7.
35. Jurado JO, Alvarez IB, Pasquinelli V, Martínez GJ, Quiroga MF, Abbate E, et al. Programmed death (PD)-1: PD-ligand 1/PD-ligand 2 pathway inhibits T cell effector functions during human tuberculosis. The Journal of Immunology. 2008;181(1):116-25.

36. Méndez-Samperio P. The human cathelicidin hCAP18/LL-37: a multifunctional peptide involved in mycobacterial infections. Peptides. 2010;31(9):1791-8.
37. Sharma S, Verma I, Khuller G. Antibacterial activity of human neutrophil peptide-1 against Mycobacterium tuberculosis H37Rv: in vitro and ex vivo study. European Respiratory Journal. 2000;16(1):112-7.
38. Hilda JN, Das S, Tripathy SP, Hanna LE. Role of neutrophils in tuberculosis: a bird's eye view. Innate immunity. 2020;26(4):240-7.
39. Esin S, Counoupas C, Aulicino A, Brancatisano FL, Maisetta G, Bottai D, et al. Interaction of Mycobacterium tuberculosis Cell Wall Components with the Human Natural Killer Cell Receptors NK p44 and Toll-Like Receptor 2. Scandinavian journal of immunology. 2013;77(6):460-9.
40. Garg A, Barnes PF, Porgador A, Roy S, Wu S, Nanda JS, et al. Vimentin expressed on Mycobacterium tuberculosis-infected human monocytes is involved in binding to the NKp46 receptor. The Journal of Immunology. 2006;177(9):6192-8.
41. Chowdhury RR, Vallania F, Yang Q, Angel CJL, Darboe F, Penn-Nicholson A, et al. A multi-cohort study of the immune factors associated with M. tuberculosis infection outcomes. Nature. 2018;560(7720):644-8.
42. Prendergast KA, Kirman JR. Dendritic cell subsets in mycobacterial infection: control of bacterial growth and T cell responses. Tuberculosis. 2013;93(2):115-22.
43. Tian T, Woodworth J, Sköld M, Behar SM. In vivo depletion of CD11c+ cells delays the CD4+ T cell response to Mycobacterium tuberculosis and exacerbates the outcome of infection. The Journal of Immunology. 2005;175(5):3268-72.
44. Tian T, Woodworth J, Sköld M, Behar SM. In vivo depletion of CD11c+ cells delays the CD4+ T cell response to Mycobacterium tuberculosis and exacerbates the outcome of infection. The Journal of Immunology. 2005;175(5):3268-72.
45. Tailleux L, Schwartz O, Herrmann J-L, Pivert E, Jackson M, Amara A, et al. DC-SIGN is the major Mycobacterium tuberculosis receptor on human dendritic cells. The Journal of experimental medicine. 2003;197(1):121-7.
46. Mellman I. Dendritic cells: master regulators of the immune response. Cancer immunology research. 2013;1(3):145-9.
47. Khader SA, Partida-Sanchez S, Bell G, Jelley-Gibbs DM, Swain S, Pearl JE, et al. Interleukin 12p40 is required for dendritic cell migration and T cell priming after Mycobacterium tuberculosis infection. The Journal of experimental medicine. 2006;203(7):1805-15.
48. Kuo C-P, Chang K-S, Hsu J-L, Tsai I-F, Lin AB, Wei T-Y, et al. Analysis of the immune response of human dendritic cells to Mycobacterium tuberculosis by quantitative proteomics. Proteome science. 2016;14(1):1-11.
49. Larsen SL, Pedersen LO, Buus S, Stryhn A. T cell responses affected by aminopeptidase N (CD13)-mediated trimming of major histocompatibility complex class II-bound peptides. The Journal of experimental medicine. 1996;184(1):183-9.
50. Ghosh M, McAuliffe B, Subramani J, Basu S, Shapiro LH. CD13 regulates dendritic cell cross-presentation and T cell responses by inhibiting receptor-mediated antigen uptake. The Journal of immunology. 2012;188(11):5489-99.
51. Trottein F, Paget C. Natural killer T cells and mucosal-associated invariant T cells in lung infections. Frontiers in immunology. 2018;9:1750.
52. Groh V, Porcelli S, Fabbi M, Lanier LL, Picker LJ, Anderson T, et al. Human lymphocytes bearing T cell receptor gamma/delta are phenotypically diverse and evenly distributed throughout the lymphoid system. The Journal of experimental medicine. 1989;169(4):1277-94.

53. Joosten SA, Ottenhoff TH, Lewinsohn DM, Hoft DF, Moody DB, Seshadri C. Harnessing donor unrestricted T-cells for new vaccines against tuberculosis. Vaccine. 2019;37(23):3022-30.
54. Shen Y, Zhou D, Qiu L, Lai X, Simon M, Shen L, et al. Adaptive immune response of Vγ2Vδ2+ T cells during mycobacterial infections. Science. 2002;295(5563):2255-8.
55. Hoft DF, Brown RM, Roodman ST. Bacille Calmette-Guérin vaccination enhances human γδ T cell responsiveness to mycobacteria suggestive of a memory-like phenotype. The Journal of Immunology. 1998;161(2):1045-54.
56. Brandes M, Willimann K, Moser B. Professional antigen-presentation function by human γδ T cells. Science. 2005;309(5732):264-8.
57. Chai Q, Lu Z, Liu CH. Host defense mechanisms against Mycobacterium tuberculosis. Cellular and Molecular Life Sciences. 2020;77(10):1859-78.
58. Fu Y-X, Cranfill R, Vollmer M, Van Der Zee R, O'Brien RL, Born W. In vivo response of murine gamma delta T cells to a heat shock protein-derived peptide. Proceedings of the National Academy of Sciences. 1993;90(1):322-6.
59. Haregewoin A, Soman G, Horn RC, Finberg RW. Human γδ+ T cells respond to mycobacterial heat-shock protein. Nature. 1989;340(6231):309-12.
60. Casetti R, Martino A. The plasticity of γδ T cells: innate immunity, antigen presentation and new immunotherapy. Cellular & molecular immunology. 2008;5(3):161-70.
61. Conti L, Casetti R, Cardone M, Varano B, Martino A, Belardelli F, et al. Reciprocal activating interaction between dendritic cells and pamidronate-stimulated γδ T cells: role of CD86 and inflammatory cytokines. The Journal of Immunology. 2005;174(1):252-60.
62. McGill JL, Sacco RE, Baldwin CL, Telfer JC, Palmer MV, Waters WR. The role of gamma delta T cells in immunity to Mycobacterium bovis infection in cattle. Veterinary immunology and immunopathology. 2014;159(3-4):133-43.
63. Baldwin CL, Yirsaw A, Gillespie A, Le Page L, Zhang F, Damani-Yokota P, et al. γδ T cells in livestock: Responses to pathogens and vaccine potential. Transboundary and emerging diseases. 2020;67:119-28.
64. Salou M, Franciszkiewicz K, Lantz O. MAIT cells in infectious diseases. Current opinion in immunology. 2017;48:7-14.
65. Jiang J, Yang B, An H, Wang X, Liu Y, Cao Z, et al. Mucosal-associated invariant T cells from patients with tuberculosis exhibit impaired immune response. Journal of Infection. 2016;72(3):338-52.
66. Paquin-Proulx D, Costa PR, Terrassani Silveira CG, Marmorato MP, Cerqueira NB, Sutton MS, et al. Latent Mycobacterium tuberculosis infection is associated with a higher frequency of mucosal-associated invariant T and invariant natural killer T cells. Frontiers in immunology. 2018;9:1394.
67. Chua W-J, Truscott SM, Eickhoff CS, Blazevic A, Hoft DF, Hansen TH. Polyclonal mucosa-associated invariant T cells have unique innate functions in bacterial infection. Infection and immunity. 2012;80(9):3256-67.
68. Sakai S, Kauffman KD, Oh S, Nelson CE, Barry CE, Barber DL. MAIT cell-directed therapy of Mycobacterium tuberculosis infection. Mucosal immunology. 2021;14(1):199-208.
69. Sada-Ovalle I, Chiba A, Gonzales A, Brenner MB, Behar SM. Innate invariant NKT cells recognize Mycobacterium tuberculosis–infected macrophages, produce interferon-γ, and kill intracellular bacteria. PLoS pathogens. 2008;4(12):e1000239.

70. Rothchild AC, Jayaraman P, Nunes-Alves C, Behar SM. iNKT cell production of GM-CSF controls Mycobacterium tuberculosis. PLoS pathogens. 2014;10(1):e1003805.
71. Gansert JL, Kieβler V, Engele M, Wittke F, Röllinghoff M, Krensky AM, et al. Human NKT cells express granulysin and exhibit antimycobacterial activity. The Journal of Immunology. 2003;170(6):3154-61.
72. Behar SM, Dascher CC, Grusby MJ, Wang C-R, Brenner MB. Susceptibility of mice deficient in CD1D or TAP1 to infection with Mycobacterium tuberculosis. The Journal of experimental medicine. 1999;189(12):1973-80.
73. Shekhar S, Joyee AG, Yang X. Invariant natural killer T cells: boon or bane in immunity to intracellular bacterial infections? Journal of Innate Immunity. 2014;6(5):575-84.
74. Al Majid F, Abba A. Immunophenotypic characterisation of peripheral T lymphocytes in pulmonary tuberculosis. Journal of Postgraduate Medicine. 2008;54(1):7.
75. Snyder-Cappione JE, Nixon DF, Loo CP, Chapman JM, Meiklejohn DA, Melo FF, et al. Individuals with pulmonary tuberculosis have lower levels of circulating CD1d-restricted NKT cells. The Journal of infectious diseases. 2007;195(9):1361-4.
76. Im JS, Kang T-J, Lee S-B, Kim C-H, Lee S-H, Venkataswamy MM, et al. Alteration of the relative levels of iNKT cell subsets is associated with chronic mycobacterial infections. Clinical immunology. 2008;127(2):214-24.
77. Rijnink WF, Ottenhoff TH, Joosten SA. B-cells and antibodies as contributors to effector immune responses in tuberculosis. Frontiers in Immunology. 2021;12:383.
78. Geldmacher C, Ngwenyama N, Schuetz A, Petrovas C, Reither K, Heeregrave EJ, et al. Preferential infection and depletion of Mycobacterium tuberculosis–specific CD4 T cells after HIV-1 infection. Journal of Experimental Medicine. 2010;207(13):2869-81.
79. Bell LC, Noursadeghi M. Pathogenesis of HIV-1 and Mycobacterium tuberculosis co-infection. Nature Reviews Microbiology. 2018;16(2):80-90.
80. Kalsdorf B, Scriba TJ, Wood K, Day CL, Dheda K, Dawson R, et al. HIV-1 infection impairs the bronchoalveolar T-cell response to mycobacteria. American journal of respiratory and critical care medicine. 2009;180(12):1262-70.
81. Mogues T, Goodrich ME, Ryan L, LaCourse R, North RJ. The relative importance of T cell subsets in immunity and immunopathology of airborne Mycobacterium tuberculosis infection in mice. The Journal of experimental medicine. 2001;193(3):271-80.
82. Krogsgaard M, Davis MM. How T cells' see'antigen. Nature immunology. 2005;6(3):239-45.
83. Ngai P, McCormick S, Small C, Zhang X, Zganiacz A, Aoki N, et al. Gamma interferon responses of CD4 and CD8 T-cell subsets are quantitatively different and independent of each other during pulmonary Mycobacterium bovis BCG infection. Infection and immunity. 2007;75(5):2244-52.
84. Lindestam Arlehamn CS, Gerasimova A, Mele F, Henderson R, Swann J, Greenbaum JA, et al. Memory T cells in latent Mycobacterium tuberculosis infection are directed against three antigenic islands and largely contained in a CXCR3+ CCR6+ Th1 subset. PLoS pathogens. 2013;9(1):e1003130.
85. Green AM, DiFazio R, Flynn JL. IFN-γ from CD4 T cells is essential for host survival and enhances CD8 T cell function during Mycobacterium tuberculosis infection. The Journal of Immunology. 2013;190(1):270-7.

86. Cowley SC, Elkins KL. CD4+ T cells mediate IFN-γ-independent control of Mycobacterium tuberculosis infection both in vitro and in vivo. The Journal of Immunology. 2003;171(9):4689-99.
87. Sia JK, Rengarajan J. Immunology of Mycobacterium tuberculosis infections. Microbiology spectrum. 2019;7(4):7.4. 6.
88. Lyadova I, Panteleev A. Th1 and Th17 cells in tuberculosis: protection, pathology, and biomarkers. Mediators of inflammation. 2015;2015.
89. Serbina NV, Lazarevic V, Flynn JL. CD4+ T cells are required for the development of cytotoxic CD8+ T cells during Mycobacterium tuberculosis infection. The Journal of Immunology. 2001;167(12):6991-7000.
90. Fletcher HA, Snowden MA, Landry B, Rida W, Satti I, Harris SA, et al. T-cell activation is an immune correlate of risk in BCG vaccinated infants. Nature communications. 2016;7(1):1-11.
91. Tippalagama R, Singhania A, Dubelko P, Arlehamn CSL, Crinklaw A, Pomaznoy M, et al. HLA-DR marks recently divided antigen-specific effector CD4 T cells in active tuberculosis patients. The Journal of Immunology. 2021;207(2):523-33.
92. Adekambi T, Ibegbu CC, Cagle S, Kalokhe AS, Wang YF, Hu Y, et al. Biomarkers on patient T cells diagnose active tuberculosis and monitor treatment response. The Journal of clinical investigation. 2015;125(5):1827-38.
93. Riou C, Berkowitz N, Goliath R, Burgers WA, Wilkinson RJ. Analysis of the phenotype of Mycobacterium tuberculosis-specific CD4+ T cells to discriminate latent from active tuberculosis in HIV-uninfected and HIV-infected individuals. Frontiers in immunology. 2017;8:968.
94. Silveira-Mattos PS, Barreto-Duarte B, Vasconcelos B, Fukutani KF, Vinhaes CL, Oliveira-de-Souza D, et al. Differential expression of activation markers by Mycobacterium tuberculosis-specific CD4+ T cell distinguishes extrapulmonary from pulmonary tuberculosis and latent infection. Clinical Infectious Diseases. 2020;71(8):1905-11.
95. Jasenosky LD, Scriba TJ, Hanekom WA, Goldfeld AE. T cells and adaptive immunity to Mycobacterium tuberculosis in humans. Immunological reviews. 2015;264(1):74-87.
96. Day CL, Abrahams DA, Lerumo L, van Rensburg EJ, Stone L, O'rie T, et al. Functional capacity of Mycobacterium tuberculosis-specific T cell responses in humans is associated with mycobacterial load. The Journal of Immunology. 2011;187(5):2222-32.
97. Caccamo N, Guggino G, Joosten SA, Gelsomino G, Di Carlo P, Titone L, et al. Multifunctional CD4+ T cells correlate with active Mycobacterium tuberculosis infection. European journal of immunology. 2010;40(8):2211-20.
98. Kagina BM, Abel B, Scriba TJ, Hughes EJ, Keyser A, Soares A, et al. Specific T cell frequency and cytokine expression profile do not correlate with protection against tuberculosis after bacillus Calmette-Guerin vaccination of newborns. American journal of respiratory and critical care medicine. 2010;182(8):1073-9.
99. Lewinsohn DA, Lewinsohn DM, Scriba TJ. Polyfunctional CD4+ T cells as targets for tuberculosis vaccination. Frontiers in immunology. 2017;8:1262.
100. Gopal R, Monin L, Slight S, Uche U, Blanchard E, A. Fallert Junecko B, et al. Unexpected role for IL-17 in protective immunity against hypervirulent Mycobacterium tuberculosis HN878 infection. PLoS pathogens. 2014;10(5):e1004099.
101. Scriba TJ, Kalsdorf B, Abrahams D-A, Isaacs F, Hofmeister J, Black G, et al. Distinct, specific IL-17-and IL-22-producing CD4+ T cell subsets contribute to the

human anti-mycobacterial immune response. The Journal of Immunology. 2008;180(3):1962-70.
102. Jurado JO, Pasquinelli V, Alvarez IB, Peña D, Rovetta AI, Tateosian NL, et al. IL-17 and IFN-γ expression in lymphocytes from patients with active tuberculosis correlates with the severity of the disease. Journal of leukocyte biology. 2012;91(6):991-1002.
103. Serbina NV, Liu C-C, Scanga CA, Flynn JL. CD8+ CTL from lungs of Mycobacterium tuberculosis-infected mice express perforin in vivo and lyse infected macrophages. The Journal of Immunology. 2000;165(1):353-63.
104. Stenger S, Hanson DA, Teitelbaum R, Dewan P, Niazi KR, Froelich CJ, et al. An antimicrobial activity of cytolytic T cells mediated by granulysin. Science. 1998;282(5386):121-5.
105. Harriff MJ, Cansler ME, Toren KG, Canfield ET, Kwak S, Gold MC, et al. Human lung epithelial cells contain Mycobacterium tuberculosis in a late endosomal vacuole and are efficiently recognized by CD8+ T cells. PloS one. 2014;9(5):e97515.
106. Bermudez LE, Goodman J. Mycobacterium tuberculosis invades and replicates within type II alveolar cells. Infection and immunity. 1996;64(4):1400-6.
107. Lu LL, Chung AW, Rosebrock TR, Ghebremichael M, Yu WH, Grace PS, et al. A functional role for antibodies in tuberculosis. Cell. 2016;167(2):433-43. e14.
108. Bitencourt J, Peralta Alvarez MP, Wilkie M, Jacobs A, Wright D, Almujri S, et al. Induction of functional specific antibodies, IgG-secreting plasmablasts and memory B cells following BCG vaccination. Frontiers in Immunology.5664.
109. Zimmermann N, Thormann V, Hu B, Köhler AB, Imai-Matsushima A, Locht C, et al. Human isotype-dependent inhibitory antibody responses against Mycobacterium tuberculosis. EMBO molecular medicine. 2016;8(11):1325-39.
110. Chen T, Blanc C, Eder AZ, Prados-Rosales R, Souza ACO, Kim RS, et al. Association of human antibodies to arabinomannan with enhanced mycobacterial opsonophagocytosis and intracellular growth reduction. The Journal of infectious diseases. 2016;214(2):300-10.
111. Silva Miranda M, Breiman A, Allain S, Deknuydt F, Altare F. The tuberculous granuloma: an unsuccessful host defence mechanism providing a safety shelter for the bacteria? Clinical and Developmental Immunology. 2012;2012.
112. Colangeli R, Gupta A, Vinhas SA, Chippada Venkata UD, Kim S, Grady C, et al. Mycobacterium tuberculosis progresses through two phases of latent infection in humans. Nature communications. 2020;11(1):1-10.
113. Ernst JD. The immunological life cycle of tuberculosis. Nature Reviews Immunology. 2012;12(8):581-91.
114. Geldmacher C, Schuetz A, Ngwenyama N, Casazza JP, Sanga E, Saathoff E, et al. Early depletion of Mycobacterium tuberculosis-specific T helper 1 cell responses after HIV-1 infection. The Journal of infectious diseases. 2008;198(11):1590-8.
115. Robert M, Miossec P. Reactivation of latent tuberculosis with TNF inhibitors: critical role of the beta 2 chain of the IL-12 receptor. Cellular & Molecular Immunology. 2021;18(7):1644-51.
116. Minozzi S, Bonovas S, Lytras T, Pecoraro V, Gonzalez-Lorenzo M, Bastiampillai AJ, et al. Risk of infections using anti-TNF agents in rheumatoid arthritis, psoriatic arthritis, and ankylosing spondylitis: a systematic review and meta-analysis. Expert opinion on drug safety. 2016;15(sup1):11-34.
117. Wallis RS. Tumour necrosis factor antagonists: structure, function, and tuberculosis risks. The Lancet infectious diseases. 2008;8(10):601-11.

118. Saliu OY, Sofer C, Stein DS, Schwander SK, Wallis RS. Tumor-necrosis-factor blockers: differential effects on mycobacterial immunity. The Journal of infectious diseases. 2006;194(4):486-92.
119. Wallis RS, editor Reactivation of latent tuberculosis by TNF blockade: the role of interferon γ. Journal of Investigative Dermatology Symposium Proceedings; 2007: Elsevier.
120. Rieder HL, Tuberculosis IUa, IUATLD. LD. Interventions for tuberculosis control and elimination: International Union Against Tuberculosis and Lung Disease Paris; 2002.
121. Hesseling A, Rabie H, Marais B, Manders M, Lips M, Schaaf H, et al. Bacille Calmette-Guérin vaccine—induced disease in HIV-infected and HIV-uninfected children. Clinical infectious diseases. 2006;42(4):548-58.
122. Dockrell HM, Smith SG. What have we learnt about BCG vaccination in the last 20 years? Frontiers in immunology. 2017;8:1134.
123. WHO. Safety of BCG vaccination in immunocompromised individuals [Available from: https://www.who.int/groups/global-advisory-committee-on-vaccine-safety/topics/bcg-vaccines.
124. Martin C, Aguilo N, Marinova D, Gonzalo-Asensio J. Update on TB vaccine pipeline. Applied Sciences. 2020;10(7):2632.
125. Hatherill M, White RG, Hawn TR. Clinical development of new TB vaccines: recent advances and next steps. Frontiers in microbiology. 2020;10:3154.
126. Bellini C, Horváti K. Recent Advances in the Development of Protein-and Peptide-Based Subunit Vaccines against Tuberculosis. Cells. 2020;9(12):2673.
127. Tameris MD, Hatherill M, Landry BS, Scriba TJ, Snowden MA, Lockhart S, et al. Safety and efficacy of MVA85A, a new tuberculosis vaccine, in infants previously vaccinated with BCG: a randomised, placebo-controlled phase 2b trial. The Lancet. 2013;381(9871):1021-8.
128. Schrager LK, Vekemens J, Drager N, Lewinsohn DM, Olesen OF. The status of tuberculosis vaccine development. The Lancet Infectious Diseases. 2020;20(3):e28-e37.
129. Gillard P, Yang P-C, Danilovits M, Su W-J, Cheng S-L, Pehme L, et al. Safety and immunogenicity of the M72/AS01E candidate tuberculosis vaccine in adults with tuberculosis: a phase II randomised study. Tuberculosis. 2016;100:118-27.
130. Tait DR, Hatherill M, Van Der Meeren O, Ginsberg AM, Van Brakel E, Salaun B, et al. Final analysis of a trial of M72/AS01E vaccine to prevent tuberculosis. New England Journal of Medicine. 2019;381(25):2429-39.
131. Nemes E, Geldenhuys H, Rozot V, Rutkowski KT, Ratangee F, Bilek N, et al. Prevention of M. tuberculosis Infection with H4:IC31 Vaccine or BCG Revaccination. N Engl J Med. 2018;379(2):138-49.
132. Vasina DV, Kleymenov DA, Manuylov VA, Mazunina EP, Koptev EY, Tukhovskaya EA, et al. First-in-human trials of GamTBvac, a recombinant subunit tuberculosis vaccine candidate: safety and immunogenicity assessment. Vaccines. 2019;7(4):166.
133. Tkachuk AP, Bykonia EN, Popova LI, Kleymenov DA, Semashko MA, Chulanov VP, et al. Safety and immunogenicity of the GamTBvac, the recombinant subunit tuberculosis vaccine candidate: A Phase II, multi-center, double-blind, randomized, placebo-controlled study. Vaccines. 2020;8(4):652.
134. Penn-Nicholson A, Tameris M, Smit E, Day TA, Musvosvi M, Jayashankar L, et al. Safety and immunogenicity of the novel tuberculosis vaccine ID93+ GLA-SE in BCG-vaccinated healthy adults in South Africa: a randomised, double-blind, placebo-controlled phase 1 trial. The Lancet Respiratory Medicine. 2018;6(4):287-98.

135. Smaill F, Jeyanathan M, Smieja M, Medina MF, Thanthrige-Don N, Zganiacz A, et al. A human type 5 adenovirus–based tuberculosis vaccine induces robust T cell responses in humans despite preexisting anti-adenovirus immunity. Science translational medicine. 2013;5(205):205ra134-205ra134.
136. Wilkie M, Satti I, Minhinnick A, Harris S, Riste M, Ramon RL, et al. A phase I trial evaluating the safety and immunogenicity of a candidate tuberculosis vaccination regimen, ChAdOx1 85A prime–MVA85A boost in healthy UK adults. Vaccine. 2020;38(4):779-89.
137. Initiative TV. The current TB vaccine pipeline Online2022 [updated October 2021; cited 2022 April]. Available from: https://www.tbvi.eu/what-we-do/pipeline-of-vaccines/.
138. Plotkin SA, Plotkin SA. Correlates of vaccine-induced immunity. Clinical infectious diseases. 2008;47(3):401-9.
139. Cole S, Brosch R, Parkhill J, Garnier T, Churcher C, Harris D, et al. Deciphering the biology of Mycobacterium tuberculosis from the complete genome sequence. Nature. 1998;396(6707):190-.
140. Geluk A, van Meijgaarden KE, Joosten SA, Commandeur S, Ottenhoff TH. Innovative strategies to identify M. tuberculosis antigens and epitopes using genome-wide analyses. Frontiers in immunology. 2014;5:256.
141. Coppola M, Ottenhoff TH, editors. Genome wide approaches discover novel Mycobacterium tuberculosis antigens as correlates of infection, disease, immunity and targets for vaccination. Seminars in immunology; 2018: Elsevier.
142. Skeiky YA, Lodes MJ, Guderian JA, Mohamath R, Bement T, Alderson MR, et al. Cloning, expression, and immunological evaluation of two putative secreted serine protease antigens of Mycobacterium tuberculosis. Infection and immunity. 1999;67(8):3998-4007.
143. Dillon DC, Alderson MR, Day CH, Lewinsohn DM, Coler R, Bement T, et al. Molecular characterization and human T-cell responses to a member of a novel Mycobacterium tuberculosis mtb39 gene family. Infection and immunity. 1999;67(6):2941-50.
144. Hawkridge T, Scriba TJ, Gelderbloem S, Smit E, Tameris M, Moyo S, et al. Safety and immunogenicity of a new tuberculosis vaccine, MVA85A, in healthy adults in South Africa. The Journal of infectious diseases. 2008;198(4):544-52.
145. Tait DR, Hatherill M, Van Der Meeren O, Ginsberg AM, Van Brakel E, Salaun B, et al. Final Analysis of a Trial of M72/AS01(E) Vaccine to Prevent Tuberculosis. N Engl J Med. 2019;381(25):2429-39.
146. Coppola M, van Meijgaarden KE, Franken KL, Commandeur S, Dolganov G, Kramnik I, et al. New genome-wide algorithm identifies novel in-vivo expressed Mycobacterium tuberculosis antigens inducing human T-cell responses with classical and unconventional cytokine profiles. Scientific reports. 2016;6(1):1-16.
147. Schuck SD, Mueller H, Kunitz F, Neher A, Hoffmann H, Franken KL, et al. Identification of T-cell antigens specific for latent Mycobacterium tuberculosis infection. PloS one. 2009;4(5):e5590.
148. Singh S, Saraav I, Sharma S. Immunogenic potential of latency associated antigens against Mycobacterium tuberculosis. Vaccine. 2014;32(6):712-6.
149. Tantivitayakul P, Juthayothin T, Ruangchai W, Smittipat N, Disratthakit A, Mahasirimongkol S, et al. Identification and in silico functional prediction of lineage-specific SNPs distributed in DosR-related proteins and resuscitation-promoting factor proteins of Mycobacterium tuberculosis. Heliyon. 2020;6(12):e05744.

150. Leyten EM, Lin MY, Franken KL, Friggen AH, Prins C, van Meijgaarden KE, et al. Human T-cell responses to 25 novel antigens encoded by genes of the dormancy regulon of Mycobacterium tuberculosis. Microbes and Infection. 2006;8(8):2052-60.
151. Coppola M, Van Den Eeden SJ, Wilson L, Franken KL, Ottenhoff TH, Geluk A. Synthetic long peptide derived from Mycobacterium tuberculosis latency antigen Rv1733c protects against tuberculosis. Clinical and Vaccine Immunology. 2015;22(9):1060-9.
152. Wang X, Zhang J, Liang J, Zhang Y, Teng X, Yuan X, et al. Protection against Mycobacterium tuberculosis infection offered by a new multistage subunit vaccine correlates with increased number of IFN-γ+ IL-2+ CD4+ and IFN-γ+ CD8+ T cells. PloS one. 2015;10(3):e0122560.
153. Aagaard C, Hoang T, Dietrich J, Cardona P-J, Izzo A, Dolganov G, et al. A multistage tuberculosis vaccine that confers efficient protection before and after exposure. Nature medicine. 2011;17(2):189-94.
154. Lin PL, Dietrich J, Tan E, Abalos RM, Burgos J, Bigbee C, et al. The multistage vaccine H56 boosts the effects of BCG to protect cynomolgus macaques against active tuberculosis and reactivation of latent Mycobacterium tuberculosis infection. The Journal of clinical investigation. 2012;122(1):303-14.
155. Luabeya AKK, Kagina BM, Tameris MD, Geldenhuys H, Hoff ST, Shi Z, et al. First-in-human trial of the post-exposure tuberculosis vaccine H56: IC31 in Mycobacterium tuberculosis infected and non-infected healthy adults. Vaccine. 2015;33(33):4130-40.
156. Suliman S, Luabeya AKK, Geldenhuys H, Tameris M, Hoff ST, Shi Z, et al. Dose optimization of H56: IC31 vaccine for tuberculosis-endemic populations. A double-blind, placebo-controlled, dose-selection trial. American journal of respiratory and critical care medicine. 2019;199(2):220-31.
157. Behr M, Wilson M, Gill W, Salamon H, Schoolnik G, Rane S, et al. Comparative genomics of BCG vaccines by whole-genome DNA microarray. Science. 1999;284(5419):1520-3.
158. Mustafa AS. Cell mediated immunity assays identify proteins of diagnostic and vaccine potential from genomic regions of difference of Mycobacterium tuberculosis. Kuwait Medical Journal. 2010;42(2):98-105.
159. Al-Attiyah Ra, Mustafa AS. Characterization of human cellular immune responses to Mycobacterium tuberculosis proteins encoded by genes predicted in RD15 genomic region that is absent in Mycobacterium bovis BCG. FEMS Immunology & Medical Microbiology. 2010;59(2):177-87.
160. Neagu A-N, Jayathirtha M, Baxter E, Donnelly M, Petre BA, Darie CC. Applications of Tandem Mass Spectrometry (MS/MS) in Protein Analysis for Biomedical Research. Molecules. 2022;27(8):2411.
161. van der Gugten JG. Tandem mass spectrometry in the clinical laboratory: a tutorial overview. Clinical Mass Spectrometry. 2020;15:36-43.
162. Wu X, Edwards N, Tseng C-W. Peptide identification via tandem mass spectrometry. Advances in Computers. 2006;68:253-78.
163. Rozanova S, Barkovits K, Nikolov M, Schmidt C, Urlaub H, Marcus K. Quantitative mass spectrometry-based proteomics: an overview. Quantitative Methods in Proteomics. 2021:85-116.
164. Liebler DC, Zimmerman LJ. Targeted quantitation of proteins by mass spectrometry. Biochemistry. 2013;52(22):3797-806.

165. Anand S, Samuel M, Ang C-S, Keerthikumar S, Mathivanan S. Label-based and label-free strategies for protein quantitation. Proteome bioinformatics: Springer; 2017. p. 31-43.
166. Nesvizhskii AI. Protein identification by tandem mass spectrometry and sequence database searching. Mass Spectrometry Data Analysis in Proteomics. 2007:87-119.
167. Zhang J, Xin L, Shan B, Chen W, Xie M, Yuen D, et al. PEAKS DB: de novo sequencing assisted database search for sensitive and accurate peptide identification. Molecular & cellular proteomics. 2012;11(4).
168. Cormican JA, Horokhovskyi Y, Soh WT, Mishto M, Liepe J. inSPIRE: An open-source tool for increased mass spectrometry identification rates using Prosit spectral prediction. Molecular & Cellular Proteomics. 2022;21(12).
169. Bettencourt P, Müller J, Nicastri A, Cantillon D, Madhavan M, Charles PD, et al. Identification of antigens presented by MHC for vaccines against tuberculosis. npj Vaccines. 2020;5(1):1-14.
170. Purcell AW, Ramarathinam SH, Ternette N. Mass spectrometry–based identification of MHC-bound peptides for immunopeptidomics. Nature protocols. 2019;14(6):1687-707.
171. Bassani-Sternberg M, Coukos G. Mass spectrometry-based antigen discovery for cancer immunotherapy. Current opinion in immunology. 2016;41:9-17.
172. Chen R, Fulton KM, Twine SM, Li J. Identification of MHC peptides using mass spectrometry for neoantigen discovery and cancer vaccine development. Mass spectrometry reviews. 2021;40(2):110-25.
173. Neidert MC, Kowalewski DJ, Silginer M, Kapolou K, Backert L, Freudenmann LK, et al. The natural HLA ligandome of glioblastoma stem-like cells: antigen discovery for T cell-based immunotherapy. Acta neuropathologica. 2018;135(6):923-38.
174. Bassani-Sternberg M, Bräunlein E, Klar R, Engleitner T, Sinitcyn P, Audehm S, et al. Direct identification of clinically relevant neoepitopes presented on native human melanoma tissue by mass spectrometry. Nature communications. 2016;7(1):1-16.
175. Karunakaran KP, Rey-Ladino J, Stoynov N, Berg K, Shen C, Jiang X, et al. Immunoproteomic discovery of novel T cell antigens from the obligate intracellular pathogen Chlamydia. The Journal of Immunology. 2008;180(4):2459-65.
176. Karunakaran KP, Yu H, Jiang X, Chan Q, Goldberg MF, Jenkins MK, et al. Identification of MHC-bound peptides from dendritic cells infected with Salmonella enterica strain SL1344: implications for a nontyphoidal Salmonella vaccine. Journal of proteome research. 2017;16(1):298-306.
177. Flyer DC, Ramakrishna V, Miller C, Myers H, McDaniel M, Root K, et al. Identification by mass spectrometry of CD8+-T-cell Mycobacterium tuberculosis epitopes within the Rv0341 gene product. Infection and immunity. 2002;70(6):2926-32.
178. Mayer RL, Impens F. Immunopeptidomics for next-generation bacterial vaccine development. Trends in Microbiology. 2021.
179. Reynisson B, Barra C, Kaabinejadian S, Hildebrand WH, Peters B, Nielsen M. Improved prediction of MHC II antigen presentation through integration and motif deconvolution of mass spectrometry MHC eluted ligand data. Journal of proteome research. 2020;19(6):2304-15.
180. Wieczorek M, Abualrous ET, Sticht J, Álvaro-Benito M, Stolzenberg S, Noé F, et al. Major histocompatibility complex (MHC) class I and MHC class II proteins: conformational plasticity in antigen presentation. Frontiers in immunology. 2017;8:292.

181. Abbas A, Lichtman A, Pillai S. Antigen presentation to T lymphocytes and the Functions of Major Histocompatibility Complex Molecules. Cellular and Molecular Immunology 9th ed Philadelphia: Elsevier Health Sciences. 2017:117-42.
182. Abualrous ET, Sticht J, Freund C. Major histocompatibility complex (MHC) class I and class II proteins: impact of polymorphism on antigen presentation. Current Opinion in Immunology. 2021;70:95-104.
183. Taylor HB, Klaeger S, Clauser KR, Sarkizova S, Weingarten-Gabbay S, Graham DB, et al. MS-based HLA-II peptidomics combined with multiomics will aid the development of future immunotherapies. Molecular & Cellular Proteomics. 2021;20.
184. Unanue ER, Turk V, Neefjes J. Variations in MHC class II antigen processing and presentation in health and disease. Annual review of immunology. 2016;34:265-97.
185. Jones EY, Fugger L, Strominger JL, Siebold C. MHC class II proteins and disease: a structural perspective. Nature Reviews Immunology. 2006;6(4):271-82.
186. Rossjohn J, Gras S, Miles JJ, Turner SJ, Godfrey DI, McCluskey J. T cell antigen receptor recognition of antigen-presenting molecules. Annual review of immunology. 2015;33:169-200.
187. Reith W, LeibundGut-Landmann S, Waldburger J-M. Regulation of MHC class II gene expression by the class II transactivator. Nature Reviews Immunology. 2005;5(10):793-806.
188. LeibundGut-Landmann S, Waldburger JM, Krawczyk M, Otten LA, Suter T, Fontana A, et al. Mini-review: specificity and expression of CIITA, the master regulator of MHC class II genes. European journal of immunology. 2004;34(6):1513-25.
189. Harding CV, Boom WH. Regulation of antigen presentation by Mycobacterium tuberculosis: a role for Toll-like receptors. Nature Reviews Microbiology. 2010;8(4):296-307.
190. Sendide K, Deghmane A-E, Pechkovsky D, Av-Gay Y, Talal A, Hmama Z. Mycobacterium bovis BCG attenuates surface expression of mature class II molecules through IL-10-dependent inhibition of cathepsin S. The Journal of Immunology. 2005;175(8):5324-32.
191. Cobelens F, Suri RK, Helinski M, Makanga M, Weinberg AL, Schaffmeister B, et al. Accelerating research and development of new vaccines against tuberculosis: a global roadmap. The Lancet Infectious Diseases. 2022.
192. Gong W, Liang Y, Wu X. Animal models of tuberculosis vaccine research: an important component in the fight against tuberculosis. BioMed Research International. 2020;2020.
193. Cardona P-J, Williams A. Experimental animal modelling for TB vaccine development. International Journal of Infectious Diseases. 2017;56:268-73.
194. Chebib J, Jackson BC, López-Cortegano E, Tautz D, Keightley PD. Inbred lab mice are not isogenic: genetic variation within inbred strains used to infer the mutation rate per nucleotide site. Heredity. 2021;126(1):107-16.
195. Stylianou E, Harrington-Kandt R, Beglov J, Bull N, Pinpathomrat N, Swarbrick GM, et al. Identification and evaluation of novel protective antigens for the development of a candidate tuberculosis subunit vaccine. Infection and immunity. 2018;86(7):e00014-18.
196. Li J, Zhao A, Tang J, Wang G, Shi Y, Zhan L, et al. Tuberculosis vaccine development: from classic to clinical candidates. European Journal of Clinical Microbiology & Infectious Diseases. 2020;39(8):1405-25.
197. Tanner R, O'Shea MK, Fletcher HA, McShane H. In vitro mycobacterial growth inhibition assays: a tool for the assessment of protective immunity and evaluation of tuberculosis vaccine efficacy. Vaccine. 2016;34(39):4656-65.

198. Parra M, Yang AL, Lim J, Kolibab K, Derrick S, Cadieux N, et al. Development of a murine mycobacterial growth inhibition assay for evaluating vaccines against Mycobacterium tuberculosis. Clinical and vaccine immunology. 2009;16(7):1025-32.
199. Kolibab K, Parra M, Yang AL, Perera LP, Derrick SC, Morris SL. A practical in vitro growth inhibition assay for the evaluation of TB vaccines. Vaccine. 2009;28(2):317-22.
200. Marsay L, Matsumiya M, Tanner R, Poyntz H, Griffiths KL, Stylianou E, et al. Mycobacterial growth inhibition in murine splenocytes as a surrogate for protection against Mycobacterium tuberculosis (M. tb). Tuberculosis. 2013;93(5):551-7.
201. Pepponi I, Khatri B, Tanner R, Villarreal-Ramos B, Vordermeier M, McShane H. A mycobacterial growth inhibition assay (MGIA) for bovine TB vaccine development. Tuberculosis. 2017;106:118-22.
202. Tanner R, Hoogkamer E, Bitencourt J, White A, Boot C, Sombroek CC, et al. The in vitro direct mycobacterial growth inhibition assay (MGIA) for the early evaluation of TB vaccine candidates and assessment of protective immunity: a protocol for non-human primate cells. F1000Research. 2021;10.
203. Tanner R, Smith SG, van Meijgaarden KE, Giannoni F, Wilkie M, Gabriele L, et al. Optimisation, harmonisation and standardisation of the direct mycobacterial growth inhibition assay using cryopreserved human peripheral blood mononuclear cells. Journal of immunological methods. 2019;469:1-10.
204. Fletcher HA, Tanner R, Wallis RS, Meyer J, Manjaly Z-R, Harris S, et al. Inhibition of mycobacterial growth in vitro following primary but not secondary vaccination with Mycobacterium bovis BCG. Clinical and Vaccine Immunology. 2013;20(11):1683-9.
205. Yang AL, Schmidt TE, Stibitz S, Derrick SC, Morris SL, Parra M. A simplified mycobacterial growth inhibition assay (MGIA) using direct infection of mouse splenocytes and the MGIT system. Journal of microbiological methods. 2016;131:7-9.
206. Zelmer A, Tanner R, Stylianou E, Damelang T, Morris S, Izzo A, et al. A new tool for tuberculosis vaccine screening: Ex vivo Mycobacterial Growth Inhibition Assay indicates BCG-mediated protection in a murine model of tuberculosis. BMC infectious diseases. 2016;16(1):1-9.
207. Tanner R, McShane H. Replacing, reducing and refining the use of animals in tuberculosis vaccine research. ALTEX-Alternatives to animal experimentation. 2017;34(1):157-66.
208. O'Shea MK, Tanner R, Müller J, Harris SA, Wright D, Stockdale L, et al. Immunological correlates of mycobacterial growth inhibition describe a spectrum of tuberculosis infection. Scientific reports. 2018;8(1):1-13.
209. Painter H, Prabowo SA, Cia F, Stockdale L, Tanner R, Willcocks S, et al. Adaption of the ex vivo mycobacterial growth inhibition assay for use with murine lung cells. Scientific reports. 2020;10(1):1-9.
210. Meier NR, Jacobsen M, Ottenhoff TH, Ritz N. A systematic review on novel Mycobacterium tuberculosis antigens and their discriminatory potential for the diagnosis of latent and active tuberculosis. Frontiers in immunology. 2018;9:2476.
211. Bertholet S, Ireton GC, Kahn M, Guderian J, Mohamath R, Stride N, et al. Identification of human T cell antigens for the development of vaccines against Mycobacterium tuberculosis. The Journal of Immunology. 2008;181(11):7948-57.
212. Brennan MJ, Tanner R, Morris S, Scriba TJ, Achkar JM, Zelmer A, et al. The cross-species mycobacterial growth inhibition assay (MGIA) project, 2010–2014. Clinical and vaccine immunology. 2017;24(9):e00142-17.

213. Chanput W, Peters V, Wichers H. THP-1 and U937 Cells. In: Verhoeckx K, Cotter P, López-Expósito I, Kleiveland C, Lea T, Mackie A, et al., editors. The Impact of Food Bioactives on Health: in vitro and ex vivo models. Cham (CH): Springer Copyright 2015, The Author(s). 2015. p. 147-59.
214. Bettencourt P, Carmo N, Pires D, Timóteo P, Anes E. Mycobacterial infection of macrophages: the effect of the multiplicity of infection. Antimicrobial Research: Novel Bioknowledge and Educational Programs; Méndez-Vilas, A, Ed. 2017:651-64.
215. Chan LL, Cheung BK, Li JC, Lau AS. A role for STAT3 and cathepsin S in IL-10 down-regulation of IFN-γ-induced MHC class II molecule on primary human blood macrophages. Journal of leukocyte biology. 2010;88(2):303-11.
216. Kim H, Kwon KW, Kim WS, Shin SJ. Virulence-dependent induction of interleukin-10-producing-tolerogenic dendritic cells by Mycobacterium tuberculosis impedes optimal T helper type 1 proliferation. Immunology. 2017;151(2):177-90.
217. Ramachandra L, Smialek JL, Shank SS, Convery M, Boom WH, Harding CV. Phagosomal processing of Mycobacterium tuberculosis antigen 85B is modulated independently of mycobacterial viability and phagosome maturation. Infection and immunity. 2005;73(2):1097-105.
218. Kiritsy MC, Ankley LM, Trombley J, Huizinga GP, Lord AE, Orning P, et al. A genetic screen in macrophages identifies new regulators of IFNγ-inducible MHCII that contribute to T cell activation. Elife. 2021;10:e65110.
219. Keer S, Dennis WM. Inhibition of pulmonary antibacterial defense by interferon-γ during recovery from influenza infection. Nature Medicine. 2008;14(5):558.
220. Logsdon MM, Aldridge BB. Stable regulation of cell cycle events in mycobacteria: Insights from inherently heterogeneous bacterial populations. Frontiers in Microbiology. 2018;9:514.
221. van den Elsen SH, van der Laan T, Akkerman OW, van der Zanden AG, Alffenaar J-WC, van Soolingen D. Membrane filtration is suitable for reliable elimination of Mycobacterium tuberculosis from saliva for therapeutic drug monitoring. Journal of Clinical Microbiology. 2017;55(11):3292-3.
222. Duque A, Lin S-YG, Desmond E, Rienthong S, Rienthong D, Boonin C. Evaluation of the BD Bactec MGIT 320 system for detection of mycobacteria and drug susceptibility testing of Mycobacterium tuberculosis. Journal of clinical microbiology. 2013;51(10):3403-5.
223. Tran NH, Qiao R, Xin L, Chen X, Liu C, Zhang X, et al. Deep learning enables de novo peptide sequencing from data-independent-acquisition mass spectrometry. Nature methods. 2019;16(1):63-6.
224. Greenbaum J, Sidney J, Chung J, Brander C, Peters B, Sette A. Functional classification of class II human leukocyte antigen (HLA) molecules reveals seven different supertypes and a surprising degree of repertoire sharing across supertypes. Immunogenetics. 2011;63(6):325-35.
225. Vadalà M, Poddighe D, Laurino C, Palmieri B. Vaccination and autoimmune diseases: is prevention of adverse health effects on the horizon? EPMA Journal. 2017;8(3):295-311.
226. Xiang Z, He Y. Vaxign: a web-based vaccine target design program for reverse vaccinology. Procedia in Vaccinology. 2009;1(1):23-9.
227. Pearson WR. An introduction to sequence similarity ("homology") searching. Current protocols in bioinformatics. 2013;42(1):3.1. -3.1. 8.
228. Ong E, Wang H, Wong MU, Seetharaman M, Valdez N, He Y. Vaxign-ML: supervised machine learning reverse vaccinology model for improved prediction of bacterial protective antigens. Bioinformatics. 2020;36(10):3185-91.

229. Weiskopf D, Angelo MA, de Azeredo EL, Sidney J, Greenbaum JA, Fernando AN, et al. Comprehensive analysis of dengue virus-specific responses supports an HLA-linked protective role for CD8+ T cells. Proceedings of the National Academy of Sciences. 2013;110(22):E2046-E53.
230. Griffiths KL, Khader SA. Novel vaccine approaches for protection against intracellular pathogens. Current opinion in immunology. 2014;28:58-63.
231. Titball RW. Vaccines against intracellular bacterial pathogens. Drug discovery today. 2008;13(13-14):596-600.
232. Madhvi A, Mishra H, Leisching G, Mahlobo P, Baker B. Comparison of human monocyte derived macrophages and THP1-like macrophages as in vitro models for M. tuberculosis infection. Comparative immunology, microbiology and infectious diseases. 2019;67:101355.
233. Mendoza-Coronel E, Castanon-Arreola M. Comparative evaluation of in vitro human macrophage models for mycobacterial infection study. Pathogens and disease. 2016;74(6).
234. Partridge T, Nicastri A, Kliszczak AE, Yindom L-M, Kessler BM, Ternette N, et al. Discrimination between human leukocyte antigen class I-bound and co-purified HIV-derived peptides in immunopeptidomics workflows. Frontiers in Immunology. 2018;9:912.
235. Chanput W, Peters V, Wichers H. THP-1 and U937 Cells. The impact of food bioactives on health. 2015:147-59.
236. Cayabyab MJ, Qin L, Kashino SS, Izzo A, Campos-Neto A. An unbiased peptide-wide discovery approach to select Mycobacterium tuberculosis antigens that target CD8+ T cell response during infection. Vaccine. 2013;31(42):4834-40.
237. Ernst JD. Mechanisms of M. tuberculosis immune evasion as challenges to TB vaccine design. Cell host & microbe. 2018;24(1):34-42.
238. Kincaid EZ, Ernst JD. Mycobacterium tuberculosis exerts gene-selective inhibition of transcriptional responses to IFN-γ without inhibiting STAT1 function. The Journal of Immunology. 2003;171(4):2042-9.
239. Pai RK, Convery M, Hamilton TA, Boom WH, Harding CV. Inhibition of IFN-γ-induced class II transactivator expression by a 19-kDa lipoprotein from Mycobacterium tuberculosis: a potential mechanism for immune evasion. The Journal of Immunology. 2003;171(1):175-84.
240. Wang Y, Curry HM, Zwilling BS, Lafuse WP. Mycobacteria inhibition of IFN-γ induced HLA-DR gene expression by up-regulating histone deacetylation at the promoter region in human THP-1 monocytic cells. The Journal of Immunology. 2005;174(9):5687-94.
241. Sun K, Metzger DW. Inhibition of pulmonary antibacterial defense by interferon-γ during recovery from influenza infection. Nature medicine. 2008;14(5):558-64.
242. Goncalves G, Mullan KA, Duscharla D, Ayala R, Croft NP, Faridi P, et al. IFNγ modulates the immunopeptidome of triple negative breast cancer cells by enhancing and diversifying antigen processing and presentation. Frontiers in Immunology. 2021;12.
243. Asai M, Li Y, Khara JS, Robertson BD, Langford PR, Newton SM. Galleria mellonella: an infection model for screening compounds against the Mycobacterium tuberculosis complex. Frontiers in Microbiology. 2019:2630.
244. Minassian AM, Ronan EO, Poyntz H, Hill AV, McShane H. Preclinical development of an in vivo BCG challenge model for testing candidate TB vaccine efficacy. PloS one. 2011;6(5):e19840.

245. Minassian AM, Satti I, Poulton ID, Meyer J, Hill AV, McShane H. A Human Challenge Model for Mycobacterium tuberculosis Using M ycobacterium bovis Bacille Calmette-Guérin. Journal of Infectious Diseases. 2012;205(7):1035-42.
246. Brosch R, Gordon SV, Pym A, Eiglmeier K, Garnier T, Cole ST. Comparative genomics of the mycobacteria. International journal of medical microbiology. 2000;290(2):143-52.
247. Gonzalo-Asensio J, Marinova D, Martin C, Aguilo N. MTBVAC: attenuating the human pathogen of tuberculosis (TB) toward a promising vaccine against the TB epidemic. Frontiers in immunology. 2017;8:1803.
248. Liu X-Q, Dosanjh D, Varia H, Ewer K, Cockle P, Pasvol G, et al. Evaluation of T-cell responses to novel RD1-and RD2-encoded Mycobacterium tuberculosis gene products for specific detection of human tuberculosis infection. Infection and immunity. 2004;72(5):2574-81.
249. Cockle P, Gordon S, Lalvani A, Buddle B, Hewinson R, Vordermeier H. Identification of novel Mycobacterium tuberculosis antigens with potential as diagnostic reagents or subunit vaccine candidates by comparative genomics. Infection and immunity. 2002;70(12):6996-7003.
250. Mariani F, Cappelli G, Riccardi G, Colizzi V. Mycobacterium tuberculosis H37Rv comparative gene-expression analysis in synthetic medium and human macrophage. Gene. 2000;253(2):281-91.
251. Coppola M, van Meijgaarden K, Franken K, Commandeur S, Dolganov G, Kramnik I, et al. New genome-wide algorithm identifies novel in-vivo expressed Mycobacterium tuberculosis antigens inducing human T-cell responses with classical and unconventional cytokine profiles. Sci Rep 6: 37793. 2016.
252. Gallegos AM, Van Heijst JW, Samstein M, Su X, Pamer EG, Glickman MS. A gamma interferon independent mechanism of CD4 T cell mediated control of M. tuberculosis infection in vivo. PLoS pathogens. 2011;7(5):e1002052.
253. Leddy OK, White FM, Bryson BD. Leveraging Immunopeptidomics To Study and Combat Infectious Disease. Msystems. 2021;6(4):e00310-21.
254. Cecílio P, Oristian J, Meneses C, Serafim TD, Valenzuela JG, Cordeiro da Silva A, et al. Engineering a vector-based pan-Leishmania vaccine for humans: proof of principle. Scientific reports. 2020;10(1):1-20.
255. Bemani P, Amirghofran Z, Mohammadi M. Designing a multi-epitope vaccine against blood-stage of Plasmodium falciparum by in silico approaches. Journal of Molecular Graphics and Modelling. 2020;99:107645.
256. Mahata D, Mukherjee D, Malviya V, Mukherjee G. Targeting "Immunogenic Hotspots" in Dengue and Zika Virus: A Novel Approach to a Common Vaccine. bioRxiv. 2021.
257. Sheikh QM, Gatherer D, Reche PA, Flower DR. Towards the knowledge-based design of universal influenza epitope ensemble vaccines. Bioinformatics. 2016;32(21):3233-9.
258. Humayun F, Cai Y, Khan A, Farhan SA, Khan F, Rana UI, et al. Structure-guided design of multi-epitopes vaccine against variants of concern (VOCs) of SARS-CoV-2 and validation through In silico cloning and immune simulations. Computers in Biology and Medicine. 2022;140:105122.
259. Zhang L, Udaka K, Mamitsuka H, Zhu S. Toward more accurate pan-specific MHC-peptide binding prediction: a review of current methods and tools. Briefings in bioinformatics. 2012;13(3):350-64.
260. Crotty S. T follicular helper cell differentiation, function, and roles in disease. Immunity. 2014;41(4):529-42.

261. Lu Y-J, Barreira-Silva P, Boyce S, Powers J, Cavallo K, Behar SM. CD4 T cell help prevents CD8 T cell exhaustion and promotes control of Mycobacterium tuberculosis infection. Cell reports. 2021;36(11):109696.
262. Ritzau-Jost J, Hutloff A. T Cell/B Cell Interactions in the Establishment of Protective Immunity. Vaccines. 2021;9(10):1074.
263. Griffin JE, Gawronski JD, DeJesus MA, Ioerger TR, Akerley BJ, Sassetti CM. High-resolution phenotypic profiling defines genes essential for mycobacterial growth and cholesterol catabolism. PLoS pathogens. 2011;7(9):e1002251.
264. Dwivedy A, Ashraf A, Jha B, Kumar D, Agarwal N, Biswal BK. De novo histidine biosynthesis protects Mycobacterium tuberculosis from host IFN-γ mediated histidine starvation. Communications biology. 2021;4(1):1-15.
265. Agüero F, Al-Lazikani B, Aslett M, Berriman M, Buckner FS, Campbell RK, et al. Genomic-scale prioritization of drug targets: the TDR Targets database. Nature reviews Drug discovery. 2008;7(11):900-7.
266. Mawuenyega KG, Forst CV, Dobos KM, Belisle JT, Chen J, Bradbury EM, et al. Mycobacterium tuberculosis functional network analysis by global subcellular protein profiling. Molecular Biology of the cell. 2005;16(1):396-404.
267. De Souza GA, Leversen NA, Målen H, Wiker HG. Bacterial proteins with cleaved or uncleaved signal peptides of the general secretory pathway. Journal of proteomics. 2011;75(2):502-10.
268. Minato Y, Gohl DM, Thiede JM, Chacón JM, Harcombe WR, Maruyama F, et al. Genomewide assessment of Mycobacterium tuberculosis conditionally essential metabolic pathways. MSystems. 2019;4(4):e00070-19.
269. Sassetti CM, Boyd DH, Rubin EJ. Genes required for mycobacterial growth defined by high density mutagenesis. Molecular microbiology. 2003;48(1):77-84.
270. DeJesus MA, Gerrick ER, Xu W, Park SW, Long JE, Boutte CC, et al. Comprehensive essentiality analysis of the Mycobacterium tuberculosis genome via saturating transposon mutagenesis. MBio. 2017;8(1):e02133-16.
271. Teahan B, Ong E, Yang Z. Identification of Mycobacterium tuberculosis Antigens with Vaccine Potential Using a Machine Learning-Based Reverse Vaccinology Approach. Vaccines. 2021;9(10):1098.
272. Wang X, Wu Y, Jiao J, Huang Q. Mycobacterium tuberculosis infection induces IL-10 gene expression by disturbing histone deacetylase 6 and histonedeacetylase 11 equilibrium in macrophages. Tuberculosis. 2018;108:118-23.
273. Harishankar M, Selvaraj P, Bethunaickan R. Influence of genetic polymorphism towards pulmonary tuberculosis susceptibility. Frontiers in medicine. 2018;5:213.
274. Tervi A, Junna N, Broberg M, Jones SE, Strausz S, Kreivi H-R, et al. Large Registry Based Analysis of Genetic Predisposition to Tuberculosis Identifies Genetic Risk Factors at HLA. medRxiv. 2022.
275. Tong X, Chen L, Liu S, Yan Z, Peng S, Zhang Y, et al. Polymorphisms in HLA-DRB1 gene and the risk of tuberculosis: a meta-analysis of 31 studies. Lung. 2015;193(2):309-18.
276. Seedat F, James I, Loubser S, Waja Z, Mallal SA, Hoffmann C, et al. Human leukocyte antigen associations with protection against tuberculosis infection and disease in human immunodeficiency virus-1 infected individuals, despite household tuberculosis exposure and immune suppression. Tuberculosis. 2021;126:102023.
277. Zhou F, Xu X, Wu S, Cui X, Fan L, Pan W. Influence of HLA-DRB1 alleles on the variations of antibody response to tuberculosis Serodiagnostic antigens in active tuberculosis patients. PloS one. 2016;11(10):e0165291.

278. Sarno A, Daltro CB, Mendes CMC, Barbosa T. Distribution of HLA-DRB1 alleles in BRICS countries with a high tuberculosis burden: a systematic review and meta-analysis. Revista da Sociedade Brasileira de Medicina Tropical. 2021;54.
279. Diedrichs M, Schendel D. Differential surface expression of class II isotypes on activated CD4 and CD8 cells correlates with levels of locus-specific mRNA. The Journal of Immunology. 1989;142(9):3275-80.
280. Laupeze B, Fardel O, Onno M, Bertho N, Drenou B, Fauchet R, et al. Differential expression of major histocompatibility complex class Ia, Ib and II molecules on monocytes and monocyte-derived dendritic and macrophagic cells. Human immunology. 1999;60(7):591-7.
281. van Lith M, McEwen-Smith RM, Benham AM. HLA-DP, HLA-DQ, and HLA-DR have different requirements for invariant chain and HLA-DM. Journal of Biological Chemistry. 2010;285(52):40800-8.
282. Goeminne LJ, Gevaert K, Clement L. Experimental design and data-analysis in label-free quantitative LC/MS proteomics: A tutorial with MSqRob. Journal of proteomics. 2018;171:23-36.
283. Välikangas T, Suomi T, Elo LL. A comprehensive evaluation of popular proteomics software workflows for label-free proteome quantification and imputation. Briefings in Bioinformatics. 2017;19(6):1344-55.
284. Kaabinejadian S, Barra C, Alvarez B, Yari H, Hildebrand WH, Nielsen M. Accurate MHC Motif Deconvolution of Immunopeptidomics Data Reveals a Significant Contribution of DRB3, 4 and 5 to the Total DR Immunopeptidome. Front Immunol. 2022;13:835454.
285. Hmama Z, Gabathuler R, Jefferies WA, de Jong G, Reiner NE. Attenuation of HLA-DR expression by mononuclear phagocytes infected with Mycobacterium tuberculosis is related to intracellular sequestration of immature class II heterodimers. The Journal of Immunology. 1998;161(9):4882-93.
286. Jeyanathan M, McCormick S, Lai R, Afkhami S, Shaler C, Horvath C, et al. Pulmonary M. tuberculosis infection delays Th1 immunity via immunoadaptor DAP12-regulated IRAK-M and IL-10 expression in antigen-presenting cells. Mucosal immunology. 2014;7(3):670-83.
287. Singhal A, Jie L, Kumar P, Hong GS, Leow MK-S, Paleja B, et al. Metformin as adjunct antituberculosis therapy. Science translational medicine. 2014;6(263):263ra159-263ra159.
288. Campo M, Heater S, Peterson GJ, Simmons JD, Skerrett SJ, Mayanja-Kizza H, et al. HDAC3 inhibitor RGFP966 controls bacterial growth and modulates macrophage signaling during Mycobacterium tuberculosis infection. Tuberculosis. 2021;127:102062.
289. Yamamoto F, Suzuki S, Mizutani A, Shigenari A, Ito S, Kametani Y, et al. Capturing differential allele-level expression and genotypes of all classical HLA loci and haplotypes by a new capture RNA-Seq method. Frontiers in immunology. 2020:941.
290. Kaabinejadian S, Barra C, Alvarez B, Yari H, Hildebrand WH, Nielsen M. Accurate MHC motif deconvolution of immunopeptidomics data reveals a significant contribution of DRB3, 4 and 5 to the total DR immunopeptidome. Frontiers in immunology. 2022;13.
291. Doerr A. Mass spectrometry–based targeted proteomics. Nature methods. 2013;10(1):23-.
292. Casasola-LaMacchia A, Ritorto M, Seward R, Ahyi-Amendah N, Ciarla A, Hickling T, et al. Human leukocyte antigen class II quantification by targeted mass spectrometry in dendritic-like cell lines and monocyte-derived dendritic cells. Scientific reports. 2021;11(1):1-11.

293. Carey BS, Poulton KV, Poles A. Factors affecting HLA expression: A review. International journal of immunogenetics. 2019;46(5):307-20.
294. Prat E, Tomaru U, Sabater L, Park DM, Granger R, Kruse N, et al. HLA-DRB5*0101 and -DRB1*1501 expression in the multiple sclerosis-associated HLA-DR15 haplotype. J Neuroimmunol. 2005;167(1-2):108-19.
295. Li J, Zhang Y, Yang C, Rong R. Discrepant mRNA and protein expression in immune cells. Current Genomics. 2020;21(8):560-3.
296. Ramagopalan SV, Maugeri NJ, Handunnetthi L, Lincoln MR, Orton S-M, Dyment DA, et al. Expression of the multiple sclerosis-associated MHC class II Allele HLA-DRB1* 1501 is regulated by vitamin D. PLoS genetics. 2009;5(2):e1000369.
297. Genetic risk and a primary role for cell-mediated immune mechanisms in multiple sclerosis. Nature. 2011;476(7359):214-9.
298. Kular L, Liu Y, Ruhrmann S, Zheleznyakova G, Marabita F, Gomez-Cabrero D, et al. DNA methylation as a mediator of HLA-DRB1* 15: 01 and a protective variant in multiple sclerosis. Nature communications. 2018;9(1):1-15.
299. Kumar P, Agarwal R, Siddiqui I, Vora H, Das G, Sharma P. ESAT6 differentially inhibits IFN-γ-inducible class II transactivator isoforms in both a TLR2-dependent and-independent manner. Immunology and cell biology. 2012;90(4):411-20.
300. Sengupta S, Naz S, Das I, Ahad A, Padhi A, Naik SK, et al. Mycobacterium tuberculosis EsxL inhibits MHC-II expression by promoting hypermethylation in class-II transactivator loci in macrophages. Journal of Biological Chemistry. 2017;292(17):6855-68.
301. Sendide K, Deghmane A-E, Reyrat J-M, Talal A, Hmama Z. Mycobacterium bovis BCG urease attenuates major histocompatibility complex class II trafficking to the macrophage cell surface. Infection and immunity. 2004;72(7):4200-9.
302. Chan MM, Cheung BK, Li JC, Chan LL, Lau AS. A role for glycogen synthase kinase-3 in antagonizing mycobacterial immune evasion by negatively regulating IL-10 induction. Journal of leukocyte biology. 2009;86(2):283-91.
303. Das S, Banerjee S, Majumder S, Paul Chowdhury B, Goswami A, Halder K, et al. Immune subversion by Mycobacterium tuberculosis through CCR5 mediated signaling: involvement of IL-10. PLoS One. 2014;9(4):e92477.
304. Richardson ET, Shukla S, Sweet DR, Wearsch PA, Tsichlis PN, Boom WH, et al. Toll-like receptor 2-dependent extracellular signal-regulated kinase signaling in Mycobacterium tuberculosis-infected macrophages drives anti-inflammatory responses and inhibits Th1 polarization of responding T cells. Infection and immunity. 2015;83(6):2242-54.
305. Koppelman B, Neefjes JJ, de Vries JE, de Waal Malefyt R. Interleukin-10 down-regulates MHC class II αβ peptide complexes at the plasma membrane of monocytes by affecting arrival and recycling. Immunity. 1997;7(6):861-71.
306. Cheng F, Lienlaf M, Perez-Villarroel P, Wang H-W, Lee C, Woan K, et al. Divergent roles of histone deacetylase 6 (HDAC6) and histone deacetylase 11 (HDAC11) on the transcriptional regulation of IL10 in antigen presenting cells. Molecular immunology. 2014;60(1):44-53.
307. Cheng F, Lienlaf M, Wang H-W, Perez-Villarroel P, Lee C, Woan K, et al. A novel role for histone deacetylase 6 in the regulation of the tolerogenic STAT3/IL-10 pathway in APCs. The Journal of Immunology. 2014;193(6):2850-62.
308. Woan KV, Sahakian E, Sotomayor EM, Seto E, Villagra A. Modulation of antigen-presenting cells by HDAC inhibitors: implications in autoimmunity and cancer. Immunology and cell biology. 2012;90(1):55-65.

309. Osborne A, Zhang H, Yang WM, Seto E, Blanck G. Histone deacetylase activity represses gamma interferon-inducible HLA-DR gene expression following the establishment of a DNase I-hypersensitive chromatin conformation. Mol Cell Biol. 2001;21(19):6495-506.
310. Wang X, Tang X, Zhou Z, Huang Q. Histone deacetylase 6 inhibitor enhances resistance to Mycobacterium tuberculosis infection through innate and adaptive immunity in mice. Pathogens and disease. 2018;76(6):fty064.
311. Woan K, Lienlaf M, Perez-Villaroel P, Lee C, Cheng F, Knox T, et al. Targeting histone deacetylase 6 mediates a dual anti-melanoma effect: Enhanced antitumor immunity and impaired cell proliferation. Molecular oncology. 2015;9(7):1447-57.
312. Zhang F, Yu S, Chai Q, Wang J, Wu T, Liu R, et al. HDAC6 contributes to human resistance against Mycobacterium tuberculosis infection via mediating innate immune responses. The FASEB Journal. 2021;35(11):e22009.
313. Verrall AJ, G. Netea M, Alisjahbana B, Hill PC, van Crevel R. Early clearance of m ycobacterium tuberculosis: a new frontier in prevention. Immunology. 2014;141(4):506-13.
314. Lombardi G, del Gallo F, Vismara D, Piccolella E, De Martino C, Garzelli C, et al. Epstein-Barr virus-transformed B cells process and present Mycobacterium tuberculosis particulate antigens to T-cell clones. Cellular immunology. 1987;107(2):281-92.
315. Zhu Q, Zhang M, Shi M, Liu Y, Zhao Q, Wang W, et al. Human B cells have an active phagocytic capability and undergo immune activation upon phagocytosis of Mycobacterium tuberculosis. Immunobiology. 2016;221(4):558-67.
316. Uplekar M, Weil D, Lonnroth K, Jaramillo E, Lienhardt C, Dias HM, et al. WHO's new end TB strategy. The Lancet. 2015;385(9979):1799-801.
317. Organization WH. Regional framework for action on implementation of the end TB strategy in the Western Pacific, 2016-2020. 2016.
318. Gopalaswamy R, Subbian S. An Update on Tuberculosis Vaccines. Vaccine Design: Springer; 2022. p. 387-409.
319. Sterne J, Rodrigues L, Guedes I. Does the efficacy of BCG decline with time since vaccination? The international journal of tuberculosis and lung disease. 1998;2(3):200-7.
320. Barreto M, Cunha S, Pereira S, Genser B, Hijjar M, Yury Ichihara M, et al. Neonatal BCG protection against tuberculosis lasts for 20 years in Brazil. The international journal of tuberculosis and lung disease. 2005;9(10):1171-3.
321. Aronson NE, Santosham M, Comstock GW, Howard RS, Moulton LH, Rhoades ER, et al. Long-term efficacy of BCG vaccine in American Indians and Alaska Natives: a 60-year follow-up study. Jama. 2004;291(17):2086-91.
322. Triccas JA, Counoupas C. Novel vaccination approaches to prevent tuberculosis in children. Pneumonia. 2016;8(1):1-7.
323. Vogelzang A, Perdomo C, Zedler U, Kuhlmann S, Hurwitz R, Gengenbacher M, et al. Central memory CD4+ T cells are responsible for the recombinant bacillus Calmette-Guerin Δ ureC:: hly vaccine's superior protection against tuberculosis. The Journal of infectious diseases. 2014;210(12):1928-37.
324. Ellner JJ, Hirsch CS, Whalen CC. Correlates of protective immunity to Mycobacterium tuberculosis in humans. Clinical Infectious Diseases. 2000;30(Supplement_3):S279-S82.
325. Bhatt K, Verma S, Ellner JJ, Salgame P. Quest for correlates of protection against tuberculosis. Clinical and Vaccine Immunology. 2015;22(3):258-66.

326. Counoupas C, Triccas JA. The generation of T-cell memory to protect against tuberculosis. Immunology and Cell Biology. 2019;97(7):656-63.
327. Kaveh DA, Garcia-Pelayo MC, Hogarth PJ. Persistent BCG bacilli perpetuate CD4 T effector memory and optimal protection against tuberculosis. Vaccine. 2014;32(51):6911-8.
328. Sakai S, Mayer-Barber KD, Barber DL. Defining features of protective CD4 T cell responses to Mycobacterium tuberculosis. Current opinion in immunology. 2014;29:137-42.
329. de Cassan SC, Pathan AA, Sander CR, Minassian A, Rowland R, Hill AV, et al. Investigating the induction of vaccine-induced Th17 and regulatory T cells in healthy, Mycobacterium bovis BCG-immunized adults vaccinated with a new tuberculosis vaccine, MVA85A. Clinical and Vaccine Immunology. 2010;17(7):1066-73.
330. Lindenstrøm T, Knudsen NPH, Agger EM, Andersen P. Control of chronic Mycobacterium tuberculosis infection by CD4 KLRG1− IL-2–secreting central memory cells. The Journal of Immunology. 2013;190(12):6311-9.
331. Dockrell HM, Butkeviciute E. Can what have we learnt about BCG vaccination in the last 20 years help us to design a better tuberculosis vaccine? Vaccine. 2022;40(11):1525-33.
332. Loxton AG, Knaul JK, Grode L, Gutschmidt A, Meller C, Eisele B, et al. Safety and immunogenicity of the recombinant Mycobacterium bovis BCG vaccine VPM1002 in HIV-unexposed newborn infants in South Africa. Clinical and Vaccine Immunology. 2017;24(2):e00439-16.
333. Fonseca JA, McCaffery JN, Caceres J, Kashentseva E, Singh B, Dmitriev IP, et al. Inclusion of the murine IgGκ signal peptide increases the cellular immunogenicity of a simian adenoviral vectored Plasmodium vivax multistage vaccine. Vaccine. 2018;36(20):2799-808.
334. Güler-Gane G, Kidd S, Sridharan S, Vaughan TJ, Wilkinson TC, Tigue NJ. Overcoming the refractory expression of secreted recombinant proteins in mammalian cells through modification of the signal peptide and adjacent amino acids. PloS one. 2016;11(5):e0155340.
335. Almagro Armenteros JJ, Tsirigos KD, Sønderby CK, Petersen TN, Winther O, Brunak S, et al. SignalP 5.0 improves signal peptide predictions using deep neural networks. Nature biotechnology. 2019;37(4):420-3.
336. Ko H-J, Ko S-Y, Kim Y-J, Lee E-G, Cho S-N, Kang C-Y. Optimization of codon usage enhances the immunogenicity of a DNA vaccine encoding mycobacterial antigen Ag85B. Infection and immunity. 2005;73(9):5666-74.
337. Saramago S, Magalhães J, Pinheiro M. Tuberculosis vaccines: an update of recent and ongoing clinical trials. Applied Sciences. 2021;11(19):9250.
338. Qin F, Xia F, Chen H, Cui B, Feng Y, Zhang P, et al. A Guide to nucleic acid vaccines in the prevention and treatment of infectious diseases and cancers: from basic principles to current applications. Frontiers in cell and developmental biology. 2021:830.
339. Garçon N, Vaughn DW, Didierlaurent AM. Development and evaluation of AS03, an Adjuvant System containing α-tocopherol and squalene in an oil-in-water emulsion. Expert review of vaccines. 2012;11(3):349-66.
340. Shi S, Zhu H, Xia X, Liang Z, Ma X, Sun B. Vaccine adjuvants: Understanding the structure and mechanism of adjuvanticity. Vaccine. 2019;37(24):3167-78.
341. Gad E, Rastetter L, Herendeen D, Curtis B, Slota M, Koehniein M, et al. Optimizing the cryopreservation of murine splenocytes for improved antigen-specific T cell function in ELISPOT. Journal for ImmunoTherapy of Cancer. 2013;1(1):1-.

342. Ford T, Wenden C, Mbekeani A, Dally L, Cox JH, Morin M, et al. Cryopreservation-related loss of antigen-specific IFNγ producing CD4+ T-cells can skew immunogenicity data in vaccine trials: Lessons from a malaria vaccine trial substudy. Vaccine. 2017;35(15):1898-906.
343. Hartman H, Wang Y, Schroeder Jr HW, Cui X. Absorbance summation: a novel approach for analyzing high-throughput ELISA data in the absence of a standard. PloS one. 2018;13(6):e0198528.
344. Frey A, Di Canzio J, Zurakowski D. A statistically defined endpoint titer determination method for immunoassays. Journal of immunological methods. 1998;221(1-2):35-41.
345. Weisberg SP, Connors TJ, Zhu Y, Baldwin MR, Lin W-H, Wontakal S, et al. Distinct antibody responses to SARS-CoV-2 in children and adults across the COVID-19 clinical spectrum. Nature immunology. 2021;22(1):25-31.
346. Kober-Hasslacher M, Oh-Strauß H, Kumar D, Soberon V, Diehl C, Lech M, et al. c-Rel gain in B cells drives germinal center reactions and autoantibody production. The Journal of clinical investigation. 2020;130(6):3270-86.
347. Tyllis TS, Fenix KA, Norton TS, Kara EE, McKenzie DR, David SC, et al. CXCR5+ CD8+ T Cells Shape Antibody Responses In Vivo Following Protein Immunisation and Peripheral Viral Infection. Frontiers in Immunology. 2021:2781.
348. Voss G, Casimiro D, Neyrolles O, Williams A, Kaufmann SH, McShane H, et al. Progress and challenges in TB vaccine development. F1000Research. 2018;7.
349. Tanner R, White AD, Boot C, Sombroek CC, O'Shea MK, Wright D, et al. A non-human primate in vitro functional assay for the early evaluation of TB vaccine candidates. npj Vaccines. 2021;6(1):1-11.
350. Tanner R, Satti I, Harris SA, O'Shea MK, Cizmeci D, O'Connor D, et al. Tools for assessing the protective efficacy of TB vaccines in humans: in vitro mycobacterial growth inhibition predicts outcome of in vivo mycobacterial infection. Frontiers in Immunology. 2020;10:2983.
351. Hassett DE, Whitton JL. DNA immunization. Trends in microbiology. 1996;4(8):307-12.
352. Okada M, Kita Y. Tuberculosis vaccine development: The development of a novel (preclinical) DNA vaccine. Human vaccines. 2010;6(4):297-308.
353. Vatakis D, McMillan M. The signal peptide sequence impacts the immune response elicited by a DNA epitope vaccine. Clinical and Vaccine Immunology. 2011;18(10):1776-80.
354. Wang G, Pan L, Zhang Y. Approaches to improved targeting of DNA vaccines. Human vaccines. 2011;7(12):1271-81.
355. Baldwin S, D'souza C, Orme I, Liu M, Huygen K, Denis O, et al. Immunogenicity and protective efficacy of DNA vaccines encoding secreted and non-secreted forms of Mycobacterium tuberculosis Ag85A. Tubercle and Lung Disease. 1999;79(4):251-9.
356. Kou Y, Xu Y, Zhao Z, Liu J, Wu Y, You Q, et al. Tissue plasminogen activator (tPA) signal sequence enhances immunogenicity of MVA-based vaccine against tuberculosis. Immunology letters. 2017;190:51-7.
357. Bertholet S, Ireton GC, Ordway DJ, Windish HP, Pine SO, Kahn M, et al. A defined tuberculosis vaccine candidate boosts BCG and protects against multidrug-resistant Mycobacterium tuberculosis. Science translational medicine. 2010;2(53):53ra74-53ra74.
358. Bruffaerts N, Huygen K, Romano M. DNA vaccines against tuberculosis. Expert opinion on biological therapy. 2014;14(12):1801-13.

359. Sefidi-Heris Y, Jahangiri A, Mokhtarzadeh A, Shahbazi M-A, Khalili S, Baradaran B, et al. Recent progress in the design of DNA vaccines against tuberculosis. Drug Discovery Today. 2020;25(11):1971-87.
360. Hobernik D, Bros M. DNA vaccines—how far from clinical use? International journal of molecular sciences. 2018;19(11):3605.
361. MacGregor RR, Boyer JD, Ugen KE, Lacy KE, Gluckman SJ, Bagarazzi ML, et al. First human trial of a DNA-based vaccine for treatment of human immunodeficiency virus type 1 infection: safety and host response. Journal of infectious diseases. 1998;178(1):92-100.
362. Wang R, Doolan DL, Le TP, Hedstrom RC, Coonan KM, Charoenvit Y, et al. Induction of antigen-specific cytotoxic T lymphocytes in humans by a malaria DNA vaccine. Science. 1998;282(5388):476-80.
363. Rottinghaus ST, Poland GA, Jacobson RM, Barr LJ, Roy MJ. Hepatitis B DNA vaccine induces protective antibody responses in human non-responders to conventional vaccination. Vaccine. 2003;21(31):4604-8.
364. Yam KK, Gupta J, Allen EK, Burt KR, Beaulieu É, Mallett CP, et al. Comparison of AS03 and Alum on immune responses elicited by A/H3N2 split influenza vaccine in young, mature and aged BALB/c mice. Vaccine. 2016;34(12):1444-51.
365. Roberts A, Lamirande EW, Vogel L, Baras B, Goossens G, Knott I, et al. Immunogenicity and protective efficacy in mice and hamsters of a β-propiolactone inactivated whole virus SARS-CoV vaccine. Viral immunology. 2010;23(5):509-19.
366. Francica JR, Flynn BJ, Foulds KE, Noe AT, Werner AP, Moore IN, et al. Protective antibodies elicited by SARS-CoV-2 spike protein vaccination are boosted in the lung after challenge in nonhuman primates. Science translational medicine. 2021;13(607):eabi4547.
367. Grigoryan L, Lee A, Walls AC, Lai L, Franco B, Arunachalam PS, et al. Adjuvanting a subunit SARS-CoV-2 vaccine with clinically relevant adjuvants induces durable protection in mice. NPJ vaccines. 2022;7(1):1-14.
368. Leroux-Roels G, Marchant A, Levy J, Van Damme P, Schwarz TF, Horsmans Y, et al. Impact of adjuvants on CD4+ T cell and B cell responses to a protein antigen vaccine: results from a phase II, randomized, multicenter trial. Clinical immunology. 2016;169:16-27.
369. Burny W, Callegaro A, Bechtold V, Clement F, Delhaye S, Fissette L, et al. Different adjuvants induce common innate pathways that are associated with enhanced adaptive responses against a model antigen in humans. Frontiers in immunology. 2017;8:943.
370. Budroni S, Buricchi F, Cavallone A, Bourguignon P, Caubet M, Dewar V, et al. Antibody avidity, persistence, and response to antigen recall: comparison of vaccine adjuvants. NPJ vaccines. 2021;6(1):1-11.
371. Cohet C, van der Most R, Bauchau V, Bekkat-Berkani R, Doherty TM, Schuind A, et al. Safety of AS03-adjuvanted influenza vaccines: A review of the evidence. Vaccine. 2019;37(23):3006-21.
372. Walker KB, Guo M, Guo Y, Poecheim J, Velmurugan K, Schrager LK. Novel approaches to preclinical research and TB vaccine development. Tuberculosis. 2016;99:S12-S5.
373. Derrick SC, Yabe IM, Yang A, Morris SL. Vaccine-induced anti-tuberculosis protective immunity in mice correlates with the magnitude and quality of multifunctional CD4 T cells. Vaccine. 2011;29(16):2902-9.
374. Yuan X, Teng X, Jing Y, Ma J, Tian M, Yu Q, et al. A live attenuated BCG vaccine overexpressing multistage antigens Ag85B and HspX provides superior

protection against Mycobacterium tuberculosis infection. Applied microbiology and biotechnology. 2015;99(24):10587-95.
375. Ballester M, Nembrini C, Dhar N, De Titta A, De Piano C, Pasquier M, et al. Nanoparticle conjugation and pulmonary delivery enhance the protective efficacy of Ag85B and CpG against tuberculosis. Vaccine. 2011;29(40):6959-66.
376. Aagaard C, Hoang TTKT, Izzo A, Billeskov R, Troudt J, Arnett K, et al. Protection and polyfunctional T cells induced by Ag85B-TB10. 4/IC31® against Mycobacterium tuberculosis is highly dependent on the antigen dose. PloS one. 2009;4(6):e5930.
377. Forbes EK, Sander C, Ronan EO, McShane H, Hill AV, Beverley PC, et al. Multifunctional, high-level cytokine-producing Th1 cells in the lung, but not spleen, correlate with protection against Mycobacterium tuberculosis aerosol challenge in mice. The Journal of Immunology. 2008;181(7):4955-64.
378. Elvang T, Christensen JP, Billeskov R, Thi Kim Thanh Hoang T, Holst P, Thomsen AR, et al. CD4 and CD8 T cell responses to the M. tuberculosis Ag85B-TB10. 4 promoted by adjuvanted subunit, adenovector or heterologous prime boost vaccination. PloS one. 2009;4(4):e5139.
379. Lindenstrøm T, Agger EM, Korsholm KS, Darrah PA, Aagaard C, Seder RA, et al. Tuberculosis subunit vaccination provides long-term protective immunity characterized by multifunctional CD4 memory T cells. The Journal of Immunology. 2009;182(12):8047-55.
380. Tchilian EZ, Desel C, Forbes EK, Bandermann S, Sander CR, Hill AV, et al. Immunogenicity and protective efficacy of prime-boost regimens with recombinant Δ ureC hly+ Mycobacterium bovis BCG and modified vaccinia virus Ankara expressing M. tuberculosis antigen 85A against murine tuberculosis. Infection and Immunity. 2009;77(2):622-31.
381. Majlessi L, Simsova M, Jarvis Z, Brodin P, Rojas M-J, Bauche C, et al. An increase in antimycobacterial Th1-cell responses by prime-boost protocols of immunization does not enhance protection against tuberculosis. Infection and immunity. 2006;74(4):2128-37.
382. Orr MT, Windish HP, Beebe EA, Argilla D, Huang P-WD, Reese VA, et al. Interferon γ and tumor necrosis factor are not essential parameters of CD4+ T-cell responses for vaccine control of tuberculosis. The Journal of infectious diseases. 2015;212(3):495-504.
383. Smith SG, Zelmer A, Blitz R, Fletcher HA, Dockrell HM. Polyfunctional CD4 T-cells correlate with in vitro mycobacterial growth inhibition following Mycobacterium bovis BCG-vaccination of infants. Vaccine. 2016;34(44):5298-305.
384. Khader SA, Bell GK, Pearl JE, Fountain JJ, Rangel-Moreno J, Cilley GE, et al. IL-23 and IL-17 in the establishment of protective pulmonary CD4+ T cell responses after vaccination and during Mycobacterium tuberculosis challenge. Nature immunology. 2007;8(4):369-77.
385. Gopal R, Rangel-Moreno J, Slight S, Lin Y, Nawar HF, Junecko F, et al. Interleukin-17-dependent CXCL13 mediates mucosal vaccine–induced immunity against tuberculosis. Mucosal immunology. 2013;6(5):972-84.
386. Woodworth JS, Clemmensen HS, Battey H, Dijkman K, Lindenstrøm T, Laureano RS, et al. A Mycobacterium tuberculosis-specific subunit vaccine that provides synergistic immunity upon co-administration with Bacillus Calmette-Guérin. Nature communications. 2021;12(1):1-13.

387. Dijkman K, Sombroek CC, Vervenne RA, Hofman SO, Boot C, Remarque EJ, et al. Prevention of tuberculosis infection and disease by local BCG in repeatedly exposed rhesus macaques. Nature medicine. 2019;25(2):255-62.
388. Rodo MJ, Rozot V, Nemes E, Dintwe O, Hatherill M, Little F, et al. A comparison of antigen-specific T cell responses induced by six novel tuberculosis vaccine candidates. PLoS pathogens. 2019;15(3):e1007643.
389. Lindenstrøm T, Woodworth J, Dietrich J, Aagaard C, Andersen P, Agger EM. Vaccine-induced th17 cells are maintained long-term postvaccination as a distinct and phenotypically stable memory subset. Infection and immunity. 2012;80(10):3533-44.
390. Knudsen NPH, Olsen A, Buonsanti C, Follmann F, Zhang Y, Coler RN, et al. Different human vaccine adjuvants promote distinct antigen-independent immunological signatures tailored to different pathogens. Scientific reports. 2016;6(1):1-13.
391. van Dissel JT, Joosten SA, Hoff ST, Soonawala D, Prins C, Hokey DA, et al. A novel liposomal adjuvant system, CAF01, promotes long-lived Mycobacterium tuberculosis-specific T-cell responses in human. Vaccine. 2014;32(52):7098-107.
392. Scriba TJ, Netea MG, Ginsberg AM, editors. Key recent advances in TB vaccine development and understanding of protective immune responses against Mycobacterium tuberculosis. Seminars in Immunology; 2020: Elsevier.
393. Baldwin SL, Reese VA, Larsen SE, Beebe E, Guderian J, Orr MT, et al. Prophylactic efficacy against Mycobacterium tuberculosis using ID93 and lipid-based adjuvant formulations in the mouse model. Plos one. 2021;16(3):e0247990.
394. Fischer K, Collins H, Taniguchi M, Kaufmann SH, Schaible UE. IL-4 and T cells are required for the generation of IgG1 isotype antibodies against cardiolipin. The Journal of Immunology. 2002;168(6):2689-94.
395. Haile M, Schröder U, Hamasur B, Pawlowski A, Jaxmar T, Källenius G, et al. Immunization with heat-killed Mycobacterium bovis bacille Calmette–Guerin (BCG) in Eurocine™ L3 adjuvant protects against tuberculosis. Vaccine. 2004;22(11-12):1498-508.
396. Melkie ST, Arias L, Farroni C, Makek MJ, Goletti D, Vilaplana C. The role of antibodies in tuberculosis diagnosis, prophylaxis and therapy: a review from the ESGMYC study group. European Respiratory Review. 2022;31(163).
397. Tasbiti AH, Badmasti F, Siadat SD, Fateh A, Yari F, Jajin MG, et al. Recognition of specific immunogenic antigens with potential diagnostic value in multi-drug resistant Mycobacterium tuberculosis inducing humoral immunity in MDR-TB patients. Infection, Genetics and Evolution. 2022;103:105328.
398. Collins KA, Brod F, Snaith R, Ulaszewska M, Longley RJ, Salman AM, et al. Ultra-low dose immunization and multi-component vaccination strategies enhance protection against malaria in mice. Scientific reports. 2021;11(1):1-15.